Spring 1-1-2012

Finite Strain Micromorphic Finite Element Analysis of Elastoplastic Geomaterials

Volkan Isbuga
University of Colorado at Boulder, isbuga@colorado.edu

Finite strain micromorphic finite element analysis of elastoplastic geomaterials

by

Volkan Isbuga

B.S., Cukurova University, 2002

A thesis submitted to the

Faculty of the Graduate School of the

University of Colorado in partial fulfillment

of the requirements for the degree of

Doctor of Philosophy

Department of Civil, Enviromental and Architectural Engineering

2012

This thesis entitled:
Finite strain micromorphic finite element analysis of elastoplastic geomaterials
written by Volkan Isbuga
has been approved for the Department of Civil, Enviromental and Architectural Engineering

Dr. Richard A. Regueiro

Dr. Carlos A. Felippa

Dr. Ronald Y.S. Pak

Dr. Stein Sture

Dr. Franck Vernerey

Date

The final copy of this thesis has been examined by the signatories, and we find that both the content and the form meet acceptable presentation standards of scholarly work in the above mentioned discipline.

Isbuga, Volkan (Ph.D., Civil, Enviromental and Architectural Engineering)

Finite strain micromorphic finite element analysis of elastoplastic geomaterials

Thesis directed by Dr. Richard A. Regueiro

A three dimensional micromorphic finite strain linear isotropic elastoplastic model for geomaterials is developed and implemented into a finite element code. First, we present the finite element formulation and implementation for the finite strain elasticity together with various examples to investigate the effects of the additional degrees of freedom, additional elastic moduli, length scale, and boundary conditions on micro-displacement tensor field that are all introduced by the micromorphic continuum. We present some findings and results of the finite element analysis of one dimensional and three dimensional problems. Three dimensional results demonstrate that the micromorphic contribution leads to unpredicted behavior under three dimensional stress states, whereas a one dimensional example presents comparatively clear trends for different cases. Examples also present length scale effects and computational benefits of the formulation by direct finite strain elasticity by providing a comparison with rate form of semi implicit time integration formulation in the Total Lagrangian finite element implementation.

The work, then, is extended to finite strain micromorphic elastoplasticity by using slightly different types of yield criteria. We assume yield functions to be in the form of standard Drucker-Prager yield condition and a similar form of a Drucker-Prager-like yield function. The effect of elastic length scale is investigated in a one dimensional problem, together with the different yield functions and micro boundary conditions. We also consider a plain strain problem as more advanced geometry compared to the one dimensional example. The results which are obtained by Drucker-Prager-like yield criterion including micromorphic terms for this plain strain problem are presented to compare the effect of different number of additional degrees of freedom and the effect of the boundary conditions on the micro-

displacement tensor field as well.

Dedication

To my family.

Acknowledgements

I would like to express my sincere gratitude to my academic advisor Professor Richard A. Regueiro for his patience, kindness, and help throughout my dissertation. He is definitely a great inspiration to me as an academic advisor, and scientist as well as modest, hard-working, and respectful person. His knowledge in the field has been a great source for me to learn more. I consider myself lucky to know him, to have had an opportunity to work with him, and to complete my study under his guidance.

I would like to thank my committee members Professor Carlos A. Felippa, Professor Ronald Y.S. Pak, Professor Stein Sture, and Professor Franck Vernerey for serving on my committee, offering their invaluable expertise, and time to review this thesis. I also would like to thank Professor Kaspar Willam and Professor Mahmoud Hussein for their valuable comments and overall constructive approach.

I am always sincerely and deeply indebted to my father Ali Isbuga and my mother Sultan Isbuga. I heartily thank my sisters Ozlem Isbuga, Oznur Isbuga and my lovely nephew Can Isbuga. I owe my deepest gratitude to you all for your love, continued faith in me, and encouragement throughout this study and my entire life. All of your love has made this thesis possible.

I want to thank my friends Ebru Onlu Dural, Murat Yuksel Kaya, Basak Sener Kaya, and all of my friends who have been supportive throughout this journey and have made it enjoyable.

Contents

Chapter

Tables

Table

Figures

Figure

Chapter 1

Introduction

1.1 Motivation: Concurrent Multiscale Computational Modeling for Bound and Unbound Particulate Materials

The ultimate goal of multiscale modeling is to use lower length scale analytical/numerical modeling to better inform the 'macro'-scale model of interest, and to do so in a computationally-efficient manner. With regard to localized deformation (shear banding, fracture, large deformation adjacent to a contacting deformable body, ...), this takes on the additional challenge that the boundaries of the lower length scale model (we will call "grain-scale"",or "mesoscale", see Figures 1.3, 1.4) must be handled carefully so as not to artificially influence the resulting numerical simulations of localized deformation (Figures 1.1, 1.2). **The primary motivation for the research proposed for this thesis is to address such boundary condition (BC) issues**, while properly upscaling/informing/coupling to the macroscale simulation domain. This will be done by developing a finite strain micromorphic elasto-plasticity model (Figure 1.6) in a coupling/overlapping/handshaking region (see Figure 1.5 for unbound particulate material, and Figure 1.7 for penetration into bound particulate material). Because some of the classes of materials of interest are bound (Figure 1.3) and unbound particulate materials (Figure 1.4) that are frictional in nature, a pressure-sensitive finite strain micromorphic elastoplastic model is formulated and implemented in a research finite element code, Tahoe `sourceforge.net/projects/tahoe`.

The failure in bound particulate materials may be considered as the combination of

some processes such as grain and matrix deformation, intra-granular cracking, matrix cracking, inter-granular cracking/debonding. The global boundary conditions on the materials can influence the resulting failure mode. One example of that is shown in Figure 1.1 which presents that the confinement pressure influences fragmentation and causes the micro-cracks to coalescence and fracture. The bound particulate materials contain grains bound by a matrix. The heterogeneous particulate structure of these materials governs their response at grain/micro-to macro-scales especially in initial boundary value problems in which the localized deformation may form. The cracking in the asphalt, Figure 1.3, shows the physical problem of localized deformation in another bound particulate material.

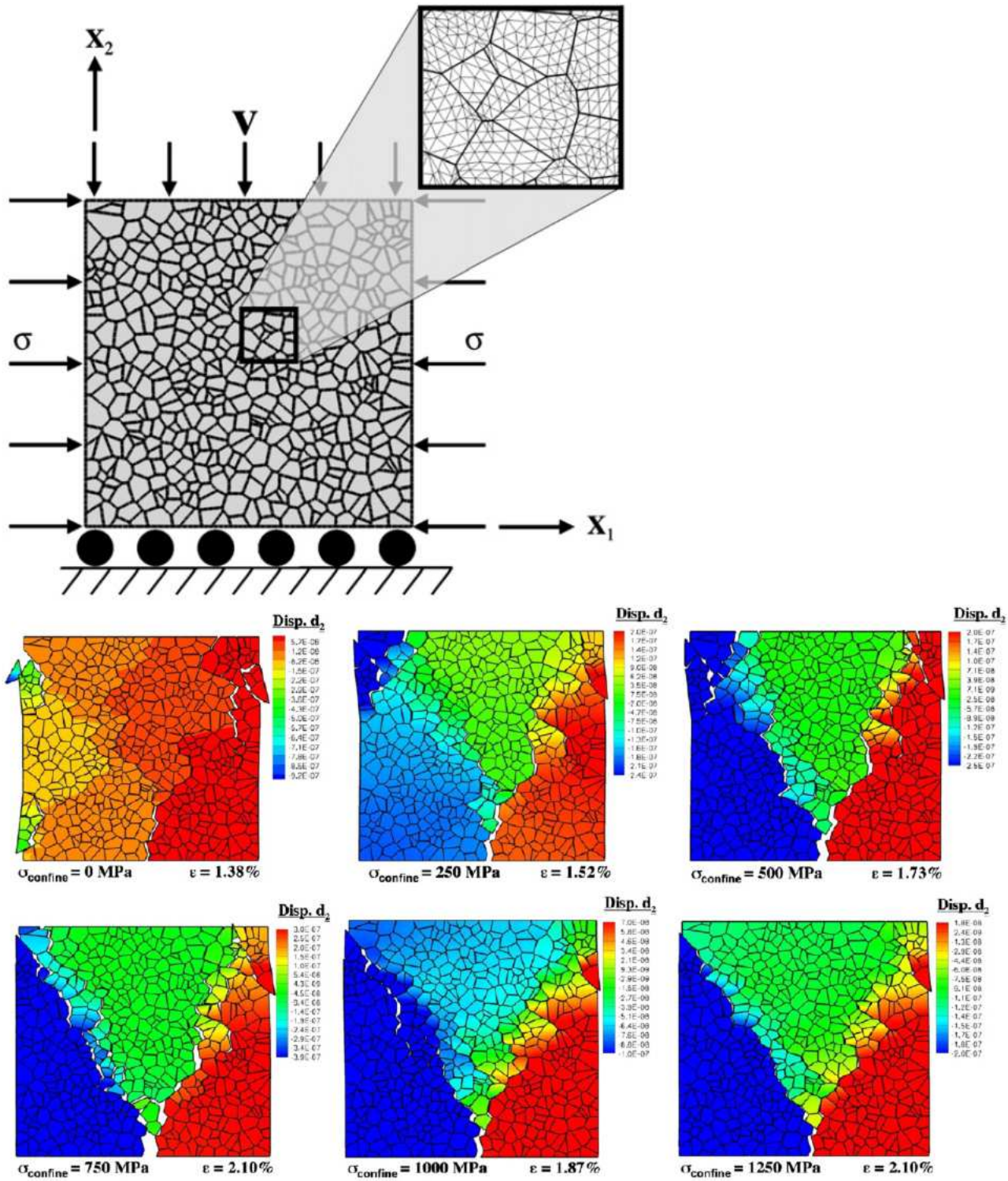

Figure 1.1: 2D FE/CSE dynamic simulations of inter-granular cracking (bottom) in brittle bound particulate material Kraft et al. (2008) showing effect of BCs (top, bottom) on coalesced micro-cracks into fracture.

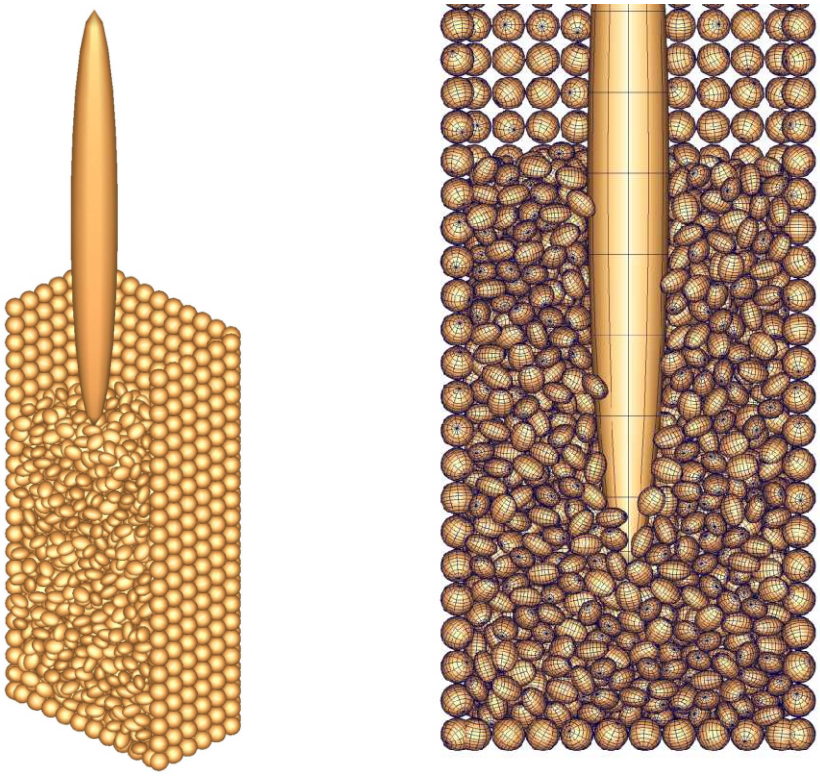

(a) 3D view

(b) 2D view

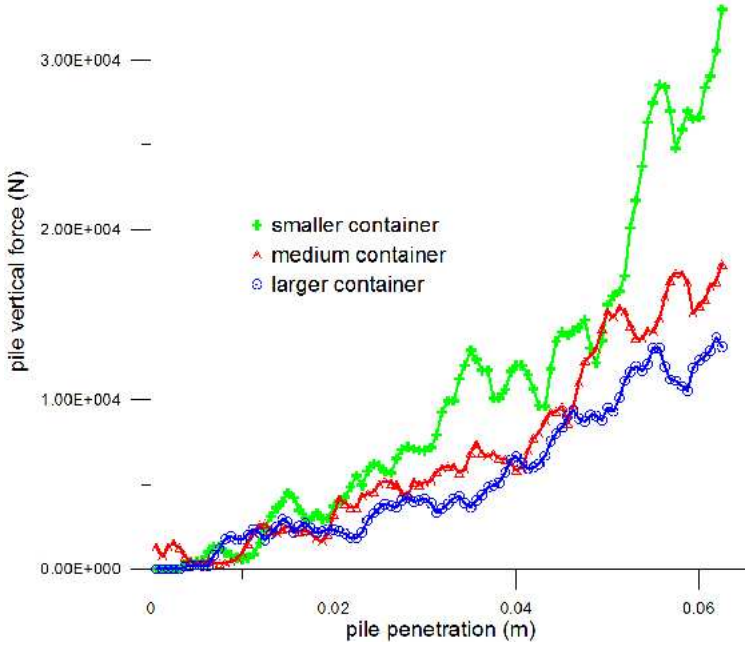

(c) force-displacement curves

Figure 1.2: Cross-sectional views of pile penetration (showing the medium container with 4260 ellipsoidal particles), and force-displacement curves showing influence of boundaries on pile resistance force Yan et al. (2010).


(a)


(b)


(c)

Figure 1.3: Grain-scale influence on fracture in asphalt: (a) road section, (b) close-up of fracture pattern, and (c) grain-binder fracture path (no intra-granular fracture observed).

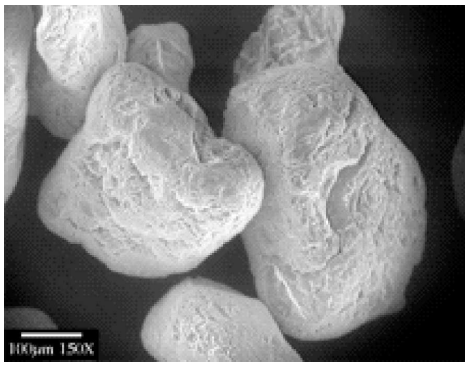

(a) Granular material like sand (image courtesy of Khalid Alshibli, University of Tennessee, Knoxville)

(b) Picture is from http://geosystems.ce.gatech.edu /Faculty/Mayne/Research/index.html

Figure 1.4: (a) Sand grains (b) Cone penetrometers

Multiscale modeling may be a way to account for the micro-structural behavior of the bound particulate materials, in which particles/grains are connected by a binder material, such as concrete(aggregate and cement), asphalt (aggregate and viscoelastic binder), sandstone (sand and clay matrix), etc., and also unbound particulate materials, in which no binder exists, such as sand, gravel. Multiscale methods are expected to give accurate results but with less computational cost compared to Direct Numerical Simulation (DNS) over the whole spatial domain of interest (Fish (2006)).

Fish (2006) reviewed the methods available to bridge the grain/particle/fibers and macro continuum scales by grouping them into two main parts as: information-passing (hierarchical) methods and concurrent methods. The information-passing methods in which discrete scale and continuum scale is modeled separately but the overall response of the discrete system is transferred to the continuum scale are divided into subclasses as: Force field calibration, generalized mathematical homogenization, quasi continuum, multiscale enrichment based on the partition of unity, variational multiscale methods, heterogeneous multiscale method, coarse-grained molecular dynamics, discontinuous Galerkin method, equation free method, proper orthogonal decomposition, the Kinetic Monte Carlo based information passing methods, atomistically informed dislocation dynamics, for instance. Whereas in

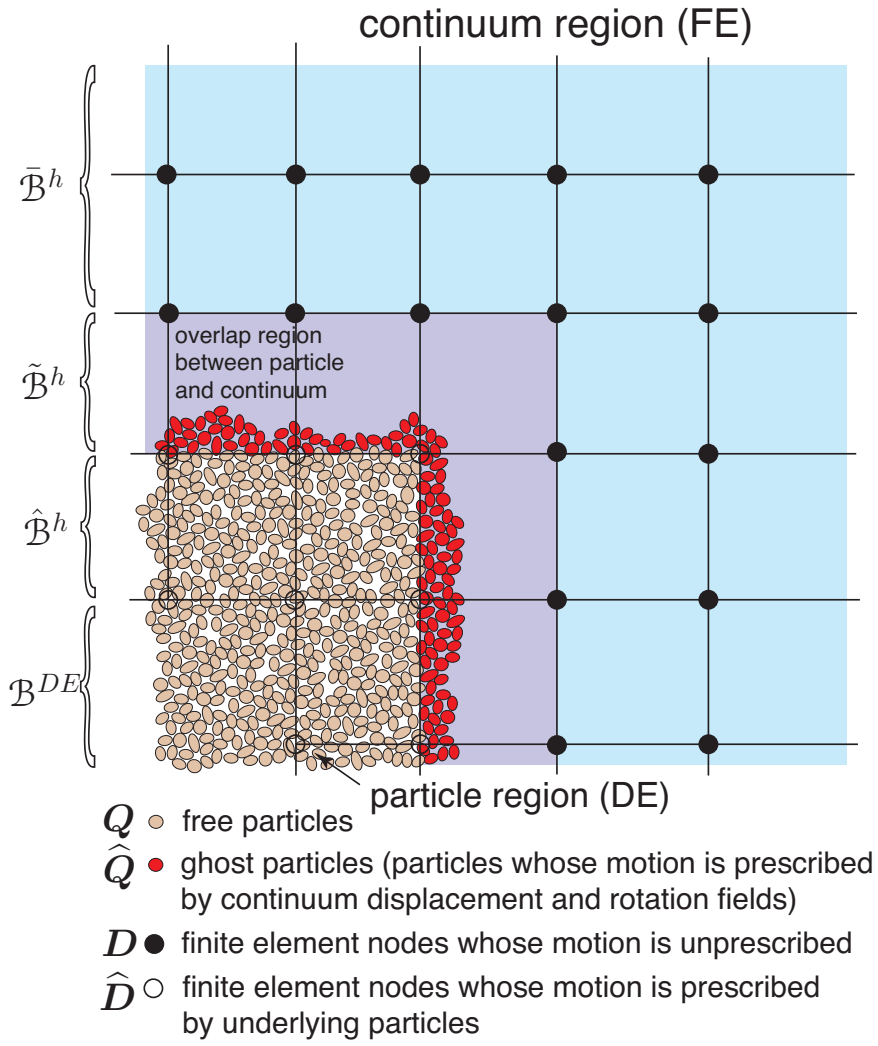

Figure 1.5: Two-dimensional illustration of the coupling between particle and micromorphic continuum regions. The purple background denotes the FE overlap region $\tilde{\mathcal{B}}^h$ with underlying ghost particles, aqua blue the FE continuum region $\bar{\mathcal{B}}^h$ with no underlying particles, and white background (with brown particles) the free particle region $\hat{\mathcal{B}}^h \cup \mathcal{B}^{DE}$. In summary, the finite element domain $\mathcal{B}^h$ is the union of pure continuum FE domain $\bar{\mathcal{B}}^h$, overlapping FE domain with underlying ghost particles $\tilde{\mathcal{B}}^h$, and overlapping FE domain with underlying free particles $\hat{\mathcal{B}}^h$, such that $\mathcal{B}^h = \bar{\mathcal{B}}^h \cup \tilde{\mathcal{B}}^h \cup \hat{\mathcal{B}}^h$. The pure particle domain with no overlapping FE domain is indicated by $\mathcal{B}^{DE}$.

concurrent methods the discrete scale and continuum scale should be simultaneously resolved, oftentimes involving a "handshaking" or overlapping region Liu et al. (2006). The concurrent methods are classified as: Domain bridging based concurrent multiscale method, local enrichment based concurrent multiscale method, multigrid based concurrent multiscale

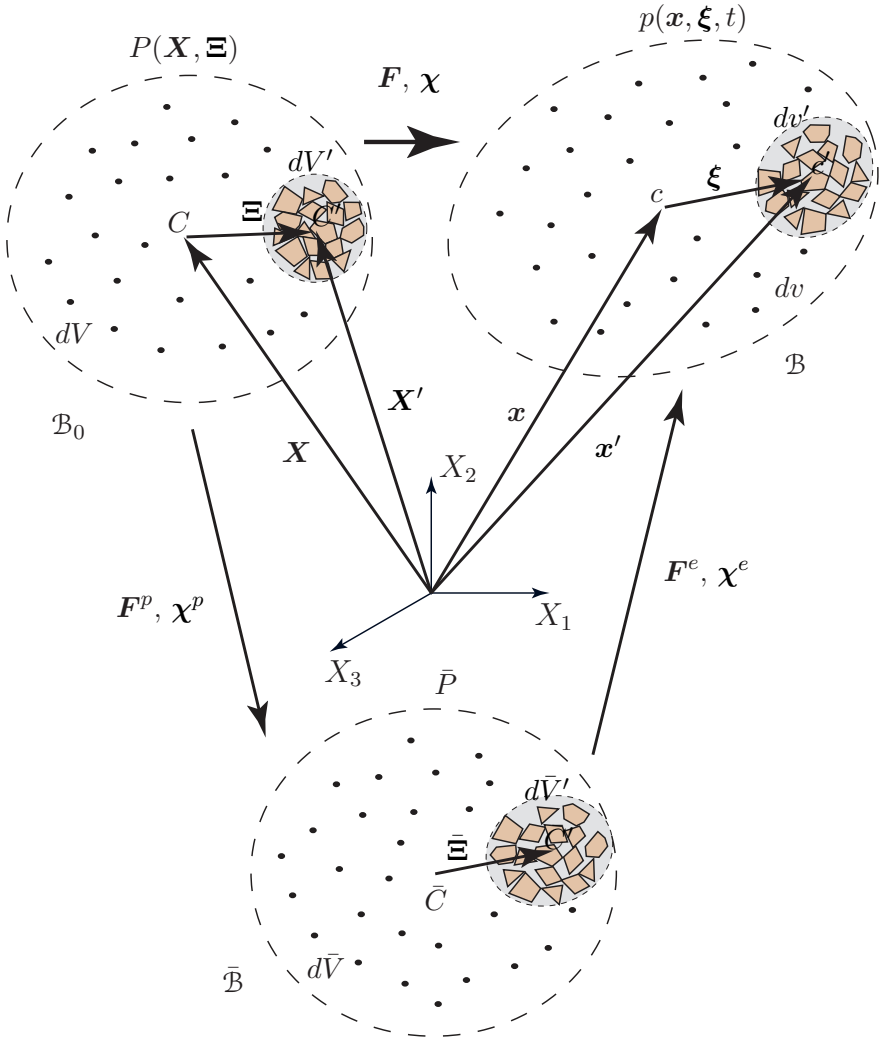

Figure 1.6: Multiplicative decomposition of deformation gradient $\boldsymbol{F}$ and micro-deformation tensor $\boldsymbol{\chi}$. Geometrical points ("macro-elements") with centroids C, $\bar{C}$, and c live in their respective configurations: $P \in \mathcal{B}_0$, $\bar{P} \in \bar{\mathcal{B}}$, and $p \in \mathcal{B}$. Material points ("micro-elements") with centroids C', $\bar{C}'$, and c'. Differential vectors and deformable directors are mapped accordingly: $d\boldsymbol{x} = \boldsymbol{F} d\boldsymbol{X}$, $d\boldsymbol{x} = \boldsymbol{F}^e d\bar{\boldsymbol{X}}$, $d\bar{\boldsymbol{X}} = \boldsymbol{F}^p d\boldsymbol{X}$, $\boldsymbol{\xi} = \boldsymbol{\chi}\boldsymbol{\Xi}$, $\boldsymbol{\xi} = \boldsymbol{\chi}^e\bar{\boldsymbol{\Xi}}$, and $\bar{\boldsymbol{\Xi}} = \boldsymbol{\chi}^p\boldsymbol{\Xi}$.

method.

1.1.1 A Possible Approach to Concurrent Multiscale Modeling

Discrete element method (DEM)(Cundall and Strack (1979); Scott and Craig (1980); Bashir and Goddard (1991); Anandarajah (1994); Wren, J.R. and Borja, R.I. (1997); Luding et al. (2001); Masson and Martinez (2001)) can treat each particle with their real physical

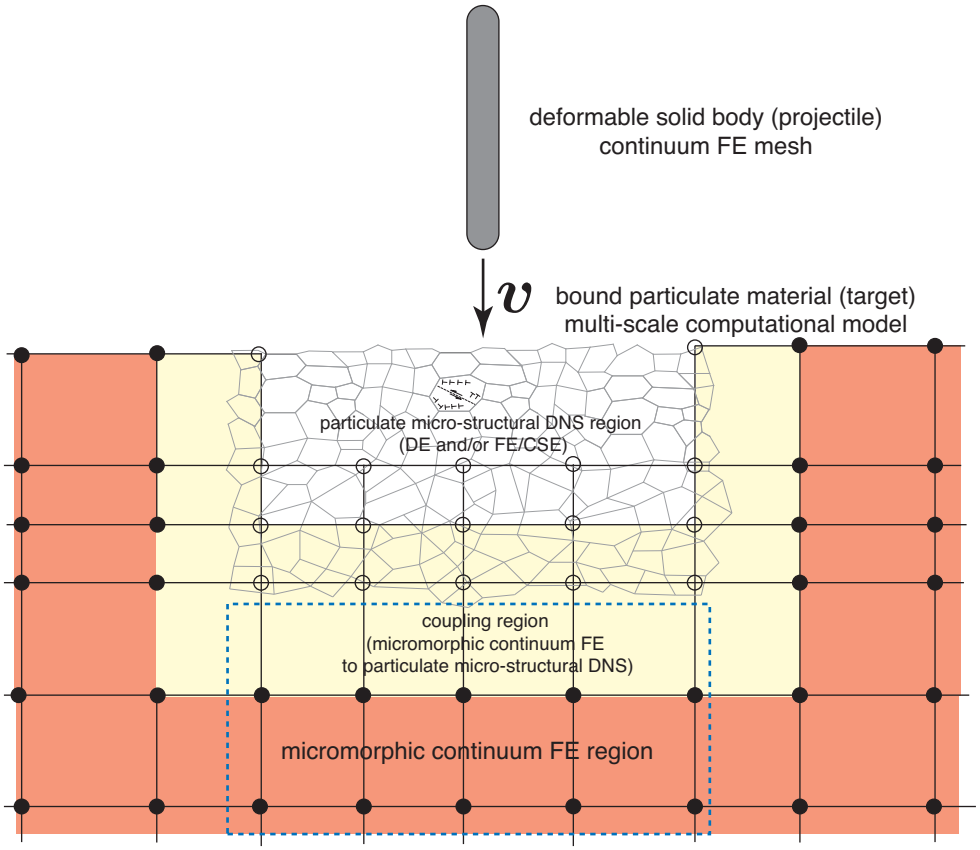

Figure 1.7: 2D illustration of concurrent computational multi-scale modeling approach in the contact interface region between a bound particulate material (e.g., ceramic target) and deformable solid body (e.g., refractory metal projectile). The DE and/or FE representation of the particulate micro-structure is intentionally not shown in order not to clutter the drawing of the micro-structure. The grains (binder matrix not shown) of the micro-structure are 'meshed' using DEs and/or FEs with cohesive surface elements (CSEs). The open circles denote continuum FE nodes that have prescribed degrees of freedom (dofs) $\widehat{\boldsymbol{D}}$ based on the underlying grain-scale response, while the solid circles denote continuum FE nodes that have free dofs $\boldsymbol{D}$ governed by the micromorphic continuum model. We intentionally leave an 'open window' (i.e., DNS) on the particulate micro-structural mesh in order to model dynamic failure. If the continuum mesh overlays the whole particulate micro-structural region, as in Klein and Zimmerman (2006) for atomistic-continuum coupling, then the continuum FEs would eventually become too deformed by following the micro-structural motion during fragmentation. The blue-dashed box at the bottom-center of the illustration is a micromorphic continuum FE region that can be converted to a DNS region for adaptive high-fidelity material modeling as the projectile penetrates the target.

sizes separately. The method takes into account the contacts between the particles rather than applying a homogenization rule over the domain. Therefore, DEM may be the most suitable approach to model the granular materials. However, DEM requires extensive com-

putational power which does not make it very useful for many problems even for small regions. One approach to utilize this method is to couple the DEM method with higher order continuum models.

Although DEM is an effective approach for modeling the micro-structure, its applicability is limited by the available computational power. A proposed approach by Regueiro (2010) aims to resolve this problem by developing a concurrent multiscale model which is coupling the region of the dry flowing particulate to the region of continuum deformation. In this method, the total domain is simply formed by subregions shown in the figures 1.5 and 1.7; (i) the first region is consisting of only discrete particles modeled by DEM. This particle region is including particle mechanics and assumed to go under large deformation. Thus, it important here is to apply the higher-resolution models; (ii) the second region is the overlap region which is bridging the particulate structure to the FE micromorphic continuum field and it is including ghost particles whose motion is prescribed by the continuum field; (iii) the third region is the modeled again by the FE micromorphic higher order continuum theory but with underlying free particles. The regions, (ii) and (iii) have a lower-resolution model compared to the part (i), although it has a better and higher-resolution approach than the classical continuum theory; (iv) the last region is the FE micromorphic continuum region which is assumed to not to have any underlying structure. Compared to modeling the whole region by DE, this approach provides a computationally less expensive, thus, preferable approximation to the problem without ignoring underlying micro-structure.

The particle-continuum coupling method is following the method called " bridging scale decomposition" proposed by Wagner and Liu (2003) and then developed by Klein and Zimmerman (2006). The method is known to minimize the fictitious forces which occurs due to improper distribution of the potential energy in the overlap region for quasi-static case and wave reflections for dynamic case. However, these two studies were based on the atomistic structure coupling with continuum region. In the current research, the atomistic structure is replaced by particulate structure. Besides, this approach will have a different energy

partitioning and it will involve the only quasi-static case. The proposed approach by Regueiro (2010) is involving the inelastic deformation modeling in both particle and continuum regions, and providing a higher resolution over the continuum regions by introducing higher order micromorphic continuum theory. The kinematics of the coupling may be summarized by using the same notation of Wagner and Liu (2003); Klein and Zimmerman (2006). The particle displacements and rotations are defined as:

$$\breve{\boldsymbol{U}} = \left[\begin{array}{ccccccccc} \boldsymbol{u}_\alpha, & \boldsymbol{u}_\beta, & ...., & \boldsymbol{u}_\gamma, & \boldsymbol{\theta}_\alpha, & \boldsymbol{\theta}_\beta, & ... & , \boldsymbol{\theta}_\gamma \end{array} \right]^T, \ \alpha, \beta, ..., \gamma \in \breve{\mathcal{A}} \tag{1.1}$$

where $\boldsymbol{u}_\alpha$ is the α particle's displacement, $\boldsymbol{\theta}_\alpha$ is the α particle's rotation and $\breve{\mathcal{A}}$ is the set of all particles. Likewise, the nodal displacements and micro-displacement gradient fields associated with the finite element mesh are :

$$\breve{\boldsymbol{D}} = \left[\begin{array}{ccccccccc} \boldsymbol{d}_a, & \boldsymbol{d}_b, & ...., & \boldsymbol{d}_c, & \boldsymbol{\phi}_a, & \boldsymbol{\phi}_b, & ..., & \boldsymbol{\phi}_c \end{array} \right]^T, \ a, b, ..., c \in \breve{\mathcal{N}} \tag{1.2}$$

where $\boldsymbol{d}_a$ is the displacement of the node a, $\boldsymbol{\phi}_a$ is the micro-displacement gradient field at the node a, $\breve{\mathcal{N}}$ is the set of the all nodes. The particles shown in the overlap region in the Figure 1.5 are called the "ghost particles" and their motions are prescribed by the continuum displacement field. It can be written as $\hat{\boldsymbol{U}} \in \hat{\mathcal{A}}$, where $\hat{\boldsymbol{U}}$ shows the prescribed particle motions. The unprescribed particle motions are denoted by $\boldsymbol{U}$ and $\boldsymbol{U} \in \mathcal{A}$ where $\hat{A} \cup \mathcal{A} = \breve{\mathcal{A}}$ and $\hat{A} \cap \mathcal{A} = \emptyset$. Likely, the node displacements and micro-deformation of continuum finite element on the particle region are prescribed by the particle motion and represented as $\hat{\boldsymbol{D}} \in \hat{\mathcal{N}}$, and the unprescribed node displacements and micro-deformations are $\boldsymbol{D} \in \mathcal{N}, \mathcal{M}$ where $\hat{\mathcal{N}} \cup \mathcal{N} = \breve{\mathcal{N}}$, $\hat{\mathcal{N}} \cap \mathcal{N} = \emptyset$. The energy partitioning will follow the concept in Klein and Zimmerman (2006) and it depends on the DE equations for particles and micromorphic continuum FE equations for the continuum field on the overlap region.

Coupling and bridging should not be confused by each other. Coupling mentioned above means taking part interactively between particle and micromorphic continuum region and vice versa. Whereas, bridging between underlying particle structure and overlaying

continuum scale is an issue accounted by micromorphic continuum theory within a finite strain inelastic constitutive model proposed by Regueiro (2009),Regueiro (2010) (the details on this model and its application to a soil model will be given in the next chapters).

Eringen (1999) states that if the ratio of the characteristic length associated with the applied load to the internal characteristic length is close to one, then, the response of the particles may change the behavior of the body dramatically. It must be noted that we have a pure particle approach in particle region in which the particle dimensions (characteristic length) become a very important factor. Therefore, having extra degrees of freedom, the micromorphic continuum theory helps to define proper B.C.'s on particles in the overlap region, thereby, it is expected to provide a smoother transition between the regions. The standard continuum models do not have this extra kinematic property so that the BC's may not simulate this transition and also the shear bands in particle region. Since the micromorphic continuum theory involves plasticity parameters, initially, the micromorphic continuum and particle region will be assumed to overlap each other completely so that these parameters can be obtained by inverse analysis via the particle based triaxial compression simulation tests. For fully overlapped regions, these particle scale parameters can be related to micromorphic continuum scale parameters via a homogenization approach with weighted averaging integrals for each desired field. If the averaging operator is shown by $\langle \bullet \rangle$, for instance, Cauchy stress tensor $\boldsymbol{\sigma}$ and higher order stress tensor $\boldsymbol{m}$ can be obtained as:

$$\sigma_{ij} \overset{def}{=} \left\langle \sigma_{ij}^{particle} \right\rangle, \qquad m_{ijk} \overset{def}{=} \left\langle \sigma_{ij}^{particle} \xi_k \right\rangle \tag{1.3}$$

It may be summarized that the higher order continuum theories are more applicable than the standard continuum theories in modeling (Chambon et al., 2004; Regueiro, 2009, 2010) when (i) size effects of the micro-structure becomes important under large deformation gradient as in granular materials, (ii) strain localization which yields to failure occurs, (iii) bridging the different scales in the multiscale modeling is needed. The theory of higher order micromorphic continuum including balance equations and definition of the higher order stress

tensors appearing in the balance equations will be explained in the next sections.

1.2 Background on Generalized Continuum Theories

The classical continuum theories have been applied widely to model the behavior of physical bodies which may be subjected to some external forces, for instance: mechanical forces such as traction forces or subjected to some body forces such as gravity and magnetism. Generally, these bodies may be in the form of a collection of many deformable sub-bodies. The classical continuum approaches ignore the micro continua of a body, accordingly, the independent micro particulate motion and its contribution on the total response to the applied forces. This kind of continua, formed by many small bodies and whose material points are endowed with additional degree of freedoms, are referred as generalized continua (E. Kröner, ed. (1968),Green and Naghdi (1995)). Therefore, a continuum theory which incorporates the local motion of sub-bodies in the continuum body by introducing additional degrees of freedom with higher derivatives of a continuum field can be shown to provide a means for accounting for these sub-bodies's physical response on the overall continuum body.

One important potential use for generalized continua is to bridge the length scale of the micro-structure on mesoscale to the macro-scale engineering applications (see previous section). The significant aspect of bridging the grain/particle/fiber micro-structure to the macro continuum is to transfer the essential information from the micro-structure to macro continuum response while proposing a cost efficient approach which is needed to apply to solve problems for the region of interest.

The classical continuum theories with constitutive relations accounting for the microstructural mechanics have been applied to model the granular materials(Christoffersen et al. (1981); Rothenburg and Selvadurai (1981); Jefferson et al. (2002); Chang et al. (1992); Gardiner and Tordesillas (2004); Luding (2004); Nemat-Nasser (2004); Peters (2005)). These approaches were mainly based on the particle contact interaction and aimed to infuse particulate structure into continuum theory. A wide range of study exists in the literature on the

constitutive modeling for granular media which is not possible to review here, however, some of the recent research give an overall idea about common assumptions for the derivations of these approaches. For instance, Chang et al. (1992) described a model to predict the initial moduli, secant moduli and damping ratio of the granular materials at small strain and stress strain behavior of the material subjected to different stress paths at large strains. In the same work for finite strain case, they introduced the term "micro-elements" which are formed by spherical particles. In their approach, they had to idealize the material with certain number of the micro-elements which were consisting of the same micro-elements but rotated on the axes. They observed similar behavior for sands under different loading conditions. Jefferson et al. (2002) presented a discrete element model for a cohesive aggregate consisting of elastic particles. A superposition approximation was utilized to obtain the coupled force and displacement on a particle due to interaction by neighbor particles within the aggregate. The model was found capable to capture the rigid body rotations of the aggregate, however, it was stated by the authors that the relative rotational motion between particles were ignored and additional rotational degrees of freedom are required to capture the particle rotations and moments. Gardiner and Tordesillas (2004) proposed a model incorporating the sliding and non sliding particles contact as well as rolling resistance of the particles and loss of contacts among them. It was based on homogenization for the discrete elements at small strains. The stress tensor and the higher order stress tensor appearing in the micro-polar theory, constitutive laws, were determined by these homogenization integrals.

Generally, these approaches are limited by rigid body rotation of elastic, small strain response of a single particle, particle cluster or some formations including these particles such as micro-element as aforementioned above. Often times, the main assumption made in these models is limiting the micro-structural behavior to have only rigid rotations, although the particles(or,rather, cluster of particles) represent not only micro-rotation but also micro-shear and micro-dilatation/compaction(stretch). The research on the constitutive modeling for granular media is on going and, for the readers interested in this topic, the more detailed

reviews and the methods are available in the literature, such as Kolymbas (2000).

1.3 Summary and Comparison of Modeling Efforts on Micromorphic Continua

Generalized continua are classified into two main categories; (i) the higher grade continua in which displacement field and its higher derivatives are involved such as strain gradient methods, (ii) the higher order continua in which additional independent kinematic degrees of freedom and higher order stresses are incorporated at each material point in the continuum (Forest and Sievert (2003)).

As aforementioned, the higher order (or generalized) continua incorporates additional independent kinematic degrees of freedom. A higher order continuum may be called differently depending on the number of additional independent kinematic degrees of freedom it involves. Eringen (1999) classifies the theories as: The first and the most generalized case of the higher order continuum is the micromorphic case which has nine extra degrees of freedom through the unsymmetric micro deformation tensor $\boldsymbol{\chi}$ which is actually representation of a material point with three deformable directors. Then, the microstretch continuum is the case of four extra degrees of freedom which are three microrotations and one microstretch. Lastly, the micropolar continuum has three extra degrees of freedom which are only microrotations which occurs when a material point has three rigid directors.

A wider classification of the generalized continuum theories (based on the degrees of freedom they include) at finite strain and at infinitesimal strain cases can be summarized in the following table:

Table 1.1: Hierarchy of the generalized continua by Forest and Sievert (2006)

Name	**Number of DOF**	**DOF (finite case)**	**DOF (infinitesimal case)**	**References**
Cauchy	3	$\boldsymbol{u}$	$\boldsymbol{u}$	Truesdell and Toupin (1960)
Microdilation	4	$\boldsymbol{u}, \chi$	$\boldsymbol{u}, \chi$	-
Cosserat	6	$\boldsymbol{u}, \boldsymbol{r}$	$\boldsymbol{u}, \boldsymbol{\Phi}$	Cosserat and Cosserat (1909); Eringen (1968b)
Microstretch	7	$\boldsymbol{u}, \chi, \boldsymbol{r}$	$\boldsymbol{u}, \chi, \boldsymbol{\Phi}$	Kafadar and Eringen (1971)
Incompressible microstrain	8	$\boldsymbol{u}, {}^{\chi}\boldsymbol{C}$ $det({}^{\chi}\boldsymbol{C}) = 1$	$\boldsymbol{u}, {}^{\chi}\boldsymbol{\varepsilon}$ $trace({}^{\chi}\boldsymbol{\varepsilon}) = 0$	-
Microstrain	9	$\boldsymbol{u}, {}^{\chi}\boldsymbol{C}$	$\boldsymbol{u}, {}^{\chi}\boldsymbol{\varepsilon}$	Forest and Sievert (2006)
Incompressible micromorphic	11	$\boldsymbol{u}, \boldsymbol{\chi}$ $det(\boldsymbol{\chi}) = 1$	$\boldsymbol{u}, \boldsymbol{\chi}$ $trace(\boldsymbol{\chi}) = 0$	-
Micromorphic	12	$\boldsymbol{u}, \boldsymbol{\chi}$	$\boldsymbol{u}, \boldsymbol{\chi}^s + \boldsymbol{\chi}^a$	Eringen and Suhubi (1964); Mindlin (1964)

In the table above, $\boldsymbol{u}$ is the displacement vector, $\boldsymbol{r}$ is the independent micro-rotation tensor in finite strain case, $\boldsymbol{\Phi}$ is the independent micro-rotation tensor for infinitesimal case, χ is the scalar representing the microdilatation, $\boldsymbol{\chi}$ is the microdeformation tensor, ${}^{\chi}\boldsymbol{C} = \boldsymbol{\chi}^T\boldsymbol{\chi}$

is the tensor with the components of the symmetric right Cauchy-Green tensor associated with the microdeformation tensor, ${}^{\chi}\boldsymbol{\varepsilon}$ is a symmetric tensor defined by ${}^{\chi}\boldsymbol{\varepsilon} = \boldsymbol{\chi}^s - \mathbf{1}$, $\boldsymbol{\chi}^s$ and $\boldsymbol{\chi}^a$ are the symmetric part and antisymmetric part of the microdeformation tensor respectively.

Efforts on modeling generalized continua may be said to start with the Cosserat brothers who introduced three additional degrees of freedom to the standard Cauchy continuum (Cosserat and Cosserat, 1909). The theory assumed that each material point is represented by a rigid body including three additional degrees of freedom which correspond to the rigid body rotations of particles (or sub-continuum bodies) also called microrotations. The theory has been developed and generalized by the contributions of many authors by the time. Some of these works and some kinematics relations which were used to derive the balance equations and these resulting equations are briefly mentioned below.

Mindlin (1964) for small strain theory assumed that in each material volume V which has the material position vector X_i and bounded by a surface S has an embedded micro volume with material position vector X_i' before deformation and the spatial position vector x_i' after deformation. The macro displacement $\boldsymbol{u}$ also was expressed as:

$$u_i = x_i - X_i \tag{1.4}$$

and the micro displacement $\boldsymbol{u}'$ was defined as:

$$u_i' = x_i' - X_i' \tag{1.5}$$

Then, it was assumed that the micro displacements can be written as a function of the specified spatial micro position vector x_i' and an arbitrary function that depends on the macro spatial position vector x_i and time t as:

$$u_i' = x_k' \psi_{ki}(\boldsymbol{x}, t) \tag{1.6}$$

The displacement gradients were assumed small so that the displacement gradients in material and spatial coordinate system were approximately the same (small strain and rotation

assumption).

$$\frac{\partial u_i}{\partial X_j} \approx \frac{\partial u_i}{\partial x_j} \overset{def}{=} \partial_j u_i, \qquad \frac{\partial u'_i}{\partial X'_j} \approx \frac{\partial u'_i}{\partial x'_j} \overset{def}{=} \partial'_j u'_i \tag{1.7}$$

where the macro displacement and the micro displacement were defined, respectively, as $u_i = u_i(x_i, t)$ and $u'_i = u'_i(x_i, x'_i, t)$. Then, the macro strain, the micro displacement gradient, the micro deformation gradient, and the relative deformation, were obtained respectively as:

$$\varepsilon_{ij} = \frac{1}{2}\left(u_{i,j} + u_{j,i}\right) \tag{1.8}$$

$$\partial'_i u'_j = \psi_{ij} \tag{1.9}$$

$$\varkappa_{ijk} = \partial_i \psi_{jk} \tag{1.10}$$

$$\gamma_{ij} = \partial_i u_j - \psi_{ij} \tag{1.11}$$

A graphical interpretation of the displacement gradient, micro displacement gradient, and relative deformation, may be shown in Figure 1.8. The micro strain and micro rotation was

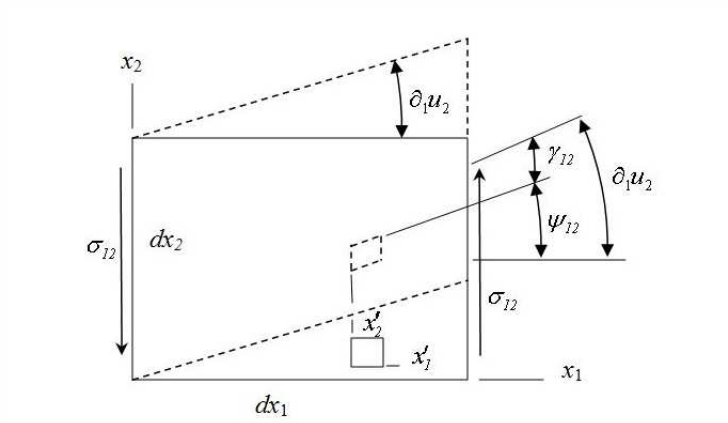

Figure 1.8: Graphical representation of γ_{12} component of the relative deformation by Mindlin (1964).

defined respectively by the symmetric part and antisymmetric part of ψ_{ij} as :

$$\psi_{(ij)} = \frac{1}{2}\left(\psi_{ij} + \psi_{ji}\right) \tag{1.12}$$

$$\psi_{[ij]} = \frac{1}{2}\left(\psi_{ij} - \psi_{ji}\right) \tag{1.13}$$

The physical explanation of the some components of micro deformation gradient $\varkappa_{ijk}$ and associated higher order stress tensor μ_{ijk} appearing in Mindlin (1964) can be shown in Figure 1.9. Following the kinematic assumptions mentioned above, Mindlin (1964) formulated an approach in small strain linear elasticity with micro-structure and obtained the stress equations of motions and constitutive equations as well. The assumed potential function, stress definitions and field equations will be mentioned here without the details in order to point out the differences with the work proposed by Eringen and Suhubi (1964), however, the constitutive equations and details on the formulation will not be considered. Mindlin

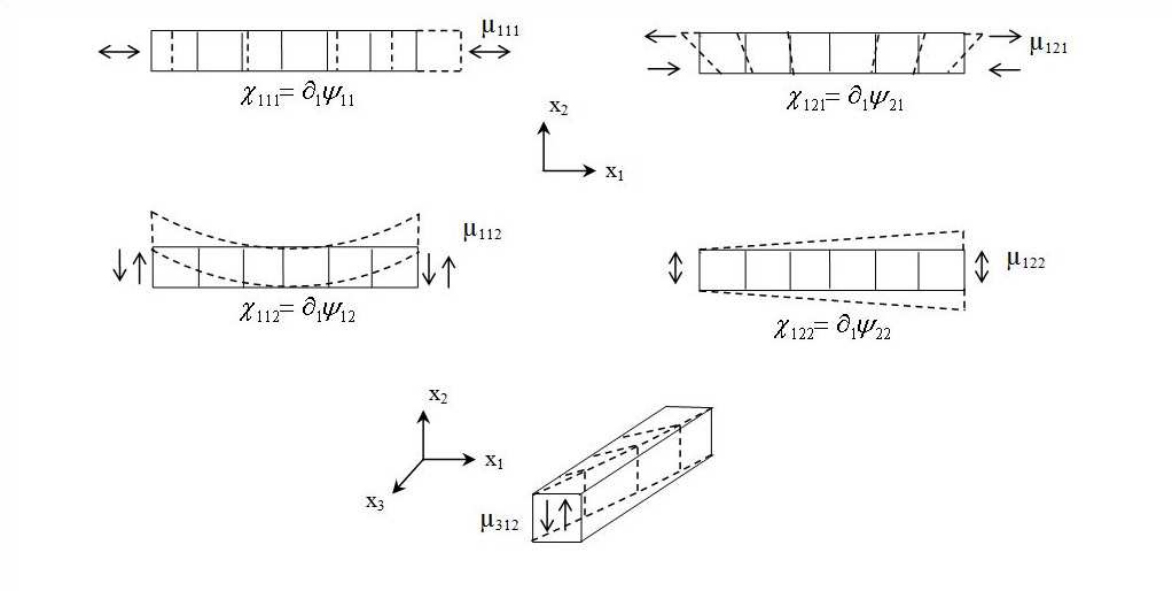

Figure 1.9: Graphical interpretation of higher order stress tensor by Mindlin (1964).

assumed a potential energy function which depends on $\boldsymbol{\varepsilon}$, $\boldsymbol{\gamma}$ and $\varkappa$ as:

$$W = W(\boldsymbol{\varepsilon}, \boldsymbol{\gamma}, \varkappa) \tag{1.14}$$

then, applying the Hamilton's principle and defining the stress tensors as:

$$\tau_{ij} = \frac{\partial W}{\partial \varepsilon_{ij}} \tag{1.15}$$

$$\sigma_{ij} = \frac{\partial W}{\partial \gamma_{ij}} \tag{1.16}$$

$$\mu_{ijk} = \frac{\partial W}{\partial \varkappa_{ijk}} \tag{1.17}$$

resulted in the field equations:

$$\partial_i(\tau_{ij} + \sigma_{ij}) + f_j = \rho \ddot{u}_j \tag{1.18}$$

$$\partial_i \mu_{ijk} + \sigma_{jk} + \Phi_{jk} = \frac{1}{3}\rho' d_{lj}^2 \ddot{\psi}_{lk} \tag{1.19}$$

where

$$d_{kl}^2 = d_p d_q \left(\delta_{p1}\delta_{q1} l_{k1} l_{l1} + \delta_{p2}\delta_{q2} l_{k2} l_{l2} + \delta_{p3}\delta_{q3} l_{k3} l_{l3}\right) \tag{1.20}$$

and the boundary conditions are:

$$t_j = n_i(\tau_{ij} + \sigma_{ij}) \tag{1.21}$$

$$T_{jk} = n_i \mu_{ijk} \tag{1.22}$$

where ρ' is the mass of the micro material per unit macro volume, d_i are the edge lengths of a parallelepiped considered as micro-volume, l_{ij} is the direction cosines with respect to axes x_i', Φ_{ij} is a tensor representing body double force per unit volume which is work conjugate to ψ_{ij}, τ_{ij} is the symmetric Cauchy stress tensor which is the work conjugate to ε_{ij}, σ_{ij} was called "relative stress" tensor by Mindlin and work conjugate to γ_{ij} tensor, and the higher order stress tensor μ_{ijk} is called "double stress tensor" in which the components are interpreted as the double forces and work conjugate to $\varkappa_{ijk}$.

Eringen and Suhubi (1964) proposed a finite strain theory to provide field equations, boundary conditions and constitutive equations for a micromorphic continuum by making use of kinematic relations mentioned below.

They started with a representative macro volume element, dV, in the reference configuration, with a differential mass dM and associated mass center $\boldsymbol{X}$. The macro element occupies a space after deformation in spatial coordinates with a center $\boldsymbol{x}$. The macro elements were assumed to involve micro volume elements, dV', in the reference configuration.

A material point in reference configuration has a position vector expressed with $\boldsymbol{X'}$ also occupies a unique point in spatial coordinates $\boldsymbol{x'}$ after deformation that means a one to one mapping which can be defined as (see Figure 1.10):

$$\boldsymbol{x}' = \boldsymbol{x}(\boldsymbol{X}', t), \qquad \boldsymbol{X}' = \boldsymbol{X}(\boldsymbol{x}', t) \tag{1.23}$$

It was assumed that there was a continuous mass density over the macro element. Then, the total mass of the macro differential volume element dM was assumed to be average of local masses of the micro volume element by some integral approximations as follows:

$$\int_{dV} \rho_0' dV' = \rho_0 dV, \qquad \int_{dv} \rho' dv' = \rho dv \tag{1.24}$$

where ρ_0', ρ' are the mass densities, respectively, at material point $\boldsymbol{X}'$ and spatial point $\boldsymbol{x}'$. The average mass densities of the undeformed macro differential volume dV and the deformed macro differential volume dv are ρ_0 and ρ respectively. It should be noted that all the quantities associated with the microelements are primed letters.

A point in the micro volume at undeformed and deformed configurations, respectively, $\boldsymbol{X}'$ and $\boldsymbol{x}'$ can be expressed in terms of the mass center point coordinates of the macro volume $\boldsymbol{X}$ and the relative position vector with respect to the macro volume mass center $\boldsymbol{\Xi}$ as:

$$\boldsymbol{X}' = \boldsymbol{X} + \boldsymbol{\Xi}, \qquad \boldsymbol{x}' = \boldsymbol{x} + \boldsymbol{\xi} \tag{1.25}$$

where $\boldsymbol{\xi} = \boldsymbol{\xi}(\boldsymbol{X}, \boldsymbol{\Xi}, t)$. It was assumed that for small length of $\boldsymbol{\Xi}$, $\boldsymbol{\xi}$ can be accepted as the analytical function of $\boldsymbol{\Xi}$ and written as:

$$\boldsymbol{\xi} = \boldsymbol{\xi}(\boldsymbol{X}, 0, t) + \frac{\partial \boldsymbol{\xi}}{\partial \boldsymbol{\Xi}} \boldsymbol{\Xi} + H.O.T. \tag{1.26}$$

Since $\boldsymbol{\xi}(\boldsymbol{X}, 0, t) = 0$ if $\boldsymbol{\Xi} = 0$, and the higher order terms (H.O.T.) are ignored, this equation reduces to

$$\boldsymbol{\xi} = \frac{\partial \boldsymbol{\xi}}{\partial \boldsymbol{\Xi}} \boldsymbol{\Xi} \tag{1.27}$$

and a micro deformation tensor is defined as:

$$\boldsymbol{\chi} \overset{def}{=} \left.\frac{\partial \boldsymbol{\xi}}{\partial \boldsymbol{\Xi}}\right|_{\boldsymbol{\Xi}=0} \Longrightarrow \boldsymbol{\xi} = \boldsymbol{\chi}\boldsymbol{\Xi} \tag{1.28}$$

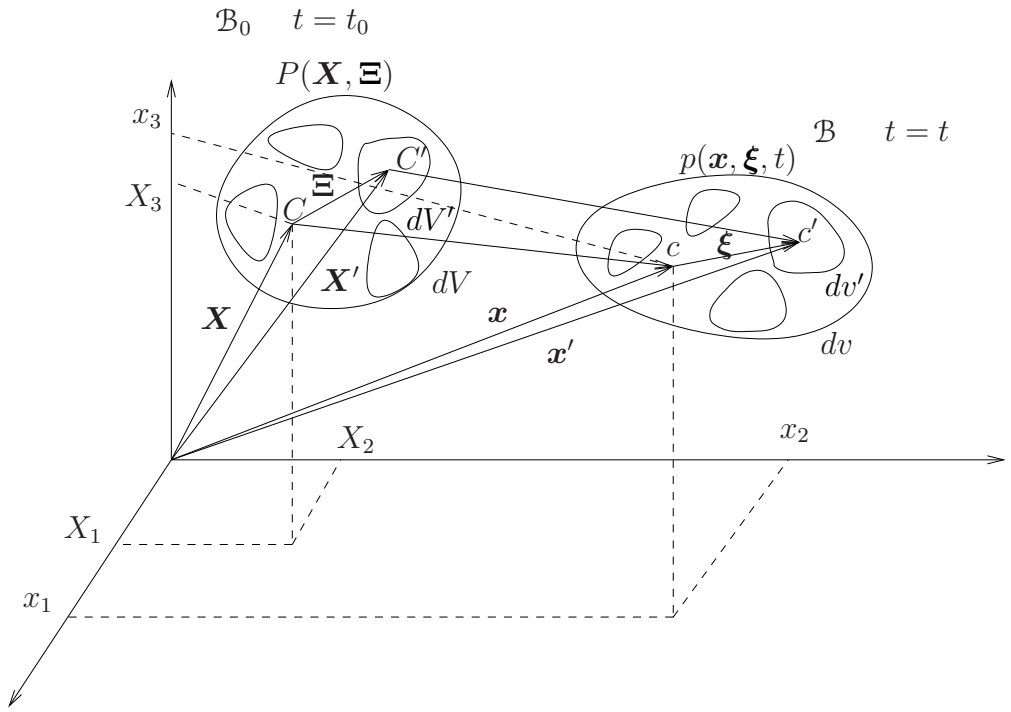

Figure 1.10: Deformation of macro differential volume and micro differential volume by Eringen (1968a).

The equation (1.28) is based on the assumption of the affine transformation of macro differential volume dV (but the overall continuum body $\mathcal{B}$ can deform heterogeneously). Then, with this assumption, the spatial position vector of the micro differential volume centroid can be written as:

$$\boldsymbol{x}'(\boldsymbol{X}, \boldsymbol{\Xi}, t) = \boldsymbol{x}(\boldsymbol{X}, t) + \boldsymbol{\xi}(\boldsymbol{X}, \boldsymbol{\Xi}, t) \tag{1.29}$$

Then, taking time derivative of the equation (1.29) by keeping $\boldsymbol{X}$ and $\boldsymbol{\Xi}$ fixed gave :

$$\dot{\boldsymbol{x}}' = \dot{\boldsymbol{x}} + \dot{\boldsymbol{\chi}}\boldsymbol{\Xi} \tag{1.30}$$

$$= \dot{\boldsymbol{x}} + \dot{\boldsymbol{\chi}}\boldsymbol{\chi}^{-1}\boldsymbol{\xi} \tag{1.31}$$

$$\boldsymbol{v}' = \boldsymbol{v} + \boldsymbol{\nu}\boldsymbol{\xi} \tag{1.32}$$

where

$$\boldsymbol{\nu} = \dot{\boldsymbol{\chi}}\boldsymbol{\chi}^{-1} \tag{1.33}$$

where $\boldsymbol{v}'$ is the velocity vector of the micro differential volume in the current configuration, $\boldsymbol{v}$ is the mean velocity vector of the macro differential volume in the current configuration, and $\boldsymbol{\nu}$ is the micro-gyration tensor. Similarly, the acceleration vector $\boldsymbol{a}'$ for micro differential volume was defined by taking the second time derivative of the displacement field as:

$$\boldsymbol{a}' = \ddot{\boldsymbol{x}}' = \ddot{\boldsymbol{x}} + \ddot{\boldsymbol{\chi}}\boldsymbol{\chi}^{-1}\boldsymbol{\xi} + \dot{\boldsymbol{\chi}}\dot{\boldsymbol{\chi}}^{-1}\boldsymbol{\xi} + \dot{\boldsymbol{\chi}}\boldsymbol{\chi}^{-1}\dot{\boldsymbol{\xi}} \tag{1.34}$$

$$\boldsymbol{a}' = \boldsymbol{a} + (\dot{\boldsymbol{\nu}} + \boldsymbol{\nu}\boldsymbol{\nu})\,\boldsymbol{\xi} \tag{1.35}$$

The deformation measures which were constructed to be invariant under the rigid body motions were defined in Cartesian coordinates as:

$$C_{KL} = x_{k,K}x_{k,L}\,, \qquad \Psi_{KL} = x_{k,K}\chi_{kL}\,, \qquad \Gamma_{KLM} = x_{k,K}\chi_{kL,M} \tag{1.36}$$

where $x_{k,K} = \frac{\partial x_k}{\partial X_K}$. This set of deformation measures can be found by calculating the square of the deformed arc length starting from writing the incremental form of the equation (1.29) as (Suhubi and Eringen (1964); Eringen (1999)):

$$dx'_k = x_{k,K}dX_K + \chi_{kK}d\Xi_K + \chi_{kK,L}\Xi_K dX_L \tag{1.37}$$

the square of the arc length in the current configuration is:

$$\begin{aligned}(ds')^2 = dx'_k dx'_k = [&x_{k,K}x_{k,L} + 2(x_{k,K}\chi_{k,L} + x_{k,L}\chi_{kM,K})\Xi_M \\ &+\chi_{kM,K}\chi_{kN,L}\Xi_M\Xi_N]\,dX_K dX_L \\ &+2(x_{k,K}\chi_{kL} + \chi_{kL}\chi_{kM,K}\Xi_M)dX_K d\Xi_L + \chi_{kK}\chi_{kL}d\Xi_K d\Xi_L\end{aligned} \tag{1.38}$$

where $\chi_{kL} = \Psi_{KL} X_{K,k}$ and $\chi_{kL,M} = \Gamma_{KLM} X_{K,k}$. If the deformation measures defined in the equation (1.36) are inserted in the equation (1.38), it becomes:

$$\begin{aligned}(ds')^2 = &\left(C_{KL} + 2\Xi_M \Gamma_{KML} + \Xi_M \Xi_N \Gamma_{PML} \Gamma_{RNK} C^{-1}_{PR}\right) dX_K dX_L \\ &+ 2\left(\Psi_{KL} + \Xi_M \Psi_{NL} \Gamma_{RMK} C^{-1}_{NR}\right) d\Xi_K dX_L \\ &+ \Psi_{MK} \Psi_{NL} C^{-1}_{MN} d\Xi_K d\Xi_L \end{aligned} \tag{1.39}$$

where $C^{-1}_{KL} = X_{K,k} X_{L,k}$. It is seen from the equation (1.39) that the arc length can be expressed in terms of the deformation measures defined in the equation (1.36). The different deformation measures have been defined by different authors (Eringen and Suhubi (1964); Suhubi and Eringen (1964); Sansour (1998); Forest and Sievert (2003, 2006)) for the various constitutive assumptions. We will use the set in Suhubi and Eringen (1964) which comprise one distinct set.

In order to obtain the local balance of momenta at mass center of the macro differential volume at deformed configuration, Eringen and Suhubi (1964) multiplied the Cauchy's law of motion with the two weight functions separately and integrated it over the macro differential volume (details about deriving the balance equations and approach will be given in section 2.2). It resulted in the two balance equations; (i) the well known balance of linear momentum, and (ii) the balance of first moment of momentum. They may be given in the Cartesian coordinate system as:

$$\sigma_{lk,l} + \rho(f_k - a_k) = 0 \tag{1.40}$$

$$\sigma_{ml} - s_{ml} + m_{klm,k} + \rho(\lambda_{lm} - \omega_{lm}) = 0 \tag{1.41}$$

where σ_{lk} are the components of the unsymmetric Cauchy stress, ρ is the mass density, f_k are the components of the body force vector per unit mass, a_k are the components of the acceleration vector per unit mass, s_{ml} are the components of the symmetric micro-stress tensor, m_{klm} are the components of the higher order couple stress, λ_{lm} are the components of the body force couple tensor per unit mass, ω_{lm} are the components of the micro-spin

inertia tensor per unit mass. This research is following the method of Eringen and Suhubi (1964) in application of the finite strain plasticity approach proposed by Regueiro (2010), therefore, the balance equations will be visited separately in the next chapters while giving the detail on the finite strain elasticity equations.

Germain (1973) provided a new approach in determining the balance equations of the generalized continua by implementing the classical method of virtual work principle. The method presented that the virtual power method can be a short way and an applicable tool besides the conventional methods used by other researchers in the literature. He mentioned that the significant point in constructing a continuum theory is to choose the kinematics relations which will be used in the virtual power method. In his work, Germain assumed that there was a continuum particle point $P(M)$ of small extent with the mass center M, then there exist a point M' in the $P(M)$. The coordinates of M and M' were denoted by $\boldsymbol{x}$ and $\boldsymbol{x}'$ respectively. The velocity of the M was shown by U_i and the velocity of M' was shown by U_i' . Taylor expansion of U_i' with respect to $\boldsymbol{x}'$ was given for the first order approximation as:

$$U_i' = U_i + \chi_{ij} x_j' \tag{1.42}$$

where χ_{ij} is the gradient of the relative velocities of $P(M)$. The relative microvelocity, η_{ij}, and the gradient of the microdeformation tensor, $\varkappa_{ijk}$, were defined similarly by Mindlin (1964)'s approach but in terms of gradient of the velocities as:

$$\eta_{ij} = U_{i,j} - \chi_{ij} \,, \qquad \varkappa_{ijk} = \chi_{ij,k} \tag{1.43}$$

By choosing the independent kinematic fields as U_i and χ_{ij}, and the first gradient theory which indicates that the first gradients of the chosen fields with their work conjugate stresses will be also in the virtual power density, the virtual power of the internal forces, $\mathcal{P}_{(int)}$, was consisting of the linear combination of the set $U_{i,j}, \eta_{ij}, \varkappa_{ijk}$ and their work conjugates $\sigma_{ij}, s_{ij}, \nu_{ijk}$ respectively. Then, omitting the details, the virtual power of the internal forces

in the domain D was expressed as:

$$\mathcal{P}_{(int)} = \int_D \left\{ (\sigma_{ij} + s_{ij})\, U_{i,j} - s_{ij}\chi_{ij} + \nu_{ijk}\varkappa_{ijk} \right\} dv \tag{1.44}$$

Then, the virtual power of external forces was introduced as:

$$\mathcal{P}_{(ext)} = \int_D \left(f_i U_i + \Psi_{ij}\chi_{ij} \right) dv \tag{1.45}$$

and the virtual power of the contact forces was also expressed as:

$$\mathcal{P}_{(cont)} = \int_S \left(T_i U_i + M_{ij}\chi_{ij} \right) dA \tag{1.46}$$

where f_i are the components of the body force vector, σ_{ij} are the components of the intrinsic part of the stress tensor, s_{ij} are the components the microstress tensor, ν_{ijk} are the components of the second microstress tensor, Ψ_{ij} are called the components of a volumetric body force couple, M_{ij} are the components of a double force traction tensor, and T_i are the components the traction vector. The power of the internal forces should be equal to the summation of the power of the external and the contact forces as :

$$\mathcal{P}_{(int)} = \mathcal{P}_{(ext)} + \mathcal{P}_{(cont)} \tag{1.47}$$

For arbitrary variations of U_i and χ_{ij} , one can get the equations below:

$$\tau_{ij} = \sigma_{ij} + s_{ij} \tag{1.48}$$

$$\tau_{ij,j} + f_i = 0 \tag{1.49}$$

$$s_{ij} + \nu_{ijk,k} + \Psi_{ij} = 0 \qquad \text{or} \qquad \tau_{ij} - \sigma_{ij} + \nu_{ijk,k} + \Psi_{ij} = 0 \tag{1.50}$$

with boundary conditions

$$T_i = \tau_{ij} n_j \tag{1.51}$$

$$M_{ij} = \nu_{ijk} n_k \tag{1.52}$$

where $\boldsymbol{\tau}$ is the Cauchy stress tensor. In summary, if we compare all these three methods, we see that although the balance equations obtained by these three authors are including the

higher order stress tensors and/or microstress tensors as a result of accounting for micro-continuum, the resulting balance equations are different. Mindlin (1964) applied Hamilton's principle to derive the governing equations and assumed a potential energy density which depends on the deformation measures that he chose. Then, he defined the stresses as the partial derivative of the potential energy function. However, Germain (1973) applied the virtual power method and found different field equations depending on the different stress tensors than those of Mindlin. On the other hand, Eringen and Suhubi (1964) wrote balance equations for microfield and applied an integral averaging method with a variational approach to obtain the macro continuum field equations. As forementioned, the micro-stress tensor, the higher order couple stress tensor, Cauchy stress tensor, body force per unit mass tensor and micro spin inertia tensor were given in integral form by Eringen and Suhubi (1964). Defining especially the macro stress tensors in integral form provides an insight for physical meanings of these tensors which are based on the micro field parameters.

Lastly, we may summarize some of the recent research on micromorphic continua very briefly. Sansour (1998) modified the strain measure set used by Eringen and his co-workers to be invariant with respect to not translations but rotations only. Sansour introduced the constitutive laws in the microstructure scale and introduced an approach for modeling finite strain viscoplasticity. He obtained higher order stress tensors with some integral averaging definitions of microstructure which were assumed to be computed numerically. However, Sansour did not carry his work on a detailed formulation of micromorphic elastoviscoplastic constitutive model.

Vernerey et al. (2007) applied a multiscale micromorphic model for hierarchical materials. They followed the approach of Mindlin (1964) and Germain (1973). The theory considered the material in different scales depending on the variations in its inherent microstructure such as mass density variation at different I scales. The assumed virtual power density was a linear combination of velocity of macroscale, velocity differences between macro and microscale, and velocity gradient of microscale. The work conjugate to these measures

were defined respectively as the macrostress, the microstress, and the microstress couple which were defined in a statistical averaging manner. Having I different scales, the virtual power density involves a summation of velocity differences between macro and each Ith micro scale and velocity gradient each Ith microscale. The first governing equation in which the summation of the microstresses are subtracted from the macrostress reduces to the well known balance of linear momentum if these microstresses are ignored. The second governing equation was expressed as the local equilibrium between microstresses and written for each microscale separately.

Lee and Chen (2003) formulated the constitutive equations for micromorphic thermoplasticity using the Eringen and Suhubi (1964)'s kinematics and balance laws. Their work was different than that of Regueiro (2009, 2010) in a sense that they applied entropy inequality in Lagrangian form and used Lagrangian definitions of the strain tensors and their time rates as well as temperature and its spatial and time derivatives rather than utilizing multiplicative kinematics and intermediate configuration.

Forest and Sievert (2003, 2006) reviewed the models for generalized continua. Forest and Sievert (2003) constructed a framework for elastoviscoplastic constitutive modeling of generalized continua. They applied virtual power method in formulating the balance equations as Germain (1973). They used different invariant deformation measures than the set proposed by Eringen (1999) and also used by Regueiro (2010, 2009) which will be followed in this research.

The research on the generalized continuum theories in the both higher order continua and higher grade continua is still on going. Since our interest is on the micromorphic continuum, we do not review the higher grade continuum theories here. However, for the higher grade continua, the strain gradient methods for elastic and inelastic application have been done by the many authors. Some examples on higher grade media can be given as Mindlin and Eshel (1968); Ramaswamy and Aravas (1998); Zervos et al. (2001, 2009); Chambon et al. (2004, 2001b,a); Tamagnini et al. (2001); Matsushima et al. (2000); Voyiadjis and Al-Rub

(2005); Forest and Sievert (2006, 2003).

Forest and Sievert (2006) gave some guidelines based on the previous research done in literature to choose the proper higher order continuum or higher grade continuum in modeling material response. According to Forest and Sievert (2006) and references therein, use of microdilatation theory which is including only one additional degree of freedom may be an efficient way in modeling the material in which the microvolume changes are important. If the rotation effects are dominant, as mentioned in previous sections, the Cosserat continuum (or Micropolar) can be applied to simulate the material behavior. The microstretch theory, on the other hand, was found to be applicable in modeling deformations of biomaterials. The microstrain theory was candidated in order to model the strain localization in metallic foams where the other higher order continuum models are neither appropriate nor sufficient.

Some of the recent works are: Sansour et al. (2010) presented a formulation for the micromorphic continuum at finite strains inelasticity by following his previous work (Sansour, 1998) that is within viscoplasticity concept. In his work, he specifically mentioned the importance of choice of additional degrees of freedom; Zhang et al. (2011b) presented a small strain micromorphic mixed hardening plasticity model to capture the size effect and Bauschinger effect in cyclic response of thin films; Zhang et al. (2011a) used to same approach to analyze the wedge indention of a thin film on a substrate by using elasto-plasticity;Grammenoudis et al. (2009) and Grammenoudis et al. (2010),respectively, demonstrated the theoretical formulation of finite deformation plasticity a micrmorphic continuum coupled with damage and small deformation plasticity coupled with damage, together with the implementation.

1.4 Determining the Micromorphic Material Parameters

Apparently, one of the main issues in implementation will be the determination of the additional micromorphic material parameters. To determine the micromorphic parameters, it may be possible to make use of the underlying DNS domain by assuming that the micromorphic continuum FE and underlying DNS synthetic domain are initially completely

overlapped. The material parameters of DNS domain can be determined by using existing experimental data or some future experiments. To use this approach, various simulations on the DNS domain may be performed and micromorphic continuum homogenization (Figure 1.11) can be utilized to calculate stresses and deformation. Then, having the stresses and deformation, we may be able to do an inverse analysis to fit the micromorphic parameters. The micromorphic homogenization formula is expressed below to express how to relate a micro-scale field parameter to its corresponding micromorphic continuum field parameter by using a weighted average of a micro-scale field given below.

$$\boldsymbol{a}^m \overset{\text{def}}{=} \langle \boldsymbol{a}^{micro} \rangle \overset{\text{def}}{=} \frac{1}{\upsilon^{\omega,avg}} \int_{\upsilon^{\omega,avg}} \omega\left(r,\theta,\vartheta\right) \boldsymbol{a}^{micro} dv \tag{1.53}$$

where $\boldsymbol{a}^m$ is a micromorphic continuum scale field, $\boldsymbol{a}^{micro}$ is the corresponding micro-scale field, $\langle . \rangle$ shows the averaging operator, $\upsilon^{\omega,avg} \overset{\text{def}}{=} \int_{\Omega^{avg}} \omega\left(r,\theta,\vartheta\right) dv$ is the weighted average current volume, $\omega\left(r,\theta,\vartheta\right)$ is the kernel function, $\boldsymbol{\xi}$ is the relative position vector within the the macro-element with respect to its centroid, Ω^{avg} is the micro-scale domain. In the equation (1.53), the left hand side will be equal to the micromorphic parameter.

Another approach proposed by Vernerey et al. (2007) may be also applicable to determine these parameters. As mentioned in the previous section, they have multiple scales in their work. In determination of the elasticity constants, they introduced also the meso-scale in the transition of the macro-scale and micro-scale. They applied an integral averaging approach to micro-scale fields in the meso-scale domain to obtain the elasticity constants. This approach may be utilized in DNS micro-scale domain a similar way to determine integral averaged elasticity constants. Then, they can be assigned to the micromorphic elasticity constants.

1.5 Novel Contributions of This Research

The main contribution of this research is that we developed a finite strain linear isotropic elastoplastic model which is based on the most general case of the higher order

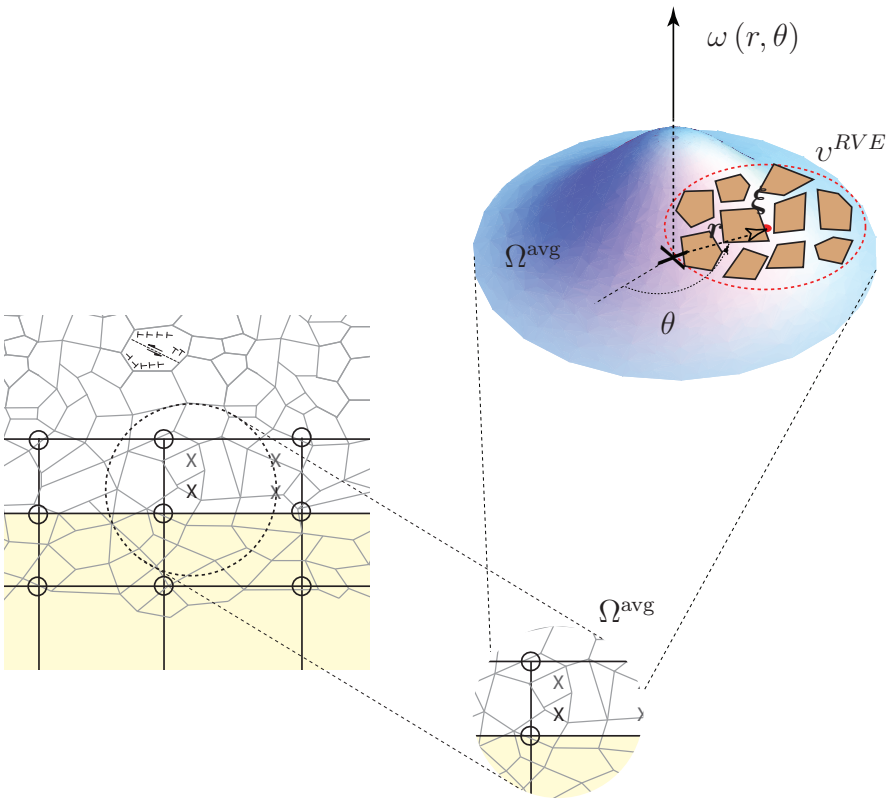

Figure 1.11: Two-dimensional illustration of micromorphic continuum homogenization of micro-scale response at a Gauss integration point x in the overlap region

continua (micromorphic continuum) and implemented it into the open source finite element code "Tahoe". These contributions will enable future researchers to resolve the issues about the artificial boundary condition influence on the numerical simulations in the coupling/overlapping/handshaking region. To determine the necessary parameters appearing in the theory, we considered the positiveness of the strain energy and related the additional elastic moduli to the existing elastic Lamé parameters as proposed by other researchers in literature. We investigated the proper boundary conditions to be used on the micro-field. Then, it is expected to be computationally possible to make use of this higher order continuum theory to be used in the proposed concurrent multiscale context aforementioned above. This will allow us to model the problems in engineering science by allowing multiscale methods to reduce the computational cost associated with attempting to predict at the grain-scale, the

interfacial mechanics problem (deformable solid and particulate material) and/or localized deformation in particulate materials.

Table 1.2: Notations used in this work

Notations	Definitions
$\boldsymbol{u}$	displacement vector
$\boldsymbol{\Phi}$	micro-displacement tensor
$\boldsymbol{\chi}$	micro-deformation tensor
$\boldsymbol{\sigma}$	unsymmetric Cauchy stress tensor in current configuration
$\boldsymbol{S}$	Second Piola Kirchhoff tensor in reference configuration
$\bar{\boldsymbol{S}}$	Second Piola Kirchhoff tensor in intermediate configuration
$\boldsymbol{s}$	symmetric micro stress tensor in current configuration
$\boldsymbol{\Sigma}$	symmetric micro stress tensor in reference configuration
$\bar{\boldsymbol{\Sigma}}$	symmetric micro stress tensor in intermediate configuration
$\boldsymbol{m}$	higher order couple stress tensor in current configuration
$\boldsymbol{M}$	higher order couple stress tensor in reference configuration
$\bar{\boldsymbol{M}}$	higher order couple stress tensor in reference configuration
	body force vector per unit mass
$\boldsymbol{a}$	acceleration vector per unit mass
$\boldsymbol{\lambda}$	body force couple tensor per unit mass
$\boldsymbol{\omega}$	micro-spin inertia per unit mass
n_{el}	number of elements
n^{u}_{en}	number of elements nodes for $\boldsymbol{u}$
n^{χ}_{en}	number of elements nodes for $\boldsymbol{\chi}$
n_{sd}	number of spatial dimensions
N^{u}_{a}	shape functions associated with $\boldsymbol{u}$
$\boldsymbol{grad}\,(\boldsymbol{N}^{u})$	gradient of $\boldsymbol{N}^{u}$ in current configuration
$\boldsymbol{GRAD}\,(\boldsymbol{N}^{u})$	gradient of $\boldsymbol{N}^{u}$ in reference configuration
N^{χ}_{a}	shape functions associated with $\boldsymbol{\chi}$
$\boldsymbol{grad}\,(\boldsymbol{N}^{\chi})$	gradient of $\boldsymbol{N}^{\chi}$ in current configuration
$\boldsymbol{GRAD}\,(\boldsymbol{N}^{\chi})$	gradient of $\boldsymbol{N}^{\chi}$ in reference configuration
$div\,(.)$	divergence operator
$\delta\,(.)$	variation operator
$\lambda, \mu, \tau, \eta, \sigma, \kappa, \nu$	elastic material moduli in micromorphic continuum
$\tau_1, \tau_2, \tau_3, \tau_4, \tau_5, \tau_6, \tau_7, \tau_8, \tau_9, \tau_{10}, \tau_{11}$	elastic parameters in micromorphic continuum
λ^*, μ^*	Lamé parameters
e	element number
$n^{u,e}_{dof} = n_{sd} * n^{u}_{en}$	number of element degrees of freedom $\boldsymbol{u}$
$n^{\chi,e}_{dof} = n_{sd} * n_{sd} * n^{\chi}_{en}$	number of element degrees of freedom $\boldsymbol{\chi}$

Chapter 2

Finite Strain Micromorphic Elasticity

In this chapter, we review the theory of finite strain micromorphic elasticity proposed by the authors Eringen and Suhubi (1964) in detail. We start with kinematics, then we review the balance equations and thermodynamics. Constitutive equations for material linear isotropic elasticity at finite strain and their maps into current configuration will be presented afterward. Then, we consider the positive definiteness of the strain energy and how this condition introduces the restrictions on the elastic moduli of a micromorphic continuum. This chapter ends with the simplification of the model to small strain micropolar elasticity.

2.1 Kinematics

In Chapter 1, we summarized the kinematics for the finite strain micromorphic elasticity given by Eringen and Suhubi (1964). We go through the kinematics mentioned in the previous section and give more details about derivation of the terms in the theory actually proposed by the authors Eringen and Suhubi (1964); Suhubi and Eringen (1964); Eringen (1968a, 1999).

Eringen (1999) explains the kinematics of the micromorphic continuum as follows: Let a material point P (macroelement) have the centroid P_1 which have a position vector $\boldsymbol{X}$ in a body consisting of deformable particles and some vectors attached to this point which are accounting for the inherent structure (microelements) of the body and denoted by $\boldsymbol{\Xi}_\alpha$, $\alpha = 1, 2, ..., N$. Eringen (1999) defined this medium as microcontinuum with *grade* N and

he classified all the microfield theories; micromorphic, micropolar, and microstrech theories as the microcontinuum field theories of grade 1 ($\alpha = 1$). The material point $P(\boldsymbol{X}, \boldsymbol{\Xi})$ was defined with its centroid C and the vectors attached to this point $\boldsymbol{\Xi}$ in reference configuration. The motion maps this material point $P(\boldsymbol{X}, \boldsymbol{\Xi})$ and $\boldsymbol{\Xi}$ respectively, to $p(\boldsymbol{x}, t)$ and $\boldsymbol{\xi}(\boldsymbol{X}, \boldsymbol{\Xi}, t)$ and the centroid, C, to the centroid, c, of the deformed element in the spatial configuration. Then, the macromotion which is mapping the macroelement in reference configuration to macroelement in spatial configuration, and the micromotion which is mapping the microelement in reference configuration into microelement in spatial configuration were defined, respectively, as (Eringen (1999)):

$$\boldsymbol{X} \rightarrow \boldsymbol{x} = \boldsymbol{x}(\boldsymbol{X}, t) \tag{2.1}$$

$$\boldsymbol{\Xi} \rightarrow \boldsymbol{\xi} = \boldsymbol{\xi}(\boldsymbol{x}, \boldsymbol{\Xi}, t) \tag{2.2}$$

The micromotion was approximated with a linear expansion of $\boldsymbol{\Xi}$ that is called affine (or homogenous) deformation. This is a valid assumption considering the size of the microelements which is assumed to be very small compared to that of macroelement. As mentioned in previous chapter, this assumption yields the first degree approximation of Taylor's expansion of $\boldsymbol{\Xi}$ where we rewrite equation (1.28) in indicial notation and in terms of $\boldsymbol{X}$ and t as:

$$\xi_k = \chi_{kK}(\boldsymbol{X}, t)\, \Xi_K \tag{2.3}$$

where $k = 1, 2, 3$ and $K = 1, 2, 3$. The relative position vectors $\boldsymbol{\Xi}$ and $\boldsymbol{\xi}$ are defined as the relative position of the center of microelements, respectively, C' and c' with respect to maco-element centroids (Figure 1.10). Then, the position vector of a point (previously given in equation (1.29)) in the particle in deformed configuration was defined in terms of $\boldsymbol{X}, \boldsymbol{\Xi}$ and t as:

$$\boldsymbol{x}'(\boldsymbol{X}, \boldsymbol{\Xi}, t) = \boldsymbol{x}(\boldsymbol{X}, t) + \boldsymbol{\xi}(\boldsymbol{X}, \boldsymbol{\Xi}, t)$$

The motions given by equations (2.3) and (2.1) have unique inverse motions defined by:

$$X_K = X_K(\boldsymbol{x}, t) \tag{2.4}$$

$$\Xi_K = \mathfrak{X}_{Kk}(\boldsymbol{x}, t)\,\xi_k \tag{2.5}$$

where $k, K = 1, 2, 3$. Having a unique inverse of the both motions indicates continuity and no matter loss. Then, if we substitute equation (2.5) in equation (2.3), we get:

$$\xi_k = \chi_{kK}\mathfrak{X}_{Kl}\xi_l \tag{2.6}$$

then from the equation above, someone can get:

$$\chi_{kK}\mathfrak{X}_{Kl} = \delta_{kl} \tag{2.7}$$

and similarly we can find

$$\mathfrak{X}_{Kk}\chi_{kL} = \delta_{KL} \tag{2.8}$$

To show the derivation of material time derivatives of the kinematic terms, we start with the gyration tensor given in equation (1.33) as:

$$\nu_{kl} = \dot{\chi}_{kK}\mathfrak{X}_{Kl} \tag{2.9}$$

Then, multiplying both sides with χ_{lL}, we get:

$$\nu_{kl}\chi_{lL} = \dot{\chi}_{kK}\mathfrak{X}_{Kl}\chi_{lL} \tag{2.10}$$

$$\nu_{kl}\chi_{lL} = \dot{\chi}_{kK}\delta_{KL} \tag{2.11}$$

it gives:

$$\dot{\chi}_{kL} = \nu_{kl}\chi_{lL} \tag{2.12}$$

and material time derivative of the equation (2.7) is:

$$\dot{\chi}_{kK}\mathfrak{X}_{Lk} + \chi_{kK}\dot{\mathfrak{X}}_{Lk} = 0 \tag{2.13}$$

If we multiply this equation with $\mathfrak{X}_{Km}$, we get;

$$\dot{\chi}_{kK}\mathfrak{X}_{Lk}\mathfrak{X}_{Km} + \chi_{kK}\dot{\mathfrak{X}}_{Lk}\mathfrak{X}_{Km} = 0 \tag{2.14}$$

and applying equation (2.12) gives:

$$\nu_{kl}\chi_{lK}\mathfrak{X}_{Lk}\mathfrak{X}_{Km} + \chi_{kK}\dot{\mathfrak{X}}_{Lk}\mathfrak{X}_{Km} = 0 \tag{2.15}$$

it can be found as:

$$\dot{\mathfrak{X}}_{Lm} = -\nu_{km}\mathfrak{X}_{Lk} \tag{2.16}$$

If we take the material time derivative of (2.3) and apply the equation (2.12), we get $\dot{\boldsymbol{\xi}}$ as:

$$\dot{\xi}_k = \dot{\chi}_{kK}\Xi_K \tag{2.17}$$

$$\dot{\xi}_k = \nu_{kl}\chi_{lK}\Xi_K \tag{2.18}$$

then, $\dot{\boldsymbol{\xi}}$ can be found as:

$$\dot{\xi}_k = \nu_{kl}\xi_l \tag{2.19}$$

The velocity and acceleration of the microfield have been already expressed in equations (1.32) and (1.35) respectively. The mass of the macro-elements have been expressed in terms of the integral sum of the microelements in equation (1.24) in previous chapter. The microelement and macro-element masses were assumed to be conserved during the deformation and expressed respectively as:

$$\rho_0' dV' = \rho' dv', \qquad \rho_0 \iota_{kl} dV = \rho dv \tag{2.20}$$

and principal of conservation of mass in current configuration can be expressed by:

$$\frac{D\left(\rho dv\right)}{Dt} = 0, \quad \text{or} \qquad \frac{\partial \rho}{\partial t} + \left(\rho v_k\right)_{,k} = 0 \tag{2.21}$$

The relative position vectors $\boldsymbol{\Xi}$ and $\boldsymbol{\xi}$ also were given to satisfy the expressions below which are the first moment of the micro-elements with respect to centroids of the macroelements, respectively, in deformed and undeformed configurations.

$$\int_{dV} \rho_0' \boldsymbol{\Xi} dV' = 0, \qquad \int_{dv} \rho' \boldsymbol{\xi} dv' = 0 \tag{2.22}$$

The second moments of $\rho_0' dV'$ and $\rho' dv'$ were given by:

$$\rho_0 I_{KL} dV = \int_{dV} \rho_0' \Xi_K \Xi_L dV', \qquad \rho_0 dv = \int_{dv} \rho' \xi_k \xi_l dv' \tag{2.23}$$

The displacement field of macrocontinuum can be defined with well know definition in continuum mechanics as:

$$x_{k,K} = X_{k,K} + u_{k,K} \tag{2.24}$$

$$x_{k,K} = (\delta_{LK} + U_{L,K})\, \delta_{kL} \tag{2.25}$$

Eringen (1968b) proposed a similar definition for the microdisplacement tensor, $\Phi_{LK}(\boldsymbol{X}, t)$, and explained the details on the kinematics as follows :

$$\chi_{kK} = (\delta_{LK} + \Phi_{LK})\, \delta_{kL} \tag{2.26}$$

then, he inserted equations (2.25) and (2.26) into the deformation measures given in equation (1.36) and obtained deformation measures in terms of macro and micro displacements as:

$$C_{KL} = \delta_{KL} + U_{K,L} + U_{L,K} + U_{M,K} U_{M,L} \tag{2.27}$$

$$\Psi_{KL} = \delta_{KL} + \Phi_{KL} + U_{L,K} + U_{M,K} \Phi_{ML} \tag{2.28}$$

$$\Gamma_{KLM} = \Phi_{KL,M} + U_{N,K} \Phi_{NL,M} \tag{2.29}$$

Although we use finite strain measures in the analysis, it will be useful to show how they reduce to small strain elasticity by ignoring the higher order terms that gives a linear approximation to the equations above as:

$$C_{KL} \approx \delta_{KL} + U_{K,L} + U_{L,K} \tag{2.30}$$

$$\Psi_{KL} \approx \delta_{KL} + \Phi_{K,L} + U_{L,K} \tag{2.31}$$

$$\Gamma_{KLM} \approx \Phi_{KL,M} \tag{2.32}$$

the linearized strain tensors E_{KL},$\mathcal{E}_{KL}$, and Γ_{KLM} may be defined based on equations from (2.30) to (2.32) as:

$$E_{KL} = \frac{1}{2}\left(C_{KL} - \delta_{KL}\right) = \frac{1}{2}\left(U_{K,L} + U_{L,K}\right) \tag{2.33}$$

$$\mathcal{E}_{KL} = \Psi_{KL} - \delta_{KL} = \Phi_{KL} + U_{L,K} \tag{2.34}$$

$$\Gamma_{KLM} = \Phi_{KL,M} \tag{2.35}$$

Then, these linearized strain measures given in equations (2.33),(2.34), and (2.35) take the forms below in current configuration.

$$e_{kl} = \frac{1}{2}\left(u_{k,l} + u_{l,k}\right) \tag{2.36}$$

$$\epsilon_{kl} = \phi_{kl} + u_{l,k} \tag{2.37}$$

$$\gamma_{klm} = -\phi_{kl,m} \tag{2.38}$$

These linearized strain tensors in reference and current configuration will be used, respectively, in Section 2.6 to show simplification of constitutive equations of a micromorphic small strain elasticity to that of small strain micropolar elasticity, and in Section 2.5 to express the restrictions on the elastic material moduli of a micromorphic continuum.

Remember the square of the arc length in current configuration was expressed in equation (1.38), the square of the arc length in reference configuration can be also found as:

$$\begin{aligned}\left(dS'\right)^2 &= d\boldsymbol{X}' \cdot d\boldsymbol{X}' \\ &= \left(dX_K + d\Xi_K\right)\left(dX_K + d\Xi_K\right)\end{aligned} \tag{2.39}$$

$$\left(dS'\right)^2 = \delta_{KL} dX_K dX_L + 2\delta_{KL} dX_K \Xi_L + \delta_{KL} d\Xi_K d\Xi_L \tag{2.40}$$

the difference between the squares of arc lengths in reference and current configuration follow from equation (1.38) and equation (2.40):

$$\begin{aligned}\left(ds'\right)^2 - \left(dS'\right)^2 = &\left(2E_{KL} + 2\Xi_M \Gamma_{KML} + \Xi_M \Xi_N \Gamma_{PML} \Gamma_{RNK} C^{-1}_{PR}\right) dX_K dX_L \\ &+ 2\left(\mathcal{E}_{KL} + \Xi_M \Psi_{NL} \Gamma_{RMK} C^{-1}_{NR}\right) d\Xi_M dX_L \\ &+ \left(\Psi_{MK} \Psi_{NL} C^{-1}_{MN} - \delta_{KL}\right) d\Xi_K d\Xi_L\end{aligned} \tag{2.41}$$

For the linear theory, this equation reduces to :

$$\begin{aligned}(ds')^2 - (dS')^2 \approx\ & 2\left(E_{KL} + \Xi_M \Gamma_{KML}\right) dX_K dX_L \\ & + 2\left(\mathcal{E}_{KL} + \Gamma_{LMK}\Xi_M\right) d\Xi_M dX_L \\ & + \left(\mathcal{E}_{KL} + \mathcal{E}_{LK} - 2E_{KL}\right) d\Xi_K d\Xi_L \end{aligned} \tag{2.42}$$

It can be easily seen that when $E_{KL} = \mathcal{E}_{KL} = 0$ and $\Gamma_{KLM} = 0$, it represents the rigid body motion since no change in arc length will occur associated with the deformation.

2.2 Balance Equations and Thermodynamics

This section is devoted to balance equations of a micromorphic continuum and the stress definitions appearing in these equations. To obtain the balance of momenta, Eringen and Suhubi (1964) started with the local form of balance of momentum and angular momentum, respectively, at a point in a micro-element in deformed configuration as:

$$\sigma'_{kl,k} + \rho'\left(f'_l - a'_l\right) = 0 \tag{2.43}$$

$$\sigma'_{kl} = \sigma'_{lk} \tag{2.44}$$

where σ'_{kl} is the Cauchy stress tensor for micro element, f'_l and a'_l are the body force vector per unit mass over the micro-element and acceleration respectively. They multiplied equation (2.43) by a function $\varphi' \overset{def}{=} \varphi'(\boldsymbol{x}')$ and integrated over the volume v. The function $\varphi'(\boldsymbol{x}')$ was assumed for special cases (1) $\varphi' = 1$ and (2) $\varphi' = x'_m = x_m + \xi_m$ as mentioned in chapter one, choosing $\varphi' = 1$ gave:

$$\int_v \left[\int_{dv} \sigma'_{kl,k}\varphi' dv' + \int_v \rho'\left(f'_l - a'_l\right)\varphi' dv'\right] dv = 0 \tag{2.45}$$

and apply

$$\sigma'_{kl,k}\varphi' = \left(\sigma'_{kl}\varphi'\right)_{,k} - \sigma'_{kl}\varphi'_{,k} \tag{2.46}$$

if equation (2.46) is inserted into (2.45), we get:

$$\int_v \left[\int_{dv} \left(\left(\sigma'_{kl}\varphi'\right)_{,k} - \sigma'_{kl}\varphi'_{,k} \right) dv' + \int_{dv} \rho' \left(f'_l - a'_l\right) \varphi' dv' \right] dv = 0 \tag{2.47}$$

$$\int_s \left[\int_{da} \sigma'_{kl}\varphi' n'_k da' \right] da + \int_v \left[\int_{dv} \left(-\sigma'_{kl}\varphi'_{,k} + \rho' \left(f'_l - a'_l\right) \varphi' \right) dv' \right] dv = 0 \tag{2.48}$$

$$\int_s \sigma_{kl} n_k da + \int_v \rho \left(f_l - a_l\right) dv = 0 \tag{2.49}$$

where

$$\int_{da} \sigma'_{kl} n'_k da' \overset{def}{=} \sigma_{kl} n_k da, \qquad \int_{dv} \rho' f'_l dv' \overset{def}{=} \rho f_l dv, \qquad \int_{dv} \rho' a'_l dv' \overset{def}{=} \rho a_l dv \tag{2.50}$$

Now, chose $\varphi' = x'_m = x_m + \xi_m$

$$\int_v \left[\int_{dv} \sigma'_{kl,k} x'_m dv' + \int_{dv} \rho' \left(f'_l - a'_l\right) x'_m dv' \right] dv = 0 \tag{2.51}$$

$$\int_s \left(\sigma_{kl} x_m + m_{klm}\right) n_k da + \int_v \left(-s_{lm} + \rho \left(f_l - a_l\right) x_m + \rho \left(\lambda_{lm} - \omega_{ml}\right) \right) dv = 0 \tag{2.52}$$

where the definitions below were used

$$s_{ml} dv \overset{def}{=} \int_{dv} \sigma'_{ml} dv' \,, \qquad m_{klm} n_k da \overset{def}{=} \int_{da} \sigma'_{kl} \xi_m n'_k da' \tag{2.53}$$

$$\rho \lambda_{lm} dv \overset{def}{=} \int_{dv} \rho' f'_l \xi_m dv' \,, \qquad \rho \omega_{lm} dv \overset{def}{=} \int_{dv} \rho' \ddot{\xi}_l \xi_m dv' \tag{2.54}$$

The quantities; $\rho, \sigma_{kl}, f_k, a_l, s_{ml}, m_{klm}, \lambda_{ml}$, and ω_{ml} were already explained in Section 1.3. To convert surface integrals to volume integrals Eringen and Suhubi (1964) applied Green-Gauss theorem which is defined as:

$$\int_{\partial\Upsilon - \varsigma} A_k n_k da = \int_{\Upsilon - \varsigma} A_{k,k} dv + \int_{\varsigma} \left[\left[A_k\right]\right] n_k da \tag{2.55}$$

where A_k is any vector, Υ is the volume, $\partial\Upsilon$ is the surface, and ς is the surfaces, n_k is the normal to the discontinuity surface. The exclusion of discontinuity surface from volume and surface are shown respectively as:

$$\Upsilon - \varsigma \overset{def}{=} \Upsilon - \Upsilon \cap \varsigma, \qquad \partial\Upsilon - \varsigma \overset{def}{=} \partial\Upsilon - \partial\Upsilon \cap \varsigma \tag{2.56}$$

and $[[A_k]]$ denotes the jump of A_k across the discontinuity surface ς. Applying the Green-Gauss theorem to surface integrals in (2.45) and (2.52) gave:

$$\int_v \left(\sigma_{kl,k} + \rho\left(f_l - a_l\right)\right) dv - \int_{s_d} [[\sigma_{kl}]]\, n_k da = 0 \tag{2.57}$$

and

$$\int_v \left\{x_m \left[\sigma_{kl,k} + \rho\left(f_l - a_l\right)\right] + \sigma_{ml} - s_{ml} + m_{klm,k} + \rho\left(\lambda_{ml} - \omega_{ml}\right)\right\} dv - \int_{s_d} [[\sigma_{kl} x_m + m_{klm}]]\, n_k da = 0 \tag{2.58}$$

From (2.58) they got the local balance of momenta on volume v as previously mentioned in chapter one:

$$\sigma_{lk,l} + \rho(f_k - a_k) = 0 \tag{2.59}$$

$$\sigma_{ml} - s_{ml} + m_{klm,k} + \rho(\lambda_{lm} - \omega_{lm}) = 0 \tag{2.60}$$

with jump conditions on s_d :

$$[[\sigma_{kl}]]\, n_k = 0, \qquad [[\sigma_{kl} x_m + m_{klm}]]\, n_k = 0 \tag{2.61}$$

and the boundary conditions on s :

$$\sigma_{lk} n_k = t_k \tag{2.62}$$

$$m_{klm} n_k = T_{lm} \tag{2.63}$$

They followed the same approach to derive the balance law of the micromorphic continuum. The local conservation of energy at a point in deformed configuration was given as:

$$\rho' \dot{e}' = \sigma'_{kl} v'_{l,k} + q'_{k,k} + \rho' r' \tag{2.64}$$

where e' is the internal energy density, r' is the heat source per unit mass of micro-element, q'_k is the heat flux vector. Then, (2.64) was integrated over the volume v as:

$$\int_v \left[\int_{dv} \rho' \dot{e}' dv' = \int_{dv} \sigma'_{kl} v'_{l,k} dv' + \int_{dv} q'_{k,k} dv' + \int_{dv} \rho' r' dv'\right] dv \tag{2.65}$$

the internal energy density per unit mass of macro element was defined by:

$$\rho e dv \stackrel{\text{def}}{=} \int_{dv} \rho' e' dv' \tag{2.66}$$

and the left hand side of equation (2.65) was written as:

$$\int_{dv} \rho' e' dv' = \frac{D}{Dt} \int_{dv} \rho' e' dv' = \frac{D}{Dt} (\rho e dv) = \rho \dot{e} dv \tag{2.67}$$

Note that equation (2.21) was applied in equation (2.67). Similarly, heat source average per unit mass of macro-element was given by:

$$\rho r dv \stackrel{\text{def}}{=} \int_{dv} \rho' r' dv' \tag{2.68}$$

and the heat flux vector of the macro-element is:

$$\int_v \left(\int_{dv} q'_{k,k} dv' \right) = \int_s \left(\int_{ds} q'_k n'_k da' \right) = \int_s q_k n_k da \tag{2.69}$$

Then,

$$q_k n_k da \stackrel{\text{def}}{=} \int_{ds} q'_k n'_k da' \tag{2.70}$$

the second term in equation (2.65) can be written as:

$$\begin{aligned} \int_v \left(\int_{dv} \sigma'_{kl} v'_{l,k} dv' \right) dv &= \int_v \left(\int_{dv} \left(\sigma'_{kl} v'_l \right)_k dv' \right) dv - \int_v \left(\int_{dv} \sigma'_{kl,k} v'_l dv' \right) dv \\ &= \int_v \left(\int_{da} \sigma'_{kl} v'_l n_k da' \right) dv - \int_v \left(\int_{dv} \sigma'_{kl,k} v'_l dv' \right) dv \end{aligned} \tag{2.71}$$

Using equation (1.32) for microvelocity v' gives:

$$\begin{aligned} \int_v \left(\int_{dv} \sigma'_{kl} v'_{l,k} dv' \right) dv &= \int_v \left(\int_{dv} \rho' \left(a'_k - f'_k \right) \left(v_l + \nu_{lm} \xi_m \right) dv' \right) dv \\ &= \int_v \left(\rho \left(a_k - f_k \right) v_l + \rho \nu_{lm} \left(\lambda_{lm} - \omega_{lm} \right) \right) dv \end{aligned} \tag{2.72}$$

Applying the definitions of $\rho f_l dv$, $\rho a_l dv$, $\rho \lambda_{lm} dv$, and $\rho a_l dv$ results in:

$$\begin{aligned} \int_v \rho \dot{e} dv = &\int_s \left(\sigma_{lk} v_l + m_{klm} \nu_{lm} + q_k \right) n_k da \\ &+ \int_v \left(\rho \left(f_l - a_l \right) v_l + \rho \left(\lambda_{lm} - \omega_{lm} \right) \right) dv \end{aligned} \tag{2.73}$$

and by converting the surface integrals to volume integrals, they got:

$$\begin{aligned}
&\int_v \left[\rho\dot{e} - \sigma_{lk}v_{l,k} - m_{klm}\nu_{lm,k} - q_{k,k} - \rho r\right] dv \\
&- \int_v \left[\left(\sigma_{kl,k} + \rho f_l - \rho a_l\right) v_l - \left(m_{klm,k} + \rho\lambda_{lm} - \rho\omega_{lm}\right)\nu_{lm}\right] dv \\
&- \int_s \left[\sigma_{kl}v_l + m_{klm}\nu_{lm} + q_k\right] n_k da = 0
\end{aligned} \tag{2.74}$$

and using equations of balance of momenta (2.59) and (2.60) balance of energy was given as:

$$\rho\dot{e} = \sigma_{kl}v_{l,k} + \left(s_{lk} - \sigma_{lk}\right)\nu_{lk} + m_{klm}\nu_{lm,k} + q_{k,k} + \rho r \qquad \text{in v} \tag{2.75}$$

with jump condition:

$$\left[\left[\sigma_{kl}v_l + m_{klm}\nu_{lm} + q_k\right]\right] n_k = 0 \qquad \text{on } s_d \tag{2.76}$$

Assuming discontinuous surface s_d is equal to continuous surface s which gives continuity of v_k, and ν_{lm} and considering equation (2.61), (2.76) reduced to:

$$q_k n_k = q_n \qquad \text{on } s \tag{2.77}$$

Introducing the Helmholtz free energy in terms of energy density, temperature and entropy gives:

$$\psi = e - \theta\eta \tag{2.78}$$

where η is entropy, θ is the temperature. Then, $\dot{\eta}$ can be expressed as:

$$\dot{\eta} = \frac{\dot{e}}{\theta} - \frac{\dot{\psi}}{\theta} - \frac{\dot{\theta}\eta}{\theta} \tag{2.79}$$

the second law of thermodynamics can be expressed as:

$$\frac{d}{dt}\int_v \rho\eta dv - \int_{ds} \frac{1}{\theta} q_k n_k da - \int_v \left(\frac{\rho h}{\theta}\right) \geq 0 \tag{2.80}$$

time differentiation and converting surface integral to volume integral gives:

$$\int_v \left[\rho\dot{\eta} - \left(\frac{q_k}{\theta}\right)_{,k} - \frac{\rho h}{\theta}\right] dv \geq 0 \tag{2.81}$$

the local form of the integral is:

$$\rho\dot{\eta} - \left(\frac{q_k}{\theta}\right)_{,k} - \frac{\rho h}{\theta} \geq 0 \tag{2.82}$$

inserting equation (2.79) into equation (2.82), solving equation (2.75) for r and inserting into equation (2.82), they obtained Clausius-Duhem inequality for the micromorphic continuum as:

$$-\rho\left(\dot{\psi} + \eta\dot{\theta}\right) + q_k\frac{\theta_{,k}}{\theta} + \sigma_{kl}v_{l,k} + \left(s_{kl} - \sigma_{kl}\right)\nu_{lk} + m_{klm}\nu_{lm,k} \geq 0 \tag{2.83}$$

2.3 Constitutive Equations for Material Linear Isotropic Elasticity at Finite Strain

Clausius-Duhem inequality given in equation (2.83) in the previous section takes the form given below in reference configuration by using the relation $\rho = \rho_0/J$, $dv = JdV$, and $q_k\theta_{,k} = Q_K\theta_{,K}\frac{1}{J}$.

$$\int_{\mathcal{B}_0}\{-\frac{1}{J}\rho_0\left(\dot{\psi} + \eta\dot{\theta}\right) + \sigma_{kl}\left(\nu_{l,k} - v_{lk}\right) + s_{kl}v_{lk} + \nu_{lm,k}m_{klm} + \frac{1}{J}\frac{1}{\theta}Q_K\theta_{,K}\}JdV \geq 0 \tag{2.84}$$

the local form of the equation is:

$$-\rho_0\left(\dot{\psi} + \eta\dot{\theta}\right) + J\sigma_{kl}\left(\nu_{l,k} - v_{lk}\right) + Js_{kl}v_{lk} + J\nu_{lm,k}m_{klm} + \frac{1}{\theta}Q_K\theta_{,K} \geq 0 \tag{2.85}$$

for isothermal and homogeneous temperature problems, the Clausius-Duhem inequality in reference configuration reduces to:

$$-\rho_0\dot{\psi} + J\sigma_{kl}\left(\nu_{l,k} - v_{lk}\right) + Js_{kl}v_{lk} + J\nu_{lm,k}m_{klm} \geq 0 \tag{2.86}$$

The stress tensors σ_{kl}, s_{kl}, and m_{klm} are mapped to reference configuration by the relations:

$$\sigma_{lk} = \frac{1}{J}F_{lL}S_{KL}F_{kK} \tag{2.87}$$

$$s_{lk} = \frac{1}{J}F_{lL}\Sigma_{KL}F_{kK} \tag{2.88}$$

$$m_{klm} = \frac{1}{J}F_{kK}F_{lL}M_{KLM}\chi_{mM} \tag{2.89}$$

Note that the first two equations (2.88) and (2.87) map to the current configuration by well know Piola transform relation. However, equation (2.89) involves the microdeformation tensor $\boldsymbol{\chi}$ in the mapping. This difference actually comes from the definition of the higher order couple stress tensor in current configuration. The definition of the higher order stress couple tensor may be expressed in current configuration by a volume average definition instead of area average definition as (Regueiro (2010)):

$$m_{klm}dv \overset{def}{=} \int_{dv} \sigma'_{kl}\xi_m dv' \tag{2.90}$$

and applying Piola transform to S'_{KL} and mapping ξ_m to reference configuration by $\xi_k = \chi_{kK}\Xi_K$, $dv' = J'dV'$ give:

$$m_{klm}dv \overset{def}{=} \int_{dv} \sigma'_{kl}\xi_m dv' = \int_{dV} F'_{kK}F'_{lL}\chi_{mM}S_{KL}\Xi_M dV' \tag{2.91}$$

$$F_{kK}F_{lL}\chi_{mM}M_{KLM}dV \overset{def}{=} \int_{dV} F'_{kK}F'_{lL}\chi_{mM}S_{KL}\Xi_M dV' \tag{2.92}$$

and

$$m_{klm}JdV = F_{kK}F_{lL}\chi_{mM}M_{KLM}dV$$

$$m_{klm} = \frac{1}{J}F_{kK}F_{lL}\chi_{mM}M_{KLM} \tag{2.93}$$

where F'_{kK} is the micro-element deformation gradient will be given in detail in the next chapter. Note that micro-deformation tensor χ_{kK} can be pulled out from the integral as it is not a function of X'_K(Eringen and Suhubi (1964)).

Eringen and Suhubi (1964) assumed a strain energy function in terms of the deformation gradient tensor F_{kK}, the micro-deformation tensor χ_{kK}, and the micro-deformation gradient tensor $\chi_{kK,L}$ for a micromorphic elastic material as :

$$\rho_0\psi\left(F_{kK}, \chi_{kK}, \chi_{kK,L}\right) \tag{2.94}$$

Then, the strain energy function rate can be expressed as :

$$\rho_0\dot{\psi} = \frac{\partial\left(\rho_0\psi\right)}{\partial F_{kK}}\dot{F}_{kK} + \frac{\partial\left(\rho_0\psi\right)}{\partial \chi_{kK}}\dot{\chi}_{kK} + \frac{\partial\left(\rho_0\psi\right)}{\partial \chi_{lK,L}}\dot{\chi}_{lK,L} \tag{2.95}$$

where $\dot{\rho}_0 = 0$ for a single phase solid material. Inserting this equation given above into equation (2.86) yields:

$$-\left(\frac{\partial(\rho_0\psi)}{\partial F_{lK}}\dot{F}_{lK}+\frac{\partial(\rho_0\psi)}{\partial \chi_{lK}}\dot{\chi}_{lK}+\frac{\partial(\rho_0\psi)}{\partial \chi_{lK,L}}\dot{\chi}_{lK,L}\right)+J\sigma_{kl}\left(\dot{F}_{lK}F^{-1}_{Kk}\right.$$
$$\left.-\dot{\chi}_{lK}\chi^{-1}_{Kk}\right)+Js_{kl}\dot{\chi}_{lK}\chi^{-1}_{Kk}+Jm_{klm}\left(\dot{\chi}_{lK,L}\chi^{-1}_{Km}F^{-1}_{Lk}+\dot{\chi}_{lK}\chi^{-1}_{Km,L}F^{-1}_{Lk}\right)\geq 0 \tag{2.96}$$

after collecting the terms with the same multiplier;

$$\left(J\sigma_{kl}F^{-1}_{Kk}-\frac{\partial(\rho_0\psi)}{\partial F_{lK}}\right)\dot{F}_{lK}+\left(Js_{kl}\chi^{-1}_{Kk}-J\sigma_{kl}\chi^{-1}_{Kk}+Jm_{klm}\chi^{-1}_{Km,L}F^{-1}_{Lk}\right.$$
$$\left.-\frac{\partial(\rho_0\psi)}{\partial \chi_{lK}}\right)\dot{\chi}^{-1}_{lK}+\left(Jm_{klm}\chi^{-1}_{Km}F^{-1}_{Lk}-\frac{\partial(\rho_0\psi)}{\partial \chi_{lK,L}}\right)\dot{\chi}_{lK,L}\geq 0 \tag{2.97}$$

For this equation to hold with the stress mapping relations given from (2.87) to (2.89):

$$J\left(\frac{1}{J}F_{kA}S_{AB}F_{lB}\right)F^{-1}_{Kk}=\frac{\partial(\rho_0\psi)}{\partial F_{lK}} \tag{2.98}$$

$$J\left(\frac{1}{J}F_{kA}\Sigma_{AB}F_{lB}\right)\chi^{-1}_{Kk}=F_{kC}\frac{\partial(\rho_0\psi)}{\partial F_{aC}}F^{-1}_{Da}F_{lD}\chi^{-1}_{Kk}+\frac{\partial(\rho_0\psi)}{\partial \chi_{lK}}$$
$$+F_{kE}F_{lF}\chi_{mG}\frac{\partial(\rho_0\psi)}{\partial \chi_{bG,E}}F^{-1}_{Fb}\chi^{-1}_{Ka}\chi_{aR,L}\chi^{-1}_{Rm}F^{-1}_{Lk} \tag{2.99}$$

$$J\left(\frac{1}{J}F_{kA}F_{lB}\chi_{mC}M_{ABC}\right)\chi^{-1}_{Km}F^{-1}_{Lk}=\frac{\partial(\rho_0\psi)}{\partial \chi_{lK,L}} \tag{2.100}$$

After some algebra definitions of stress tensors at reference configuration in terms of Helmholtz free energy function per unit mass ψ, deformation gradient F_{kK}, and microdeformation tensor χ_{kK} were obtained as (Regueiro (2010)):

$$S_{KL}=\frac{\partial(\rho_0\psi)}{\partial F_{kK}}F^{-1}_{Lk} \tag{2.101}$$

$$\Sigma_{KL}=\frac{\partial(\rho_0\psi)}{\partial F_{kK}}F^{-1}_{Lk}+F^{-1}_{Kc}\chi_{cA}\frac{\partial(\rho_0\psi)}{\partial \chi_{aA}}F^{-1}_{La}$$
$$+F^{-1}_{Kd}\chi_{dM,E}\frac{\partial(\rho_0\psi)}{\partial \chi_{fM,E}}F^{-1}_{Lf} \tag{2.102}$$

$$M_{KLM}=\frac{\partial(\rho_0\psi)}{\partial \chi_{kM,K}}F^{-1}_{Lk} \tag{2.103}$$

Another approach is to express the strain energy function in terms of the invariant elastic deformation measures given in equation (1.36) which are invariant with respect to rigid body

motion on current configuration and proposed by Eringen and Suhubi (1964).

$$\rho_0\psi\left(\boldsymbol{C},\boldsymbol{\psi},\boldsymbol{\Gamma}\right),\text{ or}\qquad \rho_0\psi\left(C_{KL},\psi_{KL},\Gamma_{KLM}\right) \tag{2.104}$$

Quadratic form assumption for the Helmholtz free energy function in reference configuration can be expressed as:

$$\begin{aligned}\rho_0\psi = &\frac{1}{2}E_{KL}A_{KLMN}E_{MN}+\frac{1}{2}\mathcal{E}_{KL}B_{KLMN}\mathcal{E}_{MN}\\ &+\frac{1}{2}\Gamma_{KLM}C_{KLMNPQ}\Gamma_{NPQ}+E_{KL}D_{KLMN}\mathcal{E}_{MN}\end{aligned} \tag{2.105}$$

and the following symmetry properties of these tensor were given by:

$$\begin{aligned}A_{KLMN}=A_{MNKL}=A_{LKMN}=A_{NMKL},\quad B_{KLMN}=B_{MNKL}\\ C_{KLMNPQ}=C_{NPQKLM},\quad D_{KLMN}=D_{LKMN}\end{aligned} \tag{2.106}$$

where elastic material moduli tensors A_{KLMN}, B_{KLMN}, D_{KLMN}, and C_{KLMNPQ} were defined for isotropic solids as (Suhubi and Eringen (1964); Eringen (1999)):

$$\begin{aligned}A_{KLMN} &= \lambda\delta_{KL}\delta_{MN}+\mu\left(\delta_{KM}\delta_{LN}+\delta_{KN}\delta_{LM}\right)\\ B_{KLMN} &= \left(\eta-\tau\right)\delta_{KL}\delta_{MN}+\left(\kappa-\sigma\right)\delta_{KM}\delta_{LN}+\left(\nu-\sigma\right)\delta_{KN}\delta_{LM}\\ C_{KLMNPQ} &= \tau_1\left(\delta_{KL}\delta_{MN}\delta_{PQ}+\delta_{KQ}\delta_{LM}\delta_{NP}\right)+\tau_2\left(\delta_{KL}\delta_{MP}\delta_{NQ}+\delta_{KM}\delta_{LQ}\delta_{NP}\right)\\ &\quad+\tau_3\delta_{KL}\delta_{MQ}\delta_{NP}+\tau_4\delta_{KN}\delta_{LM}\delta_{PQ}+\tau_5\left(\delta_{KM}\delta_{LN}\delta_{PQ}+\delta_{KP}\delta_{LM}\delta_{NQ}\right)\\ &\quad+\tau_6\delta_{KM}\delta_{LP}\delta_{NQ}+\tau_7\delta_{KN}\delta_{LP}\delta_{MQ}+\tau_8\left(\delta_{KP}\delta_{LQ}\delta_{MN}+\delta_{KQ}\delta_{LN}\delta_{MP}\right)\\ &\quad+\tau_9\delta_{KN}\delta_{LQ}\delta_{MP}+\tau_{10}\delta_{KP}\delta_{LN}\delta_{MQ}+\tau_{11}\delta_{KQ}\delta_{LP}\delta_{MN}\\ D_{KLMN} &= \tau\delta_{KL}\delta_{MN}+\sigma\left(\delta_{KN}\delta_{LM}+\delta_{LN}\delta_{KM}\right)\end{aligned} \tag{2.107}$$

where δ_{KL} is well known Kronecker delta function defined by:

$$\begin{aligned}\text{if}\quad K=L,\quad \delta_{KL}=1\\ \text{otherwise}\quad \delta_{KL}=0\end{aligned} \tag{2.108}$$

then, the constitutive equations were obtained as (Suhubi and Eringen (1964); Regueiro (2010)):

$$S_{KL} = 2\frac{\partial(\rho_0\psi)}{\partial C_{KL}} + \frac{\partial(\rho_0\psi)}{\partial \Psi_{KB}} C^{-1}_{LA}\Psi_{AB} + \frac{\partial(\rho_0\psi)}{\partial \Gamma_{KBC}} C^{-1}_{LA}\Gamma_{ABC} \tag{2.109}$$

$$\Sigma_{KL} = 2\frac{\partial(\rho_0\psi)}{\partial C_{KL}} + 2sym\left[\frac{\partial(\rho_0\psi)}{\partial \psi_{KB}} C^{-1}_{LA}\psi_{AB}\right] + 2sym\left[\frac{\partial(\rho_0\psi)}{\partial \Gamma_{KBC}} C^{-1}_{LA}\Gamma_{ABC}\right] \tag{2.110}$$

$$M_{KLM} = \frac{\partial(\rho_0\psi)}{\partial \Gamma_{LMK}} \tag{2.111}$$

If the strain energy function given in equation (2.105) is inserted and after some algebra, we get (Regueiro (2010)):

$$\begin{aligned}
S_{KL} &= A_{KLMN}E_{MN} + D_{KBMN}\mathcal{E}_{MN} \\
&\quad + \left(D_{KBMN}E_{MN} + B_{KBMN}\mathcal{E}_{MN}\right)\left[C^{-1}_{LA}\left(\mathcal{E}_{AB} + \delta_{AB}\right)\right] \\
&\quad + C_{KBCNPQ}\Gamma_{NPQ}C^{-1}_{LQ}\Gamma_{QBC} \\
\Sigma_{KL} &= A_{KLMN}E_{MN} + D_{KBMN}\mathcal{E}_{MN} \\
&\quad + 2sym\{\left(D_{KLMN}E_{MN} + B_{KBMN}\mathcal{E}_{MN}\right)\left[C^{-1}_{LA}\mathcal{E}_{AB} + \delta_{AB}\right] \\
&\quad + C_{KBCNPQ}\Gamma_{NPQ}C^{-1}_{LQ}\Gamma_{QBC}\} \\
M_{KLM} &= C_{KLMNPQ}\Gamma_{NPQ}
\end{aligned} \tag{2.112}$$

Assuming small elastic deformation cancels the quadratic terms out and inserting elastic moduli tensors given in equations (2.107) in (2.112) gives:

$$S_{KL} = (\lambda + \tau)E_{MM}\delta_{KL} + 2(\mu + \sigma)E_{KL} + \eta\mathcal{E}_{MM}\delta_{KL} + \kappa\mathcal{E}_{KL} + \nu\mathcal{E}_{LK} \tag{2.113}$$

$$\begin{aligned}
\Sigma_{KL} &= (\lambda + 2\tau)E_{MM}\delta_{KL} + 2(\mu + 2\sigma)E_{KL} + (2\eta - \tau)\mathcal{E}_{MM}\delta_{KL} \\
&\quad + (\nu + \kappa - \sigma)(\mathcal{E}_{KL} + \mathcal{E}_{LK})
\end{aligned} \tag{2.114}$$

$$\begin{aligned}
M_{KLM} &= \tau_1(\Gamma_{KRR}\delta_{LM} + \Gamma_{RRL}\delta_{KM}) + \tau_2(\Gamma_{RKR}\delta_{LM} + \Gamma_{RRM}\delta_{KL}) + \tau_3\Gamma_{RRK}\delta_{LM} \\
&\quad + \tau_4\Gamma_{LRR}\delta_{KM} + \tau_5(\Gamma_{RLR}\delta_{KM} + \Gamma_{MRR}\delta_{KL}) + \tau_6\Gamma_{RMR}\delta_{KL} + \tau_7\Gamma_{LMK} \\
&\quad + \tau_8(\Gamma_{MKL} + \Gamma_{KLM}) + \tau_9\Gamma_{LKM} + \tau_{10}\Gamma_{MLK} + \tau_{11}\Gamma_{KML}
\end{aligned} \tag{2.115}$$

where S_{KL} is the symmetric second Piola-Kirchhoff stress tensor of micro-element in reference configuration (over dV), Σ_{KL} is the symmetric second Piola-Kirchhoff micro-stress in reference configuration, and M_{KLM} is the higher order couple stress in reference configuration.

2.4 Map to Current Configuration

The constitutive equations obtained in reference configuration in equations (2.113), (2.114), and (2.115) can be mapped to obtain constitutive relations the current configuration by following the stress mappings given in equations (2.87), (2.88), and (2.89).

$$\begin{aligned}
\sigma_{kl} &= \frac{1}{J}\left[(\lambda+\tau)\,E_{MM}F_{kK}\delta_{KL}F_{lL} + 2\,(\mu+\sigma)\,F_{kK}E_{KL}F_{lL} + \eta\mathcal{E}_{MM}F_{kK}\delta_{KL}F_{lL}\right.\\
&\quad \left.+\kappa F_{kK}\mathcal{E}_{KL}F_{lL} + \nu F_{kK}\mathcal{E}_{LK}F_{lL}\right]\\
s_{kl} &= \frac{1}{J}\left[(\lambda+2\tau)\,E_{MM}F_{kK}\delta_{KL}F_{lL} + 2\,(\mu+2\sigma)\,F_{kK}E_{KL}F_{lL}\right.\\
&\quad \left.+\,(2\eta-\tau)\,\mathcal{E}_{MM}F_{kK}\delta_{KL}F_{lL} + (\nu+\kappa-\sigma)\,F_{kK}\left(\mathcal{E}_{KL}+\mathcal{E}_{LK}\right)F_{kK}\right] \qquad (2.116)
\end{aligned}$$

and

$$\begin{aligned}
m_{klm} &= \frac{1}{J}\left[\tau_1 F_{kK}F_{lL}\left(\Gamma_{KRR}\chi_{mL}+\Gamma_{RRL}\chi_{mK}\right)\right.\\
&\quad +\tau_2\left(\Gamma_{RKR}F_{kK}F_{lL}\chi_{mL}+\Gamma_{RRM}F_{kK}F_{lK}\chi_{mM}\right)\\
&\quad +\tau_3 F_{kK}F_{lL}\chi_{mL}\Gamma_{RRK}+\tau_4\Gamma_{LRR}F_{kK}F_{lL}\chi_{mK}\\
&\quad +\tau_5\left(\Gamma_{RLR}F_{kK}F_{lL}\chi_{mK}+\Gamma_{MRR}F_{kK}F_{lK}\chi_{mM}\right)\\
&\quad +\tau_6\Gamma_{RMR}F_{kK}F_{lK}\chi_{mM}+\tau_7\Gamma_{LMK}F_{kK}F_{lL}\chi_{mM}\\
&\quad +\tau_8 F_{kK}F_{lL}\chi_{mM}\left(\Gamma_{MKL}+\Gamma_{KLM}\right)+\tau_9 F_{kK}F_{lL}\chi_{mM}\Gamma_{LKM}\\
&\quad \left.+\tau_{10}F_{kK}F_{lL}\chi_{mM}\Gamma_{MLK}+\tau_{11}F_{kK}F_{lL}\chi_{mM}\Gamma_{KML}\right] \qquad (2.117)
\end{aligned}$$

introducing $\gamma_{klm} = F_{kK}F_{lL}\chi_{mM}\Gamma_{KLM}$, $\gamma_k^{F,1} = F_{kK}\Gamma_{KRR}$, $\gamma_k^{F,2} = F_{kK}\Gamma_{RRK}$, $\gamma_k^{F,3} = F_{kK}\Gamma_{RKR}$, $\gamma_k^{F,3} = F_{kK}\Gamma_{RKR}$,$\gamma_m^{\chi,1} = \chi_{mM}\Gamma_{RRM}$, $\gamma_m^{\chi,2} = \chi_{mM}\Gamma_{MRR}$, $\gamma_m^{\chi,3} = \chi_{mM}\Gamma_{RMR}$, $\psi_{kl} = F_{kK}\chi_{lK}$, $\vartheta_{kl} = F_{kK}\mathcal{E}_{KL}F_{lL}$, the left Cauchy-Green strain tensor $b_{kl} = F_{kK}F_{lK}$, and Eulerian-Almansi

strain tensor $e_{kl} = \frac{1}{2}\left(\delta_{kl} - b_{kl}^{-1}\right)$ the equations above will reduce to:

$$\sigma_{kl} = \frac{1}{J}\left[(\lambda+\tau)\, tr\,(\boldsymbol{E})\, b_{kl} + 2\,(\mu+\sigma)\, b_{ki} e_{ij} b_{jl} + \eta tr\,(\boldsymbol{\mathcal{E}})\, b_{kl}\right.$$
$$\left. +\kappa\vartheta_{kl} + \nu\vartheta_{lk}\right] \tag{2.118}$$

$$s_{kl} = \frac{1}{J}\left[(\lambda+2\tau)\, tr\,(\boldsymbol{E})\, b_{kl} + 2\,(\mu+2\sigma)\, b_{ki} e_{ij} b_{jl}\right.$$
$$\left. + (2\eta-\tau)\, tr\,(\boldsymbol{\mathcal{E}})\, b_{kl} + (\nu+\kappa-\sigma)\,(\vartheta_{kl}+\vartheta_{lk})\right] \tag{2.119}$$

and

$$m_{klm} = \frac{1}{J}\left[\tau_1\left(\gamma_k^{F,1}\psi_{lm} + \gamma_l^{F,2}\psi_{km}\right) + \tau_2\left(\gamma_k^{F,3}\psi_{lm} + \gamma_m^{\chi,1} b_{kl}\right)\right.$$
$$+ \tau_3\gamma_k^{F,2}\psi_{lm} + \tau_4\gamma_l^{F,1}\psi_{km} + \tau_5\left(\gamma_l^{F,3}\psi_{km} + \gamma_m^{\chi,2} b_{kl}\right) + \tau_6\gamma_m^{\chi,3} b_{kl} + \tau_7\gamma_{lmk}$$
$$\left. + \tau_8\left(\gamma_{mkl} + \gamma_{klm}\right) + \tau_9\gamma_{lkm} + \tau_{10}\gamma_{mlk} + \tau_{11}\gamma_{kml}\right] \tag{2.120}$$

where σ_{kl} is the unsymmetric Cauchy stress tensor, s_{kl} is the symmetric micro stress tensor, and m_{klm} is the higher order couple stress tensor.

2.5 Positiveness of The Strain Energy Function and Constraints on Elastic Parameters

The constitutive equations in the standard linear isotropic elastic Cauchy continuum involves two Lamé parameters. The isotropic micromorphic elasticity approach introduces five more elastic material moduli in unsymmetric Cauchy stress tensor, as well as in microstress tensor and eleven elastic constants in higher order couple stress tensor. In order to achieve the positivity of quadratic energy function, the restrictions among those material moduli were first proposed by Smith (1968) in the form of inequalities. Smith used the same strain tensors as Suhubi and Eringen (1964) used in constructing the free energy function. Eringen (1999) followed Smith's method to derive the inequalities which puts restrictions on the material moduli appearing in the constitutive equations obtained by using different set of deformation measures than that of Smith used. In this section, we present these inequalities proposed by Smith (1968) by following same notation applied in Smith (1968); Eringen

(1999).

Smith (1968) started with splitting energy function into :

$$\rho W(\boldsymbol{e}, \boldsymbol{\varepsilon}, \boldsymbol{\gamma}) = U(\boldsymbol{e}, \boldsymbol{\varepsilon}) + U(\boldsymbol{\gamma}) \tag{2.121}$$

where e_{kl}, ε_{kl}, and γ_{klm} were given in equations (2.36), (2.37), and (2.38) respectively. The strain energy is to be nonnegative for all the variations in strain measures.

$$U(\boldsymbol{e}, \boldsymbol{\varepsilon}) \geqslant 0 \qquad \text{for all } e_{ij} \text{ and } \varepsilon_{ij} \tag{2.122}$$

$$U(\boldsymbol{\gamma}) \geqslant 0 \qquad \text{for all } \gamma_{ijk} \tag{2.123}$$

where $U(\boldsymbol{e}, \boldsymbol{\varepsilon})$ and $U(\boldsymbol{\gamma})$ are respectively given in indicial notations as:

$$\begin{aligned} U(e_{kl}, \varepsilon_{kl}) = {} & \frac{\lambda}{2}(e_{ii})^2 + \mu e_{ij}e_{ji} + 2\sigma e_{ij}\varepsilon_{ji} + \frac{1}{2}(\kappa - \sigma)\varepsilon_{ij}\varepsilon_{ij} \\ & + \frac{1}{2}(\eta - \tau)(\varepsilon_{ii})^2 + \frac{1}{2}(\nu - \sigma)\varepsilon_{ij}\varepsilon_{ji} + \tau e_{ii}\varepsilon_{jj} \end{aligned} \tag{2.124}$$

and

$$\begin{aligned} U(\boldsymbol{\gamma}) = {} & \frac{\tau_1}{2}(\gamma_{iij}\gamma_{jkk} + \gamma_{ijj}\gamma_{kki}) + \frac{\tau_2}{2}(\gamma_{iij}\gamma_{kjk} + \gamma_{iji}\gamma_{kkj}) + \frac{\tau_3}{2}\gamma_{iij}\gamma_{kkj} \\ & + \frac{\tau_4}{2}\gamma_{ijj}\gamma_{ikk} + \frac{\tau_5}{2}(\gamma_{ijj}\gamma_{kik} + \gamma_{iji}\gamma_{jkk}) + \frac{\tau_6}{2}\gamma_{iji}\gamma_{kjk} + \frac{\tau_7}{2}\gamma_{ijk}\gamma_{ijk} \\ & + \frac{\tau_8}{2}(\gamma_{ijk}\gamma_{jki} + \gamma_{ijk}\gamma_{kij}) + \frac{\tau_9}{2}\gamma_{ijk}\gamma_{ikj} + \frac{\tau_{10}}{2}\gamma_{ijk}\gamma_{jik} + \frac{\tau_{11}}{2}\gamma_{ijk}\gamma_{kji} \end{aligned} \tag{2.125}$$

Smith (1968) defined set of variables by considering several uncoupled, symmetric, and anti-symmetric components of strain measures and took the second parial derivative with respect to those components. This method can be summarized by following Eringen (1999) notation as follows: $U(\boldsymbol{e}, \boldsymbol{\varepsilon})$, and $U(\boldsymbol{\gamma})$ are decomposed into several uncoupled, symmetric quadratic forms.

$$\begin{aligned} (\varepsilon_{11}, \varepsilon_{22}, \varepsilon_{33}, e_{11}, e_{22}, e_{33}) &= (x_1, x_2, x_3, x_4, x_5, x_6) \\ (\varepsilon_{12}, \varepsilon_{21}, e_{12}) &= (y_1, y_2, y_3) \\ (\varepsilon_{23}, \varepsilon_{31}, e_{23}) &= (z_1, z_2, z_3) \\ (\varepsilon_{31}, \varepsilon_{13}, e_{31}) &= (\xi_1, \xi_2, \xi_3) \end{aligned} \tag{2.126}$$

and Eringen (1999) wrote $U(\boldsymbol{e},\boldsymbol{\varepsilon})$ in terms of these sets as :

$$U(\boldsymbol{e},\boldsymbol{\varepsilon}) = a_{ij}x_i x_j + b_{kl}y_k y_l + b_{kl}z_k z_l + b_{kl}\xi_k \xi_l \tag{2.127}$$

we open $U(\boldsymbol{e},\boldsymbol{\varepsilon})$ to its components as :

$$\begin{aligned}
U(\boldsymbol{e},\boldsymbol{\varepsilon}) = {} & \frac{\lambda}{2}e_{11}e_{11} + \frac{\lambda}{2}e_{22}e_{22} + \frac{\lambda}{2}e_{33}e_{33} + \frac{\lambda}{2}e_{11}e_{22} + \frac{\lambda}{2}e_{22}e_{11} + \frac{\lambda}{2}e_{22}e_{33} \\
& + \frac{\lambda}{2}e_{33}e_{22} + \frac{\lambda}{2}e_{11}e_{33} + \frac{\lambda}{2}e_{33}e_{11} + \mu e_{11}e_{11} + \mu e_{12}e_{21} + \mu e_{13}e_{31} \\
& + \mu e_{21}e_{12} + \mu e_{22}e_{22} + \mu e_{23}e_{32} + \mu e_{31}e_{13} + \mu e_{32}e_{23} + \mu e_{33}e_{33} \\
& + 2\sigma e_{11}e_{11} + 2\sigma e_{12}e_{21} + 2\sigma e_{13}e_{31} + 2\sigma e_{13}e_{31} + 2\sigma e_{21}e_{12} + 2\sigma e_{22}e_{22} \\
& + 2\sigma e_{31}e_{13} + 2\sigma e_{32}e_{23} + 2\sigma e_{23}e_{32} + \tau e_{11}\varepsilon_{11} + \tau e_{11}\varepsilon_{22} + \tau e_{11}\varepsilon_{33} \\
& + \tau e_{22}\varepsilon_{11} + \tau e_{22}\varepsilon_{22} + \tau e_{22}\varepsilon_{33} + \tau e_{33}\varepsilon_{11} + \tau e_{33}\varepsilon_{22} + \tau e_{33}\varepsilon_{33} \\
& + \frac{1}{2}(\kappa-\sigma)\varepsilon_{11}\varepsilon_{11} + \frac{1}{2}(\kappa-\sigma)\varepsilon_{12}\varepsilon_{12} + \frac{1}{2}(\kappa-\sigma)\varepsilon_{13}\varepsilon_{13} \\
& + \frac{1}{2}(\kappa-\sigma)\varepsilon_{21}\varepsilon_{21} + \frac{1}{2}(\kappa-\sigma)\varepsilon_{22}\varepsilon_{22} + \frac{1}{2}(\kappa-\sigma)\varepsilon_{23}\varepsilon_{23} \\
& + \frac{1}{2}(\kappa-\sigma)\varepsilon_{31}\varepsilon_{31} + \frac{1}{2}(\kappa-\sigma)\varepsilon_{32}\varepsilon_{32} + \frac{1}{2}(\kappa-\sigma)\varepsilon_{33}\varepsilon_{33} \\
& + \frac{1}{2}(\eta-\tau)\varepsilon_{11}\varepsilon_{11} + \frac{1}{2}(\eta-\tau)\varepsilon_{22}\varepsilon_{22} + \frac{1}{2}(\eta-\tau)\varepsilon_{33}\varepsilon_{33} \\
& + \frac{1}{2}(\eta-\tau)\varepsilon_{11}\varepsilon_{22} + \frac{1}{2}(\eta-\tau)\varepsilon_{22}\varepsilon_{11} + \frac{1}{2}(\eta-\tau)\varepsilon_{22}\varepsilon_{33} \\
& + \frac{1}{2}(\eta-\tau)\varepsilon_{33}\varepsilon_{22} + \frac{1}{2}(\eta-\tau)\varepsilon_{11}\varepsilon_{33} + \frac{1}{2}(\eta-\tau)\varepsilon_{33}\varepsilon_{11} \\
& + \frac{1}{2}(\nu-\sigma)\varepsilon_{11}\varepsilon_{11} + \frac{1}{2}(\nu-\sigma)\varepsilon_{12}\varepsilon_{21} + \frac{1}{2}(\nu-\sigma)\varepsilon_{13}\varepsilon_{31} \\
& + \frac{1}{2}(\nu-\sigma)\varepsilon_{21}\varepsilon_{12} + \frac{1}{2}(\nu-\sigma)\varepsilon_{22}\varepsilon_{22} + \frac{1}{2}(\nu-\sigma)\varepsilon_{23}\varepsilon_{32} \\
& + \frac{1}{2}(\nu-\sigma)\varepsilon_{31}\varepsilon_{13} + \frac{1}{2}(\nu-\sigma)\varepsilon_{32}\varepsilon_{23} + \frac{1}{2}(\nu-\sigma)\varepsilon_{33}\varepsilon_{33}
\end{aligned} \tag{2.128}$$

Then, a_{ij} is found to be a 6×6 symmetric matrix and if we take $\frac{1}{2}$ factor out of the matrix, its components were obtained from equation (2.128) as:

$$
\begin{aligned}
a_{11} = a_{22} = a_{33} &= (\kappa + \eta + \nu - \tau - 2\sigma) \\
a_{44} = a_{55} = a_{66} &= \lambda + 2\mu \\
a_{12} = a_{13} = a_{23} = a_{21} = a_{31} = a_{32} &= \eta - \tau \\
a_{14} = a_{25} = a_{36} = a_{41} = a_{52} = a_{63} &= \tau + 2\sigma \\
a_{24} = a_{34} = a_{35} = a_{42} = a_{43} = a_{53} &= \tau \\
a_{45} = a_{46} = a_{56} = a_{54} = a_{64} = a_{65} &= \lambda
\end{aligned} \tag{2.129}
$$

Smith (1968) showed by adding and subtracting some rows and columns that the conditions on the elastic constants to have positive eigenvalues of the matrix a_{ij} are:

$$
\begin{aligned}
\mu &> 0 \\
\kappa + \nu &> 2\sigma \\
(\kappa + \nu - 2\sigma)\,\mu &> 2\sigma^2 \\
3\lambda + 2\mu &> 0 \\
\kappa + \nu + 3\mu &> 3\tau + 2\sigma \\
(\kappa + \nu + 3\eta - 3\tau - 2\sigma)\,(3\lambda + 2\mu) &> (3\tau + 2\sigma)^2
\end{aligned} \tag{2.130}
$$

Similarly the components of the matrix b_{kl} are:

$$
\begin{aligned}
b_{11} = b_{22} &= \kappa - \sigma \\
b_{12} = b_{21} &= \nu - \sigma \\
b_{13} = b_{31} = b_{23} = b_{32} &= 2\sigma \\
b_{33} &= 4\mu
\end{aligned} \tag{2.131}
$$

Smith (1968) again determined the conditions on elastic constants to have positive roots of the characteristic equation of b_{kl} which correspond to the eigenvalues of the matrix. We list

the only different conditions than the conditions listed for the matrix a_{ij} as:

$$\kappa - \nu > 0$$
$$4\mu\left(\kappa + \nu - 2\sigma\right) > 2\sigma \tag{2.132}$$

Although Eringen (1999) followed a different constitutive model than Smith (1968) who considered the model which is involving the strain measures in Suhubi and Eringen (1964), the restrictions on τ_i's coming from $U\left(\boldsymbol{\gamma}\right)$ are the same. Smith further introduced the two more symmetric 6×6 and 7×7 matrices d_{ij} and c_{ij} respectively by taking the second partial derivative of $U\left(\boldsymbol{\gamma}\right)$ with respect to these sets of variables in the same order :

$$\left(\gamma_{123},\gamma_{231},\gamma_{312},\gamma_{132},\gamma_{321},\gamma_{213}\right) = \left(x_1,x_2,x_3,x_4,x_5,x_6\right)$$
$$\left(\gamma_{111},\gamma_{122},\gamma_{133},\gamma_{212},\gamma_{313},\gamma_{221},\gamma_{331}\right) = \left(y_1,y_2,y_3,y_4,y_5,y_6,y_7\right) \tag{2.133}$$

where $U\left(\boldsymbol{\gamma}\right)$ is decomposed into two polynomials including the component of the symmetric matrices d_{ij} and c_{ij} as:

$$U\left(\boldsymbol{\gamma}\right) = \sum_{i=1}^{6}\sum_{j=1}^{6} c_{ij}x_i x_j + \sum_{k=1}^{7}\sum_{l=1}^{7} d_{kl}x_k x_l \tag{2.134}$$

Smith expressed the components of the matrices c_{ij}, d_{ij} and the restrictive conditions on the constants respectively as follows:

$$c_{11} = c_{22} = c_{33} = c_{44} = c_{55} = c_{66} = \tau_7$$
$$c_{12} = c_{13} = c_{23} = c_{45} = c_{46} = c_{56} = \tau_8$$
$$c_{14} = c_{35} = c_{26} = \tau_9$$
$$c_{24} = c_{15} = c_{36} = \tau_{11}$$
$$c_{34} = c_{25} = c_{16} = \tau_{10} \tag{2.135}$$

and the components of d_{ij} :

$$d_{11} = 2\tau_1 + 2\tau_3 + \tau_3 + \tau_4 + 2\tau_5 + \tau_6 + \tau_7 + 2\tau_8 + \tau_9 + \tau_{10} + \tau_{11}$$

$$
\begin{aligned}
&d_{12} = d_{13} = \tau_1 + \tau_4 + \tau_5 \quad && d_{14} = d_{15} = \tau_2 + \tau_5 + \tau_6 \\
&d_{16} = d_{17} = \tau_1 + \tau_2 + \tau_3 \quad && d_{22} = d_{33} = \tau_4 + \tau_7 + \tau_9 \\
&d_{23} = \tau_4 && d_{24} = d_{35} = \tau_5 + \tau_8 + \tau_{10} \\
&d_{25} = d_{34} = \tau_5 && d_{26} = d_{37} = \tau_1 + \tau_8 + \tau_{11} \\
&d_{27} = d_{36} = \tau_1 && d_{44} = d_{55} = \tau_6 + \tau_7 + \tau_{11} \\
&d_{45} = \tau_6 && d_{46} = d_{57} = \tau_2 + \tau_8 + \tau_9 \\
&d_{47} = d_{56} = \tau_2 && d_{66} = d_{77} = \tau_3 + \tau_7 + \tau_{10} \\
&d_{67} = \tau_8
\end{aligned}
\tag{2.136}
$$

and the restrictions on τ_i's are :

$$
\begin{aligned}
&\tau_7 + 2\tau_8 > |\tau_9 + \tau_{10} + \tau_{11}| \\
&\tau_7 - \tau_8 > \frac{1}{\sqrt{2}} \left| (\tau_9 - \tau_{10})^2 + (\tau_{10} - \tau_{11})^2 + (\tau_{11} - \tau_9)^2 \right|^{1/2} \\
&tr(\boldsymbol{T}) > 0, \qquad tr\,(\boldsymbol{COT}) > 0, \qquad det\,(\boldsymbol{T}) > 0
\end{aligned}
\tag{2.137}
$$

2.6 Simplification to Small Strain Micropolar Elasticity

Eringen (1999) showed that constitutive equations of a micromorphic elasticity can be simplified to microstretch and micropolar elasticities. Comparison of the constitutive equations may give us additional opinion about how to relate the material moduli of micostretch and micropolar theories obtained from previous works. Eringen proposed that this approach may be used to define additional inequalities among the material constant of a micromorphic continuum as well . However, Eringen used different set of strain measures accordingly had different constitutive equations. Here we apply his approach to provide a passage between micromorphic and micropolar elasticities for the constitutive equations given in the section 2.3.

We can derive the constitutive equations based on small strain assumption in current configuration in a similar way presented in section 2.3 for reference configuration. There-

fore, the constitutive equations (2.113), (2.114), and (2.115) can be expressed in current configuration as (Suhubi and Eringen (1964)):

$$\sigma_{kl} = (\lambda + \tau)\, e_{mm}\delta_{kl} + 2\,(\mu + \sigma)\, e_{kl} + \eta\varepsilon_{mm}\delta_{kl} + \kappa\varepsilon_{kl} + \nu\varepsilon_{lk} \tag{2.138}$$

$$\begin{aligned} s_{kl} &= (\lambda + 2\tau)\, e_{mm}\delta_{kl} + 2\,(\mu + 2\sigma)\, e_{kl} + (2\eta - \tau)\, \varepsilon_{mm}\delta_{kl} \\ &\quad + (\nu + \kappa - \sigma)\,(\varepsilon_{kl} + \varepsilon_{lk}) \end{aligned} \tag{2.139}$$

$$\begin{aligned} m_{klm} &= \tau_1\,(\gamma_{krr}\delta_{lm} + \gamma_{rrl}\delta_{km}) + \tau_2\,(\gamma_{rkr}\delta_{lm} + \gamma_{rrm}\delta_{kl}) + \tau_3\gamma_{rrk}\delta_{lm} \\ &\quad + \tau_4\gamma_{lrr}\delta_{km} + \tau_5\,(\gamma_{rlr}\delta_{km} + \gamma_{mrr}\delta_{kl}) + \tau_6\gamma_{rmr}\delta_{kl} + \tau_7\gamma_{lmk} \\ &\quad + \tau_8\,(\gamma_{mkl} + \gamma_{klm}) + \tau_9\gamma_{lkm} + \tau_{10}\gamma_{mlk} + \tau_{11}\gamma_{kml} \end{aligned} \tag{2.140}$$

where the strain tensors were already defined in equations (2.36), (2.37), and (2.38). If we write the unsymmetric Cauchy stress tensor in terms of displacement components and microdeformation components, we get :

$$\begin{aligned} \sigma_{kl} &= (\lambda + \tau)\, u_{m,m}\delta_{kl} + 2\,(\mu + \sigma)\, u_{k,l} + \eta\,(\phi_{mm} + u_{m,m})\,\delta_{kl} \\ &\quad + \kappa\,(\phi_{kl} + u_{l,k}) + \nu\,(\phi_{lk} + u_{k,l}) \end{aligned} \tag{2.141}$$

Then, we express the unsymmetric Cauchy stress tensor and the higher order couple stress tensor in terms of their symmetric and antisymmetric forms.

$$\begin{aligned} \sigma_{(kl)} &= [(\lambda + \tau + \eta)\, u_{m,m} + \eta\phi_{mm}]\,\delta_{kl} + (2\mu + 2\sigma + \kappa + \nu)\, u_{(k,l)} \\ &\quad + \kappa\phi_{(kl)} + \nu\phi_{(lk)} \end{aligned} \tag{2.142}$$

$$\sigma_{[kl]} = (2\mu + 2\sigma + \kappa)\, u_{[k,l]} + \nu u_{[l,k]} + \kappa\phi_{[kl]} + \nu\phi_{[lk]} \tag{2.143}$$

Eringen (1999) provides the passage to microstretch theory by setting:

$$\phi_{(kl)} = \phi\delta_{kl}, \qquad \phi_{[kl]} = -\epsilon_{klm}\phi_m \tag{2.144}$$

where ϵ_{klm} is the permutation tensor. After substitution, we get:

$$\begin{aligned} \sigma_{kl} &= [(\lambda + \tau + \eta)\, u_{m,m} + (3\eta + \kappa + \nu)\,\phi]\,\delta_{kl} + (2\mu + 2\sigma + \kappa)\, u_{k,l} \\ &\quad + \nu u_{l,k} + (\nu - \kappa)\,\epsilon_{klm}\phi_m \end{aligned} \tag{2.145}$$

By equaling $3\eta+\kappa+\nu=0$, we have the passage to the micropolar case. It also can be obtained from equation (2.144) by setting $\phi=0$. Eringen (1999) gave the constitutive equation for the higher order couple stress tensor m_{klm} associated with the its strain tensor $\gamma_{klm}=\phi_{kl,m}$ in terms of its symmetric and antisymmetic components. The symmetric and antisymmetic part of the higher order stress tensor m_{klm} are expressed below. These are different than that of Eringen (1999) by a factor -1 due to our strain tensor definition $\gamma_{klm}=-\phi_{kl,m}$.

$$\begin{aligned}
m_{k(lm)} = -\Bigg[& \left[(\tau_1+\tau_2)\,\phi_{(kr),r}+\tau_3\phi_{rr,k}\right]\delta_{lm} \\
& + \left[\frac{1}{2}(\tau_4+2\tau_5+\tau_6)\,\phi_{(lr),r}+\frac{1}{2}(\tau_1+\tau_2)\,\phi_{rr,l}\right]\delta_{km} \\
& + \left[\frac{1}{2}(\tau_4+2\tau_5+\tau_6)\,\phi_{(mr),r}+\frac{1}{2}(\tau_1+\tau_2)\,\phi_{rr,m}\right]\delta_{kl} \\
& + (\tau_7+\tau_{10})\,\phi_{(lm),k}+\frac{1}{2}(2\tau_8+\tau_9+\tau_{11})\,\phi_{(kl),m} \\
& + \frac{1}{2}(2\tau_8+\tau_9+\tau_{11})\,\phi_{(km),l}+\frac{1}{2}(\tau_4-\tau_6)\,\phi_{[lr],r}\delta_{km} \\
& + (\tau_1-\tau_2)\,\phi_{[kr],r}\delta_{lm}+\frac{1}{2}(\tau_4-\tau_6)\,\phi_{[mr],r}\delta_{kl} \\
& + \frac{1}{2}(\tau_{11}-\tau_9)\left(\phi_{[kl],m}+\phi_{[km],l}\right)\Bigg]
\end{aligned} \tag{2.146}$$

and

$$\begin{aligned}
m_{k[lm]} = -\Bigg[& \frac{1}{2}\left[(\tau_4-\tau_6)\,\phi_{(lr),r}+(\tau_1-\tau_2)\,\phi_{rr,l}\right]\delta_{km} \\
& - \frac{1}{2}\left[(\tau_4-\tau_6)\,\phi_{(mr),r}+(\tau_1-\tau_2)\,\phi_{rr,m}\right]\delta_{lk} \\
& + \frac{1}{2}(\tau_{11}-\tau_9)\,\phi_{(km),l}-\frac{1}{2}(\tau_{11}-\tau_9)\,\phi_{(kl),m} \\
& + \frac{1}{2}(\tau_4-2\tau_5+\tau_6)\,\phi_{[lr],r}\delta_{km}-\frac{1}{2}(\tau_4-2\tau_5+\tau_6)\,\phi_{[mr],r}\delta_{kl} \\
& + \frac{1}{2}(2\tau_8-\tau_9-\tau_{11})\,\phi_{[kl],m}-\frac{1}{2}(2\tau_8-\tau_9-\tau_{11})\,\phi_{[km],l} \\
& + (\tau_7-\tau_{10})\,\phi_{[lm],k}\Bigg]
\end{aligned} \tag{2.147}$$

Eringen (1999) decomposed the m_{klm} for microstretch continua:

$$m_{klm}=\frac{1}{3}m_k\delta_{lm}-\frac{1}{2}\epsilon_{lmr}m_{kr} \tag{2.148}$$

recalling equation (2.144) with (2.148), it can be reduced to microstretch case as:

$$m_k = m_{kll} = a_0\phi_{,k} - b_0\epsilon_{krj}\phi_{j,r} \tag{2.149}$$

$$m_{kl} = \epsilon_{lmp}m_{kpm} = \alpha\phi_{r,r}\delta_{kl} + \beta\phi_{k,l} + \gamma\phi_{l,k} + \alpha_0\epsilon_{klp}\phi_{,p} \tag{2.150}$$

where

$$a_0 = -\left(6\tau_6 + 6\tau_2 + 9\tau_3 + \tau_4 + 2\tau_5 + \tau_6 + 3\tau_7 + 2\tau_8 + \tau_9 + 3\tau_{10} + \tau_{11}\right) \tag{2.151}$$

$$b_0 = -\left(3\tau_1 - 3\tau_2 + \tau_4 - \tau_6 - \tau_9 + \tau_{11}\right) \tag{2.152}$$

$$\alpha_0 = -\left(-3\tau_1 + 3\tau_2 - \tau_4 - \tau_6 + \tau_9 - \tau_{11}\right) \tag{2.153}$$

where

$$\alpha = 2\tau_8 - \tau_9 - \tau_{11}, \quad \beta = -\tau_4 + 2\tau_5 - \tau_6$$

$$\gamma = \tau_4 - 2\tau_5 + \tau_6 + 2\tau_7 - 2\tau_8 + \tau_9 - 2\tau_{10} + \tau_{11}$$

by setting $a_0 = 0$, $b_0 = 0$, and $\alpha_0 = 0$, micropolar material moduli will be obtained.

Chapter 3

Finite Strain Micromorphic Elastoplasticity

In this chapter, we present the finite strain micromorphic elastoplasticity formulation originally proposed by Regueiro (2009, 2010). It is extension of micromorphic finite strain elasticity theory proposed by Eringen and Suhubi (1964); Suhubi and Eringen (1964); Eringen (1999) to elasto-plasticity with Drucker-Prager plasticity model. The chapter starts with the kinematics of elasto-plastic formulation such as decomposition of deformation gradient tensor $\boldsymbol{F}$, and micro-deformation tensor $\boldsymbol{\chi}$ assuming the existence of intermediate configuration. Then, we present Clausius-Duhem inequality and its reduced form which is used to attain the plastic evolution equations as well as constitutive equations on intermediate configuration. We conclude this chapter with the mapping of constitutive equations to the current configuration and numerical time integration scheme in conjunction with the yield function assumptions of pressure-sensitive plasticity formulation for the macro-scale plasticity, micro-scale plasticity and micro-scale gradient plasticity.

3.1 Kinematics Based on Multiplicative Decomposition of Deformation Gradient and Micro-deformation Tensor

Some materials may present elastic behavior which simply implies that after the deformation if the body is freed from stresses, it will return the its initial undeformed configuration. Contrarily, many materials which have practical use such as metals may behave inelastically (plastically) under large loads which indicates that permanent deformations will

remain in the body after it is relieved from stresses. If a body is deformed plastically, after cutting out the forces and relieving all the stresses in the body, it will reach a new unloaded configuration, and the motion between the last loaded configuration and this configuration may be described as elastic unloading. This configuration is free of forces and called intermediate configuration (Lubliner (1990); Bonet and Wood (1997)). The approach of introducing of the intermediate configuration is based on the works by Kondo (1952); Bilby et al. (1955); Kröner (1960); E.H. Lee and D.T. Liu (1967); Lee (1969). In general, to incorporate the plasticity within finite strain theory, the deformation gradient tensor is decomposed into its elastic and plastic parts on intermediate configuration in which constitutive equations are formulated. Intermediate configuration can be accepted as a elastically-unloaded reference configuration for current configuration such that elastic deformations govern between the intermediate configuration $\bar{\mathcal{B}}$ and current configuration $\mathcal{B}$ while the plastic deformations govern between reference configuration $\mathcal{B}_0$ and intermediate configuration $\bar{\mathcal{B}}$. Therefore, the mapping of a differential line, dx_k, in current configuration into the intermediate configuration may be described as $dx_k = F^e_{k\bar{K}} d\bar{X}_{\bar{K}}$ while same reasoning holds for a differential line, dX_K, in reference configuration to the intermediate configuration as $dX_K = F^p_{K\bar{K}} d\bar{X}_{\bar{K}}$. Note that all the expressions with a bar on top are associated with the intermediate configuration. In this section, we present a similar approach for a micromorphic continuum kinematics considering the multiplicative decomposition of deformation gradient tensor and micro-deformation tensor in conjunction with the elasto-plastic formulation which was originally proposed by Regueiro (2009); **?**.

For a micromorphic continuum, the mapping of the macro element and micro element also multiplicative decomposition of the deformation gradient and microdeformation tensor is illustrated in the figure 1.6. The position vector of a micro element in current configuration, x'_k, was expressed in equation (1.29). If we take the partial derivative of x'_k with respect to the reference micro-element position vector X'_K by using chain rule, we get the micro-

deformation gradient tensor F'_{kK} as (**?**):

$$F'_{kK} = \frac{\partial x'_k}{\partial X'_K} = \frac{\partial x'_k}{\partial X_L}\frac{\partial X_L}{\partial X'_K} \tag{3.1}$$

where

$$\frac{\partial x'_k}{\partial X_K} = \frac{\partial x_k\left(\boldsymbol{X},t\right)}{\partial X_K} + \frac{\partial \chi_{kL}\left(\boldsymbol{X},t\right)}{\partial X_K}\Xi_L + \chi_{kL}\frac{\partial \Xi_L}{\partial X_K} \tag{3.2}$$

and

$$\begin{aligned} X'_K &= X_K + \Xi_K \\ \frac{\partial X'_K}{\partial X_L} &= \delta_{KL} + \frac{\partial \Xi_K}{\partial X_L} \end{aligned} \tag{3.3}$$

$$\frac{\partial X_L}{\partial X'_K} = \left(\delta_{KL} + \frac{\partial \Xi_K}{\partial X_L}\right)^{-1} \Rightarrow \left(\delta_{KL} + \frac{\partial \Xi_K}{\partial X_L}\right)^{-1} \approx \left(\delta_{KL} - \frac{\partial \Xi_K}{\partial X_L}\right) \tag{3.4}$$

also the assumption of small gradient of micro-structure over the volume,
$\|\frac{\partial \Xi_K}{\partial X_L}\| \ll 1$, indicates that the quadratic terms can be ignored as:

$$\left(\frac{\partial \Xi_K}{\partial X_L}\right)^2 \approx 0 \tag{3.5}$$

Then, the micro-element deformation gradient tensor given in equation (3.1) can be rewritten as

$$F'_{kK} \;=\; F_{k\bar{K}} + \frac{\partial \chi_{kL}}{\partial X_K}\Xi_L + \left(\chi_{kA} - F_{kA} - \frac{\partial \chi_{kM}}{\partial X_A}\Xi_M\right)\frac{\partial \Xi_A}{\partial X_K} \tag{3.6}$$

Similar to the deformation gradient tensor F_{kK} of macro-element, the micro-element deformation gradient F'_{kK} maps the micro-element differential line segments $dx'_k = F'_{kK}dX'_L$. If the micro-element Jacobian of deformation is defined as $J' = \det\boldsymbol{F'}$, the micro-volume element in current configuration is related to micro-volume in reference configuration as $dv' = J'dV'$. Regueiro (2010) proposed that that micro-element deformation gradient tensor can be different than deformation gradient tensor, however, the constitutive equations formulated at intermediate configuration will not require the determination of F'_{kK} because they are involved in mapping of the stress tensors at micro level in the integral definitions. But, macro

level stress mappings are done by deformation gradient tensor. This is seen explicitly in equations (3.23), (3.25), and previously (2.91).

Multiplicative decomposition of the deformation gradient tensor (Lee (1969)) and micro-deformation tensor (Sansour (1998); Forest and Sievert (2003, 2006); Regueiro (2010)) gives

$$\begin{aligned} \boldsymbol{F} = \boldsymbol{F}^e\boldsymbol{F}^p \quad &, \qquad \boldsymbol{\chi} = \boldsymbol{\chi}^e\boldsymbol{\chi}^p \\ F_{kK} = F^e{}_{k\bar{K}}F^p{}_{\bar{K}K} \quad &, \qquad \chi_{kK} = \chi^e{}_{k\bar{K}}\chi^p{}_{\bar{K}K} \end{aligned} \tag{3.7}$$

The velocity gradient $v_{l,k} = \dot{F}_{lL}F^{-1}_{Lk}$ and the micro-gyration tensor $\nu_{lk} = \dot{\chi}_{lL}\chi^{-1}_{Lk}$ can be also decomposed in to elastic and plastic part as

$$\begin{aligned} \boldsymbol{\ell} &= \dot{\boldsymbol{F}}^e(\boldsymbol{F}^{e-1}) + \boldsymbol{F}^e\bar{\boldsymbol{L}}^p(\boldsymbol{F}^{e-1}) = \boldsymbol{\ell}^e + \boldsymbol{\ell}^p \\ v_{l,k} &= \dot{F}^e_{l\bar{A}}(F^{e-1})_{\bar{A}k} + F^e{}_{l\bar{B}}\bar{L}^p_{\bar{B}\bar{C}}(F^{e-1})_{\bar{C}k} = \ell^e{}_{lk} + \ell^p{}_{lk} \end{aligned} \tag{3.8}$$

and

$$\begin{aligned} \boldsymbol{\nu} &= \dot{\boldsymbol{\chi}}^e(\boldsymbol{\chi}^{e-1}) + \boldsymbol{\chi}^e\bar{\boldsymbol{L}}^{\chi,p}(\boldsymbol{\chi}^{e-1}) = \boldsymbol{\nu}^e + \boldsymbol{\nu}^p \\ \nu_{lk} &= \dot{\chi}^e_{l\bar{A}}(\chi^{e-1})_{\bar{A}k} + \chi^e{}_{l\bar{B}}\bar{L}^{\chi,p}_{\bar{B}\bar{C}}(\chi^{e-1})_{\bar{C}k} = \nu^e{}_{lk} + \nu^p{}_{lk} \end{aligned} \tag{3.9}$$

where

$$\begin{aligned} \bar{\boldsymbol{L}}^p = \dot{\boldsymbol{F}}^p(\boldsymbol{F}^{p-1}) \quad &, \qquad \bar{\boldsymbol{L}}^{\chi,p} = \dot{\boldsymbol{\chi}}^p(\boldsymbol{\chi}^{p-1}) \\ \bar{L}^p_{\bar{B}\bar{C}} = \dot{F}^p_{\bar{B}K}(F^{p-1})_{K\bar{C}} \quad &, \qquad \bar{L}^{\chi,p}_{\bar{B}\bar{C}} = \dot{\chi}^p_{\bar{B}K}(\chi^{p-1})_{K\bar{C}} \end{aligned} \tag{3.10}$$

The gradient of the micro-gyration tensor can be also split into elastic and plastic part as follows

$$\begin{aligned} \boldsymbol{\nabla}\boldsymbol{\nu} &= \boldsymbol{\nabla}\boldsymbol{\nu}^e + \boldsymbol{\nabla}\boldsymbol{\nu}^p \\ \nu_{lm,k} &= \nu^e{}_{lm,k} + \nu^p{}_{lm,k} \end{aligned} \tag{3.11}$$

where

$$\nu^e_{lm,k} = \dot{\chi}^e_{l\bar{A},k}\chi^{e-1}_{\bar{A}m} - \nu^e_{ln}\chi^e_{n\bar{D},k}\chi^{e-1}_{\bar{D}m} \tag{3.12}$$

$$\nu^p_{lm,k} = \left(\chi^e_{l\bar{C},k}\dot{\chi}^p_{\bar{C}A} + \chi^e_{l\bar{E}}\dot{\chi}^p_{\bar{E}A,k} - \chi^e_{l\bar{F}}\bar{L}^{\chi,p}_{\bar{F}\bar{G}}\chi^p_{\bar{G}A,k}\right)\chi^{-1}_{Am} - \nu^p_{la}\chi^e_{\bar{A},k}\chi^{e-1}_{\bar{A}m} \tag{3.13}$$

The macro differential volume in reference configuration maps to current configuration as

$$dv = JdV = J^eJ^pdV = J^ed\bar{V} \tag{3.14}$$

similarly, the micro-element differential volume maps as

$$dv' = J'dV' = J^{e\prime}J^{p\prime}dV' = J^{e\prime}d\bar{V}' \tag{3.15}$$

where $J^{e\prime} = \det \boldsymbol{F}^{e\prime}$, $J^{p\prime} = \det \boldsymbol{F}^{p\prime}$, $J^e = \det \boldsymbol{F}^e$, and $J^p = \det \boldsymbol{F}^p$. Mass conservation rule gives the relations among the mass densities as:

$$\rho_0 = \rho J = \rho J^eJ^p = \bar{\rho}J^p \tag{3.16}$$

$$\rho'_0 = \rho' J' = \rho' J^{e\prime}J^{p\prime} = \bar{\rho}' J^{p\prime} \tag{3.17}$$

where $\bar{\rho}'$ is the mass density of micro-element at intermediate configuration, $\bar{\rho}$ is the mass density of the macro-element at intermediate configuration. The volume averaging of micro-element densities over the macro-element can be expressed as similar to equation (1.24) in the intermediate configuration as

$$\bar{\rho}d\bar{V} \overset{\text{def}}{=} \int_{d\bar{V}} \bar{\rho}'d\bar{V}' \tag{3.18}$$

Giving the kinematics of elasto-plastic formulation and associated decompositions of the deformation tensors at intermediate configurations, the Clausius-Duhem inequality may be applied to derive the constitutive equations at intermediate configuration and plastic evolution equations. Hence, the next section focus on the expression of the Clausius-Duhem inequality in intermediate configuration.

3.2 Clausius-Duhem Inequality in Intermediate Configuration

The Clausius-Duhem inequality in current configuration and its form in the reference configuration were expressed in equations, respectively, (2.83) and (2.85) for a linear isotropic elastic micromorphic continuum. Following the same approach, we apply the Piola transform to map stresses and q_k from current configuration $\mathcal{B}$ to the intermediate configuration $\bar{\mathcal{B}}$ which results in similar mappings to those given in equations (2.87), (2.87), and (2.89). Besides, we apply a volume averaging approach assumption for the higher order couple stress tensor as given in the previous chapter to obtain the Clausius-Duhem inequality in intermediate configuration such that

$$\sigma_{lk} = \frac{1}{J^e} F^e_{l\bar{L}} \bar{S}_{\bar{K}\bar{L}} F^e_{k\bar{K}} \tag{3.19}$$

$$s_{lk} = \frac{1}{J^e} F^e_{l\bar{L}} \bar{\Sigma}_{\bar{K}\bar{L}} F^e_{k\bar{K}} \tag{3.20}$$

$$m_{klm} = \frac{1}{J^e} F^e_{k\bar{K}} F^e_{l\bar{L}} \bar{M}_{\bar{K}\bar{L}\bar{M}} \chi^e_{m\bar{M}} \tag{3.21}$$

where

$$s_{kl} dv = \int_{dv} \sigma'_{kl} dv' = \int_{d\bar{V}} \frac{1}{\bar{J}^e} F'^e_{l\bar{L}} F'^e_{k\bar{K}} \bar{\Sigma}'_{\bar{K}\bar{L}} d\bar{V}' = F^e_{l\bar{L}} F^e_{k\bar{K}} \bar{\Sigma}_{\bar{K}\bar{L}} d\bar{V} \tag{3.22}$$

$$\bar{\Sigma}_{\bar{K}\bar{L}} d\bar{V} \overset{\text{def}}{=} F^{e-1}_{\bar{K}k} F^{e-1}_{\bar{L}l} \int_{d\bar{V}} F'^e_{l\bar{J}} F'^e_{k\bar{I}} \bar{\Sigma}'_{\bar{I}\bar{J}} d\bar{V}' \tag{3.23}$$

$$\begin{aligned} m_{klm} dv &\overset{\text{def}}{=} \int_{dv} \sigma'_{kl} \xi_m dv' = \int_{d\bar{V}} \frac{1}{J'^e} F'^e_{k\bar{K}} F'^e_{l\bar{L}} S'_{\bar{K}\bar{L}} \Xi_{\bar{M}} \chi^e_{m\bar{M}} J'^e d\bar{V}' \\ &= F^e_{k\bar{K}} F^e_{l\bar{L}} \bar{M}_{\bar{K}\bar{L}\bar{M}} \chi^e_{m\bar{M}} d\bar{V} \end{aligned} \tag{3.24}$$

$$\begin{aligned} m_{klm} dv &= m_{klm} J^e d\bar{V} = F^e_{k\bar{K}} F^e_{l\bar{L}} \bar{M}_{\bar{K}\bar{L}\bar{M}} \chi^e_{m\bar{M}} d\bar{V} \\ \Rightarrow m_{klm} &= \frac{1}{J^e} F^e_{k\bar{K}} F^e_{l\bar{L}} \bar{M}_{\bar{K}\bar{L}\bar{M}} \chi^e_{m\bar{M}} \\ \bar{M}_{\bar{K}\bar{L}\bar{M}} &\overset{\text{def}}{=} F^{e-1}_{\bar{K}k} F^{e-1}_{\bar{L}l} \chi^{e-1}_{\bar{M}m} \int_{d\bar{V}} F^e_{k\bar{I}} F^e_{l\bar{J}} S'_{\bar{I}\bar{J}} \Xi_{\bar{A}} \chi^e_{m\bar{A}} d\bar{V}' \\ \bar{M}_{\bar{K}\bar{L}\bar{M}} &\overset{\text{def}}{=} F^{e-1}_{\bar{K}k} F^{e-1}_{\bar{L}l} \int_{d\bar{V}} F^e_{k\bar{I}} F^e_{l\bar{J}} S'_{\bar{I}\bar{J}} \Xi_{\bar{M}} d\bar{V}' \end{aligned} \tag{3.25}$$

and the Clausius-Duhem inequality in intermediate configuration takes the form

$$\int_{\bar{\mathcal{B}}} \left(-\bar{\rho} \left(\dot{\bar{\psi}} + \bar{\eta}\dot{\theta} \right) + J^e \sigma_{kl} \left(\nu_{l,k} - v_{lk} \right) \right.$$
$$\left. + J^e s_{kl} v_{lk} + J^e \nu_{lm,k} m_{klm} + J^e \frac{1}{\theta} \bar{Q}_{\bar{K}} \theta_{,\bar{K}} \right) d\bar{V} \geq 0 \tag{3.26}$$

The heat flux term in the Clausius-Duhem inequality can be obtained as follows: Remember the heat flux term in current configuration

$$\int_{da} \frac{1}{\theta} q'_k n'_k da' = \int_{d\bar{A}} \frac{1}{\theta} \underbrace{\left(q'_k J'^e F'^{e-1}_{\bar{K}k} \right)}_{\bar{Q}'_{\bar{K}}} \bar{N}'_{\bar{K}} d\bar{A}' = \int_{d\bar{A}} \frac{1}{\theta} \bar{Q}'_{\bar{K}} \bar{N}'_{\bar{K}} d\bar{A}' \tag{3.27}$$

Note that Nanson's formula $n'_k da' = J F'^{e-1}_{Kk} \bar{N}'_{\bar{K}} d\bar{A}$ was applied in equation above to relate the areas in current configuration and intermediate configuration that gives the Piola transform of the flux over the micro-element as $q'_k = \frac{1}{J'^e} F'^e_{k\bar{K}} \bar{Q}_{\bar{K}}$. Then, flux term over the macro-volume may be expressed as:

$$\int_{d\bar{V}} \left(\frac{\bar{Q}'_{\bar{K}}}{\theta} \right)_{,\bar{K}} d\bar{V}' \overset{\text{def}}{=} \left(\frac{\bar{Q}_{\bar{K}}}{\theta} \right)_{,\bar{K}} d\bar{V} \tag{3.28}$$

The local form of the Clausius-Duhem equation at intermediate configuration

$$-\bar{\rho} \left(\dot{\bar{\psi}} + \bar{\eta}\dot{\theta} \right) + J^e \sigma_{kl} \left(\nu_{l,k} - v_{lk} \right) + J^e s_{kl} v_{lk} + J^e \nu_{lm,k} m_{klm} + J^e \frac{1}{\theta} \bar{Q}_{\bar{K}} \theta_{,\bar{K}} \geq 0 \tag{3.29}$$

and its reduced form for isothermal and homogenous temperature problems is

$$-\bar{\rho} \dot{\bar{\psi}} + J^e \sigma_{kl} \left(\nu_{l,k} - v_{lk} \right) + J^e s_{kl} v_{lk} + J^e \nu_{lm,k} m_{klm} \geq 0 \tag{3.30}$$

Using the decompositions expressed in equations (3.8), (3.9), (3.12), and (3.13), the stress power terms in equation (3.26) can be expressed in terms of elastic and plastic parts as:

$$J^e \sigma_{lk} v_{l,k} = F^e_{l\bar{L}} \bar{S}_{\bar{K}\bar{L}} F^e_{k\bar{K}} \left(\dot{F}^e_{l\bar{A}} (F^{e-1})_{\bar{A}k} + F^e{}_{l\bar{B}} \bar{L}^p_{\bar{B}\bar{C}} (F^{e-1})_{\bar{C}k} \right)$$
$$J^e \sigma_{kl} v_{l,k} = \underbrace{\bar{S}_{\bar{K}\bar{L}} F^e_{l\bar{L}} \dot{F}^e_{l\bar{K}}}_{elastic} + \underbrace{\bar{S}_{\bar{K}\bar{L}} \bar{C}^e_{\bar{L}\bar{B}} \bar{L}^p_{\bar{B}\bar{K}}}_{plastic} \tag{3.31}$$

$$
\begin{aligned}
J^e\sigma_{kl}\nu_{lk} &= F^e_{l\bar{L}}\bar{S}_{\bar{K}\bar{L}}F^e_{k\bar{K}}\left(\nu^e_{lk} + \chi^e{}_{l\bar{B}}\bar{L}^{\chi,p}_{\bar{B}\bar{C}}(\chi^{e-1})_{\bar{C}k}\right)\\
J^e\sigma_{kl}\nu_{lk} &= F^e_{l\bar{L}}\bar{S}_{\bar{K}\bar{L}}F^e_{k\bar{K}}\nu^e_{lk} + \bar{S}_{\bar{K}\bar{L}}F^e_{l\bar{L}}\chi^e_{l\bar{E}}\bar{L}^{\chi,p}_{\bar{E}\bar{F}}(\chi^{e-1})_{\bar{F}k}F^e_{k\bar{K}}\\
J^e\sigma_{kl}\nu_{lk} &= \underbrace{F^e_{l\bar{L}}\bar{S}_{\bar{K}\bar{L}}F^e_{k\bar{K}}\nu^e_{lk}}_{elastic} + \underbrace{\bar{S}_{\bar{K}\bar{L}}\bar{\Psi}^e_{\bar{L}\bar{E}}\bar{L}^{\chi,p}_{\bar{E}\bar{F}}(\chi^{e-1})_{\bar{F}k}F^e_{k\bar{K}}}_{plastic}
\end{aligned}
\tag{3.32}
$$

$$
\begin{aligned}
J^e s_{kl}\nu_{lk} &= F^e_{l\bar{L}}\bar{\Sigma}_{\bar{K}\bar{L}}F^e_{k\bar{K}}\left(\nu^e_{lk} + \chi^e{}_{l\bar{B}}\bar{L}^{\chi,p}_{\bar{B}\bar{C}}(\chi^{e-1})_{\bar{C}k}\right)\\
J^e s_{kl}\nu_{lk} &= \underbrace{F^e_{l\bar{L}}\Sigma_{\bar{K}\bar{L}}F^e_{k\bar{K}}\nu^e_{lk}}_{elastic} + \underbrace{\bar{\Sigma}_{\bar{K}\bar{L}}\bar{\Psi}^e_{\bar{L}\bar{E}}\bar{L}^{\chi,p}_{\bar{E}\bar{F}}(\chi^{e-1})_{\bar{F}k}F^e_{k\bar{K}}}_{plastic}
\end{aligned}
\tag{3.33}
$$

$$
\begin{aligned}
J^e\nu_{lm,k}m_{klm} &= F^e_{k\bar{K}}F^e_{l\bar{L}}\bar{M}_{\bar{K}\bar{L}\bar{M}}\chi^e_{m\bar{M}}\left(\dot{\chi}^e_{l\bar{A},k}\chi^{e-1}_{\bar{A}m} - \nu^e_{ln}\chi^e_{n\bar{D},k}\chi^{e-1}_{\bar{D}m}\right)\\
&\quad + F^e_{k\bar{K}}F^e_{l\bar{L}}\bar{M}_{\bar{K}\bar{L}\bar{M}}\chi^e_{m\bar{M}}\left(\left(\chi^e_{l\bar{C},k}\dot{\chi}^p_{\bar{C}A} + \chi^e_{l\bar{E}}\dot{\chi}^p_{\bar{E}A,k} - \chi^e_{l\bar{F}}\bar{L}^{\chi,p}_{\bar{F}\bar{G}}\chi^p_{\bar{G}A,k}\right)\chi^{-1}_{Am}\right.\\
&\quad \left. - \nu^p_{la}\chi^e_{\bar{A},k}\chi^{e-1}_{\bar{A}m}\right)\\
J^e\nu_{lm,k}m_{klm} &= \bar{M}_{\bar{K}\bar{L}\bar{M}}F^e_{l\bar{L}}\left(\dot{\chi}^e_{l\bar{M},\bar{K}} - \nu^e_{ln}\chi^e_{n\bar{M},\bar{K}}\right)\Big\} \text{ elastic}\\
&\quad \left.\begin{aligned}
&+\bar{M}_{\bar{K}\bar{L}\bar{M}}F^e_{l\bar{L}}\left(-\nu^p_{ln}\chi^e_{n\bar{M},\bar{K}} + \left[\chi^e_{l\bar{C},\bar{K}}\dot{\chi}^p_{\bar{C}\bar{A}} + \chi^e_{l\bar{D}}\dot{\chi}^p_{\bar{D}\bar{A},\bar{K}}\right.\right.\\
&\left.\left.-\chi^e_{l\bar{B}}\bar{L}^{\chi,p}_{\bar{B}\bar{E}}\chi^p_{\bar{E}A,\bar{K}}\right]\chi^{p-1}_{A\bar{M}}\right)
\end{aligned}\right\} \text{plastic}
\end{aligned}
\tag{3.34}
$$

Note that deformation measures for micromorphic elastic solids were expressed in equation (1.36). We give the same deformation measures for the intermediate configuration as:

$$
\bar{C}^e_{\bar{K}\bar{L}} = F^e_{k\bar{K}}F^e_{k\bar{L}}\ ,\ \bar{\Psi}^e_{\bar{k}\bar{L}} = F^e_{k\bar{K}}\chi^e_{k\bar{L}}\ ,\ \bar{\Gamma}_{\bar{K}\bar{L}\bar{M}} = F^e_{k\bar{K}}\chi^e_{k\bar{L},\bar{M}} \tag{3.35}
$$

We chose a Helmholtz Free Energy function form similar to that of given in the section 2.3 (Eringen and Suhubi (1964); Regueiro (2010))

$$
\bar{\rho}\bar{\psi} = \bar{\rho}\bar{\psi}\left(F^e_{k\bar{K}}, \chi^e_{k\bar{K}}, \chi^e_{k\bar{K},\bar{M}}, \bar{Z}_{\bar{K}}, \bar{Z}^{\chi}_{\bar{K}}, \bar{Z}^{\chi}_{\bar{K},L}\right) \tag{3.36}
$$

where $\bar{Z}_{\bar{K}}$, $\bar{Z}^{\chi}_{\bar{K}}$, and $\bar{Z}^{\chi}_{\bar{K},L}$ are a vector of macro-strain-like ISVs, a vector of micro-strain-like ISVs, and derivative of micro-strain-like ISVs respectively in the intermediate configuration

$\bar{\mathcal{B}}$. The material time derivative of Helmholtz free energy in $\bar{\mathcal{B}}$.

$$\frac{D\left(\bar{\rho}\bar{\psi}\right)}{Dt} = \frac{\partial\bar{\rho}\bar{\psi}}{\partial F^e_{k\bar{K}}}\dot{F}^e_{k\bar{K}} + \frac{\partial\bar{\rho}\bar{\psi}}{\partial\chi^e_{k\bar{K}}}\dot{\chi}^e_{k\bar{K}} + \frac{\partial\bar{\rho}\bar{\psi}}{\partial\chi^e_{k\bar{K},\bar{M}}}\frac{D\chi^e_{k\bar{K},\bar{M}}}{Dt} + \frac{\partial\bar{\rho}\bar{\psi}}{\partial\bar{Z}_{\bar{K}}}\dot{\bar{Z}}_{\bar{K}} + \frac{\partial\bar{\rho}\bar{\psi}}{\partial\bar{Z}^{\chi}_{\bar{K}}}\dot{\bar{Z}}^{\chi}_{\bar{K}} + \frac{\partial\bar{\rho}\bar{\psi}}{\partial\bar{Z}^{\chi}_{\bar{K},\bar{M}}}\frac{D\bar{Z}^{\chi}_{\bar{K},\bar{M}}}{Dt} + \frac{\partial\bar{\rho}\bar{\psi}}{\partial\theta}\dot{\theta} \tag{3.37}$$

The left hand side of the equation above can be also expressed as:

$$\frac{D\left(\bar{\rho}\bar{\psi}\right)}{Dt} = \dot{\bar{\rho}}\bar{\psi} + \bar{\rho}\dot{\bar{\psi}} \tag{3.38}$$

where

$$\rho_0 = J^p\bar{\rho} \;\Rightarrow \dot{\bar{\rho}} = \frac{D\left(\rho_0/J^p\right)}{Dt} = -\rho_0\frac{\dot{J}^p}{\left(J^p\right)^2} = -\bar{\rho}\frac{\dot{J}^p}{J^p} \tag{3.39}$$

Then, equation (3.38) can be rewritten as:

$$\frac{D\left(\bar{\rho}\bar{\psi}\right)}{Dt} = -\bar{\rho}\bar{\psi}\frac{\dot{J}^p}{J^p} + \bar{\rho}\dot{\bar{\psi}} \tag{3.40}$$

which yields

$$\bar{\rho}\dot{\bar{\psi}} = \bar{\rho}\bar{\psi}\frac{\dot{J}^p}{J^p} + \frac{D\left(\bar{\rho}\bar{\psi}\right)}{Dt} \tag{3.41}$$

Coleman and Noll (1963) argued that plastic strain rate process is independent of the elastic strain rate. If we insert equations (3.41), (3.31), (3.32), (3.33), and (3.34) into the reduced Clausius-Duhem inequality and collect the elastic and plastic terms, from the elastic terms we get;

$$\bar{S}_{\bar{K}\bar{L}} = \frac{\partial\left(\bar{\rho}\bar{\psi}\right)}{\partial F^e_{k\bar{K}}}F^{e-1}_{\bar{L}k} \tag{3.42}$$

$$\bar{\Sigma}_{\bar{K}\bar{L}} = \frac{\partial\left(\bar{\rho}\bar{\psi}\right)}{\partial F^e_{k\bar{K}}}F^{e-1}_{\bar{L}k} + F^{e-1}_{\bar{K}c}\chi_{c\bar{A}}\frac{\partial\left(\bar{\rho}\bar{\psi}\right)}{\partial\chi_{a\bar{A}}}F^{e-1}_{\bar{L}a} + F^{e-1}_{\bar{K}d}\chi_{d\bar{M},\bar{E}}\frac{\partial\left(\bar{\rho}\bar{\psi}\right)}{\partial\chi_{f\bar{M},\bar{E}}}F^{e-1}_{\bar{L}f} \tag{3.43}$$

$$\bar{M}_{\bar{K}\bar{L}\bar{M}} = \frac{\partial\left(\bar{\rho}\bar{\psi}\right)}{\partial\chi_{k\bar{M},\bar{K}}}F^{e-1}_{\bar{L}k} \tag{3.44}$$

Similiar to what we did in chapter 2 for finite strain micromorphic elasticity, we can chose the Helmholtz free energy function with different set of invariants in intermediate configuration as:

$$\begin{aligned}&\bar{\psi}(\bar{\boldsymbol{C}}^e, \bar{\boldsymbol{\Psi}}^e, \bar{\boldsymbol{\Gamma}}^e, \bar{\boldsymbol{Z}}, \bar{\boldsymbol{Z}}^\chi, \bar{\boldsymbol{\nabla}}\bar{\boldsymbol{Z}}^\chi, \theta)\\ &\bar{\psi}(\bar{C}^e_{\bar{K}\bar{L}}, \bar{\Psi}^e_{\bar{K}\bar{L}}, \bar{\Gamma}^e_{\bar{K}\bar{L}\bar{M}}, \bar{Z}_{\bar{K}}, \bar{Z}^\chi_{\bar{K}}, \bar{Z}^\chi_{\bar{K},\bar{L}}, \theta)\end{aligned} \tag{3.45}$$

Then, the constitutive equations can be defined in the intermediate configuration as:

$$\begin{aligned}\bar{S}_{\bar{K}\bar{L}} &= 2\bar{\rho}\frac{\partial\bar{\psi}}{\partial\bar{C}^e_{\bar{K}\bar{L}}} + \bar{\rho}\frac{\partial\bar{\psi}}{\partial\bar{\Psi}^e_{\bar{K}\bar{B}}}(\bar{C}^{e-1})_{\bar{L}\bar{A}}\,\bar{\Psi}^e_{\bar{A}\bar{B}}\\ &\quad +\bar{\rho}\frac{\partial\bar{\psi}}{\partial\bar{\Gamma}^e_{\bar{K}\bar{B}\bar{C}}}(\bar{C}^{e-1})_{\bar{L}\bar{A}}\,\bar{\Gamma}^e_{\bar{A}\bar{B}\bar{C}} \qquad (3.46)\\ \bar{\Sigma}^{\bar{K}\bar{L}} &= 2\bar{\rho}\frac{\partial\bar{\psi}}{\partial\bar{C}^e_{\bar{K}\bar{L}}} + 2\text{sym}\left[\bar{\rho}\frac{\partial\bar{\psi}}{\partial\bar{\Psi}^e_{\bar{K}\bar{B}}}(\bar{C}^{e-1})_{\bar{L}\bar{A}}\,\bar{\Psi}^e_{\bar{A}\bar{B}}\right]\\ &\quad +2\text{sym}\left[\bar{\rho}\frac{\partial\bar{\psi}}{\partial\bar{\Gamma}^e_{\bar{K}\bar{B}\bar{C}}}(\bar{C}^{e-1})_{\bar{L}\bar{A}}\,\bar{\Gamma}^e_{\bar{A}\bar{B}\bar{C}}\right] \qquad (3.47)\\ \bar{M}^{\bar{K}\bar{L}\bar{M}} &= \bar{\rho}\frac{\partial\bar{\psi}}{\partial\bar{\Gamma}^e_{\bar{L}\bar{M}\bar{K}}} \qquad (3.48)\end{aligned}$$

The thermodynamic stress-like conjugates ISVs of $\bar{Z}$, $\bar{Z}^\chi$, $\bar{Z}^{\nabla,\chi}$ are introduced respectively as:

$$\bar{Q}_{\bar{K}} \overset{\text{def}}{=} \bar{\rho}\frac{\partial\bar{\psi}}{\partial\bar{Z}_{\bar{K}}}\,, \quad \bar{Q}^\chi_{\bar{K}} \overset{\text{def}}{=} \bar{\rho}\frac{\partial\bar{\psi}}{\partial\bar{Z}^\chi_{\bar{K}}}\,, \quad (\bar{Q}^{\nabla\chi})_{\bar{L}\bar{K}} \overset{\text{def}}{=} \bar{\rho}\frac{\partial\bar{\psi}}{\partial\bar{Z}^\chi_{\bar{K},\bar{L}}} \tag{3.49}$$

The remaining terms in the reduced Clausius-Duhem inequality are:

$$\begin{aligned}&\bar{\rho}\bar{\psi}\frac{\dot{J}^p}{J^p} - \bar{Q}_{\bar{K}}\dot{\bar{Z}}_{\bar{K}} - \bar{Q}^\chi_{\bar{K}}\dot{\bar{Z}}^\chi{}_{\bar{K}} - (\bar{Q}^{\nabla\chi})_{\bar{L}\bar{K}}\frac{D\left(\bar{Z}^\chi_{\bar{K},\bar{L}}\right)}{Dt} + \bar{S}_{\bar{K}\bar{L}}\left(\bar{C}^e_{\bar{L}\bar{B}}\bar{L}^p_{\bar{B}\bar{K}}\right)\\ &+ (\bar{\Sigma}_{\bar{K}\bar{L}} - \bar{S}_{\bar{K}\bar{L}})\left[\bar{\Psi}^e_{\bar{L}\bar{E}}\bar{L}^{\chi,p}_{\bar{E}\bar{F}}(\bar{C}^{\chi,e-1})_{\bar{F}\bar{N}}\bar{\Psi}^e_{\bar{K}\bar{N}}\right]\\ &+ \bar{M}_{\bar{K}\bar{L}\bar{M}}\left\{\bar{\Psi}^e_{\bar{L}\bar{D}}\bar{L}^{\chi,p}_{\bar{D}\bar{M},\bar{K}} - 2\bar{\Psi}^e_{\bar{L}\bar{D}}\text{skw}\left[\bar{L}^{\chi,p}_{\bar{D}\bar{C}}(\bar{\Psi}^{e-1})_{\bar{C}\bar{F}}\bar{\Gamma}^e_{\bar{F}\bar{M}\bar{K}}\right]\right\} \geq 0\end{aligned} \tag{3.50}$$

where the tensor $\bar{\boldsymbol{C}}^{\chi,e-1}$ is defined as $\bar{C}^{\chi,e-1}_{\bar{K}\bar{N}} = \chi^{e-1}_{\bar{K}k}\chi^{e-1}_{\bar{N}k}$.

3.3 Constitutive Equations for Simple Elasto-plasticity of Geomaterials

To derive the constitutive equations, quadratic form of Helmhotz free energy function was expressed in the previous chapter for micromorphic finite strain elastic formulation. We assume the same form for the Helmholtz free energy function including quadratic form for energy terms of ISVs as well in intermediate configurations as:

$$\begin{aligned}\bar{\rho}\bar{\psi} \overset{\text{def}}{=} & \frac{1}{2}\bar{E}^e_{\bar{K}\bar{L}}\bar{A}_{\bar{K}\bar{L}\bar{M}\bar{N}}\bar{E}^e_{\bar{M}\bar{N}} + \frac{1}{2}\bar{\mathcal{E}}^e_{\bar{K}\bar{L}}\bar{B}_{\bar{K}\bar{L}\bar{M}\bar{N}}\bar{\mathcal{E}}^e_{\bar{M}\bar{N}} \\ & + \frac{1}{2}\bar{\Gamma}^e_{\bar{K}\bar{L}\bar{M}}\bar{C}_{\bar{K}\bar{L}\bar{M}\bar{N}\bar{P}\bar{Q}}\bar{\Gamma}^e_{\bar{N}\bar{P}\bar{Q}} + \frac{1}{2}\bar{E}^e_{\bar{K}\bar{L}}\bar{D}_{\bar{K}\bar{L}\bar{M}\bar{N}}\bar{\mathcal{E}}^e_{\bar{M}\bar{N}} \\ & + \frac{1}{2}\bar{H}\bar{Z}^2 + \frac{1}{2}\bar{H}^\chi(\bar{Z}^\chi)^2 + \frac{1}{2}\bar{Z}^\chi_{,\bar{K}}\bar{H}^{\nabla\chi}\bar{Z}^\chi_{,\bar{K}}\end{aligned} \tag{3.51}$$

similarly the elastic moduli tensors are expressed in the intermediate configuration as

$$\bar{A}_{\bar{K}\bar{L}\bar{M}\bar{N}} = \lambda\delta_{\bar{K}\bar{L}}\delta_{\bar{M}\bar{N}} + \mu\left(\delta_{\bar{K}\bar{M}}\delta_{\bar{L}\bar{N}} + \delta_{\bar{K}\bar{N}}\delta_{\bar{L}\bar{M}}\right) \tag{3.52}$$

$$\begin{aligned}\bar{B}_{\bar{K}\bar{L}\bar{M}\bar{N}} = & (\eta-\tau)\delta_{\bar{K}\bar{L}}\delta_{\bar{M}\bar{N}} + \kappa\delta_{\bar{K}\bar{M}}\delta_{\bar{L}\bar{N}} + \nu\delta_{\bar{K}\bar{N}}\delta_{\bar{L}\bar{M}} \\ & -\sigma(\delta_{\bar{K}\bar{M}}\delta_{\bar{L}\bar{N}} + \delta_{\bar{K}\bar{N}}\delta_{\bar{L}\bar{M}})\end{aligned} \tag{3.53}$$

$$\begin{aligned}\bar{C}_{\bar{K}\bar{L}\bar{M}\bar{N}\bar{P}\bar{Q}} = & \tau_1\left(\delta_{\bar{K}\bar{L}}\delta_{\bar{M}\bar{N}}\delta_{\bar{P}\bar{Q}} + \delta_{\bar{K}\bar{Q}}\delta_{\bar{L}\bar{M}}\delta_{\bar{N}\bar{P}}\right) + \tau_2\left(\delta_{\bar{K}\bar{L}}\delta_{\bar{M}\bar{P}}\delta_{\bar{N}\bar{Q}} + \delta_{\bar{K}\bar{M}}\delta_{\bar{L}\bar{Q}}\delta_{\bar{N}\bar{P}}\right) \\ & + \tau_3\delta_{\bar{K}\bar{L}}\delta_{\bar{M}\bar{Q}}\delta_{\bar{N}\bar{P}} + \tau_4\delta_{\bar{K}\bar{N}}\delta_{\bar{L}\bar{M}}\delta_{\bar{P}\bar{Q}} + \tau_5\left(\delta_{\bar{K}\bar{M}}\delta_{\bar{L}\bar{N}}\delta_{\bar{P}\bar{Q}} + \delta_{\bar{K}\bar{P}}\delta_{\bar{L}\bar{M}}\delta_{\bar{N}\bar{Q}}\right) \\ & + \tau_6\delta_{\bar{K}\bar{M}}\delta_{\bar{L}\bar{P}}\delta_{\bar{N}\bar{Q}} + \tau_7\delta_{\bar{K}\bar{N}}\delta_{\bar{L}\bar{P}}\delta_{\bar{M}\bar{Q}} + \tau_8\left(\delta_{\bar{K}\bar{P}}\delta_{\bar{L}\bar{Q}}\delta_{\bar{M}\bar{N}} + \delta_{\bar{K}\bar{Q}}\delta_{\bar{L}\bar{N}}\delta_{\bar{M}\bar{P}}\right) \\ & + \tau_9\delta_{\bar{K}\bar{N}}\delta_{\bar{L}\bar{Q}}\delta_{\bar{M}\bar{P}} + \tau_{10}\delta_{\bar{K}\bar{P}}\delta_{\bar{L}\bar{N}}\delta_{\bar{M}\bar{Q}} + \tau_{11}\delta_{\bar{K}\bar{Q}}\delta_{\bar{L}\bar{P}}\delta_{\bar{M}\bar{N}}\end{aligned} \tag{3.54}$$

$$\bar{D}_{\bar{K}\bar{L}\bar{M}\bar{N}} = \tau\delta_{\bar{K}\bar{L}}\delta_{\bar{M}\bar{N}} + \sigma(\delta_{\bar{K}\bar{M}}\delta_{\bar{L}\bar{N}} + \delta_{\bar{K}\bar{N}}\delta_{\bar{L}\bar{M}}) \tag{3.55}$$

Then, the constitutive equations take the form by applying equations (3.46), (3.47), and (3.48)

$$\begin{aligned}
\bar{S}_{\bar{K}\bar{L}} &= \bar{A}_{\bar{K}\bar{L}\bar{M}\bar{N}}\bar{E}^{e}_{\bar{M}\bar{N}} + \bar{D}_{\bar{K}\bar{B}\bar{M}\bar{N}}\bar{\mathcal{E}}^{e}_{\bar{M}\bar{N}} \\
&\quad +(\bar{D}_{\bar{K}\bar{B}\bar{M}\bar{N}}\bar{E}^{e}_{\bar{M}\bar{N}} + \bar{B}_{\bar{K}\bar{B}\bar{M}\bar{N}}\bar{\mathcal{E}}^{e}_{\bar{M}\bar{N}})\left[(\bar{C})^{e-1}_{\bar{L}\bar{A}}\bar{\mathcal{E}}^{e}_{\bar{A}\bar{L}} + \delta_{\bar{L}\bar{L}}\right] \\
&\quad +\bar{C}_{\bar{K}\bar{B}\bar{C}\bar{N}\bar{P}\bar{Q}}\bar{\Gamma}^{e}_{\bar{N}\bar{P}\bar{Q}}(\bar{C}^{e-1})_{\bar{L}\bar{Q}}\bar{\Gamma}^{e}_{\bar{Q}\bar{B}\bar{C}} \qquad (3.56) \\
\bar{\Sigma}_{\bar{K}\bar{L}} &= \bar{A}_{\bar{K}\bar{L}\bar{M}\bar{N}}\bar{E}^{e}_{\bar{M}\bar{N}} + \bar{D}^{\bar{K}\bar{B}\bar{M}\bar{N}}\bar{\mathcal{E}}^{e}_{\bar{M}\bar{N}} \\
&\quad +2\text{sym}\left\{(\bar{D}_{\bar{K}\bar{L}\bar{M}\bar{N}}\bar{E}^{e}_{\bar{M}\bar{N}} + \bar{B}_{\bar{K}\bar{B}\bar{M}\bar{N}}\bar{\mathcal{E}}^{e}_{\bar{M}\bar{N}})\left[(\bar{C}^{e-1})_{\bar{L}\bar{A}}\bar{\mathcal{E}}^{e}_{\bar{A}\bar{B}} + \delta_{\bar{L}\bar{B}}\right]\right. \\
&\quad \left. +\bar{C}_{\bar{K}\bar{B}\bar{C}\bar{N}\bar{P}\bar{Q}}\bar{\Gamma}^{e}_{\bar{N}\bar{P}\bar{Q}}(\bar{C}^{e-1})_{\bar{L}\bar{Q}}\bar{\Gamma}^{e}_{\bar{Q}\bar{B}\bar{C}}\right\} \qquad (3.57) \\
\bar{M}_{\bar{K}\bar{L}\bar{M}} &= \bar{C}_{\bar{K}\bar{L}\bar{M}\bar{N}\bar{P}\bar{Q}}\bar{\Gamma}^{e}_{\bar{N}\bar{P}\bar{Q}} \qquad (3.58)
\end{aligned}$$

Ignoring the quadratic terms and inserting the elastic moduli tensors yield:

$$\bar{S}_{\bar{K}\bar{L}} = (\lambda+\tau)\,\bar{E}_{\bar{M}\bar{M}}\delta_{\bar{K}\bar{L}} + 2\,(\mu+\sigma)\,\bar{E}_{\bar{K}\bar{L}} + \eta\bar{\mathcal{E}}_{\bar{M}\bar{M}}\delta_{\bar{K}\bar{L}} + \kappa\bar{\mathcal{E}}_{\bar{K}\bar{L}} + \nu\bar{\mathcal{E}}_{\bar{L}\bar{K}} \qquad (3.59)$$

$$\begin{aligned}
\bar{\Sigma}_{\bar{K}\bar{L}} &= (\lambda+2\tau)\,\bar{E}_{\bar{M}\bar{M}}\delta_{\bar{K}\bar{L}} + 2\,(\mu+2\sigma)\,\bar{E}_{\bar{K}\bar{L}} + (2\eta-\tau)\,\bar{\mathcal{E}}_{\bar{M}\bar{M}}\delta_{\bar{K}\bar{L}} \\
&\quad + (\nu+\kappa-\sigma)\left(\bar{\mathcal{E}}_{\bar{K}\bar{L}} + \bar{\mathcal{E}}_{\bar{L}\bar{K}}\right) \qquad (3.60)
\end{aligned}$$

$$\begin{aligned}
\bar{M}_{\bar{K}\bar{L}\bar{M}} &= \tau_1\left(\bar{\Gamma}_{\bar{K}\bar{R}\bar{R}}\delta_{\bar{L}\bar{M}} + \bar{\Gamma}_{\bar{R}\bar{R}\bar{L}}\delta_{\bar{K}\bar{M}}\right) + \tau_2\left(\bar{\Gamma}_{\bar{R}\bar{K}\bar{R}}\delta_{\bar{L}\bar{M}} + \bar{\Gamma}_{\bar{R}\bar{R}\bar{M}}\delta_{\bar{K}\bar{L}}\right) + \tau_3\bar{\Gamma}_{\bar{R}\bar{R}\bar{K}}\delta_{\bar{L}\bar{M}} \\
&\quad + \tau_4\bar{\Gamma}_{\bar{L}\bar{R}\bar{R}}\delta_{\bar{K}\bar{M}} + \tau_5\left(\bar{\Gamma}_{\bar{R}\bar{L}\bar{R}}\delta_{\bar{K}\bar{M}} + \bar{\Gamma}_{\bar{M}\bar{R}\bar{R}}\delta_{\bar{K}\bar{L}}\right) + \tau_6\bar{\Gamma}_{\bar{R}\bar{M}\bar{R}}\delta_{\bar{K}\bar{L}} + \tau_7\bar{\Gamma}_{\bar{L}\bar{M}\bar{K}} \\
&\quad + \tau_8\left(\bar{\Gamma}_{\bar{M}\bar{K}\bar{L}} + \bar{\Gamma}_{\bar{K}\bar{L}\bar{M}}\right) + \tau_9\bar{\Gamma}_{\bar{L}\bar{K}\bar{M}} + \tau_{10}\bar{\Gamma}_{\bar{M}\bar{L}\bar{K}} + \tau_{11}\bar{\Gamma}_{\bar{K}\bar{M}\bar{L}} \qquad (3.61)
\end{aligned}$$

also

$$\begin{aligned}
\bar{Q} &= \bar{H}\bar{Z}_{\bar{K}} \qquad (3.62) \\
\bar{Q}^{\chi} &= \bar{H}^{\chi}\bar{Z}^{\chi}_{\bar{K}} \qquad (3.63) \\
(\bar{Q}^{\chi})_{\bar{L}} &= \bar{H}^{\nabla\chi}\bar{Z}^{\chi}_{,\bar{L}} \qquad (3.64)
\end{aligned}$$

3.4 Yield Functions, Plastic Potential Functions, and Evolution Equations

Three yield functions with same forms assuming non-associative flow rule are introduced for macro-scale plasticity, micro-scale plasticity and micro-scale gradient plasticity to define the plastic deformation evolution equations. The plastic potential functions are assumed to have the same forms with the yield functions.

3.4.1 Macro-scale Yield, Plastic Potential, and Evolution Equations

For the macro scale plasticity, we have very well known Drucker-Prager plasticity form of yield function as follows:

$$\bar{F}(\bar{\boldsymbol{S}}, \bar{c}) \overset{\text{def}}{=} \|\text{dev}\bar{\boldsymbol{S}}\| - \left(A^{\phi}\bar{c} - B^{\phi}\bar{p}\right) \leq 0 \tag{3.65}$$

$$A^{\phi} = \beta^{\phi}\cos\phi \ , \ B^{\phi} = \beta^{\phi}\sin\phi \ , \ \beta^{\phi} = \frac{2\sqrt{6}}{3 + \beta\sin\phi} \tag{3.66}$$

$$\|\text{dev}\bar{\boldsymbol{S}}\| = \sqrt{(\text{dev}\bar{\boldsymbol{S}}) : (\text{dev}\bar{\boldsymbol{S}})} \tag{3.67}$$

$$(\text{dev}\bar{\boldsymbol{S}}) : (\text{dev}\bar{\boldsymbol{S}}) = (\text{dev}\bar{S}_{\bar{I}\bar{J}})(\text{dev}\bar{S}_{\bar{I}\bar{J}}) \tag{3.68}$$

$$= (\text{dev}\bar{S}_{\bar{I}\bar{J}})(\text{dev}\bar{S}_{\bar{I}\bar{J}})$$

$$\text{dev}\bar{S}_{\bar{I}\bar{J}} = \bar{S}_{\bar{I}\bar{J}} - \left(\frac{1}{3}\bar{C}^{e}_{\bar{A}\bar{B}}\bar{S}_{\bar{A}\bar{B}}\right)(\bar{C}^{e-1})_{\bar{I}\bar{J}} \tag{3.69}$$

$$\bar{p} \overset{\text{def}}{=} \frac{1}{3}\bar{C}^{e}_{\bar{A}\bar{B}}\bar{S}_{\bar{A}\bar{B}} \tag{3.70}$$

where $\bar{c}$ is the cohesion in $\bar{B}$, ϕ the friction angle, and $-1 \leq \beta \leq 1$ to intersect the Mohr-Coulomb vertices in Triaxial Compression ($\beta = 1$). The plastic potential function with

evolution equations are:

$$\bar{G}(\bar{\boldsymbol{S}},\bar{c}) \stackrel{\text{def}}{=} \|\text{dev}\bar{\boldsymbol{S}}\| - \left(A^{\psi}\bar{c} - B^{\psi}\bar{p}\right) \tag{3.71}$$

$$A^{\psi} = \beta^{\psi}\cos\psi\ ,\ B^{\psi} = \beta^{\psi}\sin\psi\ ,\ \beta^{\psi} = \frac{2\sqrt{6}}{3+\beta\sin\psi} \tag{3.72}$$

$$\bar{C}^{e}_{\bar{L}\bar{B}}\bar{L}^{p}_{\bar{B}\bar{K}} \stackrel{\text{def}}{=} \dot{\bar{\gamma}}\frac{\partial\bar{G}}{\partial\bar{S}_{\bar{K}\bar{L}}},\ \ \frac{\partial\bar{G}}{\partial\bar{S}_{\bar{K}\bar{L}}} = \hat{\bar{N}}_{\bar{K}\bar{L}} + \frac{1}{3}B^{\psi}\bar{C}^{e}_{\bar{K}\bar{L}} \tag{3.73}$$

$$\hat{\bar{N}}_{\bar{A}\bar{B}} = \frac{\text{dev}\bar{S}_{\bar{A}\bar{B}}}{\|\text{dev}\bar{\boldsymbol{S}}\|} \tag{3.74}$$

$$\dot{\bar{Z}} \stackrel{\text{def}}{=} -\dot{\bar{\gamma}}\frac{\partial\bar{G}}{\partial\bar{c}} = A^{\psi}\dot{\bar{\gamma}} \tag{3.75}$$

$$\bar{c} = \bar{H}\bar{Z} \tag{3.76}$$

$$\bar{Q} \stackrel{\text{def}}{=} \bar{c} \tag{3.77}$$

where $\dot{\bar{\gamma}}$ is the plastic multiplier rate in $\bar{\mathcal{B}}$, $\bar{\psi}$ the dilation angle. There is no cap for this model as of yet.

3.4.2 Micro-scale Yield, Plastic Potential, and Evolution Equations

The yield function and the plastic potential function with plastic evolution equations for the micro-scale are expressed as:

$$\bar{F}^{\chi}(\bar{\boldsymbol{\Sigma}} - \bar{\boldsymbol{S}},\bar{c}^{\chi}) \stackrel{\text{def}}{=} \|\text{dev}(\bar{\boldsymbol{\Sigma}} - \bar{\boldsymbol{S}})\| - \left(A^{\chi,\phi}\bar{c}^{\chi} - B^{\chi,\phi}\bar{p}^{\chi}\right) \leq 0 \tag{3.78}$$

$$A^{\chi,\phi} = \beta^{\chi,\phi}\cos\phi^{\chi}\ ,\ B^{\chi,\phi} = \beta^{\chi,\phi}\sin\phi^{\chi} \tag{3.79}$$

$$\beta^{\chi,\phi} = \frac{2\sqrt{6}}{3+\beta^{\chi}\sin\phi^{\chi}} \tag{3.80}$$

$$\text{dev}(\bar{\Sigma}_{\bar{I}\bar{J}} - \bar{S}_{\bar{I}\bar{J}}) = (\bar{\Sigma}_{\bar{I}\bar{J}} - \bar{S}_{\bar{I}\bar{J}}) - \bar{p}^{\chi}\bar{C}^{e-1}_{\bar{I}\bar{J}} \tag{3.81}$$

$$\bar{p}^{\chi} \stackrel{\text{def}}{=} \frac{1}{3}\bar{C}^{e}_{\bar{A}\bar{B}}\left(\bar{\Sigma}_{\bar{A}\bar{B}} - \bar{S}_{\bar{A}\bar{B}}\right) \tag{3.82}$$

where $\bar{c}^{\chi}$ is the micro-scale cohesion in $\bar{\mathcal{B}}$, ϕ^{χ} the micro-scale friction angle, and $-1 \leq \beta^{\chi} \leq 1$, and $\beta^{\chi} = 1$, The plastic potential function and evolution equations of the micro-scale are:

$$\bar{G}^{\chi}(\bar{\boldsymbol{\Sigma}} - \bar{\boldsymbol{S}}, \bar{c}^{\chi}) \stackrel{\text{def}}{=} \|\text{dev}(\bar{\boldsymbol{\Sigma}} - \bar{\boldsymbol{S}})\| - \left(A^{\chi,\psi}\bar{c}^{\chi} - B^{\chi,\psi}\bar{p}^{\chi}\right) \tag{3.83}$$

$$A^{\chi,\psi} = \beta^{\chi,\psi}\cos\psi^{\chi}\ ,\ B^{\chi,\psi} = \beta^{\chi,\psi}\sin\psi^{\chi} \tag{3.84}$$

$$\beta^{\chi,\psi} = \frac{2\sqrt{6}}{3 + \beta^{\chi}\sin\psi^{\chi}} \tag{3.85}$$

$$\bar{\Psi}^{e}_{\bar{L}\bar{E}}\bar{L}^{\chi,p}_{\bar{E}\bar{F}}(\bar{C}^{\chi,e-1})_{\bar{F}\bar{N}}\bar{\Psi}^{e}_{\bar{K}\bar{N}} \stackrel{\text{def}}{=} \dot{\bar{\gamma}}^{\chi}\frac{\partial\bar{G}^{\chi}}{\partial(\bar{\Sigma}_{\bar{K}\bar{L}} - \bar{S}_{\bar{K}\bar{L}})} \tag{3.86}$$

$$\frac{\partial\bar{G}^{\chi}}{\partial(\bar{\Sigma}_{\bar{K}\bar{L}} - \bar{S}_{\bar{K}\bar{L}})} = \hat{\bar{N}}^{\chi}{}_{\bar{K}\bar{L}} + \frac{1}{3}B^{\chi,\psi}\bar{C}^{e}_{\bar{K}\bar{L}} \tag{3.87}$$

$$\hat{\bar{N}}^{\chi}{}_{\bar{A}\bar{B}} = \frac{\text{dev}(\bar{\Sigma}_{\bar{A}\bar{B}} - \bar{S}_{\bar{A}\bar{B}})}{\|\text{dev}(\bar{\boldsymbol{\Sigma}} - \bar{\boldsymbol{S}})\|} \tag{3.88}$$

$$\dot{\bar{Z}}^{\chi} \stackrel{\text{def}}{=} -\dot{\bar{\gamma}}^{\chi}\frac{\partial\bar{G}^{\chi}}{\partial\bar{c}^{\chi}} = A^{\chi,\psi}\dot{\bar{\gamma}}^{\chi} \tag{3.89}$$

$$\bar{c}^{\chi} = \bar{H}^{\chi}\bar{Z}^{\chi} \tag{3.90}$$

$$\bar{Q}^{\chi} = \bar{c}^{\chi} \tag{3.91}$$

where $\dot{\bar{\gamma}}^{\chi}$ is the micro-scale plastic multiplier rate in $\bar{\mathcal{B}}$, $\bar{\psi}^{\chi}$ the micro-scale dilation angle.

3.4.3 Micro-scale Gradient Yield, Plastic Potential, and Evolution Equations

Lastly, the yield function, the plastic potential function, and evolution equations of the micro-scale gradient are:

$$\bar{F}^{\nabla\chi}(\bar{\boldsymbol{M}}, \bar{\boldsymbol{c}}^{\nabla\chi}) \stackrel{\text{def}}{=} \|\text{dev}\bar{\boldsymbol{M}}\| - \left(A^{\nabla\chi,\phi}\|\bar{\boldsymbol{c}}^{\nabla\chi}\| - B^{\nabla\chi,\phi}\|\bar{\boldsymbol{p}}^{\nabla\chi}\|\right) \leq 0 \tag{3.92}$$

$$\begin{aligned} A^{\nabla\chi,\phi} &= \beta^{\nabla\chi,\phi}\cos\phi^{\nabla\chi}\ ,\ B^{\nabla\chi,\phi} = \beta^{\nabla\chi,\phi}\sin\phi^{\nabla\chi} \\ \beta^{\nabla\chi,\phi} &= \frac{2\sqrt{6}}{3 + \beta^{\nabla\chi}\sin\phi^{\nabla\chi}} \\ \text{dev}\bar{M}_{\bar{I}\bar{J}\bar{K}} &= \bar{M}_{\bar{I}\bar{J}\bar{K}} - (\bar{C}^{e-1})_{\bar{I}\bar{J}}\,\bar{p}^{\nabla\chi}_{\bar{K}} \\ \bar{p}^{\nabla\chi}_{\bar{K}} &\stackrel{\text{def}}{=} \frac{1}{3}\bar{C}^{e}_{\bar{A}\bar{B}}\bar{M}_{\bar{A}\bar{B}\bar{K}} \end{aligned} \tag{3.93}$$

where $\bar{c}^{\nabla\chi}$ is the micro-scale gradient cohesion in $\bar{\mathcal{B}}$, $\phi^{\nabla\chi}$ the micro-scale gradient friction angle, and $-1 \leq \beta^{\nabla\chi} \leq 1$, and $\beta^{\nabla\chi} = 1$, The plastic potential function and evolution

equations are:

$$\bar{G}^{\nabla\chi}(\bar{\boldsymbol{M}},\bar{\boldsymbol{c}}^{\nabla\chi}) \stackrel{\text{def}}{=} \|\text{dev}\bar{\boldsymbol{M}}\| - \left(A^{\nabla\chi,\psi}\|\bar{\boldsymbol{c}}^{\nabla\chi}\| - B^{\nabla\chi,\psi}\|\bar{\boldsymbol{p}}^{\nabla\chi}\|\right) \tag{3.94}$$

$$\bar{\Psi}^{e}_{\bar{L}\bar{D}}\bar{L}^{\chi,p}_{\bar{D}\bar{M},\bar{K}} - 2\bar{\Psi}^{e}_{\bar{L}\bar{D}}\text{skw}\left[\bar{L}^{\chi,p}_{\bar{D}\bar{C}}(\bar{\Psi}^{e-1})_{\bar{C}\bar{F}}\bar{\Gamma}^{e}_{\bar{F}\bar{M}\bar{K}}\right] \stackrel{\text{def}}{=} \dot{\bar{\gamma}}^{\nabla\chi}\frac{\partial\bar{G}^{\nabla\chi}}{\partial\bar{M}_{\bar{K}\bar{L}\bar{M}}} \tag{3.95}$$

$$A^{\nabla\chi,\psi} = \beta^{\nabla\chi,\psi}\cos\psi^{\nabla\chi}\ ,\ B^{\nabla\chi,\psi} = \beta^{\nabla\chi,\psi}\sin\psi^{\nabla\chi}$$

$$\frac{\partial\bar{G}^{\nabla\chi}}{\partial\bar{M}_{\bar{K}\bar{L}\bar{M}}} = \frac{\text{dev}\bar{M}_{\bar{K}\bar{L}\bar{M}}}{\|\text{dev}\bar{\boldsymbol{M}}\|} + \frac{1}{3}B^{\nabla\chi,\psi}\bar{C}^{e}_{\bar{K}\bar{L}}\frac{\bar{p}^{\nabla\chi}_{\bar{M}}}{\|\bar{\boldsymbol{p}}^{\nabla\chi}\|} \tag{3.96}$$

$$\dot{\bar{Z}}^{\chi}_{\bar{A}} \stackrel{\text{def}}{=} -\dot{\bar{\gamma}}^{\nabla\chi}\frac{\partial\bar{G}^{\nabla\chi}}{\partial\bar{c}^{\nabla\chi}_{\bar{A}}} = A^{\nabla\chi,\psi}(\dot{\bar{\gamma}}^{\nabla\chi})\frac{\bar{c}^{\nabla\chi}_{\bar{A}}}{\|\bar{\boldsymbol{c}}^{\nabla\chi}\|} \tag{3.97}$$

$$\bar{c}^{\nabla\chi}_{\bar{L}} = \bar{H}^{\nabla\chi}\bar{Z}^{\chi}_{,\bar{A}}\delta_{\bar{A}\bar{L}} \tag{3.98}$$

where $\dot{\bar{\gamma}}^{\nabla\chi}$ is the micro-scale gradient plastic multiplier rate in $\bar{\mathcal{B}}$, $\bar{\psi}^{\nabla\chi}$ the micro-scale gradient dilation angle.

3.5 Map to Current Configuration and Numerical Time Integration

Mapping the constitutive equations according to stress mapping relations given in equations (3.19), (3.20), (3.21) and then taking the material time derivatives of the stress tensors provide objective stress rates in the current configuration $\mathcal{B}$. Besides, mapping evolutions to current configuration gives us the corresponding plastic evolution equations in $\mathcal{B}$ (Eringen and Suhubi (1964); Regueiro (2009); Moran et al. (1990); Simo (1998)).

$$\dot{\sigma}_{kl} = -\frac{\dot{J}^e}{(J^e)^2}F^e_{k\bar{K}}F^e_{l\bar{L}}\bar{S}_{\bar{K}\bar{L}} + \frac{1}{J^e}\dot{F}^e_{k\bar{K}}F^e_{\bar{L}}\bar{S}_{\bar{K}\bar{L}} + \frac{1}{J^e}F^e_{k\bar{K}}\dot{F}^e_{\bar{L}}\bar{S}_{\bar{K}\bar{L}} + \frac{1}{J^e}F^e_{k\bar{K}}F^e_{\bar{L}}\dot{\bar{S}}_{\bar{K}\bar{L}} \tag{3.99}$$

$$\begin{aligned}\dot{s}_{kl} - \dot{\sigma}_{kl} = &-\frac{\dot{J}^e}{(J^e)^2}F^e_{k\bar{K}}F^e_{l\bar{L}}\left(\bar{\Sigma}_{\bar{K}\bar{L}} - \bar{S}_{\bar{K}\bar{L}}\right) + \frac{1}{J^e}\dot{F}^e_{k\bar{K}}F^e_{\bar{L}}\left(\bar{\Sigma}_{\bar{K}\bar{L}} - \bar{S}_{\bar{K}\bar{L}}\right)\\ &+ \frac{1}{J^e}F^e_{k\bar{K}}\dot{F}^e_{\bar{L}}\left(\bar{\Sigma}_{\bar{K}\bar{L}} - \bar{S}_{\bar{K}\bar{L}}\right) + \frac{1}{J^e}F^e_{k\bar{K}}F^e_{\bar{L}}\left(\dot{\bar{\Sigma}}_{\bar{K}\bar{L}} - \dot{\bar{S}}_{\bar{K}\bar{L}}\right)\end{aligned} \tag{3.100}$$

$$\begin{aligned}\dot{m}_{klm} = &-\frac{\dot{J}^e}{(J^e)^2}F^e_{k\bar{K}}F^e_{l\bar{L}}\chi^e_{m\bar{M}}\bar{M}_{\bar{K}\bar{L}\bar{M}} + \frac{1}{J^e}\dot{F}^e_{k\bar{K}}F^e_{\bar{L}}\chi^e_{m\bar{M}}\bar{M}_{\bar{K}\bar{L}\bar{M}}\\ &+ \frac{1}{J^e}F^e_{k\bar{K}}\dot{F}^e_{\bar{L}}\chi^e_{m\bar{M}}\bar{M}_{\bar{K}\bar{L}\bar{M}} + \frac{1}{J^e}F^e_{k\bar{K}}\dot{F}^e_{\bar{L}}\dot{\chi}^e_{m\bar{M}}\bar{M}_{\bar{K}\bar{L}\bar{M}} + \frac{1}{J^e}F^e_{k\bar{K}}F^e_{\bar{L}}\chi^e_{m\bar{M}}\dot{\bar{M}}_{\bar{K}\bar{L}\bar{M}}\end{aligned} \tag{3.101}$$

Note that in the mapping of the stress, the stress differences were used instead of micro-stress itself. It is because the stress difference appears as the work conjugate to the chosen metric strain definition in the reduced Clausius-Duhem inequality. If we implement the material time derivatives of the terms appearing in the equations above such as $\dot{F}^e_{k\bar{K}} = \ell^e_{kl} F^e_{l\bar{K}}$ and $\dot{\tilde{S}}_{\bar{K}\bar{L}}$ from equation (3.60), we get;

$$\begin{aligned}\dot{\sigma}_{kl} &= -(d^e_{ii})\sigma_{kl} + \ell^e_{ki}\sigma_{il} + \sigma_{ki}\ell^e_{il} + (\lambda+\tau)\,(d^e_{ii})\delta_{kl} + 2\,(\mu+\sigma)\,d^e_{kl} \\ &\quad + \eta(\varepsilon^e_{ii})\delta_{kl} + \kappa\varepsilon^e_{kl} + \nu\varepsilon^e_{lk} \qquad (3.102)\\ \dot{s}_{kl} - \dot{\sigma}_{kl} &= -(d^e_{ii})\,(s_{kl}-\sigma_{kl}) + \ell^e_{ki}\,(s_{il}-\sigma_{il}) + \tau(d^e_{ii})\delta_{kl} \\ &\quad + 2\sigma d^e_{kl} + (\eta-\tau)\,(\varepsilon^e_{ii})\delta_{kl} + (\nu-\sigma)\,\varepsilon^e_{kl} + (\kappa-\sigma)\,\varepsilon^e_{lk} \qquad (3.103)\\ \dot{m}_{klm} &= -(d^e_{ii})m_{klm} + \ell^e_{ki}m_{ilm} + m_{kim}\ell^e_{il} + m_{kli}\nu^e_{mi} + c_{klmnpq}\overset{\circ e}{\gamma}_{npq} \qquad (3.104)\end{aligned}$$

$$\begin{aligned}c_{klmnpq} \;=\;& \tau_1\,(\delta_{kl}\delta_{mn}\delta_{pq} + \delta_{kq}\delta_{lm}\delta_{np}) + \tau_2\,(\delta_{kl}\delta_{mp}\delta_{nq} + \delta_{km}\delta_{lq}\delta_{np}) \\ &+\tau_3\delta_{kl}\delta_{mq}\delta_{np} + \tau_4\delta_{kn}\delta_{lm}\delta_{pq} + \tau_5\,(\delta_{km}\delta_{ln}\delta_{pq} + \delta_{kp}\delta_{lm}\delta_{nq}) \\ &+\tau_6\delta_{km}\delta_{lp}\delta_{nq} + \tau_7\delta_{kn}\delta_{lp}\delta_{mq} + \tau_8\,(\delta_{kp}\delta_{lq}\delta_{mn} + \delta_{kq}\delta_{ln}\delta_{mp}) \\ &+\tau_9\delta_{kn}\delta_{lq}\delta_{mp} + \tau_{10}\delta_{kp}\delta_{ln}\delta_{mq} + \tau_{11}\delta_{kq}\delta_{lp}\delta_{mn} \qquad (3.105)\end{aligned}$$

where

$$\overset{\circ e}{\gamma}_{npq} = \dot{\gamma}^e_{npq} + \ell^e_{an}\gamma^e_{apq} + \gamma^e_{npa}\ell^e_{aq} + \gamma^e_{naq}\nu^e_{ap} \qquad (3.106)$$

In determining the objective stress rates given above, small elastic deformation is assumed so that the left Cauchy-Green strain tensor, its inverse, and some other strain tensors as well as Jacobian of elastic deformation gradient tensor become heavily unit tensor when multiplied by a deformation rate or stress (Regueiro (2009)). Mapping of the plastic evolution equations result in following yield functions and plastic evolutions equations for, respectively, macro-scale, micro-scale and micro-scale gradient plasticity.

For macro-scale plasticity, the yield function and plastic potential function take the

form below

$$F\left(\boldsymbol{\sigma}, c\right) = J^e \|\mathrm{dev}\boldsymbol{\sigma}\| - J^e\left(A^\phi c - B^\phi p\right) \leq 0 \tag{3.107}$$

$$\|\mathrm{dev}\boldsymbol{\sigma}\| = \sqrt{\mathrm{dev}\sigma_{ij}\mathrm{dev}\sigma_{ij}} \tag{3.108}$$

$$\mathrm{dev}\sigma_{ij} = \sigma_{ij} - p\delta_{ij} \tag{3.109}$$

$$p = \frac{1}{3}\sigma_{ii} \tag{3.110}$$

The plastic potential function and map of the plastic velocity and strain-like ISV in $\mathcal{B}$ become

$$G\left(\boldsymbol{\sigma}, c\right) = J^e \|\mathrm{dev}\boldsymbol{\sigma}\| - J^e\left(A^\phi c - B^\phi p\right) \tag{3.111}$$

$$\ell^p_{lk} = \dot{\gamma}\frac{\partial G}{\partial \sigma_{kl}} \tag{3.112}$$

$$\frac{\partial G}{\partial \sigma_{kl}} = \frac{\mathrm{dev}\sigma_{kl}}{\|\mathrm{dev}\boldsymbol{\sigma}\|} + \frac{1}{3}B^\psi\delta_{kl} \tag{3.113}$$

$$\dot{Z} = -\dot{\gamma}\frac{\partial G}{\partial c} \tag{3.114}$$

$$c = HZ \tag{3.115}$$

For micro-scale plasticity, the yield function in $\mathcal{B}$ is:

$$F\left(\boldsymbol{s}-\boldsymbol{\sigma}, c^\chi\right) = J^e \|\mathrm{dev}\left(\boldsymbol{s}-\boldsymbol{\sigma}\right)\| - J^e\left(A^{\chi,\phi}c^\chi - B^{\chi,\phi}p^\chi\right) \leq 0 \tag{3.116}$$

$$p^\chi = \frac{1}{3}\left(s_{ii} - \sigma_{ii}\right) \tag{3.117}$$

the plastic potential function and the plastic microgyration tensor and strain-like ISV are

$$G\left(\boldsymbol{\sigma}, c\right) = J^e \|\mathrm{dev}\boldsymbol{\sigma}\| - J^e\left(A^{\chi,\psi}c^\chi - B^{\chi,\psi}p^\chi\right) \tag{3.118}$$

$$\nu^p_{lk} = \dot{\gamma}^\chi\frac{\partial G}{\partial\left(s_{kl} - \sigma_{kl}\right)} \tag{3.119}$$

$$\frac{\partial G}{\partial \sigma_{kl}} = \frac{\mathrm{dev}\left(s_{kl} - \sigma_{kl}\right)}{\|\mathrm{dev}\left(\boldsymbol{s}-\boldsymbol{\sigma}\right)\|} + \frac{1}{3}B^{\chi,\psi}\delta_{kl} \tag{3.120}$$

$$\dot{Z}^\chi = -\dot{\gamma}^\chi\frac{\partial G}{\partial c^\chi} \tag{3.121}$$

$$c^\chi = H^\chi Z^\chi \tag{3.122}$$

and similarly for micro-scale gradient yield function

$$F\left(\boldsymbol{m}, \boldsymbol{c}^{\nabla\chi}\right) = J^e\|\mathrm{dev}\boldsymbol{m}\| - J^e\left(A^{\nabla\chi,\phi}\|\boldsymbol{c}^{\nabla\chi}\| - B^{\nabla\chi,\phi}\|\boldsymbol{p}^{\nabla\chi}\|\right) \leq 0 \tag{3.123}$$

$$\|\boldsymbol{m}\| = \sqrt{\left(\mathrm{dev}m_{ijk}\right)\left(\mathrm{dev}m_{ijk}\right)} \tag{3.124}$$

$$\mathrm{dev}m_{ijk} = m_{ijk} - \frac{1}{3}\delta_{ij}m_{aak} \tag{3.125}$$

$$\|\boldsymbol{p}^{\nabla\chi}\| = \sqrt{p_m^{\nabla\chi}p_m^{\nabla\chi}} \tag{3.126}$$

$$\|\boldsymbol{c}^{\nabla\chi}\| = \sqrt{c_m^{\nabla\chi}c_m^{\nabla\chi}} \tag{3.127}$$

$$p_m^{\nabla\chi} = \frac{1}{3}m_{kkm} \tag{3.128}$$

and the plastic potential function also the map of the gradient plastic microgyrataion tensor and strain-like ISV become

$$G^{\nabla\chi}\left(\boldsymbol{m}, \boldsymbol{c}^{\nabla\chi}\right) = J^e\|\mathrm{dev}\boldsymbol{m}\| - J^e\left(A^{\nabla\chi,\psi}\|\boldsymbol{c}^{\nabla\chi}\| - B^{\nabla\chi,\psi}\|\boldsymbol{p}^{\nabla\chi}\|\right) \tag{3.129}$$

$$\nu^p_{lm,k} = \dot{\gamma}^{\nabla\chi}\frac{\partial G^{\nabla\chi}}{\partial m_{klm}} \tag{3.130}$$

$$\frac{\partial G^{\nabla\chi}}{\partial m_{klm}} = \frac{\mathrm{dev}m_{klm}}{\|\mathrm{dev}\boldsymbol{m}\|} + \frac{1}{3}B^{\nabla\chi,\psi}\delta_{kl}\frac{p_m^{\nabla\chi}}{\|\boldsymbol{p}^{\nabla\chi}\|} \tag{3.131}$$

$$\dot{Z}^{\chi}_{,a} = -\dot{\gamma}^{\nabla\chi}\frac{\partial G^{\nabla\chi}}{\partial c_a^{\nabla\chi}} = A^{\nabla\chi,\phi}(\dot{\gamma}^{\nabla\chi})\frac{c_a^{\nabla\chi}}{\|\boldsymbol{c}^{\nabla\chi}\|} \tag{3.132}$$

$$c_l^{\nabla\chi} = H^{\nabla\chi}Z^{\nabla\chi}_{,l} \tag{3.133}$$

3.5.1 Numerical Time Integration

The objective stress rates presented in equations (3.102), (3.103), (3.104) may be integrated with a semi implicit time integration approach such that the unsymmetric Cauchy stress tensor, the difference of micro-stress tensor and Cauchy stress tensor, and higher order

couple stress tensor at $n+1$ time step can be expressed as:

$$\begin{aligned}\boldsymbol{\sigma}_{n+1} = &\left(1 - tr\left(\Delta t \boldsymbol{d}^e_{n+1}\right)\right)\boldsymbol{\sigma}_n + \left(\Delta t \boldsymbol{\ell}^e_{n+1}\right)\boldsymbol{\sigma}_n + \boldsymbol{\sigma}_n\left(\Delta t \boldsymbol{\ell}^e_{n+1}\right)^T \\ &+ (\lambda+\tau)\, tr\left(\Delta t \boldsymbol{d}^e_{n+1}\right)\mathbf{1} + 2(\mu+\sigma)\left(\Delta t \boldsymbol{d}^e_{n+1}\right) + \eta tr\left(\Delta t \boldsymbol{\varepsilon}^e_{n+1}\right)\mathbf{1} \\ &+ \kappa\left(\Delta t \boldsymbol{\varepsilon}^e_{n+1}\right) + \nu\left(\Delta t \boldsymbol{\varepsilon}^e_{n+1}\right)^T \end{aligned} \tag{3.134}$$

$$\begin{aligned}(\boldsymbol{s}-\boldsymbol{\sigma})_{n+1} = &\left(1 - tr\left(\Delta t \boldsymbol{d}^e_{n+1}\right)\right)(\boldsymbol{s}-\boldsymbol{\sigma})_n + \left(\Delta t \boldsymbol{\ell}^e_{n+1}\right)(\boldsymbol{s}-\boldsymbol{\sigma})_n \\ &+ (\boldsymbol{s}-\boldsymbol{\sigma})_n\left(\Delta t \boldsymbol{\ell}^e_{n+1}\right)^T + (\kappa-\sigma)\left(\Delta t \boldsymbol{\varepsilon}^e_{n+1}\right)^T \\ &+ (\nu-\sigma)\left(\Delta t \boldsymbol{\varepsilon}^e_{n+1}\right) + \tau tr\left(\Delta t \boldsymbol{d}^e_{n+1}\right)\mathbf{1} \\ &+ 2\sigma\Delta t \boldsymbol{d}^e_{n+1} + (\eta-\tau)\, tr\left(\Delta t \boldsymbol{\varepsilon}^e_{n+1}\right)\mathbf{1} \end{aligned} \tag{3.135}$$

$$\begin{aligned}\boldsymbol{m}_{n+1} = &\left(1 - tr\left(\Delta t \boldsymbol{d}^e_{n+1}\right)\right)\boldsymbol{m}_n + \left(\Delta t \boldsymbol{\ell}^e_{n+1}\right)\boldsymbol{m}_n + \boldsymbol{m}_n \odot \left(\Delta t \boldsymbol{\ell}^e_{n+1}\right)^T \\ &+ \boldsymbol{m}_n\left(\Delta t \boldsymbol{\nu}^e_{n+1}\right)^T + \boldsymbol{c}\vdots\left(\Delta t \overset{\circ}{\boldsymbol{\gamma}}{}^e_{n+1}\right) \end{aligned} \tag{3.136}$$

where

$$\Delta t \overset{\circ}{\boldsymbol{\gamma}}{}^e_{n+1} = \Delta t \dot{\boldsymbol{\gamma}}^e_{n+1} + \left(\Delta t \boldsymbol{\ell}^e_{n+1}\right)^T \boldsymbol{\gamma}^e_n + \boldsymbol{\gamma}^e_n\left(\Delta t \boldsymbol{\ell}^e_{n+1}\right) + \boldsymbol{\gamma}^e_n \odot \left(\Delta t \boldsymbol{\nu}^e_{n+1}\right) \tag{3.137}$$

$$\Delta t \dot{\boldsymbol{\gamma}}^e_{n+1} = \left(\Delta t \boldsymbol{\nu}^e_{n+1}\right)\boldsymbol{\gamma}^e_n - \left(\Delta t \boldsymbol{\nu}^e_{n+1}\right)^T \odot \boldsymbol{\gamma}^e_n + \Delta t \boldsymbol{\nabla}\boldsymbol{\nu}^e_{n+1} - \Delta t \boldsymbol{\nabla}\boldsymbol{\nu}^p_{n+1} \tag{3.138}$$

$$\Delta t \boldsymbol{\nabla}\boldsymbol{\nu}^e_{n+1} = \boldsymbol{\nabla}\left(\boldsymbol{\chi}_{n+1} - \boldsymbol{\chi}_n\right) \odot \boldsymbol{\chi}^{-1}_{n+1} + \left(\boldsymbol{\chi}_{n+1} - \boldsymbol{\chi}_n\right)\boldsymbol{\chi}^{-1}_{n+1}\left(\boldsymbol{\nabla}\boldsymbol{\chi}_{n+1}\right) \odot \boldsymbol{\chi}^{-1}_{n+1} \tag{3.139}$$

$$\Delta t \boldsymbol{\nabla}\boldsymbol{\nu}^p_{n+1} = \left(\Delta \gamma^{\nabla\chi}_{n+1}\right)\left(\boldsymbol{r}^{\nabla\chi,tr}\right)^{tr} \tag{3.140}$$

$$\left(\boldsymbol{r}^{\nabla\chi,tr}\right)^{tr} = \frac{\mathrm{dev}\boldsymbol{m}}{\|\mathrm{dev}\boldsymbol{m}\|} + \frac{1}{3}B^{\nabla\chi,\psi}\mathbf{1} \otimes \frac{\boldsymbol{p}^{\nabla\chi,tr}}{\|\boldsymbol{p}^{\nabla\chi,tr}\|} \tag{3.141}$$

Note that the terms with the subscript n in the right hand side of the equations are the terms converged in the previous time step while the terms with the subscript $n+1$ are belong to the current time step. Then we have two cases as:

(1) By using these equations above we calculate the trial stresses and then correct them to use in the yield functions. We have the plastic yielding checks at each scale as:

- If $F^{tr} > 0$ and $F^{\chi,tr} > 0$, yielding occurs at each scales. Then we solve for $\Delta\gamma_{n+1}$ and $\Delta\gamma^{\chi}_{n+1}$ using Newton-Raphson for coupled equations

$$F\left(\boldsymbol{\sigma}_{n+1}, c_{n+1}\right) = F\left(\Delta\gamma_{n+1}, \Delta\gamma^{\chi}_{n+1}\right) = 0 \tag{3.142}$$

$$F^{\chi}\left(\left(\boldsymbol{s}_{n+1} - \boldsymbol{\sigma}_{n+1}\right), c^{\chi}_{n+1}\right) = F^{\chi}\left(\Delta\gamma_{n+1}, \Delta\gamma^{\chi}_{n+1}\right) = 0 \tag{3.143}$$

- If $F^{tr} > 0$ and $F^{\chi,tr} < 0$, yielding occurs at macro-scale only. We solve for $\Delta\gamma_{n+1}$ and $\Delta\gamma^{\chi}_{n+1} = 0$ using Newton-Raphson

$$F\left(\boldsymbol{\sigma}_{n+1}, c_{n+1}\right) = F\left(\Delta\gamma_{n+1}, \Delta\gamma^{\chi}_{n+1} = 0\right) = 0 \tag{3.144}$$

- If $F^{tr} < 0$ and $F^{\chi,tr} > 0$, yielding occurs only in micro-scale. Then, we solve for $\Delta\gamma^{\chi}_{n+1}$ and $\Delta\gamma_{n+1} = 0$ using Newton-Raphson

$$F^{\chi}\left(\left(\boldsymbol{s}_{n+1} - \boldsymbol{\sigma}_{n+1}\right), c^{\chi}_{n+1}\right) = F^{\chi}\left(\Delta\gamma_{n+1} = 0, \Delta\gamma^{\chi}_{n+1}\right) = 0 \tag{3.145}$$

(2) We compute the trial yield function using the trial stress value $\boldsymbol{m}^{tr}$ and solve for $\Delta\gamma^{\nabla\chi}_{n+1}$ using Newton-Raphson

$$F^{\nabla\chi}\left(\boldsymbol{m}_{n+1}, \boldsymbol{c}^{\nabla\chi}_{n+1}\right) = F^{\nabla\chi}\left(\Delta\gamma^{\nabla\chi}_{n+1}\right) = 0 \tag{3.146}$$

Chapter 4

Finite Element Formulation of Finite Strain Micromorphic Elasticity at Current Configuration

4.1 Weak Form and Linearization of the Balance of Linear Momentum

The local form of balance of linear momentum is :

$$\sigma_{lk,l} + \rho(f_k - a_k) = 0 \tag{4.1}$$

If we multiply the weak form of (4.1) with a weight function and apply divergence theorem, we get :

$$\begin{aligned}\int_V w_k \left(\sigma_{lk,l} + \rho(f_k - a_k)\right) dv = &\int_S w_k \sigma_{lk} n_l da \\ &- \int_V \left[w_{k,l}\sigma_{lk} + w_k \left(\rho(f_k - a_k)\right)\right] dv = 0 \end{aligned} \tag{4.2}$$

$$\int_S w_k \sigma_{lk} J N_K F^{-1}_{Kl} dA - \int_V \left[w_{k,l}\sigma_{lk} + w_k \left(\rho(f_k - a_k)\right)\right] J dV = 0 \tag{4.3}$$

To linearize the balance equation, we should find the variation $\delta(.)$ of the equation. The aim of linearization is to obtain the consistent tangent matrix to apply within the Newton-Raphson algorithm. (4.3).

$$\begin{aligned}&\int_S w_k \sigma_{lk} J N_K F^{-1}_{Kl} dA - \int_V \left[w_{k,l}\sigma_{lk} + w_k \left(\rho(f_k - a_k)\right)\right] J dV \\ &\delta\left(\int_S w_k \sigma_{lk} J N_K F^{-1}_{Kl} dA - \int_V \left[w_{k,l}\sigma_{lk} + w_k \left(\rho(f_k - a_k)\right)\right] J dV\right) = 0 \end{aligned} \tag{4.4}$$

Note that area change is :

$$n_l da = J F^{-1}_{Kl} N_K dA \tag{4.5}$$

and Piola transform of Cauchy's stress tensor

$$P_{lL} = J\sigma_{lk}F^{-1}_{Lk} \tag{4.6}$$

Then, variation of equation (4.3) is:

$$\delta\left(\int_S w_k T_k dA\right) - \delta\left[\int_V \left[w_{k,l}\sigma_{lk}J + w_k\left(\rho(f_k - a_k)\right)J\right]dV\right] = 0 \tag{4.7}$$

where $T_k = P_{kL}N_L$ and variation of the volume integral will be:

$$\begin{aligned}\delta\left[\int_V \left(\boldsymbol{\nabla w}^T : \boldsymbol{\sigma}J + \boldsymbol{w}.\rho(\boldsymbol{f} - \boldsymbol{a})J\right)dV\right] &= \delta\left(\int_V \left(\boldsymbol{\nabla w}\right)^T : \boldsymbol{\sigma}JdV\right) \\ &+ \delta\left(\int_V \boldsymbol{w}.\left(\rho_0(\boldsymbol{f} - \boldsymbol{a})\right)dV\right)\end{aligned} \tag{4.8}$$

Variation of the first integrand at right hand side of equation (4.8) is:

$$\begin{aligned}\delta\left(\boldsymbol{\nabla w}\right)^T : \boldsymbol{\sigma}J + \left(\boldsymbol{\nabla w}\right)^T : \delta\boldsymbol{\sigma}J + \left(\boldsymbol{\nabla w}\right)^T : \boldsymbol{\sigma}\delta\left(J\right) &= \left(\boldsymbol{\nabla w}\right)^T : \delta\boldsymbol{\sigma}J \\ &+ \left(\boldsymbol{\nabla w}\right)^T : \boldsymbol{\sigma}\delta\left(J\right)\end{aligned} \tag{4.9}$$

or $\delta\left(\boldsymbol{\nabla w}\right)^T : \boldsymbol{\sigma}J$ can be assumed as:

$$\begin{aligned}\delta\left(\frac{\partial w_k}{\partial x_l}\right)\sigma_{lk}J = \delta\left(\frac{\partial w_k}{\partial X_L}F^{-1}_{Ll}\right)\sigma_{lk}J &= \left(\underbrace{\frac{\partial \delta w_k}{\partial X_L}}_{0}F^{-1}_{Ll} + \frac{\partial w_k}{\partial X_L}\delta F^{-1}_{Ll}\right)\sigma_{lk}J \\ &= -w_{k,L}F^{-1}_{Lm}\delta u_{m,l}\sigma_{lk}J\end{aligned} \tag{4.10}$$

In order to calculate the second term, $\left(\nabla \boldsymbol{w}\right)^T : \delta\boldsymbol{\sigma}J$, the variation of $\delta\boldsymbol{\sigma}$ must be determined as given below where $\boldsymbol{\sigma}_{n+1}$ was defined in equation 3.134 as:

$$\begin{aligned}\boldsymbol{\sigma}_{n+1} &= \left(1 - tr\left(\Delta t\boldsymbol{d}^e_{n+1}\right)\right)\boldsymbol{\sigma}_n + \left(\Delta t\boldsymbol{\ell}^e_{n+1}\right)\boldsymbol{\sigma}_n + \boldsymbol{\sigma}_n\left(\Delta t\boldsymbol{\ell}^e_{n+1}\right)^T \\ &+ \left(\lambda + \tau\right)tr\left(\Delta t\boldsymbol{d}^e_{n+1}\right)\mathbf{1} + 2\left(\mu + \sigma\right)\left(\Delta t\boldsymbol{d}^e_{n+1}\right) + \eta tr\left(\Delta t\boldsymbol{\varepsilon}^e_{n+1}\right)\mathbf{1} \\ &+ \kappa\left(\Delta t\boldsymbol{\varepsilon}^e_{n+1}\right) + \nu\left(\Delta t\boldsymbol{\varepsilon}^e_{n+1}\right)^T\end{aligned} \tag{4.11}$$

where

$$\Delta t\boldsymbol{\varepsilon}^e_{n+1} = \Delta t\boldsymbol{\nu}^e_{n+1} + \left(\Delta t\boldsymbol{\ell}^e_{n+1}\right)^T \tag{4.12}$$

$$\Delta t\boldsymbol{\nu}^e_{n+1} = \left(\Delta\boldsymbol{\chi}_{n+1}\right)\boldsymbol{\chi}^{-1}_{n+1} \tag{4.13}$$

$$\Rightarrow \Delta t\boldsymbol{\varepsilon}^e_{n+1} = \left(\Delta\boldsymbol{\chi}_{n+1}\right)\boldsymbol{\chi}^{-1}_{n+1} + \left(\Delta t\boldsymbol{\ell}^e_{n+1}\right)^T \tag{4.14}$$

Then variation of $\boldsymbol{\sigma}_{n+1}$ is found as :

$$\begin{aligned}
\delta\sigma_{lk} = &- \left((F_n)_{iL}\, F^{-1}_{Lm}\delta u_{m,i}\right)(\sigma_n)_{lk} + \left((F_n)_{lL}\, F^{-1}_{Lm}\delta u_{m,i}\right)(\sigma_n)_{ik} \\
&+ (\sigma_n)_{li}\left((F_n)_{kL}\, F^{-1}_{Lm}\delta u_{m,i}\right) + (\lambda+\tau)\left((F_n)_{iL}\, F^{-1}_{Lm}\delta u_{m,i}\right)\delta_{lk} \\
&+ (\mu+\sigma)\left((F_n)_{lL}\, F^{-1}_{Lm}\delta u_{m,k}\right) + (\mu+\sigma)\left((F_n)_{kL}\, F^{-1}_{Lm}\delta u_{m,l}\right) \\
&+ \eta\left((\chi_n)_{iL}\,\chi^{-1}_{Lm}\left(\delta\Phi_{mT}\right)\chi^{-1}_{Ti}\right)\delta_{lk} + \eta\left((F_n)_{iL}\, F^{-1}_{Lm}\delta u_{m,i}\right)\delta_{lk} \\
&+ \kappa\left((\chi_n)_{lL}\,\chi^{-1}_{Lm}\left(\delta\Phi_{mT}\right)\chi^{-1}_{Tk}\right) + \kappa\left((F_n)_{kL}\, F^{-1}_{Lm}\delta u_{m,l}\right) \\
&+ \nu\left((\chi_n)_{kL}\,\chi^{-1}_{Lm}\left(\delta\Phi_{mT}\right)\chi^{-1}_{Tl}\right) + \nu\left((F_n)_{lL}\, F^{-1}_{Lm}\delta u_{m,k}\right)
\end{aligned} \tag{4.15}$$

Lastly, the third term in equation (4.9) will be equal to :

$$\left(\nabla\boldsymbol{w}\right)^T : \boldsymbol{\sigma}\delta J = \left(\nabla\boldsymbol{w}\right)^T : \boldsymbol{\sigma}\left(Jdiv(\delta(\boldsymbol{u})\right) \tag{4.16}$$

Variation of the second integrand in (4.8) for quasi static case is :

$$\delta(\boldsymbol{w}\boldsymbol{f}\rho_0) = \delta(\boldsymbol{w})\boldsymbol{f}\rho_0 + \boldsymbol{w}\delta(\boldsymbol{f})\rho_0 + \boldsymbol{w}\boldsymbol{f}\delta(\rho_0) = 0 \tag{4.17}$$

Variation of the traction term :

$$\begin{aligned}
\delta\left(\int \boldsymbol{w}\boldsymbol{T}dA\right) &= \int\left(\delta\left(\boldsymbol{w}\right)\boldsymbol{T} + \boldsymbol{w}.\delta(\boldsymbol{T})\right)dA \\
\Rightarrow \delta\left(\int \boldsymbol{w}.\boldsymbol{T}dA\right) &= \int \boldsymbol{w}.\delta(\boldsymbol{T})dA
\end{aligned} \tag{4.18}$$

where $\delta\left(\boldsymbol{T}\right)$ depends on application of traction load.

4.2 Weak Form and Linearization of the Balance of First Moment of Momentum

The local form of balance of first moment of momentum is :

$$\sigma_{ml} - s_{ml} + m_{klm,k} + \rho(\lambda_{lm} - \omega_{lm}) \tag{4.19}$$

If the same procedure is applied as we did for equation (4.3), we get ;

$$\begin{aligned}\int_V \eta_{ml}(\sigma_{ml} - s_{ml} + m_{klm,k} + \rho(\lambda_{lm} - \omega_{lm}))dv = \int_S (\eta_{ml} m_{klm})\, n_k da \\ - \int_v \eta_{ml,k} m_{klm} dv + \int_v \eta_{ml}(\sigma_{ml} - s_{ml} + \rho(\lambda_{lm} - \omega_{lm}))dv\end{aligned} \tag{4.20}$$

where η_{ml} is the wighthing function for the micro-displacement tensor ϕ_{ml} If equation (4.6) is applied to equation (4.20) , we get :

$$\begin{aligned}\eta_{ml} m_{klm} n_k da &= \eta_{ml} m_{klm} J F^{-1}_{Kk} N_K dA \\ &= \eta_{ml} \underbrace{m_{klm} J F^{-1}_{Kk}}_{M_{lmK}} N_K dA \\ \eta_{ml} m_{klm} n_k da &= \eta_{ml} \underbrace{M_{lmK} N_K}_{F_{lm}} dA \\ \eta_{ml} m_{klm} n_k da &= \eta_{ml} F_{lm} dA\end{aligned} \tag{4.21}$$

Then, equation (4.20) will be :

$$\begin{aligned}\int_S \eta_{ml} M_{lmK} N_K dA - \int_V \eta_{ml,k} m_{klm} J dV \\ + \int_V \eta_{ml}(\sigma_{ml} - s_{ml} + \rho(\lambda_{lm} - \omega_{lm}))J dV = 0\end{aligned} \tag{4.22}$$

Variation of (4.22) is:

$$\begin{aligned}\int_S \eta_{ml} M_{lmK} N_K dA - \int_V \eta_{ml,k} m_{klm} J dV \\ + \int_V \eta_{ml}(\sigma_{ml} - s_{ml} + \rho(\lambda_{lm} - \omega_{lm}))J dV + \delta \left(\int_S \eta_{ml} M_{lmK} N_K dA - \int_V \eta_{ml,k} m_{klm} J dV \right. \\ \left. + \int_V \eta_{ml}(\sigma_{ml} - s_{ml} + \rho(\lambda_{lm} - \omega_{lm}))J dV \right) = 0\end{aligned} \tag{4.23}$$

$$\int_S \eta_{ml} M_{lmK} N_K dA - \int_V \eta_{ml,k} m_{klm} J dV$$
$$+ \int_V \eta_{ml}(\sigma_{ml} - s_{ml} + \rho(\lambda_{lm} - \omega_{lm}))JdV + \delta\left(\int_S \eta_{ml} \boldsymbol{F}_{lm} dA\right) - \delta\left(\int_V \eta_{ml,k} m_{klm} J dV\right)$$
$$+\delta\left(\int_V \eta_{ml}(\sigma_{ml} - s_{ml} + \rho(\lambda_{lm} - \omega_{lm}))JdV\right) = 0 \tag{4.24}$$

Variation of the area integral :

$$\delta\left(\int_S \eta_{ml} \boldsymbol{F}_{lm} dA\right) = \left(\int_S \eta_{ml} \delta\left(\boldsymbol{F}_{lm}\right) dA\right) \tag{4.25}$$

Variation of the second integral in (4.23):

$$\delta\left(\int_V \eta_{ml,k} m_{klm} J dV\right) = \int_V \delta\left(\eta_{ml,k}\right) m_{klm} J dV + \int_V \eta_{ml,k} \delta\left(m_{klm}\right) J dV$$
$$+ \int_V \eta_{ml,k} m_{klm} \delta\left(J\right) dV \tag{4.26}$$

where $\delta\left(\eta_{ml,k}\right)$ can be obtained as:

$$\delta\left(\eta_{ml,k}\right) m_{klm} J = \delta\left(\frac{\partial \eta_{ml}}{\partial X_K}\frac{\partial X_K}{\partial x_k}\right) m_{klm} J = \delta\left(\frac{\partial \eta_{ml}}{\partial X_K} F^{-1}_{Kk}\right) m_{klm} J$$
$$= \eta_{ml,K} F^{-1}_{Ka} \delta u_{a,L} F^{-1}_{Lk} \tag{4.27}$$

In order to calculate the variation of the second term at the right hand side of equation (4.26), someone should calculate the $\delta(\boldsymbol{m})$ where $\boldsymbol{m}$ was expressed in equation 3.136 as :

$$\boldsymbol{m}_{n+1} = \left(1 - tr\left(\Delta t \boldsymbol{d}^e_{n+1}\right)\right) \boldsymbol{m}_n + \left(\Delta t \boldsymbol{\ell}^e_{n+1}\right) \boldsymbol{m}_n + \boldsymbol{m}_n \odot \left(\Delta t \boldsymbol{\ell}^e_{n+1}\right)^T$$
$$+ \boldsymbol{m}_n \left(\Delta t \boldsymbol{\nu}^e_{n+1}\right)^T + \boldsymbol{c} \vdots \left(\Delta t \overset{\circ}{\boldsymbol{\gamma}}{}^e_{n+1}\right) \tag{4.28}$$

where

$$\Delta t \overset{\circ}{\boldsymbol{\gamma}}{}^e_{n+1} = \Delta t \dot{\boldsymbol{\gamma}}^e_{n+1} + \left(\Delta t \boldsymbol{\ell}^e_{n+1}\right)^T \boldsymbol{\gamma}^e_n + \boldsymbol{\gamma}^e_n \left(\Delta t \boldsymbol{\ell}^e_{n+1}\right) + \boldsymbol{\gamma}^e_n \odot \left(\Delta t \boldsymbol{\nu}^e_{n+1}\right) \tag{4.29}$$

$$\Delta t \dot{\boldsymbol{\gamma}}^e_{n+1} = \left(\Delta t \boldsymbol{\nu}^e_{n+1}\right) \boldsymbol{\gamma}^e_n - \left(\Delta t \boldsymbol{\nu}^e_{n+1}\right)^T \odot \boldsymbol{\gamma}^e_n + \Delta t \boldsymbol{\nabla} \boldsymbol{\nu}^e_{n+1} - \underbrace{\Delta t \boldsymbol{\nabla} \boldsymbol{\nu}^p_{n+1}}_{\text{0 for elastic case}} \tag{4.30}$$

$$\Delta t \boldsymbol{\nabla} \boldsymbol{\nu}^e_{n+1} = \boldsymbol{\nabla}\left(\boldsymbol{\chi}_{n+1} - \boldsymbol{\chi}_n\right) \odot \boldsymbol{\chi}^{-1}_{n+1} + \left(\boldsymbol{\chi}_{n+1} - \boldsymbol{\chi}_n\right) \boldsymbol{\chi}^{-1}_{n+1} \left(\boldsymbol{\nabla} \boldsymbol{\chi}_{n+1}\right) \odot \boldsymbol{\chi}^{-1}_{n+1} \tag{4.31}$$

Variation of the $\Delta t \boldsymbol{\nabla} \boldsymbol{\nu}^e_{n+1}$ is quite complicated. Therefore, it may be useful to give it in indicial form as:

$$\nu_{pr,s} = \left[\dot{\chi}_{pA}\chi^{-1}_{Ar}\right]_{,s} = \dot{\chi}_{pA,s}\chi^{-1}_{Ar} + \dot{\chi}_{pA}\chi^{-1}_{Ar,s}$$

Integration in time gives:

$$\begin{aligned}
\Delta t\nu_{pr,s} &= \Delta t\dot{\chi}_{pA,s}\chi^{-1}_{Ar} + \Delta t\dot{\chi}_{pA}\chi^{-1}_{Ar,s} \\
&= \left(\chi_{pA,s} - (\chi_n)_{pA,s}\right)\chi^{-1}_{Ar} + \left(\chi_{pA} - (\chi_n)_{pA}\right)\chi^{-1}_{Ar,s} \\
&= \left(\chi_{pA,s} - (\chi_n)_{pA,T}\right)F^{-1}_{Ts}\chi^{-1}_{Ar} + \left(\chi_{pA} - (\chi_n)_{pA}\right)\chi^{-1}_{Ar,T}F^{-1}_{Ts} \\
\Delta t\nu_{pr,s} &= \left(\chi_{pA,s} - (\chi_n)_{pA,T}\right)F^{-1}_{Ts}\chi^{-1}_{Ar} + \left(\chi_{pA} - (\chi_n)_{pA}\right)\chi^{-1}_{Aa}\frac{\partial \chi_{aB}}{\partial X_T}\chi^{-1}_{Br}F^{-1}_{Ts} \qquad (4.32)
\end{aligned}$$

Then, we take the varitation of the terms as :

$$\begin{aligned}
\delta\left(\Delta t\nu_{pr,s}\right) &= \delta\left(\chi_{pA,T} - (\chi_n)_{pA,T}\right)F^{-1}_{Ts}\chi^{-1}_{Ar} + \left(\chi_{pA,T} - (\chi_n)_{pA,T}\right)\delta F^{-1}_{Ts}\chi^{-1}_{Ar} \\
&+ \left(\chi_{pA,T} - (\chi_n)_{pA,T}\right)F^{-1}_{Ts}\delta\left(\chi^{-1}_{Ar}\right) + \delta\left(\chi_{pA} - (\chi_n)_{pA}\right)\chi^{-1}_{Aa}\frac{\partial \chi_{aB}}{\partial X_T}\chi^{-1}_{Br}F^{-1}_{Ts} \\
&+ \left(\chi_{pA} - (\chi_n)_{pA}\right)\delta\chi^{-1}_{Aa}\frac{\partial \chi_{aB}}{\partial X_T}\chi^{-1}_{Br}F^{-1}_{Ts} \\
&+ \left(\chi_{pA} - (\chi_n)_{pA}\right)\chi^{-1}_{Aa}\delta\left(\frac{\partial \chi_{aB}}{\partial X_T}\right)\chi^{-1}_{Br}F^{-1}_{Ts} \\
&+ \left(\chi_{pA} - (\chi_n)_{pA}\right)\chi^{-1}_{Aa}\frac{\partial \chi_{aB}}{\partial X_T}\delta\chi^{-1}_{Br}F^{-1}_{Ts} \\
&+ \left(\chi_{pA} - (\chi_n)_{pA}\right)\chi^{-1}_{Aa}\frac{\partial \chi_{aB}}{\partial X_T}\chi^{-1}_{Br}\delta F^{-1}_{Ts}
\end{aligned}$$

If we apply equations (A.3) and (A.9) as:

$$\begin{aligned}
\delta\left(\Delta t\nu_{pr,s}\right) &= \delta\left(\frac{\partial \chi_{pA}}{\partial X_T}\right)F^{-1}_{Ts}\chi^{-1}_{Ar} - \left(\chi_{pA,T} - (\chi_n)_{pA,T}\right)F^{-1}_{Ta}\delta F_{aB}F^{-1}_{Bs}\chi^{-1}_{Ar} \\
&+ \left(\chi_{pA,T} - (\chi_n)_{pA,T}\right)F^{-1}_{Ts}\chi^{-1}_{Aa}\delta\chi_{aB}\chi^{-1}_{Br} + \delta\left(\chi_{pA}\right)\chi^{-1}_{Aa}\frac{\partial \chi_{aB}}{\partial X_T}\chi^{-1}_{Br}F^{-1}_{Ts} \\
&- \left(\chi_{pA} - (\chi_n)_{pA}\right)\chi^{-1}_{Ai}\delta\chi_{iL}\chi^{-1}_{La}\frac{\partial \chi_{aB}}{\partial X_T}\chi^{-1}_{Br}F^{-1}_{Ts} \\
&+ \left(\chi_{pA} - (\chi_n)_{pA}\right)\chi^{-1}_{Aa}\delta\left(\frac{\partial \chi_{aB}}{\partial X_T}\right)\chi^{-1}_{Br}F^{-1}_{Ts} \\
&- \left(\chi_{pA} - (\chi_n)_{pA}\right)\chi^{-1}_{Aa}\frac{\partial \chi_{aB}}{\partial X_T}\chi^{-1}_{Bi}\delta\chi_{iL}\chi^{-1}_{Lr}F^{-1}_{Ts} \\
&- \left(\chi_{pA} - (\chi_n)_{pA}\right)\chi^{-1}_{Aa}\frac{\partial \chi_{aB}}{\partial X_T}\chi^{-1}_{Br}F^{-1}_{Ti}\delta F_{iL}F^{-1}_{Ls}
\end{aligned}$$

and applying equations (A.2) and (A.8) gives:

$$\begin{aligned}
\delta\left(\Delta t\nu_{pr,s}\right) = {} & \delta\left(\Phi_{pA,T}\right) F_{Ts}^{-1}\chi_{Ar}^{-1} - \left(\chi_{pA,T} - \left(\chi_n\right)_{pA,T}\right) F_{Ta}^{-1}\delta\left(u_{a,s}\right)\chi_{Ar}^{-1} \\
& + \left(\chi_{pA,T} - \left(\chi_n\right)_{pA,T}\right) F_{Ts}^{-1}\chi_{Aa}^{-1}\delta\Phi_{aB}\chi_{Br}^{-1} + \delta\left(\Phi_{pA}\right)\chi_{Aa}^{-1}\chi_{aB,T}\chi_{Br}^{-1}F_{Ts}^{-1} \\
& - \left(\chi_{pA} - \left(\chi_n\right)_{pA}\right)\chi_{Ai}^{-1}\delta\Phi_{iL}\chi_{La}^{-1}\chi_{aB,T}\chi_{Br}^{-1}F_{Ts}^{-1} \\
& + \left(\chi_{pA} - \left(\chi_n\right)_{pA}\right)\chi_{Aa}^{-1}\delta\Phi_{aB,T}\chi_{Br}^{-1}F_{Ts}^{-1} \\
& - \left(\chi_{pA} - \left(\chi_n\right)_{pA}\right)\chi_{Aa}^{-1}\chi_{aB,T}\chi_{Bi}^{-1}\delta\Phi_{iL}\chi_{Lr}^{-1}F_{Ts}^{-1} \\
& - \left(\chi_{pA} - \left(\chi_n\right)_{pA}\right)\chi_{Aa}^{-1}\chi_{aB,T}\chi_{Br}^{-1}F_{Ti}^{-1}\delta\left(u_{i,s}\right)
\end{aligned} \tag{4.33}$$

The variation of $\boldsymbol{m}_{n+1}$ depends on the variation of each term given in equation (3.136). These terms,basically, are related to the $\left(\Delta t\boldsymbol{\ell}_{n+1}^{e}\right)$, $\left(\Delta t\boldsymbol{d}_{n+1}^{e}\right)$, $\boldsymbol{\chi}_{n+1}$and $\left(\boldsymbol{\nabla\chi}_{n+1}\right)$. Note that variation of these terms are given in equations (A.5),(A.6),(A.8) and (A.11) respectively. Also variation of the term $\Delta t\boldsymbol{\nabla\nu}_{n+1}^{e}$ is given seperately in equation (4.33). Therefore, variation of $\boldsymbol{m}_{n+1}$ can be obtained as:

$$
\begin{aligned}
\delta m_{klm} = & -\left(\left(F_n\right)_{iL} F_{Ln}^{-1}\delta u_{n,i}\right)\left(m_n\right)_{klm} + \left(\left(F_n\right)_{kL} F_{Ln}^{-1}\delta u_{n,i}\right)\left(m_n\right)_{ilm} \\
& + \left(m_n\right)_{kim}\left(\left(F_n\right)_{lL} F_{Ln}^{-1}\delta u_{n,i}\right) + \left(m_n\right)_{kli}\left(\left(\chi_n\right)_{mL}\chi_{Lp}^{-1}\delta\Phi_{pT}\chi_{Ti}^{-1}\right) \\
& + c_{klmprs}\left[\left(\left(\chi_n\right)_{pL}\chi_{Ln}^{-1}\delta\Phi_{nT}\chi_{Ti}^{-1}\right)\left(\gamma_n^e\right)_{irs} - \left(\left(\chi_n\right)_{iL}\chi_{Ln}^{-1}\delta\Phi_{nT}\chi_{Tr}^{-1}\right)\left(\gamma_n^e\right)_{pis}\right. \\
& + \delta\left(\Phi_{pA,T}\right)F_{Ts}^{-1}\chi_{Ar}^{-1} - \left(\chi_{pA,T} - \left(\chi_n\right)_{pA,T}\right)F_{Ta}^{-1}\delta\left(u_{a,s}\right)\chi_{Ar}^{-1} \\
& + \left(\chi_{pA,T} - \left(\chi_n\right)_{pA,T}\right)F_{Ts}^{-1}\chi_{Aa}^{-1}\delta\Phi_{aB}\chi_{Br}^{-1} + \delta\left(\Phi_{pA}\right)\chi_{Aa}^{-1}\chi_{aB,T}\chi_{Br}^{-1}F_{Ts}^{-1} \\
& - \left(\chi_{pA} - \left(\chi_n\right)_{pA}\right)\chi_{Ai}^{-1}\delta\Phi_{iL}\chi_{La}^{-1}\chi_{aB,T}\chi_{Br}^{-1}F_{Ts}^{-1} \\
& + \left(\chi_{pA} - \left(\chi_n\right)_{pA}\right)\chi_{Aa}^{-1}\delta\Phi_{aB,T}\chi_{Br}^{-1}F_{Ts}^{-1} \\
& - \left(\chi_{pA} - \left(\chi_n\right)_{pA}\right)\chi_{Aa}^{-1}\chi_{aB,T}\chi_{Bi}^{-1}\delta\Phi_{iL}\chi_{Lr}^{-1}F_{Ts}^{-1} \\
& - \left(\chi_{pA} - \left(\chi_n\right)_{pA}\right)\chi_{Aa}^{-1}\chi_{aB,T}\chi_{Br}^{-1}F_{Ti}^{-1}\delta\left(u_{i,s}\right) \\
& + \left(\left(F_n\right)_{iL} F_{Ln}^{-1}\delta u_{n,k}\right)\left(\gamma_n^e\right)_{ilm} + \left(\gamma_n^e\right)_{kli}\left(\left(F_n\right)_{iL} F_{Ln}^{-1}\delta u_{n,m}\right) \\
& \left. + \left(\gamma_n^e\right)_{kim}\left(\left(\chi_n\right)_{iL}\chi_{Lp}^{-1}\delta\Phi_{pT}\chi_{Tl}^{-1}\right)\right]
\end{aligned} \tag{4.34}
$$

The last term at right hand side of equation (4.26) can be obtained as:

$$
\eta_{ml,k} m_{klm}\delta\left(J\right) = \eta_{ml,k} m_{klm}\left(J\delta(u_{n,n})\right) \tag{4.35}
$$

The variation of the last integral term in equation (4.23) can be written as follows:

$$
\begin{aligned}
\delta\left(\int_V \eta_{ml}(\sigma_{ml} - s_{ml} + \rho(\lambda_{lm} - \omega_{lm}))JdV\right) = & \int_V \overbrace{\delta\left(\eta_{ml}\right)}^{0}(\sigma_{ml} - s_{ml})J \\
+\eta_{ml}\delta(\sigma_{ml} - s_{ml})J + \eta_{ml}(\sigma_{ml} - s_{ml})\delta(J) + & \overbrace{\delta\left(\eta_{ml}\right)}^{0}\overbrace{\rho J}^{\rho_0}(\lambda_{lm} - \omega_{lm}) \\
+\eta_{ml}\overbrace{\delta(\rho_0)}^{0}(\lambda_{lm} - \omega_{lm}) + & \eta_{ml}\rho_0\delta(\lambda_{lm} - \omega_{lm})dV
\end{aligned} \tag{4.36}
$$

The first term in the right hand side of equation (4.36) will be zero. To determine the second term, $\delta(\sigma_{ml} - s_{ml})$ should be calculated where $(s_{ml} - \sigma_{ml})$ is defined as follows:

$$\begin{aligned}(\boldsymbol{s}-\boldsymbol{\sigma})_{n+1} &= \left(1 - tr\left(\Delta t \boldsymbol{d}^e_{n+1}\right)\right)(\boldsymbol{s}-\boldsymbol{\sigma})_n + \left(\Delta t \boldsymbol{\ell}^e_{n+1}\right)(\boldsymbol{s}-\boldsymbol{\sigma})_n \\ &+ (\boldsymbol{s}-\boldsymbol{\sigma})_n \left(\Delta t \boldsymbol{\ell}^e_{n+1}\right)^T + (\kappa - \sigma)\left(\Delta t \boldsymbol{\varepsilon}^e_{n+1}\right)^T \\ &+ (\nu - \sigma)\left(\Delta t \boldsymbol{\varepsilon}^e_{n+1}\right) + \tau tr\left(\Delta t \boldsymbol{d}^e_{n+1}\right)\mathbf{1} \\ &+ 2\sigma \Delta t \boldsymbol{d}^e_{n+1} + (\eta - \tau)\, tr\left(\Delta t \boldsymbol{\varepsilon}^e_{n+1}\right)\mathbf{1} \end{aligned} \tag{4.37}$$

where $\delta(\boldsymbol{\sigma} - \boldsymbol{s}) = -\delta(\boldsymbol{s} - \boldsymbol{\sigma})$. Note that variation of the terms appearing in equation (4.37) are given in Appendix (A). Variation of the third term of equation (4.36) :

$$\eta_{ml}(\sigma_{ml} - s_{ml})\delta(J) = \eta_{ml}(\sigma_{ml} - s_{ml})J\delta(u_{n,n}) \tag{4.38}$$

Variation of the last term in equation (4.36) :

$$\eta_{ml}\rho\delta(\lambda_{lm} - \omega_{lm})J = \eta_{ml}\rho\delta\left(\lambda_{lm}\right)J - \eta_{ml}\rho\delta\left(\omega_{lm}\right)J$$

where

$$\rho\lambda_{lm}dv = \int_{dv} \rho' f'_l \xi'_m dv' = \int_{dv} \rho' f'_l \chi_{mK} \Xi_K dv'$$

$$\rho\lambda_{lm}dv = \chi_{mK}\int_{dv} \rho' f'_l \Xi'_K dv' = \chi_{mK} \underbrace{\int_{dv} f'_l \Xi_K \underbrace{\rho' J'}_{\rho'_0} dV'}_{\rho_0 \Gamma_{lK} dV}$$

$$\rho\lambda_{lm}dv = \chi_{mK}\rho_0\Gamma_{lK}dV \tag{4.39}$$

$$\Rightarrow \rho\delta\left(\lambda_{lm}\right)dv = \delta\left[\chi_{mK}\underbrace{\int_{dV} \rho' f'_l \Xi'_K J' dV'}_{\rho_0\Gamma_{lK}dV}\right] = \delta\left(\chi_{mK}\right)\rho_0\Gamma_{lK}dV + \chi_{mK}\overbrace{\delta\left(\rho_0\Gamma_{lK}dV\right)}^{0}$$

$$\rho\delta\left(\lambda_{lm}\right)dv = \rho_0\Gamma_{lK}\delta\left(\Phi_{mK}\right)dV \tag{4.40}$$

and

$$\begin{aligned}
\rho\omega_{lm}dv &= \int_{dv} \rho'\ddot{\xi}_l\xi_m dv' \\
&= \int_{dv} \rho' \left(\ddot{\chi}_{lK}\right) \Xi_K \chi_{mL} \Xi_L dv' \\
&= \left(\ddot{\chi}_{lK}\right) \chi_{mL} \int_{dV} \rho_0' \Xi_K \Xi_L dV' \\
\Rightarrow \rho\omega_{lm}dv &= \left(\ddot{\chi}_{lK}\right) \chi_{mL}\rho_0\Omega_{KL}dV, \quad \rho_0\Omega_{KL}dV = \int_{dV} \rho_0' \Xi_K \Xi_L dV' \\
\rho\delta\left(\omega_{lm}\right) dv &= \left(\delta\left(\ddot{\Phi}_{lK}\right) \Phi_{mL} + \ddot{\Phi}_{lK}\delta\left(\Phi_{mL}\right)\right) \rho_0\Omega_{KL}dV \qquad (4.41)
\end{aligned}$$

By using (4.40) and (4.41), we get :

$$\begin{aligned}
\eta_{ml}\rho\delta\left(\lambda_{lm}\right) J - \eta_{ml}\rho\delta\left(\omega_{lm}\right) J &= \eta_{ml}\rho_0\Gamma_{lK}\delta\left(\Phi_{mK}\right) \\
&\quad - \eta_{ml}\left(\delta\left(\ddot{\Phi}_{lK}\right) \Phi_{mL} + \ddot{\Phi}_{lK}\delta\left(\Phi_{mL}\right)\right) \rho_0\Omega_{lm} \qquad (4.42)
\end{aligned}$$

Then, the last term for quasistatic case in equation (4.36) becomes :

$$\delta\left(\int \rho(\lambda_{lm} - \underbrace{\omega_{lm}}_{0})dv\right) = \int_V \rho_0\Gamma_{lK}\delta\left(\Phi_{mK}\right) dV$$

4.3 Finite Element Discretization

Displacement $\boldsymbol{u}$ can be discretized as:

$$u_i^h = \sum_{a=1}^{n_{en}^u} N_a^u d_{i(a)} \tag{4.43}$$

$$\Rightarrow \delta\left(u_i^h\right) = \sum_{a=1}^{n_{en}^u} N_a^u \delta\left(d_{i(a)}\right) \tag{4.44}$$

$$\underbrace{\left\{\boldsymbol{u}^h\right\}}_{n_{sd}\times 1} = \underbrace{[\boldsymbol{N}^{u,e}]}_{n_{sd}\times n_{dof}^{u,e}} . \underbrace{\{\boldsymbol{d}^e\}}_{n_{dof}^{u,e}\times 1} \tag{4.45}$$

$$u_{i,j}^h = \sum_{a=1}^{n_{en}} N_{a,j}^u d_{i(a)} \tag{4.46}$$

$$\underbrace{\left\{\boldsymbol{grad}(\boldsymbol{u}^h)\right\}}_{(n_{sd}*n_{sd})\times 1} = \underbrace{[\boldsymbol{grad}\left(\boldsymbol{N}^{u,e}\right)]}_{(n_{sd}*n_{sd})\times n_{dof}^{u,e}} . \underbrace{\{\boldsymbol{d}^e\}}_{n_{dof}^{u,e}\times 1} \tag{4.47}$$

$$u_{i,i}^h = \sum_{a=1}^{n_{el}} N_{a,i}^u d_{i(a)} \tag{4.48}$$

$$div(\boldsymbol{u}^h) = \underbrace{[div\left(\boldsymbol{N}^{u,e}\right)]}_{1\times n_{dof}^{u,e}} . \underbrace{\{\boldsymbol{d}^e\}}_{n_{dof}^{u,e}\times 1} \tag{4.49}$$

The weight function $\boldsymbol{w}$ can be discretized as :

$$w_{k,l}^h = \sum_{a=1}^{n_{en}^u} N_{a,l}^u c_{k(a)}^e \tag{4.50}$$

in matrix form

$$\underbrace{\left\{\boldsymbol{w}^h\right\}}_{n_{sd}\times 1} = \underbrace{[\boldsymbol{N}^{u,e}]}_{n_{sd}\times n_{dof}^{u,e}} . \underbrace{\{\boldsymbol{c}^e\}}_{n_{dof}^{u,e}\times 1} \tag{4.51}$$

then, $\boldsymbol{grad}(\boldsymbol{w})$ can be obtained as:

$$w_{k,l}^h = w_{k,L}^h F_{Ll}^{-1} \tag{4.52}$$

$$\underbrace{\left\{\boldsymbol{grad}(\boldsymbol{w}^h)\right\}}_{(n_{sd}*n_{sd})\times 1} = \underbrace{\left[\boldsymbol{F}^{-1}\right]_w^T}_{(n_{sd}*n_{sd})\times(n_{sd}*n_{sd})} . \underbrace{\left\{\boldsymbol{GRAD}(\boldsymbol{w}^h)\right\}}_{(n_{sd}*n_{sd})\times 1} \tag{4.53}$$

$$w_{k,L}^h = \sum_{a=1}^{n_{en}^u} N_{a,L}^u c_{k(a)}^e \tag{4.54}$$

in matrix form

$$\underbrace{\{\boldsymbol{GRAD}(\boldsymbol{w})\}}_{(n_{sd}*n_{sd})\times 1} = \underbrace{[\boldsymbol{GRAD}(\boldsymbol{N}^{u,e})]}_{(n_{sd}*n_{sd})\times n_{dof}^{u,e}}.\ \underbrace{\{\boldsymbol{c}^e\}}_{\left(n_{dof}^{u,e}\right)\times 1} \tag{4.55}$$

$$\underbrace{\{\boldsymbol{GRAD}(\boldsymbol{w})\}^T}_{1\times(n_{sd}*n_{sd})} = \underbrace{\{\boldsymbol{c}^e\}^T}_{1\times\left(n_{dof}^{u,e}\right)}.\underbrace{[\boldsymbol{GRAD}(\boldsymbol{N}^{u,e})]^T}_{n_{dof}^{u,e}\times(n_{sd}*n_{sd})} \tag{4.56}$$

$$\underbrace{\left\{\boldsymbol{grad}(\boldsymbol{w}^h)\right\}^T}_{1\times(n_{sd}*n_{sd})} = \underbrace{\{\boldsymbol{c}^e\}^T}_{1\times\left(n_{dof}^{u,e}\right)}.\underbrace{[\boldsymbol{GRAD}(\boldsymbol{N}^{u,e})]^T}_{n_{dof}^{u,e}\times(n_{sd}*n_{sd})}.\ \underbrace{\left[\boldsymbol{F}^{-1}\right]_w^T}_{(n_{sd}*n_{sd})\times(n_{sd}*n_{sd})} \tag{4.57}$$

$$\underbrace{[\boldsymbol{\iota}]_w}_{n_{dof}^{u,e}\times(n_{sd}*n_{sd})} = \underbrace{[\boldsymbol{GRAD}(\boldsymbol{N}^{u,e})]^T}_{n_{dof}^{u,e}\times(n_{sd}*n_{sd})}.\ \underbrace{\left[\boldsymbol{F}^{-1}\right]_w^T}_{(n_{sd}*n_{sd})\times(n_{sd}*n_{sd})} \tag{4.58}$$

Micro deformation tensor $\boldsymbol{\chi}$ can be discretized as:

$$\Phi_{mL}^h = \sum_{b=1}^{n_{en}^{\chi}} N_b^{\chi}\phi_{mL(b)} \tag{4.59}$$

$$\Rightarrow \delta\left(\chi_{mL}^h\right) = \delta\left(\Phi_{mL}^h\right) = \sum_{b=1}^{n_{en}^{\chi}} N_b^{\chi}\delta\left(\phi_{mL(b)}\right) \tag{4.60}$$

in matrix form

$$\underbrace{\{\boldsymbol{\Phi}^h\}}_{(n_{sd}*n_{sd})\times 1} = \underbrace{[\boldsymbol{N}^{\chi,e}]}_{(n_{sd}*n_{sd})\times n_{dof}^{\chi,e}}.\underbrace{\{\boldsymbol{\phi}\}}_{n_{dof}^{\chi}\times 1}$$

The weight function $\boldsymbol{\eta}$ can be discretized as :

$$\eta_{mL}^h = \sum_{b=1}^{n_{en}^{\chi}} N_b^{\chi}\alpha_{mL(b)} \tag{4.61}$$

in matrix form

$$\underbrace{\{\boldsymbol{\eta}\}}_{(n_{sd}*n_{sd})\times 1} = \underbrace{[\boldsymbol{N}^{\chi,e}]}_{(n_{sd}*n_{sd})\times n_{dof}^{\chi}}.\underbrace{\{\boldsymbol{\alpha}\}}_{n_{dof}^{\chi}\times 1} \tag{4.62}$$

The gradient of the weight function $\boldsymbol{\eta}$ can be discretized as:

$$\eta_{ml,k}^h = \sum_{b=1}^{n_{en}^{\chi}} N_{b,k}^{\chi}\alpha_{ml(b)} \tag{4.63}$$

in matrix form

$$\underbrace{\{\boldsymbol{grad}(\boldsymbol{\eta})\}}_{(n_{sd}*n_{sd}*n_{sd})\times 1} = \underbrace{[\boldsymbol{grad}(\boldsymbol{N}^{\chi,e})]}_{(n_{sd}*n_{sd}*n_{sd})\times n_{dof}^{\chi,e}}.\underbrace{\{\boldsymbol{\alpha}\}}_{n_{dof}^{\chi,e}\times 1} \tag{4.64}$$

$$\underbrace{\left\{\boldsymbol{grad}(\boldsymbol{\eta})\right\}}_{(n_{sd}*n_{sd}*n_{sd})\times 1} = \underbrace{\left[\boldsymbol{F}^{-1}\right]_{\eta}}_{(n_{sd}*n_{sd}*n_{sd})\times(n_{sd}*n_{sd}*n_{sd})} .\underbrace{\left[\boldsymbol{GRAD}(\boldsymbol{\eta})\right]}_{(n_{sd}*n_{sd}*n_{sd})\times 1} \tag{4.65}$$

$$\underbrace{\left\{\boldsymbol{grad}(\boldsymbol{\eta})\right\}^{T}}_{(n_{sd}*n_{sd}*n_{sd})\times 1} = \underbrace{\left\{\boldsymbol{\alpha}\right\}}_{1\times n_{dof}^{\chi,e}}^{T} .\underbrace{\left[\boldsymbol{GRAD}(\boldsymbol{N}^{\chi,e})\right]^{T}}_{n_{dof}^{\chi,e}\times(n_{sd}*n_{sd}*n_{sd})} \underbrace{\left[\boldsymbol{F}^{-1}\right]_{\eta}^{T}}_{(n_{sd}*n_{sd}*n_{sd})\times(n_{sd}*n_{sd}*n_{sd})} \tag{4.66}$$

$$\underbrace{\left[\boldsymbol{\iota}\right]_{\eta}}_{n_{dof}^{\chi,e}\times(n_{sd}*n_{sd}*n_{sd})} = \underbrace{\left[\boldsymbol{GRAD}(\boldsymbol{N}^{\chi,e})\right]^{T}}_{n_{dof}^{\chi,e}\times(n_{sd}*n_{sd}*n_{sd})} . \underbrace{\left[\boldsymbol{F}^{-1}\right]_{\eta}^{T}}_{(n_{sd}*n_{sd}*n_{sd})\times(n_{sd}*n_{sd}*n_{sd})} \tag{4.67}$$

4.4 Submatrices in the Matrix Form of the Balance of Linear Momentum

Equation (4.3) is separated into subintegrals as follows:

$$\mathcal{G}_1 = -\int_V \left(\boldsymbol{grad}\left(\boldsymbol{w}\right)\right)^T : \boldsymbol{\sigma} J dV \tag{4.68}$$

If we write equation (3.134) in indicial notation as:

$$\begin{aligned}\sigma_{lk} &= \left(1-\Delta t d_{ii}^{e}\right)\left(\sigma_n\right)_{lk} + \left(\Delta t \ell_{li}^{e}\right)\left(\sigma_n\right)_{ik} + \left(\sigma_n\right)_{li}\left(\Delta t \ell_{n+1}^{e}\right)_{ki} \\ &+ \left(\lambda+\tau\right)\Delta t d_{ii}^{e}\delta_{lk} + 2\left(\mu+\sigma\right)\left(\Delta t d_{lk}^{e}\right) + \eta t \Delta t \varepsilon_{ii}^{e}\delta_{lk} \\ &+ \kappa \Delta t \varepsilon_{lk}^{e} + \nu \Delta t \varepsilon_{kl}^{e}\end{aligned} \tag{4.69}$$

then,

$$\left(\mathcal{G}\right)_1 = -\int_V w_{k,l}\sigma_{lk} J dV \tag{4.70}$$

if the all the expressions given in Appendix (A) are inserted, Galerkin from of the $\mathcal{G}_1^h$ can be obtained as:

$$\left(\mathcal{G}^{e,h}\right)_1 = -\int_{V^e} \underbrace{\left\{\boldsymbol{c}^{e}\right\}^{T}}_{1\times\left(n_{dof}^{u,e}\right)} .\underbrace{\left[\boldsymbol{grad}(\boldsymbol{N}^{u,e})\right]^{T}}_{n_{dof}^{u,e}\times(n_{sd}*n_{sd})} . \underbrace{\left\{\boldsymbol{G}_1\right\}}_{(n_{sd}*n_{sd})\times 1} J dV \tag{4.71}$$

$$\underbrace{\left\{\boldsymbol{U}_1^{e,Int}\right\}}_{n_{dof}^{u,e}\times 1} = -\int_{V^e} \underbrace{\left[\boldsymbol{grad}(\boldsymbol{N}^{u,e})\right]^{T}}_{n_{dof}^{u,e}\times(n_{sd}*n_{sd})} . \underbrace{\left\{\boldsymbol{G}_1\right\}}_{(n_{sd}*n_{sd})\times 1} J dV \tag{4.72}$$

$$\underbrace{\left\{\boldsymbol{U}_1^{e,Int}\right\}}_{n_{dof}^{u,e}\times 1} = -\int_{V^e} \underbrace{\left[\boldsymbol{GRAD}(\boldsymbol{N}^{u,e})\right]^{T}}_{n_{dof}^{u,e}\times(n_{sd}*n_{sd})} . \underbrace{\left[\boldsymbol{F}^{-1}\right]_{w}}_{(n_{sd}*n_{sd})\times(n_{sd}*n_{sd})} . \underbrace{\left\{\boldsymbol{G}_1\right\}}_{(n_{sd}*n_{sd})\times 1} J dV \tag{4.73}$$

$$\left(\mathcal{G}_1^h\right) = \underset{e=1}{\overset{n_{el}}{\mathbb{A}}} \underbrace{\left\{\boldsymbol{c}^e\right\}^T}_{1\times n_{dof}^{u,e}} . \underbrace{\left\{\boldsymbol{U}_1^{e,Int}\right\}}_{n_{dof}^{u,e}\times 1} \tag{4.74}$$

The second term:

$$\left(\mathcal{G}\right)_2 = -\int_V \rho_0 w_k f_k dV \tag{4.75}$$

$$\left(\mathcal{G}^{e,h}\right)_2 = -\int_{V^e} \left\{\boldsymbol{c}^e\right\}^T . \left[\boldsymbol{N}^{u,e}\right]^T . \left\{\boldsymbol{f}\right\} \rho_0 dV \tag{4.76}$$

$$\left(\mathcal{G}^{e,h}\right)_2 = -\int_{V^e} \rho_0 \underbrace{\left\{\boldsymbol{c}^e\right\}^T}_{1\times\left(n_{dof}^{u,e}\right)} . \underbrace{\left[\boldsymbol{N}^{u,e}\right]^T}_{n_{dof}^{u,e}\times n_{sd}} . \underbrace{\left\{\boldsymbol{f}\right\}}_{n_{sd}\times 1} dV \tag{4.77}$$

$$\underbrace{\left\{\boldsymbol{U}_2^{e,Int}\right\}}_{n_{dof}^{u,e}\times 1} = -\int_{V^e} \rho_0 \underbrace{\left[\boldsymbol{N}^{u,e}\right]^T}_{n_{dof}^{u,e}\times n_{sd}} . \underbrace{\left\{\boldsymbol{f}\right\}}_{n_{sd}\times 1} dV \tag{4.78}$$

$$\left(\mathcal{G}^h\right)_2 = \underset{e=1}{\overset{n_{el}}{\mathbb{A}}} \underbrace{\left\{\boldsymbol{c}^e\right\}}_{1\times\left(n_{dof}^{u,e}\right)}^T . \underbrace{\left\{\boldsymbol{U}_2^{e,Int}\right\}}_{n_{dof}^{u,e}\times 1} \tag{4.79}$$

and

$$\left(\mathcal{G}_{ext}\right) = \int_S \rho_0 \boldsymbol{w}^T . \boldsymbol{T} dA \tag{4.80}$$

$$\left(\mathcal{G}_{ext}\right) = \int_{S^e} \rho_0 w_k T_k dA \tag{4.81}$$

$$\left(\mathcal{G}_{ext}^h\right) = \int_{S^e} \underbrace{\left\{\boldsymbol{c}^e\right\}}_{1\times\left(n_{dof}^{u,e}\right)}^T . \underbrace{\left[\boldsymbol{N}^{u,e}\right]^T}_{n_{dof}^{u,e}\times n_{sd}} . \underbrace{\left\{\boldsymbol{T}\right\}}_{n_{sd}\times 1} \rho_0 dA \tag{4.82}$$

$$\underbrace{\left\{\boldsymbol{U}_{ext}^e\right\}}_{n_{dof}^{u,e}\times 1} = \int_{S^e} \underbrace{\left[\boldsymbol{N}^{u,e}\right]^T}_{n_{dof}^{u,e}\times n_{sd}} . \underbrace{\left\{\boldsymbol{T}\right\}}_{n_{sd}\times 1} \rho_0 dA \tag{4.83}$$

$$\left(\mathcal{G}_{ext}^h\right) = \underset{e=1}{\overset{n_{el}}{\mathbb{A}}} \underbrace{\left\{\boldsymbol{c}^e\right\}^T}_{1\times\left(n_{dof}^{u,e}\right)} . \underbrace{\left\{\boldsymbol{U}_{ext}^e\right\}}_{n_{dof}^{u,e}\times 1} \tag{4.84}$$

4.5 Submatrices in the Matrix Form of the Balance of First Moment of Momentum

The balance of first Moment of Momentum can be separated into subintegrals as follows:

The first subintegral $\mathcal{H}_1$:

$$\mathcal{H}_1 = -\int_V \eta_{ml,k} m_{klm} J dV \tag{4.85}$$

where m_{klm} is written in indicial notation as:

$$\begin{aligned} m_{klm} = &\left(1 - \Delta t d^e_{ii}\right)\left(m_n\right)_{klm} + \left(\Delta t \ell^e_{ki}\right)\left(m_n\right)_{ilm} + \left(m_n\right)_{kim}\left(\Delta t \ell^e_{li}\right) \\ &+ \left(m_n\right)_{kli}\left(\Delta t \nu^e_{mi}\right) + c_{klmprs}\left(\Delta t \overset{\circ}{\gamma}{}^e_{prs}\right) \end{aligned} \tag{4.86}$$

$$\Delta t \overset{\circ}{\gamma}{}^e_{prs} = \Delta t \dot{\gamma}^e_{prs} + \left(\Delta t \ell^e_{ip}\right)\left(\gamma^e_n\right)_{irs} + \left(\gamma^e_n\right)_{pri}\left(\Delta t \ell^e_{is}\right) + \left(\gamma^e_n\right)_{pis}\left(\Delta t \nu^e_{ir}\right) \tag{4.87}$$

$$\Delta t \dot{\gamma}^e_{prs} = \left(\Delta t \nu^e_{pi}\right)\left(\gamma^e_n\right)_{irs} - \left(\Delta t \nu^e_{ir}\right)\left(\gamma^e_n\right)_{pis} + \Delta t \nu^e_{pr,s} - \underbrace{\Delta t \nu^p_{pr,s}}_{\text{0 for elastic case}} \tag{4.88}$$

$$\Delta t \nu^e_{pr,s} = \left(\chi_{pK,s} - \left(\chi_n\right)_{pK,s}\right)\chi^{-1}_{Kr} - \left(\chi_{pK} - \left(\chi_n\right)_{pK}\right)\chi^{-1}_{Ki}\left(\chi_{iT,r}\right)\chi^{-1}_{Ts} \tag{4.89}$$

$$\Delta t \nu^e_{pr,s} = \left(\chi_{pK,S} - \left(\chi_n\right)_{pK,S}\right)F^{-1}_{Ss}\chi^{-1}_{Kr} - \left(\chi_{pK} - \left(\chi_n\right)_{pK}\right)\chi^{-1}_{Ki}\left(\chi_{iT,S}\right)F^{-1}_{Sr}\chi^{-1}_{Ts} \tag{4.90}$$

$$\mathcal{H}^{e,h}_1 = -\int_{V^e} \underbrace{\left\{\boldsymbol{\alpha}^e\right\}^T}_{1\times n^\chi_{dof}} . \underbrace{\left[\boldsymbol{grad}(\boldsymbol{N}^{\chi,e})\right]^T}_{n^\chi_{dof}\times(n_{sd}*n_{sd}*n_{sd})} . \underbrace{\left\{\boldsymbol{H}_1\right\}}_{(n_{sd}*n_{sd}*n_{sd})\times 1} J dV \tag{4.91}$$

$$\underbrace{\left\{\boldsymbol{P}^{e,Int}_1\right\}}_{n^{\chi,e}_{dof}\times 1} = -\int_{V^e} \underbrace{\left[\boldsymbol{grad}(\boldsymbol{N}^{\chi,e})\right]^T}_{n^\chi_{dof}\times(n_{sd}*n_{sd}*n_{sd})} . \underbrace{\left\{\boldsymbol{H}_1\right\}}_{(n_{sd}*n_{sd}*n_{sd})\times 1} dV \tag{4.92}$$

$$\mathcal{H}^h_1 = \mathop{\mathbb{A}}_{e=1}^{n_{el}} \underbrace{\left\{\boldsymbol{\alpha}^e\right\}^T}_{1\times n^\chi_{dof}} . \underbrace{\left\{\boldsymbol{P}^{e,Int}_1\right\}}_{n^{\chi,e}_{dof}\times 1} \tag{4.93}$$

The second subintegral $\mathcal{H}_2$:

$$\mathcal{H}_2 = \int_V \eta_{ml}(\sigma_{ml} - s_{ml}) J dV \tag{4.94}$$

$$\mathcal{H}_2 = -\int_V \eta_{ml}(s_{ml} - \sigma_{ml}) J dV \tag{4.95}$$

where $(s_{ml} - \sigma_{ml})$ is expressed in indicial forms as:

$$\begin{aligned} (s_{ml} - \sigma_{ml}) = &\left(1 - \Delta t d^e_{ii}\right)(s_{ml} - \sigma_{ml})_n + \left(\Delta t \ell^e_{mi}\right)(s_{il} - \sigma_{il})_n + (s_{mi} - \sigma_{mi})_n\left(\Delta t \ell^e_{li}\right) \\ &+ (\kappa - \sigma)\left(\Delta t \varepsilon^e_{lm}\right) + (\nu - \sigma)\left(\Delta t \varepsilon^e_{ml}\right) \end{aligned} \tag{4.96}$$

$$+ \tau \Delta t d^e_{ii}\delta_{ml} + 2\sigma \Delta t d^e_{ml} + (\eta - \tau)\,\Delta t \varepsilon^e_{ii}\delta_{ml} \tag{4.97}$$

$$\mathcal{H}_2^{e,h} = -\int_{V^e} \underbrace{\left\{\boldsymbol{\alpha}^e\right\}^T}_{1\times n_{dof}^{\chi}} . \underbrace{\left[\boldsymbol{N}^{\chi,e}\right]^T}_{n_{dof}^{\chi}\times(n_{sd}*n_{sd})} . \underbrace{\left\{\boldsymbol{H}_2\right\}}_{(n_{sd}*n_{sd})\times 1} JdV \tag{4.98}$$

$$\underbrace{\left\{\boldsymbol{P}_2^{e,Int}\right\}}_{n_{dof}^{\chi,e}\times 1} = -\int_{V^e} \underbrace{\left[\boldsymbol{N}^{\chi,e}\right]^T}_{n_{dof}^{\chi}\times(n_{sd}*n_{sd})} . \underbrace{\left\{\boldsymbol{H}_2\right\}}_{(n_{sd}*n_{sd})\times 1} JdV \tag{4.99}$$

$$\mathcal{H}_2^h = \mathop{\mathsf{A}}_{e=1}^{n_{\text{el}}} \underbrace{\left\{\boldsymbol{\alpha}^e\right\}^T}_{1\times n_{dof}^{\chi}} \underbrace{\left\{\boldsymbol{P}_2^{e,Int}\right\}}_{n_{dof}^{\chi,e}\times 1} \tag{4.100}$$

The third subintegral $\mathcal{H}_3$:

$$\mathcal{H}_3 = \int_V \eta_{ml}\rho(\lambda_{lm} - \omega_{lm}) JdV \tag{4.101}$$

$$\mathcal{H}_3^{e,h} = \int_{V^e} \underbrace{\left\{\boldsymbol{\alpha}^e\right\}^T}_{1\times n_{dof}^{\chi}} . \underbrace{\left[\boldsymbol{N}^{\chi,e}\right]^T}_{n_{dof}^{\chi}\times(n_{sd}*n_{sd})} . \underbrace{\left\{\boldsymbol{H}_3\right\}}_{(n_{sd}*n_{sd})\times 1} \rho_0 dV \tag{4.102}$$

$$\underbrace{\left\{\boldsymbol{P}_3^{e,Int}\right\}}_{n_{dof}^{\chi,e}\times 1} = \int_{V^e} \underbrace{\left[\boldsymbol{N}^{\chi,e}\right]^T}_{n_{dof}^{\chi}\times(n_{sd}*n_{sd})} . \underbrace{\left\{\boldsymbol{H}_3\right\}}_{(n_{sd}*n_{sd})\times 1} \rho_0 dV \tag{4.103}$$

$$\mathcal{H}_3^h = \mathop{\mathsf{A}}_{e=1}^{n_{\text{el}}} \underbrace{\left\{\boldsymbol{\alpha}^e\right\}^T}_{1\times n_{dof}^{\chi}} \underbrace{\left\{\boldsymbol{P}_3^{e,Int}\right\}}_{n_{dof}^{\chi,e}\times 1} \tag{4.104}$$

The fourth term $\mathcal{H}_{ext}$:

$$\mathcal{H}_{ext} = \int_S \eta_{ml} F_{km} dA \tag{4.105}$$

$$\mathcal{H}_{ext}^{e,h} = \int_{S^e} \underbrace{\left\{\boldsymbol{\alpha}^e\right\}^T}_{1\times n_{dof}^{\chi}} \underbrace{\left[\boldsymbol{N}^{\chi,e}\right]^T}_{n_{dof}^{\chi}\times(n_{sd}*n_{sd})} . \underbrace{\left\{\boldsymbol{H}_{ext}\right\}}_{(n_{sd}*n_{sd})\times 1} dA \tag{4.106}$$

$$\underbrace{\left\{\boldsymbol{P}_{ext}^{e}\right\}}_{n_{dof}^{\chi,e}\times 1} = \int_{S^e} \underbrace{\left[\boldsymbol{N}^{\chi,e}\right]^T}_{n_{dof}^{\chi}\times(n_{sd}*n_{sd})} . \underbrace{\left\{\boldsymbol{H}_{ext}\right\}}_{(n_{sd}*n_{sd})\times 1} ddA \tag{4.107}$$

$$\mathcal{H}_{ext}^h = \mathop{\mathsf{A}}_{e=1}^{n_{\text{el}}} \underbrace{\left\{\boldsymbol{\alpha}^e\right\}^T}_{1\times n_{dof}^{\chi}} . \underbrace{\left\{\boldsymbol{P}^{e,ext}\right\}}_{n_{dof}^{\chi,e}\times 1} \tag{4.108}$$

4.6 Submatrices in the Matrix Form of the Linearized Form of the Balance of Linear Momentum

Linearization of the term $\mathcal{G}_1$:

$$\left(\delta\mathcal{G}_1\right)_1 = \int_V \left(\boldsymbol{\nabla w}\right)^T : \delta\left(\boldsymbol{\sigma}\right) JdV = \int_V \frac{\partial w_k}{\partial x_l}\delta\left(\sigma_{lk}\right) JdV \tag{4.109}$$

$$\left(\delta\mathcal{G}_1\right)_1 = \int_V w_{k,l}\left(\left(F_n\right)_{iL} F^{-1}_{Lm}\delta u_{m,i}\right)\left(\sigma_n\right)_{lk} JdV \tag{4.110}$$

$$\left(\delta\mathcal{G}_1^{e,h}\right)_1 = \int_{V^e} \underbrace{\left\{\boldsymbol{c}^e\right\}^T}_{1\times\left(n^{u,e}_{dof}\right)} .\underbrace{\left[\boldsymbol{grad}(\boldsymbol{N}^{u,e})\right]^T}_{\left(n^{u,e}_{dof}\right)\times\left(n_{sd}*n_{sd}\right)} . \underbrace{\left[\boldsymbol{T}^{\sigma}_1\right]}_{\left(n_{sd}*n_{sd}\right)\times\left(n_{sd}*n_{sd}\right)} .\underbrace{\left[\boldsymbol{grad}\left(\boldsymbol{N}^{u,e}\right)\right]}_{\left(n_{sd}*n_{sd}\right)\times n^{u,e}_{dof}} .\underbrace{\left\{\delta\boldsymbol{d}^e\right\}}_{n^{u,e}_{dof}\times 1} JdV \tag{4.111}$$

$$\underbrace{\left[\mathfrak{T}^e_1\right]}_{\left(n^{u,e}_{dof}\right)\times\left(n^{u,e}_{dof}\right)} = \int_{V^e} \underbrace{\left[\boldsymbol{grad}(\boldsymbol{N}^{u,e})\right]^T}_{\left(n^{u,e}_{dof}\right)\times\left(n_{sd}*n_{sd}\right)} . \underbrace{\left[\boldsymbol{T}^{\sigma}_1\right]}_{\left(n_{sd}*n_{sd}\right)\times\left(n_{sd}*n_{sd}\right)} .\underbrace{\left[\boldsymbol{grad}\left(\boldsymbol{N}^{u,e}\right)\right]}_{\left(n_{sd}*n_{sd}\right)\times n^{u,e}_{dof}} JdV \tag{4.112}$$

$$\left(\delta\mathcal{G}_1^h\right)_1 = \mathop{\mathbf{A}}_{e=1}^{n_{\text{el}}} \underbrace{\left\{\boldsymbol{c}^e\right\}^T}_{1\times\left(n^{u,e}_{dof}\right)} . \underbrace{\left[\mathfrak{T}^e_1\right]}_{\left(n^{u,e}_{dof}\right)\times\left(n^{u,e}_{dof}\right)} .\underbrace{\left\{\delta\boldsymbol{d}^e\right\}}_{n^{u,e}_{dof}\times 1} \tag{4.113}$$

For the second term in equation (4.15), we have :

$$\left(\delta\mathcal{G}_1\right)_2 = -\int_V w_{k,l}\left(\left(F_n\right)_{lL} F^{-1}_{Lm}\delta u_{m,i}\right)\left(\sigma_n\right)_{ik} JdV \tag{4.114}$$

$$\left(\delta\mathcal{G}_1^{e,h}\right)_2 = -\int_{V^e} \underbrace{\left\{\boldsymbol{c}^e\right\}^T}_{1\times\left(n^{u,e}_{dof}\right)} .\underbrace{\left[\boldsymbol{grad}(\boldsymbol{N}^{u,e})\right]^T}_{\left(n^{u,e}_{dof}\right)\times\left(n_{sd}*n_{sd}\right)} . \underbrace{\left[\boldsymbol{T}^{\sigma}_2\right]}_{\left(n_{sd}*n_{sd}\right)\times\left(n_{sd}*n_{sd}\right)} .\underbrace{\left[\boldsymbol{grad}\left(\boldsymbol{N}^{u,e}\right)\right]}_{\left(n_{sd}*n_{sd}\right)\times n^{u,e}_{dof}} .\underbrace{\left\{\delta\boldsymbol{d}^e\right\}}_{n^{u,e}_{dof}\times 1} JdV \tag{4.115}$$

$$\underbrace{\left[\mathfrak{T}^e_2\right]}_{\left(n^{u,e}_{dof}\right)\times\left(n^{u,e}_{dof}\right)} = -\int_{V^e} \underbrace{\left[\boldsymbol{grad}(\boldsymbol{N}^{u,e})\right]^T}_{\left(n^{u,e}_{dof}\right)\times\left(n_{sd}*n_{sd}\right)} . \underbrace{\left[\boldsymbol{T}^{\sigma}_2\right]}_{\left(n_{sd}*n_{sd}\right)\times\left(n_{sd}*n_{sd}\right)} .\underbrace{\left[\boldsymbol{grad}\left(\boldsymbol{N}^{u,e}\right)\right]}_{\left(n_{sd}*n_{sd}\right)\times n^{u,e}_{dof}} JdV \tag{4.116}$$

$$\left(\delta\mathcal{G}_1^h\right)_2 = \mathop{\mathbf{A}}_{e=1}^{n_{\text{el}}} \underbrace{\left\{\boldsymbol{c}^e\right\}^T}_{1\times\left(n^{u,e}_{dof}\right)} . \underbrace{\left[\mathfrak{T}^e_2\right]}_{\left(n^{u,e}_{dof}\right)\times\left(n^{u,e}_{dof}\right)} .\underbrace{\left\{\delta\boldsymbol{d}^e\right\}}_{n^{u,e}_{dof}\times 1} \tag{4.117}$$

The third term in the equation (4.15) will be :

$$\left(\delta\mathcal{G}_1\right)_3 = -\int_V w_{k,l}\left(\sigma_n\right)_{li}\left(\left(F_n\right)_{kL} F^{-1}_{Lm}\delta u_{m,i}\right) JdV \tag{4.118}$$

$$\left(\delta \mathcal{G}_1^{e,h}\right)_3 = -\int_{V^e} \underbrace{\left\{\boldsymbol{c}^e\right\}^T}_{1\times\left(n_{dof}^{u,e}\right)} . \underbrace{\left[\boldsymbol{grad}(\boldsymbol{N}^{u,e})\right]^T}_{\left(n_{dof}^{u,e}\right)\times(n_{sd}*n_{sd})} . \underbrace{\left[\boldsymbol{T}_3^{\sigma}\right]}_{(n_{sd}*n_{sd})\times(n_{sd}*n_{sd})}$$
$$. \underbrace{\left[\boldsymbol{grad}\left(\boldsymbol{N}^{u,e}\right)\right]}_{(n_{sd}*n_{sd})\times n_{dof}^{u,e}} . \underbrace{\left\{\delta \boldsymbol{d}^e\right\}}_{n_{dof}^{u,e}\times 1} JdV \tag{4.119}$$

$$\underbrace{\left[\mathfrak{T}_3^e\right]}_{\left(n_{dof}^{u,e}\right)\times\left(n_{dof}^{u,e}\right)} = -\int_{V^e} \underbrace{\left[\boldsymbol{grad}(\boldsymbol{N}^{u,e})\right]^T}_{\left(n_{dof}^{u,e}\right)\times(n_{sd}*n_{sd})} . \underbrace{\left[\boldsymbol{T}_3^{\sigma}\right]}_{(n_{sd}*n_{sd})\times(n_{sd}*n_{sd})} . \underbrace{\left[\boldsymbol{grad}\left(\boldsymbol{N}^{u,e}\right)\right]}_{(n_{sd}*n_{sd})\times n_{dof}^{u,e}} JdV \tag{4.120}$$

$$\left(\delta \mathcal{G}_1^h\right)_3 = \mathop{\mathbf{A}}_{e=1}^{n_{\text{el}}} \underbrace{\left\{\boldsymbol{c}^e\right\}^T}_{1\times\left(n_{dof}^{u,e}\right)} . \underbrace{\left[\mathfrak{T}_3^e\right]}_{\left(n_{dof}^{u,e}\right)\times\left(n_{dof}^{u,e}\right)} . \underbrace{\left\{\delta \boldsymbol{d}^e\right\}}_{n_{dof}^{u,e}\times 1} \tag{4.121}$$

The fourth term in equation (4.15) can be found as :

$$\left(\delta \mathcal{G}_1\right)_4 = -\int_V w_{k,l}\delta_{lk}\left(\lambda+\tau\right)\left(\left(F_n\right)_{iL} F_{Lm}^{-1}\delta u_{m,i}\right) JdV \tag{4.122}$$

$$\left(\delta \mathcal{G}_1^{e,h}\right)_4 = -\left(\lambda+\tau\right)\int_{V^e} \underbrace{\left\{\boldsymbol{c}^e\right\}^T}_{1\times\left(n_{dof}^{u,e}\right)} . \underbrace{\left[\boldsymbol{grad}(\boldsymbol{N}^{u,e})\right]^T}_{\left(n_{dof}^{u,e}\right)\times(n_{sd}*n_{sd})} . \underbrace{\left[\boldsymbol{T}_1^{F_n}\right]}_{(n_{sd}*n_{sd})\times(n_{sd}*n_{sd})}$$
$$. \underbrace{\left[\boldsymbol{grad}\left(\boldsymbol{N}^{u,e}\right)\right]}_{(n_{sd}*n_{sd})\times n_{dof}^{u,e}} . \underbrace{\left\{\delta \boldsymbol{d}^e\right\}}_{n_{dof}^{u,e}\times 1} JdV \tag{4.123}$$

$$\underbrace{\left[\mathfrak{T}_4^e\right]}_{\left(n_{dof}^{u,e}\right)\times\left(n_{dof}^{u,e}\right)} = -\left(\lambda+\tau\right)\int_{V^e} \underbrace{\left[\boldsymbol{grad}(\boldsymbol{N}^{u,e})\right]^T}_{\left(n_{dof}^{u,e}\right)\times(n_{sd}*n_{sd})} . \underbrace{\left[\boldsymbol{T}_1^{F_n}\right]}_{(n_{sd}*n_{sd})\times(n_{sd}*n_{sd})} . \underbrace{\left[\boldsymbol{grad}\left(\boldsymbol{N}^{u,e}\right)\right]}_{(n_{sd}*n_{sd})\times n_{dof}^{u,e}} JdV \tag{4.124}$$

$$\left(\delta \mathcal{G}_1^h\right)_4 = \mathop{\mathbf{A}}_{e=1}^{n_{\text{el}}} \underbrace{\left\{\boldsymbol{c}^e\right\}^T}_{1\times\left(n_{dof}^{u,e}\right)} . \underbrace{\left[\mathfrak{T}_4^e\right]}_{\left(n_{dof}^{u,e}\right)\times\left(n_{dof}^{u,e}\right)} . \underbrace{\left\{\delta \boldsymbol{d}^e\right\}}_{n_{dof}^{u,e}\times 1} \tag{4.125}$$

The fifth term in equation (4.15) can be found as :

$$\left(\delta \mathcal{G}_1\right)_5 = -\left(\mu+\sigma\right)\int_V w_{k,l}\left(\left(F_n\right)_{lL} F_{Lm}^{-1}\delta u_{m,k}\right) JdV \tag{4.126}$$

$$\left(\delta \mathcal{G}_1^{e,h}\right)_5 = -\left(\mu+\sigma\right)\int_{V^e} \underbrace{\left\{\boldsymbol{c}^e\right\}^T}_{1\times\left(n_{dof}^{u,e}\right)} . \underbrace{\left[\boldsymbol{grad}(\boldsymbol{N}^{u,e})\right]^T}_{\left(n_{dof}^{u,e}\right)\times(n_{sd}*n_{sd})} . \underbrace{\left[\boldsymbol{T}_2^{F_n}\right]}_{(n_{sd}*n_{sd})\times(n_{sd}*n_{sd})}$$
$$. \underbrace{\left[\boldsymbol{grad}\left(\boldsymbol{N}^{u,e}\right)\right]}_{(n_{sd}*n_{sd})\times n_{dof}^{u,e}} . \underbrace{\left\{\delta \boldsymbol{d}^e\right\}}_{n_{dof}^{u,e}\times 1} JdV \tag{4.127}$$

$$\underbrace{\left[\mathfrak{T}_5^e\right]}_{\left(n_{dof}^{u,e}\right)\times\left(n_{dof}^{u,e}\right)} = -\left(\mu+\sigma\right)\int_{V^e}\underbrace{\left[\boldsymbol{grad}(\boldsymbol{N}^{u,e})\right]^T}_{\left(n_{dof}^{u,e}\right)\times(n_{sd}*n_{sd})}.\underbrace{\left[\boldsymbol{T}_2^{F_n}\right]}_{(n_{sd}*n_{sd})\times(n_{sd}*n_{sd})}.\underbrace{\left[\boldsymbol{grad}\left(\boldsymbol{N}^{u,e}\right)\right]}_{(n_{sd}*n_{sd})\times n_{dof}^{u,e}}JdV \quad (4.128)$$

$$\left(\delta\mathcal{G}_1^h\right)_5 = \mathop{\mathbf{A}}_{e=1}^{n_{\text{el}}}\underbrace{\left\{\boldsymbol{c}^e\right\}^T}_{1\times\left(n_{dof}^{u,e}\right)}.\underbrace{\left[\mathfrak{T}_5^e\right]}_{\left(n_{dof}^{u,e}\right)\times\left(n_{dof}^{u,e}\right)}.\underbrace{\left\{\delta\boldsymbol{d}^e\right\}}_{n_{dof}^{u,e}\times 1} \quad (4.129)$$

The sixth term in equation (4.15) can be found as :

$$\left(\delta\mathcal{G}_1\right)_6 = -\left(\mu+\sigma\right)\int_V w_{k,l}\left(\left(F_n\right)_{kL}F^{-1}_{Lm}\delta u_{m,l}\right)JdV \quad (4.130)$$

$$\left(\delta\mathcal{G}_1^{e,h}\right)_6 = \left(\mu+\sigma\right)\int_{V^e}\underbrace{\left\{\boldsymbol{c}^e\right\}^T}_{1\times\left(n_{dof}^{u,e}\right)}.\underbrace{\left[\boldsymbol{grad}(\boldsymbol{N}^{u,e})\right]^T}_{\left(n_{dof}^{u,e}\right)\times(n_{sd}*n_{sd})}.\underbrace{\left[\boldsymbol{T}_3^{F_n}\right]}_{(n_{sd}*n_{sd})\times(n_{sd}*n_{sd})}$$
$$.\underbrace{\left[\boldsymbol{grad}\left(\boldsymbol{N}^{u,e}\right)\right]}_{(n_{sd}*n_{sd})\times n_{dof}^{u,e}}.\underbrace{\left\{\delta\boldsymbol{d}^e\right\}}_{n_{dof}^{u,e}\times 1}JdV \quad (4.131)$$

$$\underbrace{\left[\mathfrak{T}_6^e\right]}_{\left(n_{dof}^{u,e}\right)\times\left(n_{dof}^{u,e}\right)} = -\left(\mu+\sigma\right)\int_{V^e}\underbrace{\left[\boldsymbol{grad}(\boldsymbol{N}^{u,e})\right]^T}_{\left(n_{dof}^{u,e}\right)\times(n_{sd}*n_{sd})}.\underbrace{\left[\boldsymbol{T}_3^{F_n}\right]}_{(n_{sd}*n_{sd})\times(n_{sd}*n_{sd})}$$
$$.\underbrace{\left[\boldsymbol{grad}\left(\boldsymbol{N}^{u,e}\right)\right]}_{(n_{sd}*n_{sd})\times n_{dof}^{u,e}}JdV \quad (4.132)$$

$$\left(\delta\mathcal{G}_1^h\right)_6 = \mathop{\mathbf{A}}_{e=1}^{n_{\text{el}}}\underbrace{\left\{\boldsymbol{c}^e\right\}^T}_{1\times\left(n_{dof}^{u,e}\right)}.\underbrace{\left[\mathfrak{T}_6^e\right]}_{\left(n_{dof}^{u,e}\right)\times\left(n_{dof}^{u,e}\right)}.\underbrace{\left\{\delta\boldsymbol{d}^e\right\}}_{n_{dof}^{u,e}\times 1} \quad (4.133)$$

The seventh term in equation (4.15) can be found as :

$$\left(\delta\mathcal{G}_1\right)_7 = -\eta\int_V w_{k,l}\left(\left(\chi_n\right)_{iL}\chi^{-1}_{Lm}\delta\Phi_{mH}\chi^{-1}_{Hi}\right)\delta_{lk}JdV \quad (4.134)$$

where

$$\left(\delta\mathcal{G}_1^{e,h}\right)_7 = -\eta\int_{V^e}\underbrace{\left\{\boldsymbol{c}^e\right\}^T}_{1\times\left(n_{dof}^{u,e}\right)}.\underbrace{\left[\boldsymbol{grad}(\boldsymbol{N}^{u,e})\right]^T}_{\left(n_{dof}^{u,e}\right)\times(n_{sd}*n_{sd})}.\underbrace{\left[\boldsymbol{T}_1^{\chi_n}\right]}_{(n_{sd}*n_{sd})\times(n_{sd}*n_{sd})}$$
$$.\underbrace{\left[\left(\boldsymbol{N}^{\chi,e}\right)\right]}_{(n_{sd}*n_{sd})\times n_{dof}^{\chi,e}}.\underbrace{\left\{\delta\boldsymbol{\phi}^e\right\}}_{n_{dof}^{\chi,e}\times 1}JdV \quad (4.135)$$

$$\underbrace{\left[\mathfrak{T}_7^e\right]}_{\left(n_{dof}^{u,e}\right)\times\left(n_{dof}^{\chi,e}\right)} = -\eta\int_{V^e}\underbrace{\left[\boldsymbol{grad}(\boldsymbol{N}^{u,e})\right]^T}_{\left(n_{dof}^{u,e}\right)\times(n_{sd}*n_{sd})}.\underbrace{\left[\boldsymbol{T}_1^{\chi_n}\right]}_{(n_{sd}*n_{sd})\times(n_{sd}*n_{sd})}.\underbrace{\left[(\boldsymbol{N}^{\chi,e})\right]}_{(n_{sd}*n_{sd})\times n_{dof}^{\chi,e}}JdV \tag{4.136}$$

$$\left(\delta\mathcal{G}_1^h\right)_7 = \mathop{\mathbf{A}}_{e=1}^{n_{\text{el}}}\underbrace{\left\{\boldsymbol{c}^e\right\}^T}_{1\times\left(n_{dof}^{u,e}\right)}.\underbrace{\left[\mathfrak{T}_7^e\right]}_{\left(n_{dof}^{u,e}\right)\times\left(n_{dof}^{\chi,e}\right)}.\underbrace{\left\{\delta\boldsymbol{\phi}^e\right\}}_{n_{dof}^{\chi,e}\times 1} \tag{4.137}$$

The eighth term in equation (4.15) can be found as :

$$\left(\delta\mathcal{G}_1\right)_8 = -\eta\int_V w_{k,l}\left(\left(F_n\right)_{iL}F^{-1}_{Lm}\delta u_{m,i}\right)\delta_{lk}JdV \tag{4.138}$$

$$\left(\delta\mathcal{G}_1^{e,h}\right)_8 = -\eta\int_{V^e}\underbrace{\left\{\boldsymbol{c}^e\right\}^T}_{1\times\left(n_{dof}^{u,e}\right)}.\underbrace{\left[\boldsymbol{grad}(\boldsymbol{N}^{u,e})\right]^T}_{\left(n_{dof}^{u,e}\right)\times(n_{sd}*n_{sd})}.\underbrace{\left[\boldsymbol{T}_4^{Fn}\right]}_{(n_{sd}*n_{sd})\times(n_{sd}*n_{sd})}$$
$$.\underbrace{\left[\boldsymbol{grad}\left(\boldsymbol{N}^{u,e}\right)\right]}_{(n_{sd}*n_{sd})\times n_{dof}^{u,e}}.\underbrace{\left\{\delta\boldsymbol{d}^e\right\}}_{n_{dof}^{u,e}\times 1}JdV \tag{4.139}$$

$$\underbrace{\left[\mathfrak{T}_8^e\right]}_{\left(n_{dof}^{u,e}\right)\times\left(n_{dof}^{u,e}\right)} = -\eta\int_{V^e}\underbrace{\left[\boldsymbol{grad}(\boldsymbol{N}^{u,e})\right]^T}_{\left(n_{dof}^{u,e}\right)\times(n_{sd}*n_{sd})}.\underbrace{\left[\boldsymbol{T}_4^{Fn}\right]}_{(n_{sd}*n_{sd})\times(n_{sd}*n_{sd})}.\underbrace{\left[\boldsymbol{grad}\left(\boldsymbol{N}^{u,e}\right)\right]}_{(n_{sd}*n_{sd})\times n_{dof}^{u,e}}JdV \tag{4.140}$$

$$\left(\delta\mathcal{G}_1^h\right)_8 = \mathop{\mathbf{A}}_{e=1}^{n_{\text{el}}}\underbrace{\left\{\boldsymbol{c}^e\right\}^T}_{1\times\left(n_{dof}^{u,e}\right)}.\underbrace{\left[\mathfrak{T}_8^e\right]}_{\left(n_{dof}^{u,e}\right)\times\left(n_{dof}^{u,e}\right)}.\underbrace{\left\{\delta\boldsymbol{d}^e\right\}}_{n_{dof}^{u,e}\times 1} \tag{4.141}$$

The ninth term in equation (4.15) will be found as :

$$\left(\delta\mathcal{G}_1\right)_9 = -\kappa\int_V w_{k,l}\left(\left(\chi_n\right)_{lL}\chi^{-1}_{Lm}\delta\Phi_{mR}\chi^{-1}_{Rk}\right)JdV \tag{4.142}$$

$$\left(\delta\mathcal{G}_1^{e,h}\right)_9 = -\kappa\int_{V^e}\underbrace{\left\{\boldsymbol{c}^e\right\}^T}_{1\times\left(n_{dof}^{u,e}\right)}.\underbrace{\left[\boldsymbol{grad}(\boldsymbol{N}^{u,e})\right]^T}_{\left(n_{dof}^{u,e}\right)\times(n_{sd}*n_{sd})}.\underbrace{\left[\boldsymbol{T}_2^{\chi_n}\right]}_{(n_{sd}*n_{sd})\times(n_{sd}*n_{sd})}$$
$$.\underbrace{\left[(\boldsymbol{N}^{\chi,e})\right]}_{(n_{sd}*n_{sd})\times n_{dof}^{\chi,e}}.\underbrace{\left\{\delta\boldsymbol{\phi}^e\right\}}_{n_{dof}^{\chi,e}\times 1}JdV \tag{4.143}$$

$$\underbrace{\left[\mathfrak{T}_9^e\right]}_{\left(n_{dof}^{u,e}\right)\times\left(n_{dof}^{\chi,e}\right)} = -\kappa\int_{V^e}\underbrace{\left[\boldsymbol{grad}(\boldsymbol{N}^{u,e})\right]^T}_{\left(n_{dof}^{u,e}\right)\times(n_{sd}*n_{sd})}.\underbrace{\left[\boldsymbol{T}_2^{\chi_n}\right]}_{(n_{sd}*n_{sd})\times(n_{sd}*n_{sd})}.\underbrace{\left[(\boldsymbol{N}^{\chi,e})\right]}_{(n_{sd}*n_{sd})\times n_{dof}^{\chi,e}}JdV \tag{4.144}$$

$$\left(\delta\mathcal{G}_1^h\right)_9 = \mathop{\mathbf{A}}_{e=1}^{n_{\text{el}}}\underbrace{\left\{\boldsymbol{c}^e\right\}^T}_{1\times\left(n_{dof}^{u,e}\right)}.\underbrace{\left[\mathfrak{T}_9^e\right]}_{\left(n_{dof}^{u,e}\right)\times\left(n_{dof}^{\chi,e}\right)}.\underbrace{\left\{\delta\boldsymbol{\phi}^e\right\}}_{n_{dof}^{\chi,e}\times 1} \tag{4.145}$$

The tenth term in equation (4.15) will be found as :

$$\left(\delta \mathcal{G}_1\right)_{10} = -\kappa \int_V w_{k,l} \left(\left(F_n\right)_{kL} F^{-1}_{Lm} \delta u_{m,l} \right) JdV \tag{4.146}$$

$$\left(\delta \mathcal{G}_1^{e,h}\right)_{10} = -\kappa \int_{V^e} \underbrace{\left\{\boldsymbol{c}^e\right\}^T}_{1\times\left(n^{u,e}_{dof}\right)} . \underbrace{\left[\boldsymbol{grad}(\boldsymbol{N}^{u,e})\right]^T}_{\left(n^{u,e}_{dof}\right)\times(n_{sd}*n_{sd})} . \underbrace{\left[\boldsymbol{T}_5^{F_n}\right]}_{(n_{sd}*n_{sd})\times(n_{sd}*n_{sd})}$$
$$. \underbrace{\left[\boldsymbol{grad}\left(\boldsymbol{N}^{u,e}\right)\right]}_{(n_{sd}*n_{sd})\times n^{u,e}_{dof}} . \underbrace{\left\{\delta \boldsymbol{d}^e\right\}}_{n^{u,e}_{dof}\times 1} JdV \tag{4.147}$$

$$\underbrace{\left[\boldsymbol{\mathcal{T}}^e_{10}\right]}_{\left(n^{u,e}_{dof}\right)\times\left(n^{u,e}_{dof}\right)} = -\kappa \int_{V^e} \underbrace{\left[\boldsymbol{grad}(\boldsymbol{N}^{u,e})\right]^T}_{\left(n^{u,e}_{dof}\right)\times(n_{sd}*n_{sd})} . \underbrace{\left[\boldsymbol{T}_5^{F_n}\right]}_{(n_{sd}*n_{sd})\times(n_{sd}*n_{sd})} . \underbrace{\left[\boldsymbol{grad}\left(\boldsymbol{N}^{u,e}\right)\right]}_{(n_{sd}*n_{sd})\times n^{u,e}_{dof}} JdV \tag{4.148}$$

$$\left(\delta \mathcal{G}_1^h\right)_{10} = \mathop{\mathbf{A}}_{e=1}^{n_{\text{el}}} \underbrace{\left\{\boldsymbol{c}^e\right\}^T}_{1\times\left(n^{u,e}_{dof}\right)} . \underbrace{\left[\boldsymbol{\mathcal{T}}^e_{10}\right]}_{\left(n^{u,e}_{dof}\right)\times\left(n^{u,e}_{dof}\right)} . \underbrace{\left\{\delta \boldsymbol{d}^e\right\}}_{n^{u,e}_{dof}\times 1} \tag{4.149}$$

The eleventh term in equation (4.15) will be found as :

$$\left(\delta \mathcal{G}_1\right)_{11} = -\nu \int_V w_{k,l} \left(\left(\chi_n\right)_{kL} \chi^{-1}_{Lm} \delta \Phi_{mR} \chi^{-1}_{Rl} \right) JdV \tag{4.150}$$

$$\left(\delta \mathcal{G}_1^{e,h}\right)_{11} = -\nu \int_{V^e} \underbrace{\left\{\boldsymbol{c}^e\right\}^T}_{1\times\left(n^{u,e}_{dof}\right)} . \underbrace{\left[\boldsymbol{grad}(\boldsymbol{N}^{u,e})\right]^T}_{\left(n^{u,e}_{dof}\right)\times(n_{sd}*n_{sd})} . \underbrace{\left[\boldsymbol{T}_3^{\chi_n}\right]}_{(n_{sd}*n_{sd})\times(n_{sd}*n_{sd})}$$
$$. \underbrace{\left[(\boldsymbol{N}^{\chi,e})\right]}_{(n_{sd}*n_{sd})\times n^{\chi,e}_{dof}} . \underbrace{\left\{\delta \boldsymbol{\phi}^e\right\}}_{n^{\chi,e}_{dof}\times 1} JdV \tag{4.151}$$

$$\underbrace{\left[\boldsymbol{\mathcal{T}}^e_{11}\right]}_{\left(n^{u,e}_{dof}\right)\times\left(n^{\chi,e}_{dof}\right)} = -\nu \int_{V^e} \underbrace{\left[\boldsymbol{grad}(\boldsymbol{N}^{u,e})\right]^T}_{\left(n^{u,e}_{dof}\right)\times(n_{sd}*n_{sd})} . \underbrace{\left[\boldsymbol{T}_3^{\chi_n}\right]}_{(n_{sd}*n_{sd})\times(n_{sd}*n_{sd})} . \underbrace{\left[(\boldsymbol{N}^{\chi,e})\right]}_{(n_{sd}*n_{sd})\times n^{\chi,e}_{dof}} JdV \tag{4.152}$$

$$\left(\delta \mathcal{G}_1^h\right)_{11} = \mathop{\mathbf{A}}_{e=1}^{n_{\text{el}}} \underbrace{\left\{\boldsymbol{c}^e\right\}^T}_{1\times\left(n^{u,e}_{dof}\right)} . \underbrace{\left[\boldsymbol{\mathcal{T}}^e_{11}\right]}_{\left(n^{u,e}_{dof}\right)\times\left(n^{\chi,e}_{dof}\right)} . \underbrace{\left\{\delta \boldsymbol{\phi}^e\right\}}_{n^{\chi,e}_{dof}\times 1} \tag{4.153}$$

The twelfth term is:

$$\left(\delta \mathcal{G}_1\right)_{12} = -\nu \int_V w_{k,l} \left(\left(F_n\right)_{lL} F^{-1}_{Lm} \delta u_{m,k} \right) JdV \tag{4.154}$$

$$\left(\delta \mathcal{G}_1^{e,h}\right)_{12} = -\nu \int_{V^e} \underbrace{\left\{\boldsymbol{c}^e\right\}^T}_{1\times\left(n_{dof}^{u,e}\right)} . \underbrace{\left[\boldsymbol{grad}(\boldsymbol{N}^{u,e})\right]^T}_{\left(n_{dof}^{u,e}\right)\times(n_{sd}*n_{sd})} . \underbrace{\left[\boldsymbol{T}_6^{F_n}\right]}_{(n_{sd}*n_{sd})\times(n_{sd}*n_{sd})}$$
$$. \underbrace{\left[\boldsymbol{grad}\left(\boldsymbol{N}^{u,e}\right)\right]}_{(n_{sd}*n_{sd})\times n_{dof}^{u,e}} . \underbrace{\left\{\delta \boldsymbol{d}^e\right\}}_{n_{dof}^{u,e}\times 1} J dV \tag{4.155}$$

$$\underbrace{\left[\mathfrak{T}_{12}^e\right]}_{\left(n_{dof}^{u,e}\right)\times\left(n_{dof}^{u,e}\right)} = -\nu \int_{V^e} \underbrace{\left[\boldsymbol{grad}(\boldsymbol{N}^{u,e})\right]^T}_{\left(n_{dof}^{u,e}\right)\times(n_{sd}*n_{sd})} . \underbrace{\left[\boldsymbol{T}_6^{F_n}\right]}_{(n_{sd}*n_{sd})\times(n_{sd}*n_{sd})} . \underbrace{\left[\boldsymbol{grad}\left(\boldsymbol{N}^{u,e}\right)\right]}_{(n_{sd}*n_{sd})\times n_{dof}^{u,e}} J dV \tag{4.156}$$

$$\left(\delta \mathcal{G}_1^h\right)_{12} = \mathop{\mathbf{A}}_{e=1}^{n_{\text{el}}} \underbrace{\left\{\boldsymbol{c}^e\right\}^T}_{1\times\left(n_{dof}^{u,e}\right)} . \underbrace{\left[\mathfrak{T}_{12}^e\right]}_{\left(n_{dof}^{u,e}\right)\times\left(n_{dof}^{u,e}\right)} . \underbrace{\left\{\delta \boldsymbol{d}^e\right\}}_{n_{dof}^{u,e}\times 1} \tag{4.157}$$

the thirteenth term is:

$$\left(\delta \mathcal{G}_1\right)_{13} = -\int_V w_{k,l}\sigma_{lk}\delta\left(J\right) dV = -\int_V w_{k,l}\sigma_{lk} J div(\delta \boldsymbol{u}) dV \tag{4.158}$$

$$\left(\delta \mathcal{G}_1\right)_{13} = -\int_V w_{k,l}\sigma_{lk}\delta\left(u_{n,n}\right) J dV \tag{4.159}$$

$$\left(\delta \mathcal{G}_1\right)_{13} = -\int_V w_{k,l}\sigma_{lk}\delta u_{n,j}\delta_{jn} J dV \tag{4.160}$$

or

$$\left(\delta \mathcal{G}_1\right)_{13} = -\int_V w_{k,l}\sigma_{lk}\delta u_{n,N} F_{Nn}^{-1} J dV \tag{4.161}$$

$$\left(\delta \mathcal{G}_1^{e,h}\right)_{13} = -\int_{V^e} \underbrace{\left\{\boldsymbol{c}^e\right\}^T}_{1\times\left(n_{dof}^{u,e}\right)} . \underbrace{\left[\boldsymbol{grad}(\boldsymbol{N}^{u,e})\right]^T}_{\left(n_{dof}^{u,e}\right)\times(n_{sd}*n_{sd})} . \underbrace{\left\{\boldsymbol{\sigma}_{curr}\right\}}_{(n_{sd}*n_{sd})\times(n_{sd}*n_{sd})}$$
$$. \underbrace{\left[\boldsymbol{GRAD}\left(\boldsymbol{N}^{u,e}\right)\right]}_{(n_{sd}*n_{sd})\times n_{dof}^{u,e}} . \underbrace{\left\{\delta \boldsymbol{d}^e\right\}}_{n_{dof}^{u,e}\times 1} J dV \tag{4.162}$$

$$\underbrace{\left[\mathfrak{T}_{13}^e\right]}_{\left(n_{dof}^{u,e}\right)\times\left(n_{dof}^{u,e}\right)} = -\int_{V^e} \underbrace{\left[\boldsymbol{grad}(\boldsymbol{N}^{u,e})\right]^T}_{\left(n_{dof}^{u,e}\right)\times(n_{sd}*n_{sd})} . \underbrace{\left\{\boldsymbol{\sigma}_{curr}\right\}}_{(n_{sd}*n_{sd})\times(n_{sd}*n_{sd})} . \underbrace{\left[\boldsymbol{GRAD}\left(\boldsymbol{N}^{u,e}\right)\right]}_{(n_{sd}*n_{sd})\times n_{dof}^{u,e}} J dV \tag{4.163}$$

$$\left(\delta \mathcal{G}_1^h\right)_{13} = \mathop{\mathbf{A}}_{e=1}^{n_{\text{el}}} \underbrace{\left\{\boldsymbol{c}^e\right\}^T}_{1\times\left(n_{dof}^{u,e}\right)} . \underbrace{\left[\mathfrak{T}_{13}^e\right]}_{\left(n_{dof}^{u,e}\right)\times\left(n_{dof}^{u,e}\right)} . \underbrace{\left\{\delta \boldsymbol{d}^e\right\}}_{n_{dof}^{u,e}\times 1} \tag{4.164}$$

contribution of variation of $\boldsymbol{F}^{-1}$ from $\boldsymbol{\nabla w}$:

$$\left(\delta \mathcal{G}_1\right)_{14} = -\int_V w_{k,l}\sigma_{lk}\delta\left(J\right) dV = -\int_V -w_{k,L} F_{Lm}^{-1}\delta u_{m,l}\sigma_{lk} J dV \tag{4.165}$$

$$\left(\delta \mathcal{G}_1\right)_{14} = \int_V w_{k,m}\sigma_{lk}\delta u_{m,l} JdV \tag{4.166}$$

$$\left(\delta \mathcal{G}_1^{e,h}\right)_{14} = -\int_{V^e} \underbrace{\left\{\boldsymbol{c}^e\right\}^T}_{1\times\left(n_{dof}^{u,e}\right)} . \underbrace{\left[\boldsymbol{grad}(\boldsymbol{N}^{u,e})\right]^T}_{\left(n_{dof}^{u,e}\right)\times(n_{sd}*n_{sd})} . \underbrace{\left\{\boldsymbol{V}_F\right\}}_{(n_{sd}*n_{sd})\times(n_{sd}*n_{sd})}$$
$$. \underbrace{\left[\boldsymbol{grad}\left(\boldsymbol{N}^{u,e}\right)\right]}_{(n_{sd}*n_{sd})\times n_{dof}^{u,e}} . \underbrace{\left\{\delta\boldsymbol{d}^e\right\}}_{n_{dof}^{u,e}\times 1} JdV \tag{4.167}$$

$$\underbrace{\left[\boldsymbol{\mathcal{T}}_{14}^e\right]}_{\left(n_{dof}^{u,e}\right)\times\left(n_{dof}^{u,e}\right)} = -\int_{V^e} \underbrace{\left[\boldsymbol{grad}(\boldsymbol{N}^{u,e})\right]^T}_{\left(n_{dof}^{u,e}\right)\times(n_{sd}*n_{sd})} . \underbrace{\left\{\boldsymbol{V}_F\right\}}_{(n_{sd}*n_{sd})\times(n_{sd}*n_{sd})} . \underbrace{\left[\boldsymbol{grad}\left(\boldsymbol{N}^{u,e}\right)\right]}_{(n_{sd}*n_{sd})\times n_{dof}^{u,e}} JdV \tag{4.168}$$

$$\left(\delta \mathcal{G}_1^h\right)_{14} = \mathop{\mathbf{A}}_{e=1}^{n_{\text{el}}} \underbrace{\left\{\boldsymbol{c}^e\right\}^T}_{1\times\left(n_{dof}^{u,e}\right)} . \underbrace{\left[\boldsymbol{\mathcal{T}}_{14}^e\right]}_{\left(n_{dof}^{u,e}\right)\times\left(n_{dof}^{u,e}\right)} . \underbrace{\left\{\delta\boldsymbol{d}^e\right\}}_{n_{dof}^{u,e}\times 1} \tag{4.169}$$

The traction term (force term);

$$\delta \mathcal{G}_{ext}^h = \int_S \boldsymbol{w}^T \cdot \delta\boldsymbol{T}\rho_0 dA \tag{4.170}$$

$$\delta \mathcal{G}_{ext}^{e,h} = \int_{S^e} \underbrace{\left\{\boldsymbol{c}^e\right\}}_{1\times\left(n_{dof}^{u,e}\right)}^T . \underbrace{\left[\boldsymbol{N}^{u,e}\right]^T}_{n_{dof}^{u,e}\times n_{sd}} . \underbrace{\left\{\delta\boldsymbol{T}\right\}}_{n_{sd}\times 1} \rho_0 dA \tag{4.171}$$

$$\underbrace{\left\{\boldsymbol{G}_{ext}^{T,e}\right\}}_{n_{dof}^{u,e}\times 1} = \int_{S^e} \underbrace{\left[\boldsymbol{N}^{u,e}\right]^T}_{n_{dof}^{u,e}\times n_{sd}} . \underbrace{\left\{\delta\boldsymbol{T}\right\}}_{n_{sd}\times 1} \rho_0 dA \tag{4.172}$$

$$\delta \mathcal{G}_{ext}^h = \mathop{\mathbf{A}}_{e=1}^{n_{\text{el}}} \underbrace{\left\{\boldsymbol{c}^e\right\}^T}_{1\times\left(n_{dof}^{u,e}\right)} . \underbrace{\left\{\boldsymbol{G}_{ext}^{T,e}\right\}}_{n_{dof}^{u,e}\times 1} \tag{4.173}$$

4.7 Submatrices in the Matrix Form of the Linearized Form of the Balance of First Moment of Momentum

Variation of $\boldsymbol{\nabla\eta}$:

$$(\delta\mathcal{H}_1)_{\nabla\eta} = -\int_V \delta\eta_{ml,k} m_{klm} JdV \tag{4.174}$$

$$(\delta\mathcal{H}_1)_{\nabla\eta} = -\int_V \eta_{ml,K}\delta F^{-1}_{Kk} m_{klm} JdV \tag{4.175}$$

$$(\delta\mathcal{H}_1)_{\nabla\eta} = \int_V \eta_{ml,K} F^{-1}_{Ki}\delta u_{i,k} m_{klm} JdV \tag{4.176}$$

$$(\delta\mathcal{H}_1)_{\nabla\eta} = \int_V \eta_{ml,i} m_{klm}\delta u_{i,k} JdV \tag{4.177}$$

$$\left(\delta\mathcal{H}_1^{e,h}\right)_{\nabla\eta} = \int_{V^e} \underbrace{\left\{\boldsymbol{\alpha}^e\right\}^T}_{1\times n^{\chi}_{dof}} . \underbrace{\left[\boldsymbol{grad}(\boldsymbol{N}^{\chi,e})\right]^T}_{n^{\chi}_{dof}\times(n_{sd}*n_{sd}*n_{sd})} . \underbrace{\left[\boldsymbol{M}^m_{\nabla\eta}\right]}_{(n_{sd}*n_{sd}*n_{sd})\times(n_{sd}*n_{sd})} . \underbrace{\left[\boldsymbol{grad}\left(\boldsymbol{N}^{u,e}\right)\right]}_{(n_{sd}*n_{sd})\times n^{u,e}_{dof}} . \underbrace{\left\{\delta\boldsymbol{d}^e\right\}}_{n^{u,e}_{dof}\times 1} JdV \tag{4.178}$$

$$\underbrace{\left[\boldsymbol{\mathfrak{M}}^e_{\nabla\eta}\right]}_{n^{\chi}_{dof}\times n^{u,e}_{dof}} = \int_{V^e} \underbrace{\left[\boldsymbol{grad}(\boldsymbol{N}^{\chi,e})\right]^T}_{n^{\chi}_{dof}\times(n_{sd}*n_{sd}*n_{sd})} . \underbrace{\left[\boldsymbol{M}^m_{\nabla\eta}\right]}_{(n_{sd}*n_{sd}*n_{sd})\times(n_{sd}*n_{sd})} . \underbrace{\left[\boldsymbol{grad}\left(\boldsymbol{N}^{u,e}\right)\right]}_{(n_{sd}*n_{sd})\times n^{u,e}_{dof}} JdV \tag{4.179}$$

$$\left(\delta\mathcal{H}_1^h\right)_1 = \mathop{\mathbf{A}}_{e=1}^{n_{\text{el}}} \underbrace{\left\{\boldsymbol{\alpha}^e\right\}^T}_{1\times n^{\chi,e}_{dof}} . \underbrace{\left[\boldsymbol{\mathfrak{M}}^e_{\nabla\eta}\right]}_{n^{\chi}_{dof}\times n^{u,e}_{dof}} . \underbrace{\left\{\delta\boldsymbol{d}^e\right\}}_{n^{u,e}_{dof}\times 1} \tag{4.180}$$

The first variation term (the first term in the variation of of $\delta\boldsymbol{m}_{n+1}$);

$$(\delta\mathcal{H}_1)_1 = \int_V \eta_{ml,k}\left((F_n)_{iL} F^{-1}_{Lp}\delta u_{p,i}\right)(m_n)_{klm} JdV \tag{4.181}$$

$$\left(\delta\mathcal{H}_1^{e,h}\right)_1 = \int_{V^e} \left\{\boldsymbol{grad}\left(\boldsymbol{\eta}\right)\right\}^T . \left[\boldsymbol{M}^m_1\right] . \left\{\boldsymbol{grad}\left(\delta\boldsymbol{u}\right)\right\} JdV \tag{4.182}$$

$$\left(\delta\mathcal{H}_1^{e,h}\right)_1 = \int_{V^e} \underbrace{\left\{\boldsymbol{\alpha}^e\right\}^T}_{1\times n^{\chi}_{dof}} . \underbrace{\left[\boldsymbol{grad}(\boldsymbol{N}^{\chi,e})\right]^T}_{n^{\chi}_{dof}\times(n_{sd}*n_{sd}*n_{sd})} . \underbrace{\left[\boldsymbol{M}^m_1\right]}_{(n_{sd}*n_{sd}*n_{sd})\times(n_{sd}*n_{sd})} . \underbrace{\left[\boldsymbol{grad}\left(\boldsymbol{N}^{u,e}\right)\right]}_{(n_{sd}*n_{sd})\times n^{u,e}_{dof}} . \underbrace{\left\{\delta\boldsymbol{d}^e\right\}}_{n^{u,e}_{dof}\times 1} JdV \tag{4.183}$$

$$\underbrace{\left[\mathfrak{M}_1^e\right]}_{n_{dof}^{\chi}\times n_{dof}^{u,e}} = \int_{V^e} \underbrace{\left[\boldsymbol{grad}(\boldsymbol{N}^{\chi,e})\right]^T}_{n_{dof}^{\chi}\times(n_{sd}*n_{sd}*n_{sd})} . \underbrace{\left[\boldsymbol{M}_1^m\right]}_{(n_{sd}*n_{sd}*n_{sd})\times(n_{sd}*n_{sd})} . \underbrace{\left[\boldsymbol{grad}\left(\boldsymbol{N}^{u,e}\right)\right]}_{(n_{sd}*n_{sd})\times n_{dof}^{u,e}} JdV \tag{4.184}$$

$$\left(\delta\mathcal{H}_1^h\right)_1 = \mathop{\mathbf{A}}_{e=1}^{n_{\text{el}}} \underbrace{\left\{\boldsymbol{\alpha}^e\right\}^T}_{1\times n_{dof}^{\chi,e}} . \underbrace{\left[\mathfrak{M}_1^e\right]}_{n_{dof}^{\chi,e}\times n_{dof}^{u,e}} . \underbrace{\left\{\delta\boldsymbol{d}^e\right\}}_{n_{dof}^{u,e}\times 1} \tag{4.185}$$

The second variation term (the second term in the variation of of $\delta\boldsymbol{m}_{n+1}$) ;

$$\left(\delta\mathcal{H}_1\right)_2 = -\int_V \eta_{ml,k}\left(\left(F_n\right)_{kL} F_{Ln}^{-1}\delta u_{n,i}\right)\left(m_n\right)_{ilm} JdV \tag{4.186}$$

$$\left(\delta\mathcal{H}_1^{e,h}\right)_2 = -\int_{V^e} \left\{\boldsymbol{grad}\left(\boldsymbol{\eta}\right)\right\}^T . \left[\boldsymbol{M}_2^m\right] . \left\{\boldsymbol{grad}\left(\delta\boldsymbol{u}\right)\right\} JdV \tag{4.187}$$

where

$$\left(\delta\mathcal{H}_1^{e,h}\right)_2 = -\int_{V^e} \underbrace{\left\{\boldsymbol{\alpha}^e\right\}^T}_{1\times n_{dof}^{\chi,e}} . \underbrace{\left[\boldsymbol{grad}(\boldsymbol{N}^{\chi,e})\right]^T}_{n_{dof}^{\chi,e}\times(n_{sd}*n_{sd}*n_{sd})} . \underbrace{\left[\boldsymbol{M}_2^m\right]}_{(n_{sd}*n_{sd}*n_{sd})\times(n_{sd}*n_{sd})} . \underbrace{\left[\boldsymbol{grad}\left(\boldsymbol{N}^{u,e}\right)\right]}_{(n_{sd}*n_{sd})\times n_{dof}^{u,e}} . \underbrace{\left\{\delta\boldsymbol{d}^e\right\}}_{n_{dof}^{u,e}\times 1} JdV \tag{4.188}$$

$$\underbrace{\left[\mathfrak{M}_2^e\right]}_{n_{dof}^{\chi,e}\times n_{dof}^{u,e}} = -\int_{V^e} \underbrace{\left[\boldsymbol{grad}(\boldsymbol{N}^{\chi,e})\right]^T}_{n_{dof}^{\chi,e}\times(n_{sd}*n_{sd}*n_{sd})} . \underbrace{\left[\boldsymbol{M}_2^m\right]}_{(n_{sd}*n_{sd}*n_{sd})\times(n_{sd}*n_{sd})} . \underbrace{\left[\boldsymbol{grad}\left(\boldsymbol{N}^{u,e}\right)\right]}_{(n_{sd}*n_{sd})\times n_{dof}^{u,e}} JdV \tag{4.189}$$

$$\left(\delta\mathcal{H}_1^h\right)_2 = \mathop{\mathbf{A}}_{e=1}^{n_{\text{el}}} \underbrace{\left\{\boldsymbol{\alpha}^e\right\}^T}_{1\times n_{dof}^{\chi,e}} . \underbrace{\left[\mathfrak{M}_2^e\right]}_{n_{dof}^{\chi,e}\times n_{dof}^{u,e}} . \underbrace{\left\{\delta\boldsymbol{d}^e\right\}}_{n_{dof}^{u,e}\times 1} \tag{4.190}$$

The third variation term (the third term in the variation of of $\delta\boldsymbol{m}_{n+1}$) ;

$$\left(\delta\mathcal{H}_1\right)_3 = -\int_V \eta_{ml,k}\left(m_n\right)_{kim}\left(\left(F_n\right)_{lL} F_{Lp}^{-1}\delta u_{p,i}\right) JdV \tag{4.191}$$

$$\left(\delta\mathcal{H}_1^{e,h}\right)_3 = -\int_{V^e} \left\{\boldsymbol{grad}\left(\boldsymbol{\eta}\right)\right\}^T . \left[\boldsymbol{M}_3^m\right] . \left\{\boldsymbol{grad}\left(\delta\boldsymbol{u}\right)\right\} JdV \tag{4.192}$$

$$\left(\delta\mathcal{H}_1^{e,h}\right)_3 = -\int_{V^e} \underbrace{\left\{\boldsymbol{\alpha}^e\right\}^T}_{1\times n_{dof}^{\chi}} . \underbrace{\left[\boldsymbol{grad}(\boldsymbol{N}^{\chi,e})\right]^T}_{n_{dof}^{\chi}\times(n_{sd}*n_{sd}*n_{sd})} . \underbrace{\left[\boldsymbol{M}_3^m\right]}_{(n_{sd}*n_{sd}*n_{sd})\times(n_{sd}*n_{sd})} . \underbrace{\left[\boldsymbol{grad}\left(\boldsymbol{N}^{u,e}\right)\right]}_{(n_{sd}*n_{sd})\times n_{dof}^{u,e}} . \underbrace{\left\{\delta\boldsymbol{d}^e\right\}}_{n_{dof}^{u,e}\times 1} JdV \tag{4.193}$$

$$\underbrace{\left[\mathfrak{M}_3^e\right]}_{n_{dof}^{\chi,e}\times n_{dof}^{u,e}} = -\int_{V^e} \underbrace{\left[\boldsymbol{grad}(\boldsymbol{N}^{\chi,e})\right]^T}_{n_{dof}^{\chi}\times(n_{sd}*n_{sd}*n_{sd})}.\underbrace{\left[\boldsymbol{M}_3^m\right]}_{(n_{sd}*n_{sd}*n_{sd})\times(n_{sd}*n_{sd})}.\underbrace{\left[\boldsymbol{grad}\left(\boldsymbol{N}^{u,e}\right)\right]}_{(n_{sd}*n_{sd})\times n_{dof}^{u,e}} JdV \tag{4.194}$$

$$\left(\delta\mathcal{H}_1^h\right)_3 = \mathop{\mathbf{A}}_{e=1}^{n_{\text{el}}} \underbrace{\left\{\boldsymbol{\alpha}^e\right\}^T}_{1\times n_{dof}^{\chi,e}}.\underbrace{\left[\mathfrak{M}_3^e\right]}_{n_{dof}^{\chi,e}\times n_{dof}^{u,e}}.\underbrace{\left\{\delta\boldsymbol{d}^e\right\}}_{n_{dof}^{u,e}\times 1} \tag{4.195}$$

The fourth variation term (the fourth term in the variation of of $\delta\boldsymbol{m}_{n+1}$) ;

$$\left(\delta\mathcal{H}_1\right)_4 = -\int_V \eta_{ml,k}\left(m_n\right)_{kli}\left(\left(\chi_n\right)_{mL}\chi_{Lp}^{-1}\delta\Phi_{pT}\chi_{Ti}^{-1}\right)JdV \tag{4.196}$$

$$\left(\delta\mathcal{H}_1^{e,h}\right)_4 = -\int_{V^e}\left\{\boldsymbol{grad}\left(\boldsymbol{\eta}\right)\right\}^T.\left[\boldsymbol{M}_4^m\right].\left\{\delta\boldsymbol{\Phi}\right\}JdV \tag{4.197}$$

$$\left(\delta\mathcal{H}_1^{e,h}\right)_4 = -\int_{V^e}\underbrace{\left\{\boldsymbol{\alpha}^e\right\}^T}_{1\times n_{dof}^{\chi,e}}.\underbrace{\left[\boldsymbol{grad}(\boldsymbol{N}^{\chi,e})\right]^T}_{n_{dof}^{\chi,e}\times(n_{sd}*n_{sd}*n_{sd})}.\underbrace{\left[\boldsymbol{M}_4^m\right]}_{(n_{sd}*n_{sd}*n_{sd})\times(n_{sd}*n_{sd})}$$
$$.\underbrace{\left[\boldsymbol{N}^{\chi,e}\right]}_{(n_{sd}*n_{sd})\times n_{dof}^{\chi,e}}.\underbrace{\left\{\delta\boldsymbol{\phi}^e\right\}}_{n_{dof}^{\chi,e}\times 1}JdV \tag{4.198}$$

$$\underbrace{\left[\mathfrak{M}_4^e\right]}_{n_{dof}^{\chi,e}\times n_{dof}^{u,e}} = -\int_{V^e}\underbrace{\left[\boldsymbol{grad}(\boldsymbol{N}^{\chi,e})\right]^T}_{n_{dof}^{\chi,e}\times(n_{sd}*n_{sd}*n_{sd})}.\underbrace{\left[\boldsymbol{M}_4^m\right]}_{(n_{sd}*n_{sd}*n_{sd})\times(n_{sd}*n_{sd})}.\underbrace{\left[\boldsymbol{N}^{\chi,e}\right]}_{(n_{sd}*n_{sd})\times n_{dof}^{\chi,e}}JdV \tag{4.199}$$

$$\left(\delta\mathcal{H}_1^h\right)_4 = \mathop{\mathbf{A}}_{e=1}^{n_{\text{el}}}\underbrace{\left\{\boldsymbol{\alpha}^e\right\}^T}_{1\times n_{dof}^{\chi,e}}.\underbrace{\left[\mathfrak{M}_4^e\right]}_{n_{dof}^{\chi,e}\times n_{dof}^{\chi,e}}.\underbrace{\left\{\delta\boldsymbol{\phi}^e\right\}}_{n_{dof}^{\chi,e}\times 1} \tag{4.200}$$

The fifth term is :

$$\left(\delta\mathcal{H}_1\right)_5 = -\int_V \eta_{ml,k}c_{klmprs}\left(\left(\chi_n\right)_{pL}\chi_{Ln}^{-1}\delta\Phi_{nT}\chi_{Ti}^{-1}\right)\left(\gamma_n^e\right)_{irs}JdV \tag{4.201}$$

$$\left(\delta\mathcal{H}_1^{e,h}\right)_5 = -\int_{V^e}\underbrace{\left\{\boldsymbol{\alpha}^e\right\}^T}_{1\times n_{dof}^{\chi,e}}.\underbrace{\left[\boldsymbol{grad}(\boldsymbol{N}^{\chi,e})\right]^T}_{n_{dof}^{\chi,e}\times(n_{sd}*n_{sd}*n_{sd})}.\underbrace{\left[\boldsymbol{M}_5^m\right]}_{(n_{sd}*n_{sd}*n_{sd})\times(n_{sd}*n_{sd})}$$
$$.\underbrace{\left[\boldsymbol{N}^{\chi,e}\right]}_{(n_{sd}*n_{sd})\times n_{dof}^{\chi,e}}.\underbrace{\left\{\delta\boldsymbol{\phi}^e\right\}}_{n_{dof}^{\chi,e}\times 1}JdV \tag{4.202}$$

$$\underbrace{\left[\mathfrak{M}_5^e\right]}_{n_{dof}^{\chi,e}\times n_{dof}^{u,e}} = -\int_{V^e}\underbrace{\left[\boldsymbol{grad}(\boldsymbol{N}^{\chi,e})\right]^T}_{n_{dof}^{\chi,e}\times(n_{sd}*n_{sd}*n_{sd})}.\underbrace{\left[\boldsymbol{M}_5^m\right]}_{(n_{sd}*n_{sd}*n_{sd})\times(n_{sd}*n_{sd})}.\underbrace{\left[\boldsymbol{N}^{\chi,e}\right]}_{(n_{sd}*n_{sd})\times n_{dof}^{\chi,e}}JdV \tag{4.203}$$

$$(\delta\mathcal{H}_1)_5 = \mathop{\mathbf{A}}_{e=1}^{n_{\text{el}}} \underbrace{\left\{\boldsymbol{\alpha}^e\right\}^T}_{1\times n_{dof}^{\chi,e}} . \underbrace{\left[\mathfrak{M}_5^e\right]}_{n_{dof}^{\chi,e}\times n_{dof}^{\chi,e}} . \underbrace{\left\{\delta\boldsymbol{\phi}^e\right\}}_{n_{dof}^{\chi,e}\times 1} \tag{4.204}$$

The sixth term is :

$$(\delta\mathcal{H}_1)_6 = \int_V \eta_{ml,k} c_{klmprs} \left((\chi_n)_{iL} \, \chi_{Ln}^{-1} \delta\Phi_{nT} \chi_{Tr}^{-1} \right) (\gamma_n^e)_{pis} \, JdV \tag{4.205}$$

$$\left(\delta\mathcal{H}_1^{e,h}\right)_6 = \int_{V^e} \underbrace{\left\{\boldsymbol{\alpha}^e\right\}^T}_{1\times n_{dof}^{\chi,e}} . \underbrace{\left[\boldsymbol{grad}(\boldsymbol{N}^{\chi,e})\right]^T}_{n_{dof}^{\chi,e}\times(n_{sd}*n_{sd}*n_{sd})} . \underbrace{\left[\boldsymbol{M}_6^m\right]}_{(n_{sd}*n_{sd}*n_{sd})\times(n_{sd}*n_{sd})}$$
$$. \underbrace{\left[\boldsymbol{N}^{\chi,e}\right]}_{(n_{sd}*n_{sd})\times n_{dof}^{\chi,e}} . \underbrace{\left\{\delta\boldsymbol{\phi}^e\right\}}_{n_{dof}^{\chi,e}\times 1} JdV \tag{4.206}$$

$$\underbrace{\left[\mathfrak{M}_6^e\right]}_{n_{dof}^{\chi,e}\times n_{dof}^{u,e}} = \int_{V^e} \underbrace{\left[\boldsymbol{grad}(\boldsymbol{N}^{\chi,e})\right]^T}_{n_{dof}^{\chi,e}\times(n_{sd}*n_{sd}*n_{sd})} . \underbrace{\left[\boldsymbol{M}_6^m\right]}_{(n_{sd}*n_{sd}*n_{sd})\times(n_{sd}*n_{sd})} . \underbrace{\left[\boldsymbol{N}^{\chi,e}\right]}_{(n_{sd}*n_{sd})\times n_{dof}^{\chi,e}} JdV \tag{4.207}$$

$$\left(\delta\mathcal{H}_1^h\right)_6 = \mathop{\mathbf{A}}_{e=1}^{n_{\text{el}}} \underbrace{\left\{\boldsymbol{\alpha}^e\right\}^T}_{1\times n_{dof}^{\chi,e}} . \underbrace{\left[\mathfrak{M}_6^e\right]}_{n_{dof}^{\chi,e}\times n_{dof}^{\chi,e}} . \underbrace{\left\{\delta\boldsymbol{\phi}^e\right\}}_{n_{dof}^{\chi,e}\times 1} \tag{4.208}$$

The seventh term is :

$$(\delta\mathcal{H}_1)_7 = \int_V \eta_{ml,k} c_{klmprs} \delta\left(\Phi_{pA,T}\right) F_{Ts}^{-1} \chi_{Ar}^{-1} JdV \tag{4.209}$$

$$\underbrace{\left[\mathfrak{M}_7^e\right]}_{n_{dof}^{\chi,e}\times n_{dof}^{\chi,e}} = \int_{V^e} \underbrace{\left[\boldsymbol{grad}(\boldsymbol{N}^{\chi,e})\right]^T}_{n_{dof}^{\chi,e}\times(n_{sd}*n_{sd}*n_{sd})} . \underbrace{\left[\boldsymbol{M}_7^m\right]}_{(n_{sd}*n_{sd}*n_{sd})\times(n_{sd}*n_{sd}*n_{sd})} . \underbrace{\left[\boldsymbol{GRAD}\left(\boldsymbol{N}^{\chi,e}\right)\right]}_{(n_{sd}*n_{sd}*n_{sd})\times n_{dof}^{\chi,e}} JdV$$

$$\left(\delta\mathcal{H}_1^h\right)_7 = \mathop{\mathbf{A}}_{e=1}^{n_{\text{el}}} \underbrace{\left\{\boldsymbol{\alpha}^e\right\}^T}_{1\times n_{dof}^{\chi,e}} . \underbrace{\left[\mathfrak{M}_7^e\right]}_{n_{dof}^{\chi,e}\times n_{dof}^{\chi,e}} . \underbrace{\left\{\delta\boldsymbol{\phi}^e\right\}}_{n_{dof}^{\chi,e}\times 1} \tag{4.210}$$

The eighth term is :

$$(\delta\mathcal{H}_1)_8 = -\int_V \eta_{ml,k} c_{klmprs} \left(\chi_{pA,T} - (\chi_n)_{pA,T}\right) F_{Ta}^{-1} \delta\left(u_{a,s}\right) \chi_{Ar}^{-1} JdV \tag{4.211}$$

$$\left(\delta\mathcal{H}_1^{e,h}\right)_8 = \int_{V^e} \underbrace{\left\{\boldsymbol{\alpha}^e\right\}^T}_{1\times n_{dof}^{\chi,e}} . \underbrace{\left[\boldsymbol{grad}(\boldsymbol{N}^{\chi,e})\right]^T}_{n_{dof}^{\chi}\times(n_{sd}*n_{sd}*n_{sd})} . \underbrace{\left[\boldsymbol{M}_8^m\right]}_{(n_{sd}*n_{sd}*n_{sd})\times(n_{sd}*n_{sd})}$$
$$. \underbrace{\left[\boldsymbol{grad}\left(\boldsymbol{N}^{u,e}\right)\right]}_{(n_{sd}*n_{sd})\times n_{dof}^{u,e}} . \underbrace{\left\{\delta\boldsymbol{d}^e\right\}}_{n_{dof}^{u,e}\times 1} JdV \tag{4.212}$$

$$\underbrace{\left[\mathfrak{M}_8^e\right]}_{n_{dof}^{\chi,e}\times n_{dof}^{u,e}} = \int_{V^e} \underbrace{\left[\boldsymbol{grad}(\boldsymbol{N}^{\chi,e})\right]^T}_{n_{dof}^{\chi,e}\times(n_{sd}*n_{sd}*n_{sd})} . \underbrace{\left[\boldsymbol{M}_8^m\right]}_{(n_{sd}*n_{sd}*n_{sd})\times(n_{sd}*n_{sd})} . \underbrace{\left[\boldsymbol{grad}\left(\boldsymbol{N}^{u,e}\right)\right]}_{(n_{sd}*n_{sd})\times n_{dof}^{u,e}} JdV$$

$$\left(\delta\mathcal{H}_1^h\right)_8 = \mathop{\mathbf{A}}_{e=1}^{n_{\text{el}}} \underbrace{\left\{\boldsymbol{\alpha}^e\right\}^T}_{1\times n_{dof}^{\chi,e}} . \underbrace{\left[\mathfrak{M}_8^e\right]}_{n_{dof}^{\chi,e}\times n_{dof}^{u,e}} . \underbrace{\left\{\delta\boldsymbol{d}^e\right\}}_{n_{dof}^{u,e}\times 1} \tag{4.213}$$

The ninth term is :

$$\left(\delta\mathcal{H}_1\right)_9 = \int_V \eta_{ml,k} c_{klmprs} \left(\chi_{pA,T} - \left(\chi_n\right)_{pA,T}\right) F_{Ts}^{-1} \chi_{Aa}^{-1} \delta\Phi_{aB} \chi_{Br}^{-1} JdV \tag{4.214}$$

$$\left(\delta\mathcal{H}_1^{e,h}\right)_9 = -\int_{V^e} \underbrace{\left\{\boldsymbol{\alpha}^e\right\}^T}_{1\times n_{dof}^{\chi,e}} . \underbrace{\left[\boldsymbol{grad}(\boldsymbol{N}^{\chi,e})\right]^T}_{n_{dof}^{\chi,e}\times(n_{sd}*n_{sd}*n_{sd})} . \underbrace{\left[\boldsymbol{M}_9^m\right]}_{(n_{sd}*n_{sd}*n_{sd})\times(n_{sd}*n_{sd})}$$
$$. \underbrace{\left[\boldsymbol{N}^{\chi,e}\right]}_{(n_{sd}*n_{sd})\times n_{dof}^{\chi,e}} . \underbrace{\left\{\delta\boldsymbol{\phi}^e\right\}}_{n_{dof}^{\chi,e}\times 1} JdV \tag{4.215}$$

$$\underbrace{\left[\mathfrak{M}_9^e\right]}_{n_{dof}^{\chi,e}\times n_{dof}^{\chi,e}} = -\int_{V^e} \underbrace{\left[\boldsymbol{grad}(\boldsymbol{N}^{\chi,e})\right]^T}_{n_{dof}^{\chi,e}\times(n_{sd}*n_{sd}*n_{sd})} . \underbrace{\left[\boldsymbol{M}_9^m\right]}_{(n_{sd}*n_{sd}*n_{sd})\times(n_{sd}*n_{sd})} . \underbrace{\left[\boldsymbol{N}^{\chi,e}\right]}_{(n_{sd}*n_{sd})\times n_{dof}^{\chi,e}} JdV \tag{4.216}$$

$$\left(\delta\mathcal{H}_1^h\right)_9 = \mathop{\mathbf{A}}_{e=1}^{n_{\text{el}}} \underbrace{\left\{\boldsymbol{\alpha}^e\right\}^T}_{1\times n_{dof}^{\chi,e}} . \underbrace{\left[\mathfrak{M}_9^e\right]}_{n_{dof}^{\chi,e}\times n_{dof}^{\chi,e}} . \underbrace{\left\{\delta\boldsymbol{\phi}^e\right\}}_{n_{dof}^{\chi,e}\times 1} \tag{4.217}$$

The tenth term:

$$\left(\delta\mathcal{H}_1\right)_{10} = \int_V \eta_{ml,k} c_{klmprs} \delta\left(\Phi_{pA}\right) \chi_{Aa}^{-1} \chi_{aB,T} \chi_{Br}^{-1} F_{Ts}^{-1} JdV \tag{4.218}$$

$$\left(\delta\mathcal{H}_1^{e,h}\right)_{10} = -\int_{V^e} \underbrace{\left\{\boldsymbol{\alpha}^e\right\}^T}_{1\times n_{dof}^{\chi,e}} . \underbrace{\left[\boldsymbol{grad}(\boldsymbol{N}^{\chi,e})\right]^T}_{n_{dof}^{\chi,e}\times(n_{sd}*n_{sd}*n_{sd})} . \underbrace{\left[\boldsymbol{M}_{10}^m\right]}_{(n_{sd}*n_{sd}*n_{sd})\times(n_{sd}*n_{sd})}$$
$$. \underbrace{\left[\boldsymbol{N}^{\chi,e}\right]}_{(n_{sd}*n_{sd})\times n_{dof}^{\chi,e}} . \underbrace{\left\{\delta\boldsymbol{\phi}^e\right\}}_{n_{dof}^{\chi,e}\times 1} JdV \tag{4.219}$$

$$\underbrace{\left[\mathfrak{M}_{10}^e\right]}_{n_{dof}^{\chi,e}\times n_{dof}^{\chi,e}} = -\int_{V^e} \underbrace{\left[\boldsymbol{grad}(\boldsymbol{N}^{\chi,e})\right]^T}_{n_{dof}^{\chi,e}\times(n_{sd}*n_{sd}*n_{sd})} . \underbrace{\left[\boldsymbol{M}_{10}^m\right]}_{(n_{sd}*n_{sd}*n_{sd})\times(n_{sd}*n_{sd})} . \underbrace{\left[\boldsymbol{N}^{\chi,e}\right]}_{(n_{sd}*n_{sd})\times n_{dof}^{\chi,e}} JdV \tag{4.220}$$

$$\left(\delta\mathcal{H}_1^h\right)_{10} = \mathop{\mathbf{A}}_{e=1}^{n_{\text{el}}} \underbrace{\left\{\boldsymbol{\alpha}^e\right\}^T}_{1\times n_{dof}^{\chi,e}} . \underbrace{\left[\mathfrak{M}_{10}^e\right]}_{n_{dof}^{\chi,e}\times n_{dof}^{\chi,e}} . \underbrace{\left\{\delta\boldsymbol{\phi}^e\right\}}_{n_{dof}^{\chi,e}\times 1} \tag{4.221}$$

The eleventh term:

$$\left(\delta\mathcal{H}_1\right)_{11} = -\int_V \eta_{ml,k} c_{klmprs} \left(\chi_{pA} - \left(\chi_n\right)_{pA}\right) \chi^{-1}_{Ai} \delta\Phi_{iL} \chi^{-1}_{La} \chi_{aB,T} \chi^{-1}_{Br} F^{-1}_{Ts} JdV \tag{4.222}$$

$$\left(\delta\mathcal{H}_1^{e,h}\right)_{11} = -\int_{V^e} \underbrace{\left\{\boldsymbol{\alpha}^e\right\}^T}_{1\times n^{\chi,e}_{dof}} . \underbrace{\left[\boldsymbol{grad}(\boldsymbol{N}^{\chi,e})\right]^T}_{n^{\chi,e}_{dof}\times(n_{sd}*n_{sd}*n_{sd})} . \underbrace{\left[\boldsymbol{M}^m_{11}\right]}_{(n_{sd}*n_{sd}*n_{sd})\times(n_{sd}*n_{sd})} . \underbrace{\left[\boldsymbol{N}^{\chi,e}\right]}_{(n_{sd}*n_{sd})\times n^{\chi,e}_{dof}} . \underbrace{\left\{\delta\boldsymbol{\phi}^e\right\}}_{n^{\chi,e}_{dof}\times 1} JdV \tag{4.223}$$

$$\underbrace{\left[\mathfrak{M}^e_{11}\right]}_{n^{\chi,e}_{dof}\times n^{\chi,e}_{dof}} = -\int_{V^e} \underbrace{\left[\boldsymbol{grad}(\boldsymbol{N}^{\chi,e})\right]^T}_{n^{\chi,e}_{dof}\times(n_{sd}*n_{sd}*n_{sd})} . \underbrace{\left[\boldsymbol{M}^m_{11}\right]}_{(n_{sd}*n_{sd}*n_{sd})\times(n_{sd}*n_{sd})} . \underbrace{\left[\boldsymbol{N}^{\chi,e}\right]}_{(n_{sd}*n_{sd})\times n^{\chi,e}_{dof}} JdV \tag{4.224}$$

$$\left(\delta\mathcal{H}^h_1\right)_{11} = \mathop{\mathbf{A}}_{e=1}^{n_{\text{el}}} \underbrace{\left\{\boldsymbol{\alpha}^e\right\}^T}_{1\times n^{\chi,e}_{dof}} . \underbrace{\left[\mathfrak{M}^e_{11}\right]}_{n^{\chi,e}_{dof}\times n^{\chi,e}_{dof}} . \underbrace{\left\{\delta\boldsymbol{\phi}^e\right\}}_{n^{\chi,e}_{dof}\times 1} \tag{4.225}$$

The twelfth term:

$$\left(\delta\mathcal{H}_1\right)_{12} = -\int_V \eta_{ml,k} c_{klmprs} \left(\chi_{pA} - \left(\chi_n\right)_{pA}\right) \chi^{-1}_{Aa} \delta\Phi_{aB,T} \chi^{-1}_{Br} F^{-1}_{Ts} JdV \tag{4.226}$$

$$\left(\delta\mathcal{H}_1^{e,h}\right)_{12} = -\int_{V^e} \underbrace{\left\{\boldsymbol{\alpha}^e\right\}^T}_{1\times n^{\chi,e}_{dof}} . \underbrace{\left[\boldsymbol{grad}(\boldsymbol{N}^{\chi,e})\right]^T}_{n^{\chi,e}_{dof}\times(n_{sd}*n_{sd}*n_{sd})} . \underbrace{\left[\boldsymbol{M}^m_{12}\right]}_{(n_{sd}*n_{sd}*n_{sd})\times(n_{sd}*n_{sd}*n_{sd})} . \underbrace{\left[\boldsymbol{GRAD}\left(\boldsymbol{N}^{\chi,e}\right)\right]}_{(n_{sd}*n_{sd}*n_{sd})\times n^{\chi,e}_{dof}} . \underbrace{\left\{\delta\boldsymbol{\phi}^e\right\}}_{n^{\chi,e}_{dof}\times 1} JdV \tag{4.227}$$

$$\underbrace{\left[\mathfrak{M}^e_{12}\right]}_{n^{\chi,e}_{dof}\times n^{\chi,e}_{dof}} = -\int_{V^e} \underbrace{\left[\boldsymbol{grad}(\boldsymbol{N}^{\chi,e})\right]^T}_{n^{\chi,e}_{dof}\times(n_{sd}*n_{sd}*n_{sd})} . \underbrace{\left[\boldsymbol{M}^m_{12}\right]}_{(n_{sd}*n_{sd}*n_{sd})\times(n_{sd}*n_{sd}*n_{sd})} . \underbrace{\left[\boldsymbol{GRAD}\left(\boldsymbol{N}^{\chi,e}\right)\right]}_{(n_{sd}*n_{sd}*n_{sd})\times n^{\chi,e}_{dof}} JdV \tag{4.228}$$

$$\left(\delta\mathcal{H}^h_1\right)_{12} = \mathop{\mathbf{A}}_{e=1}^{n_{\text{el}}} \underbrace{\left\{\boldsymbol{\alpha}^e\right\}^T}_{1\times n^{\chi,e}_{dof}} . \underbrace{\left[\mathfrak{M}^e_{12}\right]}_{n^{\chi,e}_{dof}\times n^{\chi,e}_{dof}} . \underbrace{\left\{\delta\boldsymbol{\phi}^e\right\}}_{n^{\chi,e}_{dof}\times 1} \tag{4.229}$$

The thirteenth term:

$$\left(\delta\mathcal{H}_1\right)_{13} = -\int_V \eta_{ml,k} c_{klmprs} \left(\chi_{pA} - \left(\chi_n\right)_{pA}\right) \chi^{-1}_{Aa} \chi_{aB,T} \chi^{-1}_{Bi} \delta\Phi_{iL} \chi^{-1}_{Lr} F^{-1}_{Ts} JdV \tag{4.230}$$

$$\left(\delta\mathcal{H}_1^{e,h}\right)_{13} = -\int_{V^e} \underbrace{\left\{\boldsymbol{\alpha}^e\right\}^T}_{1\times n_{dof}^{\chi,e}} . \underbrace{\left[\boldsymbol{grad}(\boldsymbol{N}^{\chi,e})\right]^T}_{n_{dof}^{\chi,e}\times(n_{sd}*n_{sd}*n_{sd})} . \underbrace{\left[\boldsymbol{M}_{13}^m\right]}_{(n_{sd}*n_{sd}*n_{sd})\times(n_{sd}*n_{sd})} . \underbrace{\left[\boldsymbol{N}^{\chi,e}\right]}_{(n_{sd}*n_{sd})\times n_{dof}^{\chi,e}} . \underbrace{\left\{\delta\boldsymbol{\phi}^e\right\}}_{n_{dof}^{\chi,e}\times 1} JdV \tag{4.231}$$

$$\underbrace{\left[\mathfrak{M}_{13}^e\right]}_{n_{dof}^{\chi,e}\times n_{dof}^{\chi,e}} = -\int_{V^e} \underbrace{\left[\boldsymbol{grad}(\boldsymbol{N}^{\chi,e})\right]^T}_{n_{dof}^{\chi,e}\times(n_{sd}*n_{sd}*n_{sd})} . \underbrace{\left[\boldsymbol{M}_{13}^m\right]}_{(n_{sd}*n_{sd}*n_{sd})\times(n_{sd}*n_{sd})} . \underbrace{\left[\boldsymbol{N}^{\chi,e}\right]}_{(n_{sd}*n_{sd})\times n_{dof}^{\chi,e}} JdV \tag{4.232}$$

$$\left(\delta\mathcal{H}_1^h\right)_{13} = \mathop{\mathbf{A}}_{e=1}^{n_{\text{el}}} \underbrace{\left\{\boldsymbol{\alpha}^e\right\}^T}_{1\times n_{dof}^{\chi,e}} . \underbrace{\left[\mathfrak{M}_{13}^e\right]}_{n_{dof}^{\chi,e}\times n_{dof}^{\chi,e}} . \underbrace{\left\{\delta\boldsymbol{\phi}^e\right\}}_{n_{dof}^{\chi,e}\times 1} \tag{4.233}$$

The fourteenth term:

$$\left(\delta\mathcal{H}_1\right)_{14} = -\int_V \eta_{ml,k} c_{klmprs} \left(\chi_{pA}\left(\chi_n\right)_{pA}\right) \chi_{Aa}^{-1}\chi_{aB,T}\chi_{Br}^{-1}F_{Ti}^{-1}\delta\left(u_{i,s}\right) JdV \tag{4.234}$$

$$\left(\delta\mathcal{H}_1^{e,h}\right)_{14} = -\int_{V^e} \underbrace{\left\{\boldsymbol{\alpha}^e\right\}^T}_{1\times n_{dof}^{\chi,e}} . \underbrace{\left[\boldsymbol{grad}(\boldsymbol{N}^{\chi,e})\right]^T}_{n_{dof}^{\chi,e}\times(n_{sd}*n_{sd}*n_{sd})} . \underbrace{\left[\boldsymbol{M}_{14}^m\right]}_{(n_{sd}*n_{sd}*n_{sd})\times(n_{sd}*n_{sd})} . \underbrace{\left[\boldsymbol{gradN}^{u,e}\right]}_{(n_{sd}*n_{sd})\times n_{dof}^{u,e}} . \underbrace{\left\{\delta\boldsymbol{d}^e\right\}}_{n_{dof}^{u,e}\times 1} JdV \tag{4.235}$$

$$\underbrace{\left[\mathfrak{M}_{14}^e\right]}_{n_{dof}^{\chi,e}\times n_{dof}^{u,e}} = -\int_{V^e} \underbrace{\left[\boldsymbol{grad}(\boldsymbol{N}^{\chi,e})\right]^T}_{n_{dof}^{\chi,e}\times(n_{sd}*n_{sd}*n_{sd})} . \underbrace{\left[\boldsymbol{M}_{13}^m\right]}_{(n_{sd}*n_{sd}*n_{sd})\times(n_{sd}*n_{sd})} . \underbrace{\left[\boldsymbol{gradN}^{u,e}\right]}_{(n_{sd}*n_{sd})\times n_{dof}^{u,e}} JdV \tag{4.236}$$

$$\left(\delta\mathcal{H}_1^h\right)_{14} = \mathop{\mathbf{A}}_{e=1}^{n_{\text{el}}} \underbrace{\left\{\boldsymbol{\alpha}^e\right\}^T}_{1\times n_{dof}^{\chi,e}} . \underbrace{\left[\mathfrak{M}_{14}^e\right]}_{n_{dof}^{\chi,e}\times n_{dof}^{u,e}} . \underbrace{\left\{\delta\boldsymbol{d}^e\right\}}_{n_{dof}^{u,e}\times 1} \tag{4.237}$$

the fifteenth term

$$\left(\delta\mathcal{H}_1\right)_{15} = -\int_V \eta_{ml,k}\left(F_n\right)_{iL} F_{Ln}^{-1}\delta u_{n,k}\left(\gamma_n\right)_{ilm} JdV \tag{4.238}$$

$$\left(\delta\mathcal{H}_1^{e,h}\right)_{15} = -\int_{V^e} \underbrace{\left\{\boldsymbol{\alpha}^e\right\}^T}_{1\times n_{dof}^{\chi,e}} . \underbrace{\left[\boldsymbol{grad}(\boldsymbol{N}^{\chi,e})\right]^T}_{n_{dof}^{\chi,e}\times(n_{sd}*n_{sd}*n_{sd})} . \underbrace{\left[\boldsymbol{M}_{15}^m\right]}_{(n_{sd}*n_{sd}*n_{sd})\times(n_{sd}*n_{sd})} . \underbrace{\left[\boldsymbol{grad}\left(\boldsymbol{N}^{u,e}\right)\right]}_{(n_{sd}*n_{sd})\times n_{dof}^{u,e}} . \underbrace{\left\{\delta\boldsymbol{d}^e\right\}}_{n_{dof}^{u,e}\times 1} JdV \tag{4.239}$$

$$\underbrace{\left[\mathfrak{M}_{15}^{e}\right]}_{n_{dof}^{\chi,e}\times n_{dof}^{u,e}} = -\int_{V^e} \underbrace{\left[\boldsymbol{grad}(\boldsymbol{N}^{\chi,e})\right]^T}_{n_{dof}^{\chi,e}\times(n_{sd}*n_{sd}*n_{sd})}.\underbrace{\left[\boldsymbol{M}_{15}^{m}\right]}_{(n_{sd}*n_{sd}*n_{sd})\times(n_{sd}*n_{sd})}.\underbrace{\left[\boldsymbol{grad}\left(\boldsymbol{N}^{u,e}\right)\right]}_{(n_{sd}*n_{sd})\times n_{dof}^{u,e}} JdV \tag{4.240}$$

$$\left(\delta\mathcal{H}_1^h\right)_{15} = \mathop{\mathbf{A}}_{e=1}^{n_{\text{el}}} \underbrace{\left\{\boldsymbol{\alpha}^e\right\}^T}_{1\times n_{dof}^{\chi,e}}.\underbrace{\left[\mathfrak{M}_{15}^{e}\right]}_{n_{dof}^{\chi,e}\times n_{dof}^{u,e}}.\underbrace{\left\{\delta\boldsymbol{d}^e\right\}}_{n_{dof}^{u,e}\times 1} \tag{4.241}$$

The sixteenth term:

$$\left(\delta\mathcal{H}_1\right)_{16} = -\int_V \eta_{ml,k}\left(\gamma_n\right)_{kli}\left(F_n\right)_{iL} F_{Ln}^{-1}\delta u_{n,m} JdV \tag{4.242}$$

$$\left(\delta\mathcal{H}_1^{e,h}\right)_{16} = -\int_{V^e} \underbrace{\left\{\boldsymbol{\alpha}^e\right\}^T}_{1\times n_{dof}^{\chi,e}}.\underbrace{\left[\boldsymbol{grad}(\boldsymbol{N}^{\chi,e})\right]^T}_{n_{dof}^{\chi,e}\times(n_{sd}*n_{sd}*n_{sd})}.\underbrace{\left[\boldsymbol{M}_{16}^{m}\right]}_{(n_{sd}*n_{sd}*n_{sd})\times(n_{sd}*n_{sd})}$$
$$.\underbrace{\left[\boldsymbol{grad}\left(\boldsymbol{N}^{u,e}\right)\right]}_{(n_{sd}*n_{sd})\times n_{dof}^{u,e}}.\underbrace{\left\{\delta\boldsymbol{d}^e\right\}}_{n_{dof}^{u,e}\times 1} JdV \tag{4.243}$$

$$\underbrace{\left[\mathfrak{M}_{16}^{e}\right]}_{n_{dof}^{\chi,e}\times n_{dof}^{u,e}} = -\int_{V^e} \underbrace{\left[\boldsymbol{grad}(\boldsymbol{N}^{\chi,e})\right]^T}_{n_{dof}^{\chi,e}\times(n_{sd}*n_{sd}*n_{sd})}.\underbrace{\left[\boldsymbol{M}_{12}^{m}\right]}_{(n_{sd}*n_{sd}*n_{sd})\times(n_{sd}*n_{sd})}.\underbrace{\left[\boldsymbol{grad}\left(\boldsymbol{N}^{u,e}\right)\right]}_{(n_{sd}*n_{sd})\times n_{dof}^{u,e}} JdV \tag{4.244}$$

$$\left(\delta\mathcal{H}_1^h\right)_{16} = \mathop{\mathbf{A}}_{e=1}^{n_{\text{el}}} \underbrace{\left\{\boldsymbol{\alpha}^e\right\}^T}_{1\times n_{dof}^{\chi,e}}.\underbrace{\left[\mathfrak{M}_{16}^{e}\right]}_{n_{dof}^{\chi,e}\times n_{dof}^{u,e}}.\underbrace{\left\{\delta\boldsymbol{d}^e\right\}}_{n_{dof}^{u,e}\times 1} \tag{4.245}$$

The seventeenth term:

$$\left(\delta\mathcal{H}_1\right)_{17} = -\int_V \eta_{ml,k}\left(\gamma_n\right)_{kim}\left(\chi_n\right)_{iL}\chi_{Ln}^{-1}\delta\Phi_{nT}\chi_{Tl}^{-1} JdV \tag{4.246}$$

$$\left(\delta\mathcal{H}_1^{e,h}\right)_{17} = -\int_{V^e} \underbrace{\left\{\boldsymbol{\alpha}^e\right\}^T}_{1\times n_{dof}^{\chi,e}}.\underbrace{\left[\boldsymbol{grad}(\boldsymbol{N}^{\chi,e})\right]^T}_{n_{dof}^{\chi,e}\times(n_{sd}*n_{sd}*n_{sd})}.\underbrace{\left[\boldsymbol{M}_{17}^{m}\right]}_{(n_{sd}*n_{sd}*n_{sd})\times(n_{sd}*n_{sd})}$$
$$.\underbrace{\left[\boldsymbol{N}^{\chi,e}\right]}_{(n_{sd}*n_{sd})\times n_{dof}^{\chi,e}}.\underbrace{\left\{\delta\boldsymbol{\phi}^e\right\}}_{n_{dof}^{\chi,e}\times 1} JdV \tag{4.247}$$

$$\underbrace{\left[\mathfrak{M}_{17}^{e}\right]}_{n_{dof}^{\chi,e}\times n_{dof}^{\chi,e}} = -\int_V \underbrace{\left\{\boldsymbol{\alpha}^e\right\}^T}_{1\times n_{dof}^{\chi,e}}.\underbrace{\left[\boldsymbol{M}_{13}^{m}\right]}_{(n_{sd}*n_{sd}*n_{sd})\times(n_{sd}*n_{sd})}.\underbrace{\left[\boldsymbol{N}^{\chi,e}\right]}_{(n_{sd}*n_{sd})\times n_{dof}^{\chi,e}} JdV \tag{4.248}$$

$$\left(\delta\mathcal{H}_1^h\right)_{17} = \mathop{\mathbf{A}}_{e=1}^{n_{\text{el}}} \underbrace{\left\{\boldsymbol{\alpha}^e\right\}^T}_{1\times n_{dof}^{\chi,e}}.\underbrace{\left[\mathfrak{M}_{17}^{e}\right]}_{n_{dof}^{\chi,e}\times n_{dof}^{\chi,e}}.\underbrace{\left\{\delta\boldsymbol{\phi}^e\right\}}_{n_{dof}^{\chi,e}\times 1} \tag{4.249}$$

The last term in equation (4.26)

$$\left(\delta\mathcal{H}_1\right)_{18} = -\int_V \eta_{ml,k} m_{klm} \delta\left(J\right) dV \tag{4.250}$$

$$\left(\delta\mathcal{H}_1\right)_{18} = -\int_V \eta_{ml,k} m_{klm} \delta\left(u_{n,n}\right) JdV \tag{4.251}$$

$$\left(\delta\mathcal{H}_1\right)_{18} = -\int_V \eta_{ml,k} m_{klm} \delta u_{n,N} F^{-1}_{N,n} JdV \tag{4.252}$$

$$\left(\delta\mathcal{H}_1^{e,h}\right)_{18} = -\int_{V^e} \underbrace{\left\{\boldsymbol{\alpha}^e\right\}^T}_{1\times n^{\chi}_{dof}} . \underbrace{\left[\boldsymbol{grad}(\boldsymbol{N}^{\chi,e})\right]^T}_{n^{\chi}_{dof}\times(n_{sd}*n_{sd}*n_{sd})} . \underbrace{\left[\boldsymbol{M}^m_{14}\right]}_{(n_{sd}*n_{sd}*n_{sd})\times(n_{sd}*n_{sd})}$$
$$. \underbrace{\left[\boldsymbol{GRAD}\left(\boldsymbol{N}^{u,e}\right)\right]}_{(n_{sd}*n_{sd})\times n^{u,e}_{dof}} . \underbrace{\left\{\delta\boldsymbol{d}^e\right\}}_{n^{u,e}_{dof}\times 1} JdV \tag{4.253}$$

$$\underbrace{\left[\boldsymbol{\mathfrak{M}}^e_{18}\right]}_{n^{\chi}_{dof}\times n^{u,e}_{dof}} = -\int_{V^e} \underbrace{\left[\boldsymbol{grad}(\boldsymbol{N}^{\chi,e})\right]^T}_{n^{\chi}_{dof}\times(n_{sd}*n_{sd}*n_{sd})} . \underbrace{\left[\boldsymbol{M}^m_{14}\right]}_{(n_{sd}*n_{sd}*n_{sd})\times(n_{sd}*n_{sd})} . \underbrace{\left[\boldsymbol{GRAD}\left(\boldsymbol{N}^{u,e}\right)\right]}_{(n_{sd}*n_{sd})\times n^{u,e}_{dof}} JdV \tag{4.254}$$

$$\left(\delta\mathcal{H}_1^h\right)_{18} = \mathop{\mathbf{A}}_{e=1}^{n_{\text{el}}} \underbrace{\left\{\boldsymbol{\alpha}^e\right\}^T}_{1\times n^{\chi,e}_{dof}} . \underbrace{\left[\boldsymbol{\mathfrak{M}}^e_{18}\right]}_{n^{\chi,e}_{dof}\times n^{u,e}_{dof}} . \underbrace{\left\{\delta\boldsymbol{d}^e\right\}}_{n^{u,e}_{dof}\times 1} \tag{4.255}$$

The other integral term in 4.23 is;

$$\delta\mathcal{H}_2 = \int \eta_{ml}\delta\left(\sigma_{ml} - s_{ml}\right) JdV + \int \eta_{ml}\left(\sigma_{ml} - s_{ml}\right)\delta\left(J\right) dV \tag{4.256}$$

The matrix form of $\delta\left(\boldsymbol{s}-\boldsymbol{\sigma}\right)$ was given in equation (3.135) where its indicial notation can be expressed as :

$$\begin{aligned}
-\delta(s-\sigma)_{ml} &= \delta\left(\Delta t d^{e}_{ii}\right)\left(s_{ml}-\sigma_{ml}\right)_{n} - \delta\left(\Delta t \ell^{e}_{mi}\right)\left(s_{il}-\sigma_{il}\right)_{n} \\
&\quad - \left(s_{mi}-\sigma_{mi}\right)_{n}\delta\left(\Delta t \ell^{e}_{li}\right) - \left(\kappa-\sigma\right)\delta\left(\Delta t \varepsilon^{e}_{lm}\right) \\
&\quad - \left(\nu-\sigma\right)\delta\left(\Delta t \varepsilon^{e}_{ml}\right) - \tau\delta\left(\Delta t d^{e}_{ii}\right)\delta_{ml} - 2\sigma\delta\left(\Delta t d^{e}_{ml}\right) \\
&\quad - \left(\eta-\tau\right)\delta\left(\Delta t \varepsilon^{e}_{ii}\right)\delta_{ml} \qquad (4.257) \\
-\delta(s-\sigma)_{ml} &= \left(\left(F_n\right)_{iL}F^{-1}_{Lk}\delta u_{k,i}\right)\left(s_{ml}-\sigma_{ml}\right)_{n} - \left(\left(F_n\right)_{mL}F^{-1}_{Lk}\delta u_{k,i}\right)\left(s_{il}-\sigma_{il}\right)_{n} \\
&\quad - \left(s_{mi}-\sigma_{mi}\right)_{n}\left(\left(F_n\right)_{lL}F^{-1}_{Lk}\delta u_{k,i}\right) \\
&\quad - \left(\kappa-\sigma\right)\left(\left(\chi_n\right)_{lT}\chi^{-1}_{Tp}\delta\left(\Phi_{pK}\right)\chi^{-1}_{Km} + \left(F_n\right)_{mK}F^{-1}_{Kp}\delta u_{p,l}\right) \\
&\quad - \left(\nu-\sigma\right)\left(\left(\chi_n\right)_{mT}\chi^{-1}_{Tp}\delta\left(\Phi_{pK}\right)\chi^{-1}_{Kl} + \left(F_n\right)_{lK}F^{-1}_{Kp}\delta u_{p,m}\right) \\
&\quad - \tau\left(\left(F_n\right)_{iL}F^{-1}_{Lk}\delta u_{k,i}\right)\delta_{ml} \\
&\quad - 2\sigma\frac{1}{2}\left(\left(F_n\right)_{mL}F^{-1}_{Lk}\delta u_{k,l} + \left(F_n\right)_{lL}F^{-1}_{Lk}\delta u_{k,m}\right) \\
&\quad - \left(\eta-\tau\right)\left(\left(\chi_n\right)_{iT}\chi^{-1}_{Tp}\delta\left(\Phi_{pK}\right)\chi^{-1}_{Ki} + \left(F_n\right)_{iK}F^{-1}_{Kp}\delta u_{p,i}\right)\delta_{ml} \qquad (4.258)
\end{aligned}$$

Then the first sub-integral is :

$$\left(\delta\mathcal{H}_2\right)_1 = \int_V \eta_{ml}\delta\left(\sigma_{ml}-s_{ml}\right)JdV \qquad (4.259)$$

The first term in the variation of $-\delta\left(\sigma_{ml}-s_{ml}\right)$

$$\left(\delta\mathcal{H}_2\right)_1 = \int_V \eta_{ml}\left(\left(F_n\right)_{iL}F^{-1}_{Lm}\delta u_{m,i}\right)\left(s_{ml}-\sigma_{ml}\right)_{n}JdV \qquad (4.260)$$

Since the most of the matrices appearing in the $\mathcal{H}^h_2$ terms were found in chapter (4.6) or similar to them,they are not going to be given here in detail.

Starting with the first terms as:

$$\left(\delta\mathcal{H}_2\right)_1 = \int_V \eta_{ml}\left(\left(F_n\right)_{iL}F^{-1}_{Lk}\delta u_{k,i}\right)\left(s_{ml}-\sigma_{ml}\right)_{n}JdV \qquad (4.261)$$

$$\left(\delta\mathcal{H}^{e,h}_2\right)_1 = \int_{V^e} \underbrace{\left\{\boldsymbol{\alpha}^e\right\}^T}_{1\times n^{\chi}_{dof}} . \underbrace{\left[\boldsymbol{N}^{\chi,e}\right]^T}_{n^{\chi}_{dof}\times(n_{sd}*n_{sd})} . \underbrace{\left[\boldsymbol{R}^u_1\right]}_{(n_{sd}*n_{sd})\times(n_{sd}*n_{sd})} . \underbrace{\left[\boldsymbol{grad}\left(\boldsymbol{N}^{u,e}\right)\right]}_{(n_{sd}*n_{sd})\times n^{u,e}_{dof}} . \underbrace{\left\{\delta\boldsymbol{d}^e\right\}}_{n^{u,e}_{dof}\times 1} JdV \qquad (4.262)$$

$$\underbrace{\left[\boldsymbol{\mathcal{R}}^{\boldsymbol{e}}{}_1\right]}_{n_{dof}^{\chi}\times n_{dof}^{u,e}} = \int_{V^e} \underbrace{\left[\boldsymbol{N}^{\chi,e}\right]^T}_{n_{dof}^{\chi}\times(n_{sd}*n_{sd})} . \underbrace{\left[\boldsymbol{R}_1^u\right]}_{(n_{sd}*n_{sd})\times(n_{sd}*n_{sd})} . \underbrace{\left[\boldsymbol{grad}\left(\boldsymbol{N}^{u,e}\right)\right]}_{(n_{sd}*n_{sd})\times n_{dof}^{u,e}} .JdV \tag{4.263}$$

$$\left(\delta\mathcal{H}_2^h\right)_1 = \mathop{\mathbf{A}}_{e=1}^{n_{\text{el}}} \underbrace{\left\{\boldsymbol{\alpha}^e\right\}^T}_{1\times n_{dof}^{\chi,e}} . \underbrace{\left[\boldsymbol{\mathcal{R}}^{\boldsymbol{e}}{}_1\right]}_{n_{dof}^{\chi,e}\times n_{dof}^{u,e}} . \underbrace{\left\{\delta\boldsymbol{d}^e\right\}}_{n_{dof}^{u,e}\times 1} \tag{4.264}$$

The next term is :

$$\left(\delta\mathcal{H}_2\right)_2 = -\int_V \eta_{ml}\left(\left(F_n\right)_{mL} F_{Lk}^{-1}\delta u_{k,i}\right)\left(s_{il}-\sigma_{il}\right)_n JdV \tag{4.265}$$

$$\left(\delta\mathcal{H}_2^{e,h}\right)_2 = -\int_{V^e} \underbrace{\left\{\boldsymbol{\alpha}^e\right\}^T}_{1\times n_{dof}^{\chi}} . \underbrace{\left[\boldsymbol{N}^{\chi,e}\right]^T}_{n_{dof}^{\chi}\times(n_{sd}*n_{sd})} . \underbrace{\left[\boldsymbol{R}_2^u\right]}_{(n_{sd}*n_{sd})\times(n_{sd}*n_{sd})} . \underbrace{\left[\boldsymbol{grad}\left(\boldsymbol{N}^{u,e}\right)\right]}_{(n_{sd}*n_{sd})\times n_{dof}^{u,e}} . \underbrace{\left\{\delta\boldsymbol{d}^e\right\}}_{n_{dof}^{u,e}\times 1} JdV \tag{4.266}$$

$$\underbrace{\left[\boldsymbol{\mathcal{R}}^{\boldsymbol{e}}{}_2\right]}_{n_{dof}^{\chi}\times n_{dof}^{u,e}} = -\int_{V^e} \underbrace{\left[\boldsymbol{N}^{\chi,e}\right]^T}_{n_{dof}^{\chi}\times(n_{sd}*n_{sd})} . \underbrace{\left[\boldsymbol{R}_2^u\right]}_{(n_{sd}*n_{sd})\times(n_{sd}*n_{sd})} . \underbrace{\left[\boldsymbol{grad}\left(\boldsymbol{N}^{u,e}\right)\right]}_{(n_{sd}*n_{sd})\times n_{dof}^{u,e}} .JdV \tag{4.267}$$

$$\left(\delta\mathcal{H}_2^h\right)_2 = \mathop{\mathbf{A}}_{e=1}^{n_{\text{el}}} \underbrace{\left\{\boldsymbol{\alpha}^e\right\}^T}_{1\times n_{dof}^{\chi,e}} . \underbrace{\left[\boldsymbol{\mathcal{R}}^{\boldsymbol{e}}{}_2\right]}_{n_{dof}^{\chi,e}\times n_{dof}^{u,e}} . \underbrace{\left\{\delta\boldsymbol{d}^e\right\}}_{n_{dof}^{u,e}\times 1} \tag{4.268}$$

The third term is :

$$\left(\delta\mathcal{H}_2\right)_3 = -\int_V \eta_{ml}\left(s_{mi}-\sigma_{mi}\right)_n\left(\left(F_n\right)_{lL} F_{Lk}^{-1}\delta u_{k,i}\right) JdV \tag{4.269}$$

$$\left(\delta\mathcal{H}_2^{e,h}\right)_3 = -\int_{V^e} \underbrace{\left\{\boldsymbol{\alpha}^e\right\}^T}_{1\times n_{dof}^{\chi}} . \underbrace{\left[\boldsymbol{N}^{\chi,e}\right]^T}_{n_{dof}^{\chi}\times(n_{sd}*n_{sd})} . \underbrace{\left[\boldsymbol{R}_3^u\right]}_{(n_{sd}*n_{sd})\times(n_{sd}*n_{sd})} . \underbrace{\left[\boldsymbol{grad}\left(\boldsymbol{N}^{u,e}\right)\right]}_{(n_{sd}*n_{sd})\times n_{dof}^{u,e}} . \underbrace{\left\{\delta\boldsymbol{d}^e\right\}}_{n_{dof}^{u,e}\times 1} JdV \tag{4.270}$$

$$\underbrace{\left[\boldsymbol{\mathcal{R}}^{\boldsymbol{e}}{}_3\right]}_{n_{dof}^{\chi}\times n_{dof}^{u,e}} = -\int_{V^e} \underbrace{\left[\boldsymbol{N}^{\chi,e}\right]^T}_{n_{dof}^{\chi}\times(n_{sd}*n_{sd})} . \underbrace{\left[\boldsymbol{R}_3^u\right]}_{(n_{sd}*n_{sd})\times(n_{sd}*n_{sd})} . \underbrace{\left[\boldsymbol{grad}\left(\boldsymbol{N}^{u,e}\right)\right]}_{(n_{sd}*n_{sd})\times n_{dof}^{u,e}} .JdV \tag{4.271}$$

$$\left(\delta\mathcal{H}_2^h\right)_3 = \mathop{\mathbf{A}}_{e=1}^{n_{\text{el}}} \underbrace{\left\{\boldsymbol{\alpha}^e\right\}^T}_{1\times n_{dof}^{\chi,e}} . \underbrace{\left[\boldsymbol{\mathcal{R}}^{\boldsymbol{e}}{}_3\right]}_{n_{dof}^{\chi,e}\times n_{dof}^{u,e}} . \underbrace{\left\{\delta\boldsymbol{d}^e\right\}}_{n_{dof}^{u,e}\times 1} \tag{4.272}$$

The fourth term is :

$$\left(\delta\mathcal{H}_2\right)_4 = -\left(\kappa-\sigma\right)\int_V \eta_{ml}\left(\chi_n\right)_{lT}\chi_{Tp}^{-1}\delta\left(\Phi_{pK}\right)\chi_{Km}^{-1} JdV \tag{4.273}$$

$$\left(\delta\mathcal{H}_2^{e,h}\right)_4 = -\left(\kappa-\sigma\right)\int_{V^e} \underbrace{\left\{\boldsymbol{\alpha}^e\right\}^T}_{1\times n_{dof}^{\chi}} . \underbrace{\left[\boldsymbol{N}^{\chi,e}\right]^T}_{n_{dof}^{\chi}\times(n_{sd}*n_{sd})} . \underbrace{\left[\boldsymbol{R}_1^{\chi}\right]}_{(n_{sd}*n_{sd})\times(n_{sd}*n_{sd})} . \underbrace{\left[\boldsymbol{N}^{\chi,e}\right]}_{(n_{sd}*n_{sd})\times n_{dof}^{\chi,e}} . \underbrace{\left\{\delta\phi^e\right\}}_{n_{dof}^{\chi,e}\times 1} JdV \tag{4.274}$$

$$\underbrace{\left[\boldsymbol{\mathcal{R}}^{\boldsymbol{e}}{}_4\right]}_{n_{dof}^{\chi}\times n_{dof}^{\chi,e}} = -\left(\kappa-\sigma\right)\int_{V^e}\underbrace{\left[\boldsymbol{N}^{\chi,e}\right]^T}_{n_{dof}^{\chi}\times(n_{sd}*n_{sd})}.\underbrace{\left[\boldsymbol{R}_1^{\chi}\right]}_{(n_{sd}*n_{sd})\times(n_{sd}*n_{sd})}.\underbrace{\left[\boldsymbol{N}^{\chi,e}\right]}_{(n_{sd}*n_{sd})\times n_{dof}^{\chi,e}}JdV \tag{4.275}$$

$$\left(\delta\mathcal{H}_2^h\right)_4 = \mathop{\mathbf{A}}_{e=1}^{n_{\text{el}}}\underbrace{\left\{\boldsymbol{\alpha}^e\right\}^T}_{1\times n_{dof}^{\chi,e}}.\underbrace{\left[\boldsymbol{\mathcal{R}}^{\boldsymbol{e}}{}_4\right]}_{n_{dof}^{\chi,e}\times n_{dof}^{\chi,e}}.\underbrace{\left\{\delta\boldsymbol{\phi}^e\right\}}_{n_{dof}^{\chi,e}\times 1} \tag{4.276}$$

The fifth term is :

$$\left(\delta\mathcal{H}_2\right)_5 = -\left(\kappa-\sigma\right)\int_V \eta_{ml}\left(F_n\right)_{mK}F_{Kk}^{-1}\delta u_{k,l}JdV \tag{4.277}$$

$$\left(\delta\mathcal{H}_2^{e,h}\right)_5 = -\left(\kappa-\sigma\right)\int_{V^e}\underbrace{\left\{\boldsymbol{\alpha}^e\right\}^T}_{1\times n_{dof}^{\chi}}.\underbrace{\left[\boldsymbol{N}^{\chi,e}\right]^T}_{n_{dof}^{\chi}\times(n_{sd}*n_{sd})}.\underbrace{\left[\boldsymbol{R}_4^u\right]}_{(n_{sd}*n_{sd})\times(n_{sd}*n_{sd})}$$
$$.\underbrace{\left[\boldsymbol{grad}\left(\boldsymbol{N}^{u,e}\right)\right]}_{(n_{sd}*n_{sd})\times n_{dof}^{u,e}}.\underbrace{\left\{\delta\boldsymbol{d}^e\right\}}_{n_{dof}^{u,e}\times 1}JdV \tag{4.278}$$

$$\underbrace{\left[\boldsymbol{\mathcal{R}}^{\boldsymbol{e}}{}_5\right]}_{n_{dof}^{\chi}\times n_{dof}^{u,e}} = -\left(\kappa-\sigma\right)\int_{V^e}\underbrace{\left[\boldsymbol{N}^{\chi,e}\right]^T}_{n_{dof}^{\chi}\times(n_{sd}*n_{sd})}.\underbrace{\left[\boldsymbol{R}_4^u\right]}_{(n_{sd}*n_{sd})\times(n_{sd}*n_{sd})}.\underbrace{\left[\boldsymbol{grad}\left(\boldsymbol{N}^{u,e}\right)\right]}_{(n_{sd}*n_{sd})\times n_{dof}^{u,e}}.JdV \tag{4.279}$$

$$\left(\delta\mathcal{H}_2^h\right)_5 = \mathop{\mathbf{A}}_{e=1}^{n_{\text{el}}}\underbrace{\left\{\boldsymbol{\alpha}^e\right\}^T}_{1\times n_{dof}^{\chi,e}}.\underbrace{\left[\boldsymbol{\mathcal{R}}^{\boldsymbol{e}}{}_5\right]}_{n_{dof}^{\chi,e}\times n_{dof}^{u,e}}.\underbrace{\left\{\delta\boldsymbol{d}^e\right\}}_{n_{dof}^{u,e}\times 1} \tag{4.280}$$

The sixth term is :

$$\left(\delta\mathcal{H}_2\right)_6 = -\left(\nu-\sigma\right)\int_V \eta_{ml}\left(\chi_n\right)_{mT}\chi_{Tp}^{-1}\delta\left(\Phi_{pK}\right)\chi_{Kl}^{-1}JdV \tag{4.281}$$

$$\left(\delta\mathcal{H}_2^{e,h}\right)_6 = -\left(\nu-\sigma\right)\int_{V^e}\underbrace{\left\{\boldsymbol{\alpha}^e\right\}^T}_{1\times n_{dof}^{\chi}}.\underbrace{\left[\boldsymbol{N}^{\chi,e}\right]^T}_{n_{dof}^{\chi}\times(n_{sd}*n_{sd})}.\underbrace{\left[\boldsymbol{R}_2^{\chi}\right]}_{(n_{sd}*n_{sd})\times(n_{sd}*n_{sd})}$$
$$.\underbrace{\left[\boldsymbol{N}^{\chi,e}\right]}_{(n_{sd}*n_{sd})\times n_{dof}^{\chi,e}}.\underbrace{\left\{\delta\phi^e\right\}}_{n_{dof}^{\chi,e}\times 1}JdV \tag{4.282}$$

$$\underbrace{\left[\boldsymbol{\mathcal{R}}^{\boldsymbol{e}}{}_6\right]}_{n_{dof}^{\chi}\times n_{dof}^{\chi,e}} = -\left(\nu-\sigma\right)\int_{V^e}\underbrace{\left[\boldsymbol{N}^{\chi,e}\right]^T}_{n_{dof}^{\chi}\times(n_{sd}*n_{sd})}.\underbrace{\left[\boldsymbol{R}_2^{\chi}\right]}_{(n_{sd}*n_{sd})\times(n_{sd}*n_{sd})}.\underbrace{\left[\boldsymbol{N}^{\chi,e}\right]}_{(n_{sd}*n_{sd})\times n_{dof}^{\chi,e}}JdV \tag{4.283}$$

$$\left(\delta\mathcal{H}_2^h\right)_6 = \mathop{\mathbf{A}}_{e=1}^{n_{\text{el}}}\underbrace{\left\{\boldsymbol{\alpha}^e\right\}^T}_{1\times n_{dof}^{\chi,e}}.\underbrace{\left[\boldsymbol{\mathcal{R}}^{\boldsymbol{e}}{}_6\right]}_{n_{dof}^{\chi,e}\times n_{dof}^{\chi,e}}.\underbrace{\left\{\delta\boldsymbol{\phi}^e\right\}}_{n_{dof}^{\chi,e}\times 1} \tag{4.284}$$

The seventh term is:

$$(\delta\mathcal{H}_2)_7 = -(\nu-\sigma)\int_V \eta_{ml}\,(F_n)_{lK}\,F^{-1}_{Kp}\delta u_{p,m}JdV \tag{4.285}$$

$$\left(\delta\mathcal{H}_2^{e,h}\right)_7 = -(\nu-\sigma)\int_{V^e} \underbrace{\left\{\boldsymbol{\alpha}^e\right\}^T}_{1\times n^{\chi}_{dof}}.\underbrace{\left[\boldsymbol{N}^{\chi,e}\right]^T}_{n^{\chi}_{dof}\times(n_{sd}*n_{sd})}.\underbrace{\left[\boldsymbol{R}^u_5\right]}_{(n_{sd}*n_{sd})\times(n_{sd}*n_{sd})}$$
$$.\underbrace{\left[\boldsymbol{grad}\left(\boldsymbol{N}^{u,e}\right)\right]}_{(n_{sd}*n_{sd})\times n^{u,e}_{dof}}.\underbrace{\left\{\delta\boldsymbol{d}^e\right\}}_{n^{u,e}_{dof}\times 1}JdV \tag{4.286}$$

$$\underbrace{\left[\boldsymbol{\mathcal{R}}^{\boldsymbol{e}}{}_7\right]}_{n^{\chi}_{dof}\times n^{u,e}_{dof}} = -(\nu-\sigma)\int_{V^e} \underbrace{\left[\boldsymbol{N}^{\chi,e}\right]^T}_{n^{\chi}_{dof}\times(n_{sd}*n_{sd})}.\underbrace{\left[\boldsymbol{R}^u_5\right]}_{(n_{sd}*n_{sd})\times(n_{sd}*n_{sd})}.\underbrace{\left[\boldsymbol{grad}\left(\boldsymbol{N}^{u,e}\right)\right]}_{(n_{sd}*n_{sd})\times n^{u,e}_{dof}}JdV \tag{4.287}$$

$$\left(\delta\mathcal{H}_2^h\right)_7 = \mathop{\mathsf{A}}_{e=1}^{n_{\mathrm{el}}}\underbrace{\left\{\boldsymbol{\alpha}^e\right\}^T}_{1\times n^{\chi,e}_{dof}}.\underbrace{\left[\boldsymbol{\mathcal{R}}^{\boldsymbol{e}}{}_7\right]}_{n^{\chi,e}_{dof}\times n^{u,e}_{dof}}.\underbrace{\left\{\delta\boldsymbol{d}^e\right\}}_{n^{u,e}_{dof}\times 1} \tag{4.288}$$

The eighth term is:

$$(\delta\mathcal{H}_2)_8 = -\tau\int_V \eta_{ml}\left(\left(F_n\right)_{iL}F^{-1}_{Lk}\delta u_{k,i}\right)\delta_{ml}JdV \tag{4.289}$$

$$\left(\delta\mathcal{H}_2^{e,h}\right)_8 = -\tau\int_{V^e} \underbrace{\left\{\boldsymbol{\alpha}^e\right\}^T}_{1\times n^{\chi}_{dof}}.\underbrace{\left[\boldsymbol{N}^{\chi,e}\right]^T}_{n^{\chi}_{dof}\times(n_{sd}*n_{sd})}.\underbrace{\left[\boldsymbol{R}^u_6\right]}_{(n_{sd}*n_{sd})\times(n_{sd}*n_{sd})}.\underbrace{\left[\boldsymbol{grad}\left(\boldsymbol{N}^{u,e}\right)\right]}_{(n_{sd}*n_{sd})\times n^{u,e}_{dof}}.\underbrace{\left\{\delta\boldsymbol{d}^e\right\}}_{n^{u,e}_{dof}\times 1}JdV \tag{4.290}$$

$$\underbrace{\left[\boldsymbol{\mathcal{R}}^{\boldsymbol{e}}{}_8\right]}_{n^{\chi}_{dof}\times n^{u,e}_{dof}} = -\tau\int_{V^e} \underbrace{\left[\boldsymbol{N}^{\chi,e}\right]^T}_{n^{\chi}_{dof}\times(n_{sd}*n_{sd})}.\underbrace{\left[\boldsymbol{R}^u_6\right]}_{(n_{sd}*n_{sd})\times(n_{sd}*n_{sd})}.\underbrace{\left[\boldsymbol{grad}\left(\boldsymbol{N}^{u,e}\right)\right]}_{(n_{sd}*n_{sd})\times n^{u,e}_{dof}}JdV \tag{4.291}$$

$$\left(\delta\mathcal{H}_2^h\right)_8 = \mathop{\mathsf{A}}_{e=1}^{n_{\mathrm{el}}}\underbrace{\left\{\boldsymbol{\alpha}^e\right\}^T}_{1\times n^{\chi,e}_{dof}}.\underbrace{\left[\boldsymbol{\mathcal{R}}^{\boldsymbol{e}}{}_8\right]}_{n^{\chi,e}_{dof}\times n^{u,e}_{dof}}.\underbrace{\left\{\delta\boldsymbol{d}^e\right\}}_{n^{u,e}_{dof}\times 1} \tag{4.292}$$

The ninth term is:

$$(\delta\mathcal{H}_2)_9 = -\sigma\int_V \eta_{ml}\left(\left(F_n\right)_{mL}F^{-1}_{Lk}\delta u_{k,l}\right)JdV \tag{4.293}$$

$$\left(\delta\mathcal{H}_2^{e,h}\right)_9 = -\sigma\int_{V^e} \underbrace{\left\{\boldsymbol{\alpha}^e\right\}^T}_{1\times n^{\chi}_{dof}}.\underbrace{\left[\boldsymbol{N}^{\chi,e}\right]^T}_{n^{\chi}_{dof}\times(n_{sd}*n_{sd})}.\underbrace{\left[\boldsymbol{R}^u_7\right]}_{(n_{sd}*n_{sd})\times(n_{sd}*n_{sd})}.\underbrace{\left[\boldsymbol{grad}\left(\boldsymbol{N}^{u,e}\right)\right]}_{(n_{sd}*n_{sd})\times n^{u,e}_{dof}}.\underbrace{\left\{\delta\boldsymbol{d}^e\right\}}_{n^{u,e}_{dof}\times 1}JdV \tag{4.294}$$

$$\underbrace{\left[\boldsymbol{\mathcal{R}}^{\boldsymbol{e}}{}_9\right]}_{n^{\chi}_{dof}\times n^{u,e}_{dof}} = -\sigma\int_{V^e} \underbrace{\left[\boldsymbol{N}^{\chi,e}\right]^T}_{n^{\chi}_{dof}\times(n_{sd}*n_{sd})}.\underbrace{\left[\boldsymbol{R}^u_7\right]}_{(n_{sd}*n_{sd})\times(n_{sd}*n_{sd})}.\underbrace{\left[\boldsymbol{grad}\left(\boldsymbol{N}^{u,e}\right)\right]}_{(n_{sd}*n_{sd})\times n^{u,e}_{dof}}JdV \tag{4.295}$$

$$\left(\delta\mathcal{H}_2^h\right)_9 = \mathop{\mathbf{A}}_{e=1}^{n_{\text{el}}} \underbrace{\left\{\boldsymbol{\alpha}^e\right\}^T}_{1\times n_{dof}^{\chi,e}} . \underbrace{\left[\boldsymbol{\mathcal{R}}^{\boldsymbol{e}}{}_9\right]}_{n_{dof}^{\chi,e}\times n_{dof}^{u,e}} . \underbrace{\left\{\delta\boldsymbol{d}^e\right\}}_{n_{dof}^{u,e}\times 1} \tag{4.296}$$

the tenth term is:

$$\left(\delta\mathcal{H}_2\right)_{10} = -\sigma \int_V \eta_{ml}\left(\left(F_n\right)_{lL} F_{Lk}^{-1}\delta u_{k,m}\right) JdV \tag{4.297}$$

$$\left(\delta\mathcal{H}_2^{e,h}\right)_{10} = -\sigma \int_{V^e} \underbrace{\left\{\boldsymbol{\alpha}^e\right\}^T}_{1\times n_{dof}^{\chi}} . \underbrace{\left[\boldsymbol{N}^{\chi,e}\right]^T}_{n_{dof}^{\chi}\times(n_{sd}*n_{sd})} . \underbrace{\left[\boldsymbol{R}_8^u\right]}_{(n_{sd}*n_{sd})\times(n_{sd}*n_{sd})} . \underbrace{\left[\boldsymbol{grad}\left(\boldsymbol{N}^{u,e}\right)\right]}_{(n_{sd}*n_{sd})\times n_{dof}^{u,e}} . \underbrace{\left\{\delta\boldsymbol{d}^e\right\}}_{n_{dof}^{u,e}\times 1} JdV \tag{4.298}$$

$$\underbrace{\left[\boldsymbol{\mathcal{R}}^{\boldsymbol{e}}{}_{10}\right]}_{n_{dof}^{\chi}\times n_{dof}^{u,e}} = -\sigma \int_{V^e} \underbrace{\left[\boldsymbol{N}^{\chi,e}\right]^T}_{n_{dof}^{\chi}\times(n_{sd}*n_{sd})} . \underbrace{\left[\boldsymbol{R}_8^u\right]}_{(n_{sd}*n_{sd})\times(n_{sd}*n_{sd})} . \underbrace{\left[\boldsymbol{grad}\left(\boldsymbol{N}^{u,e}\right)\right]}_{(n_{sd}*n_{sd})\times n_{dof}^{u,e}} JdV \tag{4.299}$$

$$\left(\delta\mathcal{H}_2^h\right)_{10} = \mathop{\mathbf{A}}_{e=1}^{n_{\text{el}}} \underbrace{\left\{\boldsymbol{\alpha}^e\right\}^T}_{1\times n_{dof}^{\chi,e}} . \underbrace{\left[\boldsymbol{\mathcal{R}}^{\boldsymbol{e}}{}_{10}\right]}_{n_{dof}^{\chi,e}\times n_{dof}^{u,e}} . \underbrace{\left\{\delta\boldsymbol{d}^e\right\}}_{n_{dof}^{u,e}\times 1} \tag{4.300}$$

The eleventh term is:

$$\left(\delta\mathcal{H}_2\right)_{11} = -\left(\eta-\tau\right)\int_V \eta_{ml}\left(\left(\chi_n\right)_{iT}\chi_{Tp}^{-1}\delta\left(\Phi_{pK}\right)\chi_{Ki}^{-1}\right)\delta_{ml}JdV \tag{4.301}$$

$$\left(\delta\mathcal{H}_2^{e,h}\right)_{11} = -\left(\eta-\tau\right)\int_{V^e} \underbrace{\left\{\boldsymbol{\alpha}^e\right\}^T}_{1\times n_{dof}^{\chi}} . \underbrace{\left[\boldsymbol{N}^{\chi,e}\right]^T}_{n_{dof}^{\chi}\times(n_{sd}*n_{sd})} . \underbrace{\left[\boldsymbol{R}_3^{\chi}\right]}_{(n_{sd}*n_{sd})\times(n_{sd}*n_{sd})} . \underbrace{\left[\boldsymbol{N}^{\chi,e}\right]}_{(n_{sd}*n_{sd})\times n_{dof}^{\chi,e}} . \underbrace{\left\{\delta\boldsymbol{\phi}^e\right\}}_{n_{dof}^{\chi,e}\times 1} JdV \tag{4.302}$$

$$\underbrace{\left[\boldsymbol{\mathcal{R}}^{\boldsymbol{e}}{}_{11}\right]}_{n_{dof}^{\chi}\times n_{dof}^{\chi,e}} = -\left(\eta-\tau\right)\int_{V^e} \underbrace{\left[\boldsymbol{N}^{\chi,e}\right]^T}_{n_{dof}^{\chi}\times(n_{sd}*n_{sd})} . \underbrace{\left[\boldsymbol{R}_3^{\chi}\right]}_{(n_{sd}*n_{sd})\times(n_{sd}*n_{sd})} . \underbrace{\left[\boldsymbol{N}^{\chi,e}\right]}_{(n_{sd}*n_{sd})\times n_{dof}^{\chi,e}} JdV \tag{4.303}$$

$$\left(\delta\mathcal{H}_2^h\right)_{11} = \mathop{\mathbf{A}}_{e=1}^{n_{\text{el}}} \underbrace{\left\{\boldsymbol{\alpha}^e\right\}^T}_{1\times n_{dof}^{\chi,e}} . \underbrace{\left[\boldsymbol{\mathcal{R}}^{\boldsymbol{e}}{}_{11}\right]}_{n_{dof}^{\chi,e}\times n_{dof}^{\chi,e}} . \underbrace{\left\{\delta\boldsymbol{\phi}^e\right\}}_{n_{dof}^{\chi,e}\times 1} \tag{4.304}$$

the twelfth term is:

$$\left(\delta\mathcal{H}_2^{e,h}\right)_{12} = -\left(\eta-\tau\right)\int_V \eta_{ml}\left(F_n\right)_{iK}F_{Kp}^{-1}\delta u_{p,i}\delta_{ml}JdV \tag{4.305}$$

$$\left(\delta\mathcal{H}_2^h\right)_{12} = -\left(\eta-\tau\right)\int_{V^e} \underbrace{\left\{\boldsymbol{\alpha}^e\right\}^T}_{1\times n_{dof}^{\chi}} . \underbrace{\left[\boldsymbol{N}^{\chi,e}\right]^T}_{n_{dof}^{\chi}\times(n_{sd}*n_{sd})} . \underbrace{\left[\boldsymbol{R}_9^u\right]}_{(n_{sd}*n_{sd})\times(n_{sd}*n_{sd})} . \underbrace{\left[\boldsymbol{grad}\left(\boldsymbol{N}^{u,e}\right)\right]}_{(n_{sd}*n_{sd})\times n_{dof}^{u,e}} . \underbrace{\left\{\delta\boldsymbol{d}^e\right\}}_{n_{dof}^{u,e}\times 1} JdV \tag{4.306}$$

$$\underbrace{\left[\boldsymbol{\mathcal{R}}^{\boldsymbol{e}}{}_{12}\right]}_{n^{\chi}_{dof}\times n^{u,e}_{dof}} = -\left(\eta-\tau\right)\int_{V^e}\underbrace{\left[\boldsymbol{N}^{\chi,e}\right]^T}_{n^{\chi}_{dof}\times(n_{sd}*n_{sd})}\cdot\underbrace{\left[\boldsymbol{R}^{u}_{9}\right]}_{(n_{sd}*n_{sd})\times(n_{sd}*n_{sd})}\cdot\underbrace{\left[\boldsymbol{grad}\left(\boldsymbol{N}^{u,e}\right)\right]}_{(n_{sd}*n_{sd})\times n^{u,e}_{dof}}JdV \tag{4.307}$$

$$\left(\delta\mathcal{H}^{h}_{2}\right)_{12} = \mathop{\mathbf{A}}_{e=1}^{n_{\text{el}}}\underbrace{\left\{\boldsymbol{\alpha}^{e}\right\}^T}_{1\times n^{\chi,e}_{dof}}\cdot\underbrace{\left[\boldsymbol{\mathcal{R}}^{\boldsymbol{e}}{}_{12}\right]}_{n^{\chi,e}_{dof}\times n^{u,e}_{dof}}\cdot\underbrace{\left\{\delta\boldsymbol{d}^{e}\right\}}_{n^{u,e}_{dof}\times 1} \tag{4.308}$$

The thirteenth term is :

$$\left(\delta\mathcal{H}_{2}\right)_{13} = -\int_{V}\eta_{ml}\left(s_{ml}-\sigma_{ml}\right)\delta u_{n,n}JdV \tag{4.309}$$

$$\left(\delta\mathcal{H}_{2}\right)_{13} = -\int_{V}\eta_{ml}\left(s_{ml}-\sigma_{ml}\right)\delta u_{n,T}F^{-1}_{Tn}JdV \tag{4.310}$$

$$\left(\delta\mathcal{H}_{2}\right)_{13} = -\int_{V}\eta_{ml}\left(s_{ml}-\sigma_{ml}\right)F^{-1}_{Tn}\delta u_{n,T}JdV \tag{4.311}$$

$$\left(\delta\mathcal{H}^{e,h}_{2}\right)_{13} = -\int_{V^e}\underbrace{\left\{\boldsymbol{\alpha}^{e}\right\}^T}_{1\times n^{\chi}_{dof}}\cdot\underbrace{\left[\boldsymbol{N}^{\chi,e}\right]^T}_{n^{\chi}_{dof}\times(n_{sd}*n_{sd})}\cdot\underbrace{\left[\boldsymbol{R}^{s-\sigma}\right]}_{(n_{sd}*n_{sd})\times(n_{sd}*n_{sd})}$$
$$\cdot\underbrace{\left[\boldsymbol{GRAD}(\boldsymbol{N}^{u,e})\right]}_{(n_{sd}*n_{sd})\times n^{u,e}_{dof}}\cdot\underbrace{\left\{\delta\boldsymbol{d}^{e}\right\}}_{n^{u,e}_{dof}\times 1}JdV \tag{4.312}$$

$$\underbrace{\left[\boldsymbol{\mathcal{R}}^{\boldsymbol{e}}{}_{13}\right]}_{n^{\chi}_{dof}\times n^{u,e}_{dof}} = -\int_{V^e}\underbrace{\left[\boldsymbol{N}^{\chi,e}\right]^T}_{n^{\chi}_{dof}\times(n_{sd}*n_{sd})}\cdot\underbrace{\left[\boldsymbol{R}^{s-\sigma}\right]}_{(n_{sd}*n_{sd})\times(n_{sd}*n_{sd})}\cdot\underbrace{\left[\boldsymbol{GRAD}(\boldsymbol{N}^{u,e})\right]}_{(n_{sd}*n_{sd})\times n^{u,e}_{dof}}JdV \tag{4.313}$$

$$\left(\delta\mathcal{H}^{h}_{2}\right)_{13} = \mathop{\mathbf{A}}_{e=1}^{n_{\text{el}}}\underbrace{\left\{\boldsymbol{\alpha}^{e}\right\}^T}_{1\times n^{\chi,e}_{dof}}\cdot\underbrace{\left[\boldsymbol{\mathcal{R}}^{\boldsymbol{e}}{}_{13}\right]}_{n^{\chi,e}_{dof}\times n^{u,e}_{dof}}\cdot\underbrace{\left\{\delta\boldsymbol{d}^{e}\right\}}_{n^{u,e}_{dof}\times 1} \tag{4.314}$$

The last integral term is:

$$\delta\left(\mathcal{H}_{3}\right) = \int_{V}\eta_{ml}\rho_0\Gamma_{lK}\delta\left(\Phi_{mK}\right)dV \tag{4.315}$$

$$\delta\left(\mathcal{H}^{e,h}_{3}\right) = \int_{V}\underbrace{\left\{\boldsymbol{\alpha}^{e}\right\}^T}_{1\times n^{\chi}_{dof}}\cdot\underbrace{\left[\boldsymbol{N}^{\chi,e}\right]^T}_{n^{\chi}_{dof}\times(n_{sd}*n_{sd})}\cdot\underbrace{\left[\boldsymbol{R}^{\Gamma}\right]}_{(n_{sd}*n_{sd})\times(n_{sd}*n_{sd})}\cdot\underbrace{\left[\boldsymbol{N}^{\chi,e}\right]}_{(n_{sd}*n_{sd})\times n^{\chi,e}_{dof}}\cdot\underbrace{\left\{\delta\boldsymbol{\phi}^{e}\right\}}_{n^{\chi,e}_{dof}\times 1}dV \tag{4.316}$$

$$\underbrace{\left[\boldsymbol{\mathcal{R}}^{\boldsymbol{e}\Gamma,e}\right]}_{n^{\chi,e}_{dof}\times n^{\chi,e}_{dof}} = \int_{V^e}\underbrace{\left[\boldsymbol{N}^{\chi,e}\right]^T}_{n^{\chi}_{dof}\times(n_{sd}*n_{sd})}\cdot\underbrace{\left[\boldsymbol{R}^{\Gamma}\right]}_{(n_{sd}*n_{sd})\times(n_{sd}*n_{sd})}\cdot\underbrace{\left[\boldsymbol{N}^{\chi,e}\right]}_{(n_{sd}*n_{sd})\times n^{\chi,e}_{dof}}\;dV \tag{4.317}$$

$$\delta\left(\mathcal{H}^{h}_{3}\right) = \mathop{\mathbf{A}}_{e=1}^{n_{\text{el}}}\underbrace{\left\{\boldsymbol{\alpha}^{e}\right\}^T}_{1\times n^{\chi,e}_{dof}}\cdot\underbrace{\left[\boldsymbol{\mathcal{R}}^{\boldsymbol{e}\Gamma,e}\right]}_{n^{\chi,e}_{dof}\times n^{\chi,e}_{dof}}\cdot\underbrace{\left\{\delta\boldsymbol{\phi}^{e}\right\}}_{n^{\chi,e}_{dof}\times 1} \tag{4.318}$$

Variation of the force term :

$$\delta\left(\mathcal{H}_{ext}\right) = \int_S \eta_{ml} F_{lm} dA$$

$$\delta\left(\mathcal{H}^{e,h}_{ext}\right) = \int_S \underbrace{\left\{\boldsymbol{\alpha}^e\right\}^T}_{1\times n^{\chi}_{dof}} \underbrace{\left[\boldsymbol{N}^{\chi,e}\right]^T}_{n^{\chi}_{dof}\times(n_{sd}*n_{sd})} \cdot \underbrace{\left\{F\right\}}_{(n_{sd}*n_{sd})\times 1} dA$$

$$\underbrace{\left[\mathfrak{N}^e\right]_{ext}}_{n^{\chi}_{dof}\times 1} = \int_S \underbrace{\left[\boldsymbol{N}^{\chi,e}\right]^T}_{n^{\chi}_{dof}\times(n_{sd}*n_{sd})} \cdot \underbrace{\left\{F\right\}}_{(n_{sd}*n_{sd})\times 1} dA$$

$$\mathcal{H}^h_{ext} = \mathop{\mathsf{A}}_{e=1}^{n_{\text{el}}} \underbrace{\left\{\boldsymbol{\alpha}^e\right\}^T}_{1\times n^{\chi}_{dof}} \underbrace{\left[\mathfrak{N}^e\right]_{ext}}_{n^{\chi}_{dof}\times 1} \tag{4.319}$$

4.8 Summary of the Finite Element Model in the Equation $\boldsymbol{K}\delta\boldsymbol{x} = -\boldsymbol{R}$

Since the $\boldsymbol{\alpha}$ and $\boldsymbol{c}$ are the arbitrary constants, the matrice equations will hold for all $\boldsymbol{\alpha}$ and $\boldsymbol{c}$. Therefore, they can be romoved from the quations and total system of the equations reduce to:

$$\begin{bmatrix} \boldsymbol{K}_{dd} & \boldsymbol{K}_{d\phi} \\ \boldsymbol{K}_{\phi d} & \boldsymbol{K}_{\phi\phi} \end{bmatrix} \cdot \begin{Bmatrix} \delta\boldsymbol{d} \\ \delta\boldsymbol{\phi} \end{Bmatrix} = \begin{Bmatrix} -\boldsymbol{R}_d \\ -\boldsymbol{R}_\phi \end{Bmatrix} \tag{4.320}$$

where

$$\underbrace{[\boldsymbol{K}_{dd}]}_{\left(n_{dof}^{u,e}\right)\times\left(n_{dof}^{u,e}\right)} = \mathop{\mathbf{A}}_{e=1}^{n_{\text{el}}}\left[\sum_{i=1,i\neq 7,9,11}^{i=14}\underbrace{\left[\mathfrak{T}_i^e\right]}_{\left(n_{dof}^{u,e}\right)\times\left(n_{dof}^{u,e}\right)}\right] \tag{4.321}$$

$$\underbrace{[\boldsymbol{K}_{d\phi}]}_{\left(n_{dof}^{u,e}\right)\times\left(n_{dof}^{\chi,e}\right)} = \mathop{\mathbf{A}}_{e=1}^{n_{\text{el}}}\left[\underbrace{\left[\mathfrak{T}_7^e\right]}_{\left(n_{dof}^{u,e}\right)\times\left(n_{dof}^{\chi,e}\right)} + \underbrace{\left[\mathfrak{T}_9^e\right]}_{\left(n_{dof}^{u,e}\right)\times\left(n_{dof}^{\chi,e}\right)} + \underbrace{\left[\mathfrak{T}_{11}^e\right]}_{\left(n_{dof}^{u,e}\right)\times\left(n_{dof}^{\chi,e}\right)}\right] \tag{4.322}$$

$$\begin{aligned}\underbrace{[\boldsymbol{K}_{\phi d}]}_{\left(n_{dof}^{\chi,e}\right)\times\left(n_{dof}^{\chi,e}\right)} = \mathop{\mathbf{A}}_{e=1}^{n_{\text{el}}}\Bigg[&\underbrace{\left[\mathfrak{M}_{\nabla\eta}^e\right]}_{n_{dof}^{\chi,e}\times n_{dof}^{\chi,e}} + \sum_{i=1,i\neq 4,5,6,7,9,10,11,12,13,17}^{i=18}\underbrace{\left[\mathfrak{M}_i^e\right]}_{\left(n_{dof}^{\chi,e}\right)\times\left(n_{dof}^{\chi,e}\right)}\\ &+\sum_{i=1,i\neq 4,6,11}^{i=13}\underbrace{\left[\mathfrak{R}_i^e\right]}_{\left(n_{dof}^{\chi,e}\right)\times\left(n_{dof}^{\chi,e}\right)}\Bigg]\end{aligned} \tag{4.323}$$

$$\begin{aligned}\underbrace{[\boldsymbol{K}_{\phi\phi}]}_{\left(n_{dof}^{\chi,e}\right)\times\left(n_{dof}^{\chi,e}\right)} = \mathop{\mathbf{A}}_{e=1}^{n_{\text{el}}}\Bigg[&\sum_{i=1,i\neq 1,2,3,8,14,15,16}^{i=17}\underbrace{\left[\mathfrak{M}_i^e\right]}_{\left(n_{dof}^{\chi,e}\right)\times\left(n_{dof}^{\chi,e}\right)}\\ &+\underbrace{\left[\mathfrak{R}_4^e\right]}_{\left(n_{dof}^{\chi,e}\right)\times\left(n_{dof}^{\chi,e}\right)} + \underbrace{\left[\mathfrak{R}_6^e\right]}_{\left(n_{dof}^{\chi,e}\right)\times\left(n_{dof}^{\chi,e}\right)} + \underbrace{\left[\mathfrak{R}_{11}^e\right]}_{\left(n_{dof}^{\chi,e}\right)\times\left(n_{dof}^{\chi,e}\right)} + \underbrace{\left[\mathfrak{R}^{\Gamma,e}\right]}_{\left(n_{dof}^{\chi,e}\right)\times\left(n_{dof}^{\chi,e}\right)}\Bigg]\end{aligned} \tag{4.324}$$

The right hand side is:

$$\underbrace{\{\boldsymbol{R}_d\}}_{n_{dof}^{u,e}\times 1} = \mathop{\mathbf{A}}_{e=1}^{n_{\text{el}}}\left[\underbrace{\{\boldsymbol{U}_1^{e,Int}\}}_{n_{dof}^{u,e}\times 1} + \underbrace{\{\boldsymbol{U}_2^{e,Int}\}}_{n_{dof}^{u,e}\times 1} - \underbrace{\{\boldsymbol{U}_{ext}^{e}\}}_{n_{dof}^{u,e}\times 1}\right] \tag{4.325}$$

$$\underbrace{\{\boldsymbol{R}_\phi\}}_{n_{dof}^{\chi,e}\times 1} = \mathop{\mathbf{A}}_{e=1}^{n_{\text{el}}}\left[\underbrace{\{\boldsymbol{P}_1^{e,Int}\}}_{n_{dof}^{\chi,e}\times 1} + \underbrace{\{\boldsymbol{P}_2^{e,Int}\}}_{n_{dof}^{\chi,e}\times 1} + \underbrace{\{\boldsymbol{P}_3^{e,Int}\}}_{n_{dof}^{\chi,e}\times 1} - \underbrace{\{\boldsymbol{P}_{ext}^{e}\}}_{n_{dof}^{\chi,e}\times 1}\right] \tag{4.326}$$

Chapter 5

Finite Element Formulation of Finite Strain Micromorphic Elasticity at Reference Configuration

5.1 Linearization of the Balance Equations at Reference Configuration

Previously in Chapter 4, we presented the weak forms of balance equations and their linearizations together with finite element equations at current configuration $\mathcal{B}$. This section presents the mapping of the balance equations to the reference configuration and their linearizations at reference configuration $\mathcal{B}_0$.

5.1.1 Linearization of Balance of Momenta at Reference Configuration

Applying the method of weighted residuals (Hughes, 1987) and integration by parts to the balance of linear momentum and balance of first moment of momentum give us the variational equations. We use the Piola transforms and volume transformation to map the balance of linear momentum to reference configuration. First, after integration by parts in the current configuration, we have

$$\int_V w_k \left[\sigma_{lk,l} + \rho(f_k - a_k)\right] dv = \int_A w_k \sigma_{lk} n_l da - \int_V \left[w_{k,l}\sigma_{lk} + w_k \rho(f_k - a_k)\right] dv = 0 \qquad (5.1)$$

If we also apply Piola transforms of the Cauchy stress tensor $P_{lL} = J\sigma_{lk}F^{-1}_{Lk}$, $\sigma_{lk} = F_{lL}S_{LK}F_{kK}/J$, and Nanson's formula $n_l da = JF^{-1}_{Kl}N_K dA$ for area change, we obtain in the reference configuration

$$\int_A w_k P_{kK} N_K dA - \int_V \left[w_{k,l}F_{lL}S_{LK}F_{kK} + w_k \rho_0 (f_k - a_k)\right] dV = 0 \qquad (5.2)$$

where P_{kK} is the first Piola-Kirchhoff stress tensor. If we define a traction $T_k = P_{kL}N_L$, equation (5.2) can be written as

$$\int_A w_k T_k dA - \int_V \left[w_{k,l} F_{lL} S_{LK} F_{kK} + w_k \rho_0 (f_k - a_k) \right] dV = 0 \tag{5.3}$$

Application of the Newton-Raphson method requires linearization of the balance equations to construct a consistent tangent, where linearization of the balance of linear momentum may be expressed as

$$\begin{aligned} &\int_A w_k T_k dA - \int_V \left[w_{k,l} F_{lL} S_{LK} F_{kK} + w_k \rho_0 (f_k - a_k) \right] dV \\ &+ \delta \left(\int_A w_k T_k dA - \int_V \left[w_{k,l} F_{lL} S_{LK} F_{kK} + w_k \rho_0 (f_k - a_k) \right] dV \right) = 0 \end{aligned} \tag{5.4}$$

where $\delta(\bullet)$ is the increment operator within a linearization procedure. Ignoring the boundary term, the body force vector, and the acceleration vector, the equation above reduces to:

$$\int_V w_{k,l} F_{lL} S_{LK} F_{kK} dV + \delta \left(\int_V w_{k,l} F_{lL} S_{LK} F_{kK} dV \right) = 0 \tag{5.5}$$

Carrying the linearization operator over the terms gives:

$$\begin{aligned} &\int_V \delta \left(w_{k,l} \right) F_{lL} S_{LK} F_{kK} dV + \int_V w_{k,l} \delta \left(F_{lL} \right) S_{LK} F_{kK} dV + \int_V w_{k,l} F_{lL} \delta \left(S_{LK} \right) F_{kK} dV \\ &+ \int_V w_{k,l} F_{lL} S_{LK} \delta \left(F_{kK} \right) dV = - \int_V w_{k,l} F_{lL} S_{LK} F_{kK} dV \end{aligned} \tag{5.6}$$

Similarly, we follow the same method for the balance of first moment of momentum. Multiplying the residual form of (2.60) with the weight function η_{ml} and applying integration by parts together with Piola transforms and area change relations expressed above, we obtain in the reference configuration

$$\begin{aligned} &\int_V \eta_{ml} \left[F_{mM} S_{ML} F_{lL} - F_{mM} \Sigma_{ML} F_{lL} + \rho_0 (\lambda_{lm} - \omega_{lm}) \right] dV - \int_V \eta_{ml,k} F_{kK} F_{lL} M_{KLM} \chi_{mM} dV \\ &+ \int_A \eta_{ml} \mathcal{M}_{lm} dA = 0 \end{aligned} \tag{5.7}$$

where $\mathcal{M}_{lm}$ is the traction couple tensor, defined as $\mathcal{M}_{lm} = Jm_{klm}F^{-1}_{Kk}N_K$. Then, linearization of (5.7) is expressed as

$$\begin{aligned}
&\int_V \eta_{ml}\left[F_{mM}S_{ML}F_{lL} - F_{mM}\Sigma_{ML}F_{lL} + \rho_0(\lambda_{lm} - \omega_{lm})\right]dV - \int_V \eta_{ml,k}F_{kK}F_{lL}M_{KLM}\chi_{mM}dV \\
&+ \int_A \eta_{ml}\mathcal{M}_{lm}dA + \delta\left(\int_V \eta_{ml}\left[F_{mM}S_{ML}F_{lL} - F_{mM}\Sigma_{ML}F_{lL} + \rho_0(\lambda_{lm} - \omega_{lm})\right]dV\right. \\
&\left. - \int_V \eta_{ml,k}F_{kK}F_{lL}M_{KLM}\chi_{mM}dV + \int_A \eta_{ml}\mathcal{M}_{lm}dA\right) = 0
\end{aligned} \tag{5.8}$$

Ignoring the boundary term, the body couple, and the micro-spin inertia tensors gives:

$$\begin{aligned}
&\int_V \eta_{ml}F_{mM}\Sigma_{ML}F_{lL} - F_{mM}S_{ML}F_{lL}dV + \int_V \eta_{ml,k}F_{kK}F_{lL}M_{KLM}\chi_{mM}dV \\
&+ \delta\left(\int_V \eta_{ml}\left[F_{mM}\Sigma_{ML}F_{lL} - F_{mM}S_{ML}F_{lL}\right]dV + \int_V \eta_{ml,k}F_{kK}F_{lL}M_{KLM}\chi_{mM}dV\right) = 0
\end{aligned} \tag{5.9}$$

Similary, carrying the linearization operator over the terms gives:

$$\begin{aligned}
&\int_V \eta_{ml}\delta\left(F_{mM}\right)\left(\Sigma_{ML} - S_{ML}\right)F_{lL}dV + \int_V \eta_{ml}F_{mM}\delta\left(\Sigma_{ML} - S_{ML}\right)F_{lL}dV \\
&+ \int_V \eta_{ml}F_{mM}\left(\Sigma_{ML} - S_{ML}\right)\delta\left(F_{lL}\right)dV + \int_V \delta\left(\eta_{ml,k}\right)F_{kK}F_{lL}M_{KLM}\chi_{mM}dV \\
&+ \int_V \eta_{ml,k}\delta\left(F_{kK}\right)F_{lL}M_{KLM}\chi_{mM}dV + \int_V \eta_{ml,k}F_{kK}\delta\left(F_{lL}\right)M_{KLM}\chi_{mM}dV \\
&+ \int_V \eta_{ml,k}F_{kK}F_{lL}\delta\left(M_{KLM}\right)\chi_{mM}dV + \int_V \eta_{ml,k}F_{kK}F_{lL}M_{KLM}\delta\left(\chi_{mM}\right)dV \\
&= -\int_V \eta_{ml}F_{mM}\left(\Sigma_{ML} - S_{ML}\right)F_{lL}dV - \int_V \eta_{ml,k}F_{kK}F_{lL}M_{KLM}\chi_{mM}dV
\end{aligned} \tag{5.10}$$

In the finite element implementation, the terms in the right hand side of (5.6) and (5.10) will yield the residual vectors $\boldsymbol{R}_d$ and $\boldsymbol{R}_\phi$ respectively. The terms involving $\delta\boldsymbol{u}$ and $\delta\boldsymbol{\Phi}$ in (5.6) result in the associated consistent tangent matrices $\boldsymbol{K}_{dd}$ and $\boldsymbol{K}_{d\phi}$, respectively. Similarly, in (5.10) the associated consistent tangent matrices are, respectively, $\boldsymbol{K}_{\phi d}$ and $\boldsymbol{K}_{\phi\phi}$. We have the following coupled finite element system of equations to solve for nodal displacement increments $\delta\boldsymbol{d}$ and nodal micro-displacement tensor increments $\delta\boldsymbol{\phi}$ at each iteration in a Newton-Raphson algorithm:

$$\begin{bmatrix} \boldsymbol{K}_{dd} & \boldsymbol{K}_{d\phi} \\ \boldsymbol{K}_{\phi d} & \boldsymbol{K}_{\phi\phi} \end{bmatrix} \begin{Bmatrix} \delta\boldsymbol{d} \\ \delta\boldsymbol{\phi} \end{Bmatrix} = \begin{Bmatrix} -\boldsymbol{R}_d \\ -\boldsymbol{R}_\phi \end{Bmatrix} \tag{5.11}$$

The sub-matrices constructing the matrices $\boldsymbol{K}_{dd}$, $\boldsymbol{K}_{d\phi}$, $\boldsymbol{K}_{\phi d}$, and $\boldsymbol{K}_{\phi\phi}$ in a same way described in Section 4.8 are presented in the next section.

5.1.2 Submatrices in the Matrix Form of the Balance of Linear Momentum at Reference Configuration

This section provides the submatrices coming from the individual terms appearing in the linearization of the balance of linear momentum. Since the dimensionalizing and putting into Galerkin form were presented in detail in Chapter 4, we present only the final form of the submatrices in the linearized form balance equations in this section and hereafter. All the submatrices denoted by $\left(\mathcal{K}_{uu}^{e,h}\right)_i$, and $\left(\mathcal{K}_{u\phi}^{h}\right)_i$ are the contributions to consistent tangent coming from the linearized form of the balance of linear momentum.

The first term in the linearization of the balance of linear momentum:

$$\int_{\mathcal{B}_0} \delta\left(w_{kl}\right) F_{lL} S_{LK} F_{kK} dV = \int_{\mathcal{B}_0} w_{k,L} \delta\left(F_{Ll}^{-1}\right) F_{lL} S_{LK} F_{kK} dV$$
$$= -\int_{\mathcal{B}_0} w_{k,L} F_{Ll}^{-1} F_{lL} S_{LK} F_{kK} \delta u_{l,L} dV \tag{5.12}$$

$$\left(\mathcal{K}_{uu}^{e,h}\right)_1 = \int_{\mathcal{B}_0^e} \left\{\boldsymbol{c}^e\right\}^T \cdot \left[\boldsymbol{GRAD}\left(\boldsymbol{N}^{u,e}\right)\right]^T \cdot \left[\boldsymbol{I}_{11}\right] \cdot \left[\boldsymbol{GRAD}\left(\boldsymbol{N}^{u,e}\right)\right] \cdot \left\{\delta \boldsymbol{d}^e\right\} dV \tag{5.13}$$

$$\left[\mathfrak{J}_{11}^e\right] = \int_{\mathcal{B}_0^e} \left[\boldsymbol{GRAD}\left(\boldsymbol{N}^{u,e}\right)\right]^T \cdot \left[\boldsymbol{I}_{11}\right] \cdot \left[\boldsymbol{GRAD}\left(\boldsymbol{N}^{u,e}\right)\right] dV \tag{5.14}$$

$$\left(\mathcal{K}_{uu}^{h}\right)_1 = \mathop{\mathsf{A}}_{e=1}^{n_{\text{el}}} \left\{\boldsymbol{c}^e\right\}^T \cdot \left[\mathfrak{J}_{11}^e\right] \cdot \left\{\delta \boldsymbol{d}^e\right\} \tag{5.15}$$

The second term in the linearization of the balance of linear momentum:

$$\int_{\mathcal{B}_0} w_{k,L} F_{Ll}^{-1} \delta\left(F_{lL}\right) S_{LK} F_{kK} dV = \int_{\mathcal{B}_0} w_{k,L} F_{Ll}^{-1} S_{LK} F_{kK} \delta u_{l,L} dV \tag{5.16}$$

$$\left(\mathcal{K}_{uu}^{e,h}\right)_2 = \int_{\mathcal{B}_0^e} \left\{\boldsymbol{c}^e\right\}^T \cdot \left[\boldsymbol{GRAD}\left(\boldsymbol{N}^{u,e}\right)\right]^T \cdot \left[\boldsymbol{I}_{12}\right] \cdot \left[\boldsymbol{GRAD}\left(\boldsymbol{N}^{u,e}\right)\right] \cdot \left\{\delta \boldsymbol{d}^e\right\} dV \tag{5.17}$$

$$\left[\mathfrak{J}_{12}^e\right] = \int_{\mathcal{B}_0^e} \left[\boldsymbol{GRAD}\left(\boldsymbol{N}^{u,e}\right)\right]^T \cdot \left[\boldsymbol{I}_{12}\right] \cdot \left[\boldsymbol{GRAD}\left(\boldsymbol{N}^{u,e}\right)\right] dV \tag{5.18}$$

$$\left(\mathcal{K}_{uu}^{h}\right)_2 = \mathop{\mathsf{A}}_{e=1}^{n_{\text{el}}} \left\{\boldsymbol{c}^e\right\}^T \cdot \left[\mathfrak{J}_{12}^e\right] \cdot \left\{\delta \boldsymbol{d}^e\right\} \tag{5.19}$$

The third term is the first term coming from the linearization the second Piola-Kirchhoff tensor δS_{LK}:

$$(\lambda+\tau)\int_{\mathcal{B}_0} w_{k,L}F^{-1}_{Ll}F_{lL}\delta\left(F_{iM}\right)F_{iM}\delta_{LK}F_{kK}dV=(\lambda+\tau)\int_{\mathcal{B}_0} w_{k,L}F^{-1}_{Ll}F_{lL}F_{iM}\delta_{LK}F_{kK}\delta u_{i,M}dV \tag{5.20}$$

$$\left(\mathcal{K}^{e,h}_{uu}\right)_3=(\lambda+\tau)\int_{\mathcal{B}^e_0}\{\boldsymbol{c}^e\}^T\cdot\left[\boldsymbol{GRAD}\left(\boldsymbol{N}^{u,e}\right)\right]^T\cdot[\boldsymbol{I}_{13}]\cdot\left[\boldsymbol{GRAD}\left(\boldsymbol{N}^{u,e}\right)\right]\cdot\{\delta\boldsymbol{d}^e\}\,dV \tag{5.21}$$

$$[\mathfrak{J}^e_{13}]=(\lambda+\tau)\int_{\mathcal{B}^e_0}\left[\boldsymbol{GRAD}\left(\boldsymbol{N}^{u,e}\right)\right]^T\cdot[\boldsymbol{I}_{13}]\cdot\left[\boldsymbol{GRAD}\left(\boldsymbol{N}^{u,e}\right)\right]dV \tag{5.22}$$

$$\left(\mathcal{K}^{h}_{uu}\right)_3=\mathop{\mathsf{A}}_{e=1}^{n_{\text{el}}}\{\boldsymbol{c}^e\}^T\cdot[\mathfrak{J}^e_{13}]\cdot\{\delta\boldsymbol{d}^e\} \tag{5.23}$$

The fourth term is:

$$(\lambda+\tau)\int_{\mathcal{B}_0} w_{k,L}F^{-1}_{Ll}F_{lL}F_{iM}\delta\left(F_{iM}\right)\delta_{LK}F_{kK}dV=(\lambda+\tau)\int_{\mathcal{B}_0} w_{k,L}F^{-1}_{Ll}F_{lL}F_{iM}\delta_{LK}F_{kK}\delta u_{i,M}dV \tag{5.24}$$

$$\left(\mathcal{K}^{e,h}_{uu}\right)_4=(\lambda+\tau)\int_{\mathcal{B}^e_0}\{\boldsymbol{c}^e\}^T\cdot\left[\boldsymbol{GRAD}\left(\boldsymbol{N}^{u,e}\right)\right]^T\cdot[\boldsymbol{I}_{4}]\cdot\left[\boldsymbol{GRAD}\left(\boldsymbol{N}^{u,e}\right)\right]\cdot\{\delta\boldsymbol{d}^e\}\,dV \tag{5.25}$$

$$[\mathfrak{J}^e_{4}]=(\lambda+\tau)\int_{\mathcal{B}^e_0}\left[\boldsymbol{GRAD}\left(\boldsymbol{N}^{u,e}\right)\right]^T\cdot[\boldsymbol{I}_{14}]\cdot\left[\boldsymbol{GRAD}\left(\boldsymbol{N}^{u,e}\right)\right]dV \tag{5.26}$$

$$\left(\mathcal{K}^{h}_{uu}\right)_4=\mathop{\mathsf{A}}_{e=1}^{n_{\text{el}}}\{\boldsymbol{c}^e\}^T\cdot[\mathfrak{J}^e_{14}]\cdot\{\delta\boldsymbol{d}^e\} \tag{5.27}$$

The fifth term is:

$$2\left(\mu+\sigma\right)\int_{\mathcal{B}_0} w_{k,L}F^{-1}_{Ll}F_{lL}\delta\left(F_{iL}\right)F_{iK}F_{kK}dV=2\left(\mu+\sigma\right)\int_{\mathcal{B}_0} w_{k,L}F^{-1}_{Ll}F_{lL}F_{iK}F_{kK}\delta u_{i,L}dV \tag{5.28}$$

$$\left(\mathcal{K}^{e,h}_{uu}\right)_5=2\left(\mu+\sigma\right)\int_{\mathcal{B}^e_0}\{\boldsymbol{c}^e\}^T\cdot\left[\boldsymbol{GRAD}\left(\boldsymbol{N}^{u,e}\right)\right]^T\cdot[\boldsymbol{I}_{15}]\cdot\left[\boldsymbol{GRAD}\left(\boldsymbol{N}^{u,e}\right)\right]\cdot\{\delta\boldsymbol{d}^e\}\,dV \tag{5.29}$$

$$[\mathfrak{J}^e_{15}]=2\left(\mu+\sigma\right)\int_{\mathcal{B}^e_0}\left[\boldsymbol{GRAD}\left(\boldsymbol{N}^{u,e}\right)\right]^T\cdot[\boldsymbol{I}_{15}]\cdot\left[\boldsymbol{GRAD}\left(\boldsymbol{N}^{u,e}\right)\right]dV \tag{5.30}$$

$$\left(\mathcal{K}^{h}_{uu}\right)_5=\mathop{\mathsf{A}}_{e=1}^{n_{\text{el}}}\{\boldsymbol{c}^e\}^T\cdot[\mathfrak{J}^e_{15}]\cdot\{\delta\boldsymbol{d}^e\} \tag{5.31}$$

The sixth term is:

$$2\left(\mu+\sigma\right)\int_{\mathcal{B}_0} w_{k,L}F^{-1}_{Ll}F_{lL}F_{iL}\delta\left(F_{iK}\right)F_{kK}dV=2\left(\mu+\sigma\right)\int_{\mathcal{B}_0} w_{k,L}F^{-1}_{Ll}F_{lL}F_{iL}F_{kK}\delta u_{i,K}dV \tag{5.32}$$

$$\left(\mathcal{K}_{uu}^{e,h}\right)_6 = 2\left(\mu+\sigma\right)\int_{\mathcal{B}_0^e}\left\{\boldsymbol{c}^e\right\}^T\cdot\left[\boldsymbol{GRAD}\left(\boldsymbol{N}^{u,e}\right)\right]^T\cdot\left[\boldsymbol{I}_{16}\right]\cdot\left[\boldsymbol{GRAD}\left(\boldsymbol{N}^{u,e}\right)\right]\cdot\left\{\delta\boldsymbol{d}^e\right\}dV \tag{5.33}$$

$$\left[\mathfrak{J}_{16}^e\right] = 2\left(\mu+\sigma\right)\int_{\mathcal{B}_0^e}\left[\boldsymbol{GRAD}\left(\boldsymbol{N}^{u,e}\right)\right]^T\cdot\left[\boldsymbol{I}_{16}\right]\cdot\left[\boldsymbol{GRAD}\left(\boldsymbol{N}^{u,e}\right)\right]dV \tag{5.34}$$

$$\left(\mathcal{K}_{uu}^{h}\right)_6 = \mathop{\mathsf{A}}_{e=1}^{n_{\text{el}}}\left\{\boldsymbol{c}^e\right\}^T\cdot\left[\mathfrak{J}_{16}^e\right]\cdot\left\{\delta\boldsymbol{d}^e\right\} \tag{5.35}$$

The seventh term is:

$$\eta\int_{\mathcal{B}_0} w_{k,L}F_{Ll}^{-1}F_{lL}\delta\left(F_{iM}\right)\chi_{iM}\delta_{LK}F_{kK}dV = \eta\int_{\mathcal{B}_0} w_{k,L}F_{Ll}^{-1}F_{lL}\chi_{iM}\delta_{LK}F_{kK}\delta u_{i,M}dV \tag{5.36}$$

$$\left(\mathcal{K}_{uu}^{e,h}\right)_7 = \eta\int_{\mathcal{B}_0^e}\left\{\boldsymbol{c}^e\right\}^T\cdot\left[\boldsymbol{GRAD}\left(\boldsymbol{N}^{u,e}\right)\right]^T\cdot\left[\boldsymbol{I}_{17}\right]\cdot\left[\boldsymbol{GRAD}\left(\boldsymbol{N}^{u,e}\right)\right]\cdot\left\{\delta\boldsymbol{d}^e\right\}dV \tag{5.37}$$

$$\left[\mathfrak{J}_{17}^e\right] = \eta\int_{\mathcal{B}_0^e}\left[\boldsymbol{GRAD}\left(\boldsymbol{N}^{u,e}\right)\right]^T\cdot\left[\boldsymbol{I}_{17}\right]\cdot\left[\boldsymbol{GRAD}\left(\boldsymbol{N}^{u,e}\right)\right]dV \tag{5.38}$$

$$\left(\mathcal{K}_{uu}^{h}\right)_7 = \mathop{\mathsf{A}}_{e=1}^{n_{\text{el}}}\left\{\boldsymbol{c}^e\right\}^T\cdot\left[\mathfrak{J}_{17}^e\right]\cdot\left\{\delta\boldsymbol{d}^e\right\} \tag{5.39}$$

The eighth term is:

$$\eta\int_{\mathcal{B}_0} w_{k,L}F_{Ll}^{-1}F_{lL}F_{iM}\delta\left(\chi_{iM}\right)\delta_{LK}F_{kK}dV = \eta\int_{\mathcal{B}_0} w_{k,L}F_{Ll}^{-1}F_{lL}F_{iM}\delta_{LK}F_{kK}\delta\Phi_{iM}dV \tag{5.40}$$

$$\left(\mathcal{K}_{u\phi}^{e,h}\right)_1 = \eta\int_{\mathcal{B}_0^e}\left\{\boldsymbol{c}^e\right\}^T\cdot\left[\boldsymbol{GRAD}\left(\boldsymbol{N}^{u,e}\right)\right]^T\cdot\left[\boldsymbol{I}_{21}\right]\cdot\left[\boldsymbol{N}^{\chi,e}\right]\cdot\left\{\delta\boldsymbol{\phi}^e\right\}dV \tag{5.41}$$

$$\left[\mathfrak{J}_{21}^e\right] = \eta\int_{\mathcal{B}_0^e}\left[\boldsymbol{GRAD}\left(\boldsymbol{N}^{u,e}\right)\right]^T\cdot\left[\boldsymbol{I}_{21}\right]\cdot\left[\boldsymbol{N}^{\chi,e}\right]dV \tag{5.42}$$

$$\left(\mathcal{K}_{u\phi}^{h}\right)_1 = \mathop{\mathsf{A}}_{e=1}^{n_{\text{el}}}\left\{\boldsymbol{c}^e\right\}^T\cdot\left[\mathfrak{J}_{21}^e\right]\cdot\left\{\delta\boldsymbol{\phi}^e\right\} \tag{5.43}$$

The ninth term is:

$$\kappa\int_{\mathcal{B}_0} w_{k,L}F_{Ll}^{-1}F_{lL}\delta\left(F_{iK}\right)\chi_{iL}F_{kK}dV = \kappa\int_{\mathcal{B}_0} w_{k,L}F_{Ll}^{-1}F_{lL}\chi_{iL}F_{kK}\delta u_{i,K}dV \tag{5.44}$$

$$\left(\mathcal{K}_{uu}^{e,h}\right)_8 = \kappa\int_{\mathcal{B}_0^e}\left\{\boldsymbol{c}^e\right\}^T\cdot\left[\boldsymbol{GRAD}\left(\boldsymbol{N}^{u,e}\right)\right]^T\cdot\left[\boldsymbol{I}_{18}\right]\cdot\left[\boldsymbol{GRAD}\left(\boldsymbol{N}^{u,e}\right)\right]\cdot\left\{\delta\boldsymbol{d}^e\right\}dV \tag{5.45}$$

$$\left[\mathfrak{J}_{18}^e\right] = \kappa\int_{\mathcal{B}_0^e}\left[\boldsymbol{GRAD}\left(\boldsymbol{N}^{u,e}\right)\right]^T\cdot\left[\boldsymbol{I}_{18}\right]\cdot\left[\boldsymbol{GRAD}\left(\boldsymbol{N}^{u,e}\right)\right]\cdot\left\{\delta\boldsymbol{d}^e\right\}dV \tag{5.46}$$

$$\left(\mathcal{K}_{uu}^{h}\right)_8 = \mathop{\mathsf{A}}_{e=1}^{n_{\text{el}}}\left\{\boldsymbol{c}^e\right\}^T\cdot\left[\mathfrak{J}_{18}^e\right]\cdot\left\{\delta\boldsymbol{d}^e\right\} \tag{5.47}$$

The tenth term is:

$$\kappa \int_{\mathcal{B}_0} w_{k,L} F_{Ll}^{-1} F_{lL} F_{iK} \delta\left(\chi_{iL}\right) F_{kK} dV = \kappa \int_{\mathcal{B}_0} w_{k,L} F_{Ll}^{-1} F_{lL} F_{iK} F_{kK} \delta\Phi_{iL} dV \tag{5.48}$$

$$\left(\mathcal{K}_{u\phi}^{e,h}\right)_2 = \kappa \int_{\mathcal{B}_0^e} \left\{\boldsymbol{c}^e\right\}^T \cdot \left[\boldsymbol{GRAD}\left(\boldsymbol{N}^{u,e}\right)\right]^T \cdot \left[\boldsymbol{I}_{22}\right] \cdot \left[\boldsymbol{N}^{\chi,e}\right] \cdot \left\{\delta\boldsymbol{\phi}^e\right\} dV \tag{5.49}$$

$$\left[\mathfrak{J}_{22}^e\right] = \kappa \int_{\mathcal{B}_0^e} \left[\boldsymbol{GRAD}\left(\boldsymbol{N}^{u,e}\right)\right]^T \cdot \left[\boldsymbol{I}_{22}\right] \cdot \left[\boldsymbol{N}^{\chi,e}\right] dV \tag{5.50}$$

$$\left(\mathcal{K}_{u\phi}^{h}\right)_2 = \mathop{\mathbf{A}}_{e=1}^{n_{\text{el}}} \left\{\boldsymbol{c}^e\right\}^T \cdot \left[\mathfrak{J}_{22}^e\right] \cdot \left\{\delta\boldsymbol{\phi}^e\right\} \tag{5.51}$$

The eleventh term is:

$$\nu \int_{\mathcal{B}_0} w_{k,L} F_{Ll}^{-1} F_{lL} \delta\left(F_{iL}\right) \chi_{iK} F_{kK} dV = \nu \int_{\mathcal{B}_0} w_{k,L} F_{Ll}^{-1} F_{lL} \chi_{iK} F_{kK} \delta u_{i,L} dV \tag{5.52}$$

$$\left(\mathcal{K}_{uu}^{e,h}\right)_9 = \nu \int_{\mathcal{B}_0^e} \left\{\boldsymbol{c}^e\right\}^T \cdot \left[\boldsymbol{GRAD}\left(\boldsymbol{N}^{u,e}\right)\right]^T \cdot \left[\boldsymbol{I}_{19}\right] \cdot \left[\boldsymbol{GRAD}\left(\boldsymbol{N}^{u,e}\right)\right] \cdot \left\{\delta\boldsymbol{d}^e\right\} dV \tag{5.53}$$

$$\left[\mathfrak{J}_{19}^e\right] = \nu \int_{\mathcal{B}_0^e} \left[\boldsymbol{GRAD}\left(\boldsymbol{N}^{u,e}\right)\right]^T \cdot \left[\boldsymbol{I}_{19}\right] \cdot \left[\boldsymbol{GRAD}\left(\boldsymbol{N}^{u,e}\right)\right] \cdot \left\{\delta\boldsymbol{d}^e\right\} dV \tag{5.54}$$

$$\left(\mathcal{K}_{uu}^{h}\right)_9 = \mathop{\mathbf{A}}_{e=1}^{n_{\text{el}}} \left\{\boldsymbol{c}^e\right\}^T \cdot \left[\mathfrak{J}_{19}^e\right] \cdot \left\{\delta\boldsymbol{d}^e\right\} \tag{5.55}$$

The twelfth term is:

$$\nu \int_{\mathcal{B}_0} w_{k,L} F_{Ll}^{-1} F_{lL} F_{iL} \delta\left(\chi_{iK}\right) F_{kK} dV = \nu \int_{\mathcal{B}_0} w_{k,L} F_{Ll}^{-1} F_{lL} F_{iL} F_{kK} \delta\Phi_{iK} dV \tag{5.56}$$

$$\left(\mathcal{K}_{u\phi}^{e,h}\right)_4 = \nu \int_{\mathcal{B}_0^e} \left\{\boldsymbol{c}^e\right\}^T \cdot \left[\boldsymbol{GRAD}\left(\boldsymbol{N}^{u,e}\right)\right]^T \cdot \left[\boldsymbol{I}_{24}\right] \cdot \left[\boldsymbol{N}^{\chi,e}\right] \cdot \left\{\delta\boldsymbol{\phi}^e\right\} dV \tag{5.57}$$

$$\left[\mathfrak{J}_{24}^e\right] = \nu \int_{\mathcal{B}_0^e} \left[\boldsymbol{GRAD}\left(\boldsymbol{N}^{u,e}\right)\right]^T \cdot \left[\boldsymbol{I}_{24}\right] \cdot \left[\boldsymbol{N}^{\chi,e}\right] dV \tag{5.58}$$

$$\left(\mathcal{K}_{u\phi}^{h}\right)_4 = \mathop{\mathbf{A}}_{e=1}^{n_{\text{el}}} \left\{\boldsymbol{c}^e\right\}^T \cdot \left[\mathfrak{J}_{24}^e\right] \cdot \left\{\delta\boldsymbol{\phi}^e\right\} \tag{5.59}$$

The thirteenth term is:

$$\int_{\mathcal{B}_0} w_{k,L} F_{Ll}^{-1} F_{lL} S_{LK} \delta\left(F_{kK}\right) dV = \int_{\mathcal{B}_0} w_{k,L} F_{Ll}^{-1} F_{lL} S_{LK} \delta u_{k,K} dV \tag{5.60}$$

$$\left(\mathcal{K}_{uu}^{e,h}\right)_{10} = \int_{\mathcal{B}_0^e} \left\{\boldsymbol{c}^e\right\}^T \cdot \left[\boldsymbol{GRAD}\left(\boldsymbol{N}^{u,e}\right)\right]^T \cdot \left[\boldsymbol{I}_{1/10}\right] \cdot \left[\boldsymbol{GRAD}\left(\boldsymbol{N}^{u,e}\right)\right] \cdot \left\{\delta\boldsymbol{d}^e\right\} dV \tag{5.61}$$

$$\left[\mathfrak{J}_{1/10}^e\right] = \int_{\mathcal{B}_0^e} \left[\boldsymbol{GRAD}\left(\boldsymbol{N}^{u,e}\right)\right]^T \cdot \left[\boldsymbol{I}_{1/10}\right] \cdot \left[\boldsymbol{GRAD}\left(\boldsymbol{N}^{u,e}\right)\right] dV \tag{5.62}$$

$$\left(\mathcal{K}_{uu}^{h}\right)_{10} = \mathop{\mathbf{A}}_{e=1}^{n_{\text{el}}} \left\{\boldsymbol{c}^e\right\}^T \cdot \left[\mathfrak{J}_{1/10}^e\right] \cdot \left\{\delta\boldsymbol{d}^e\right\} \tag{5.63}$$

5.1.3 Submatrices in the Matrix Form of the Balance of First Moment of Momentum at Reference Configuration

Similar to previous section, $\left(\mathcal{K}^h_{\phi u}\right)_i$, $\left(\mathcal{K}^h_{\phi\phi}\right)_i$, $\left(\mathcal{KM}_{\phi u}\right)_i$,and $\left(\mathcal{KM}^h_{\phi\phi}\right)_i$ are the contributions to the consistent tangent coming from the linearized form of the balance of first moment of momentum. The first term is:

$$\int_{\mathcal{B}_0} \eta_{lm}\delta\left(F_{lM}\right)\left(\Sigma_{LM}-S_{LM}\right)F_{mM}dV = \int_{\mathcal{B}_0} \eta_{lm}\left(\Sigma_{LM}-S_{LM}\right)F_{mM}\delta u_{l,M}dV \tag{5.64}$$

$$\left(\mathcal{K}^{e,h}_{\phi u}\right)_1 = \int_{\mathcal{B}^e_0} \left\{\boldsymbol{\alpha}^e\right\}^T\cdot\left[\boldsymbol{N}^{\chi,e}\right]^T\cdot\left[\boldsymbol{J}_{11}\right]\cdot\left[\boldsymbol{GRAD}\left(\boldsymbol{N}^{u,e}\right)\right]\cdot\left\{\delta\boldsymbol{d}^e\right\}dV \tag{5.65}$$

$$\left[\mathcal{J}^e_{11}\right] = \int_{\mathcal{B}^e_0} \left[\boldsymbol{N}^{\chi,e}\right]^T\cdot\left[\boldsymbol{J}_{11}\right]\cdot\left[\boldsymbol{GRAD}\left(\boldsymbol{N}^{u,e}\right)\right]dV \tag{5.66}$$

$$\left(\mathcal{K}^h_{\phi u}\right)_1 = \mathop{\mathbf{A}}_{e=1}^{n_{\text{el}}}\left\{\boldsymbol{\alpha}^e\right\}^T\cdot\left[\mathcal{J}^e_{11}\right]\cdot\left\{\delta\boldsymbol{d}^e\right\} \tag{5.67}$$

The second term which is the first term of $\left(\Sigma_{LM}-S_{LM}\right)$ is:

$$\tau\int_{\mathcal{B}_0} \eta_{lm}F_{lM}\delta\left(F_{iK}\right)F_{iK}\delta_{LM}F_{mM}dV = \tau\int_{\mathcal{B}_0} \eta_{lm}F_{lM}F_{iK}\delta_{LM}F_{mM}\delta u_{i,K}dV \tag{5.68}$$

$$\left(\mathcal{K}^{e,h}_{\phi u}\right)_2 = \tau\int_{\mathcal{B}^e_0} \left\{\boldsymbol{\alpha}^e\right\}^T\cdot\left[\boldsymbol{N}^{\chi,e}\right]^T\cdot\left[\boldsymbol{J}_{12}\right]\cdot\left[\boldsymbol{GRAD}\left(\boldsymbol{N}^{u,e}\right)\right]\cdot\left\{\delta\boldsymbol{d}^e\right\}dV \tag{5.69}$$

$$\left[\mathcal{J}^e_{12}\right] = \tau\int_{\mathcal{B}^e_0} \left[\boldsymbol{N}^{\chi,e}\right]^T\cdot\left[\boldsymbol{J}_{12}\right]\cdot\left[\boldsymbol{GRAD}\left(\boldsymbol{N}^{u,e}\right)\right]dV \tag{5.70}$$

$$\left(\mathcal{K}^h_{\phi u}\right)_2 = \mathop{\mathbf{A}}_{e=1}^{n_{\text{el}}}\left\{\boldsymbol{\alpha}^e\right\}^T\cdot\left[\mathcal{J}^e_{12}\right]\cdot\left\{\delta\boldsymbol{d}^e\right\} \tag{5.71}$$

The third term is:

$$\tau\int_{\mathcal{B}_0} \eta_{lm}F_{lM}F_{iK}\delta\left(F_{iK}\right)\delta_{LM}F_{mM}dV = \tau\int_{\mathcal{B}_0} \eta_{lm}F_{lM}F_{iK}\delta_{LM}F_{mM}\delta u_{i,K}dV \tag{5.72}$$

$$\left(\mathcal{K}^{e,h}_{\phi u}\right)_3 = \tau\int_{\mathcal{B}^e_0} \left\{\boldsymbol{\alpha}^e\right\}^T\cdot\left[\boldsymbol{N}^{\chi,e}\right]^T\cdot\left[\boldsymbol{J}_{13}\right]\cdot\left[\boldsymbol{GRAD}\left(\boldsymbol{N}^{u,e}\right)\right]\cdot\left\{\delta\boldsymbol{d}^e\right\}dV \tag{5.73}$$

$$\left[\mathcal{J}^e_{13}\right] = \tau\int_{\mathcal{B}^e_0} \left[\boldsymbol{N}^{\chi,e}\right]^T\cdot\left[\boldsymbol{J}_{13}\right]\cdot\left[\boldsymbol{GRAD}\left(\boldsymbol{N}^{u,e}\right)\right]dV \tag{5.74}$$

$$\left(\mathcal{K}^h_{\phi u}\right)_3 = \mathop{\mathbf{A}}_{e=1}^{n_{\text{el}}}\left\{\boldsymbol{\alpha}^e\right\}^T\cdot\left[\mathcal{J}^e_{13}\right]\cdot\left\{\delta\boldsymbol{d}^e\right\} \tag{5.75}$$

The fourth term is:

$$2\sigma \int_{\mathcal{B}_0} \eta_{lm} F_{lM} \delta\left(F_{iL}\right) F_{iM} F_{mM} dV = 2\sigma \int_{\mathcal{B}_0} \eta_{lm} F_{lM} F_{iM} F_{mM} \delta u_{i,L} dV \tag{5.76}$$

$$\left(\mathcal{K}_{\phi u}^{e,h}\right)_4 = 2\sigma \int_{\mathcal{B}_0^e} \left\{\boldsymbol{\alpha}^e\right\}^T \cdot \left[\boldsymbol{N}^{\chi,e}\right]^T \cdot \left[\boldsymbol{J}_{14}\right] \cdot \left[\boldsymbol{GRAD}\left(\boldsymbol{N}^{u,e}\right)\right] \cdot \left\{\delta \boldsymbol{d}^e\right\} dV \tag{5.77}$$

$$\left[\boldsymbol{\mathcal{J}}_{14}^e\right] = 2\sigma \int_{\mathcal{B}_0^e} \left[\boldsymbol{N}^{\chi,e}\right]^T \cdot \left[\boldsymbol{J}_{14}\right] \cdot \left[\boldsymbol{GRAD}\left(\boldsymbol{N}^{u,e}\right)\right] dV \tag{5.78}$$

$$\left(\mathcal{K}_{\phi u}^{h}\right)_4 = \mathop{\mathbf{A}}_{e=1}^{n_{\text{el}}} \left\{\boldsymbol{\alpha}^e\right\}^T \cdot \left[\boldsymbol{\mathcal{J}}_{14}^e\right] \cdot \left\{\delta \boldsymbol{d}^e\right\} \tag{5.79}$$

The fifth term is:

$$2\sigma \int_{\mathcal{B}_0} \eta_{lm} F_{lM} F_{iL} \delta\left(F_{iM}\right) F_{mM} dV = 2\sigma \int_{\mathcal{B}_0} \eta_{lm} F_{lM} F_{iL} F_{mM} \delta u_{i,M} dV \tag{5.80}$$

$$\left(\mathcal{K}_{\phi u}^{e,h}\right)_5 = 2\sigma \int_{\mathcal{B}_0^e} \left\{\boldsymbol{\alpha}^e\right\}^T \cdot \left[\boldsymbol{N}^{\chi,e}\right]^T \cdot \left[\boldsymbol{J}_{15}\right] \cdot \left[\boldsymbol{GRAD}\left(\boldsymbol{N}^{u,e}\right)\right] \cdot \left\{\delta \boldsymbol{d}^e\right\} dV \tag{5.81}$$

$$\left[\boldsymbol{\mathcal{J}}_{15}^e\right] = 2\sigma \int_{\mathcal{B}_0^e} \left[\boldsymbol{N}^{\chi,e}\right]^T \cdot \left[\boldsymbol{J}_{15}\right] \cdot \left[\boldsymbol{GRAD}\left(\boldsymbol{N}^{u,e}\right)\right] dV \tag{5.82}$$

$$\left(\mathcal{K}_{\phi u}^{h}\right)_5 = \mathop{\mathbf{A}}_{e=1}^{n_{\text{el}}} \left\{\boldsymbol{\alpha}^e\right\}^T \cdot \left[\boldsymbol{\mathcal{J}}_{15}^e\right] \cdot \left\{\delta \boldsymbol{d}^e\right\} \tag{5.83}$$

The sixth term is:

$$(\eta - \tau) \int_{\mathcal{B}_0} \eta_{lm} F_{lM} \delta\left(F_{iK}\right) \chi_{iK} \delta_{LM} F_{mM} dV = (\eta - \tau) \int_{\mathcal{B}_0} \eta_{lm} F_{lM} \chi_{iK} \delta_{LM} F_{mM} \delta u_{i,K} dV \tag{5.84}$$

$$\left(\mathcal{K}_{\phi u}^{e,h}\right)_6 = (\eta - \tau) \int_{\mathcal{B}_0^e} \left\{\boldsymbol{\alpha}^e\right\}^T \cdot \left[\boldsymbol{N}^{\chi,e}\right]^T \cdot \left[\boldsymbol{J}_{16}\right] \cdot \left[\boldsymbol{GRAD}\left(\boldsymbol{N}^{u,e}\right)\right] \cdot \left\{\delta \boldsymbol{d}^e\right\} dV \tag{5.85}$$

$$\left[\boldsymbol{\mathcal{J}}_{16}^e\right] = (\eta - \tau) \int_{\mathcal{B}_0^e} \left[\boldsymbol{N}^{\chi,e}\right]^T \cdot \left[\boldsymbol{J}_{16}\right] \cdot \left[\boldsymbol{GRAD}\left(\boldsymbol{N}^{u,e}\right)\right] dV \tag{5.86}$$

$$\left(\mathcal{K}_{\phi u}^{h}\right)_6 = \mathop{\mathbf{A}}_{e=1}^{n_{\text{el}}} \left\{\boldsymbol{\alpha}^e\right\}^T \cdot \left[\boldsymbol{\mathcal{J}}_{16}^e\right] \cdot \left\{\delta \boldsymbol{d}^e\right\} \tag{5.87}$$

The seventh term is:

$$(\eta - \tau) \int_{\mathcal{B}_0} \eta_{lm} F_{lM} F_{iK} \delta\left(\chi_{iK}\right) \delta_{LM} F_{mM} dV = (\eta - \tau) \int_{\mathcal{B}_0} \eta_{lm} F_{lM} F_{iK} \delta_{LM} F_{mM} \delta \Phi_{iK} dV \tag{5.88}$$

$$\left(\mathcal{K}^{e,h}_{\phi\phi}\right)_1 = (\eta-\tau)\int_{\mathcal{B}^e_0}\{\boldsymbol{\alpha}^e\}^T\cdot[\boldsymbol{N}^{\chi,e}]^T\cdot[\boldsymbol{J}_{21}]\cdot[\boldsymbol{N}^{\chi,e}]\cdot\{\delta\boldsymbol{\phi}^e\}\,dV \tag{5.89}$$

$$[\boldsymbol{\mathcal{J}}^e_{21}] = (\eta-\tau)\int_{\mathcal{B}^e_0}[\boldsymbol{N}^{\chi,e}]^T\cdot[\boldsymbol{J}_{21}]\cdot[\boldsymbol{N}^{\chi,e}]\,dV \tag{5.90}$$

$$\left(\mathcal{K}^{h}_{\phi\phi}\right)_1 = \mathop{\mathbf{A}}_{e=1}^{n_{\text{el}}}\{\boldsymbol{\alpha}^e\}^T\cdot[\boldsymbol{\mathcal{J}}^e_{21}]\cdot\{\delta\boldsymbol{\phi}^e\} \tag{5.91}$$

The eight term is:

$$(\nu-\sigma)\int_{\mathcal{B}_0}\eta_{lm}F_{lM}\delta\left(F_{iL}\right)\chi_{iM}F_{mM}dV = (\nu-\sigma)\int_{\mathcal{B}_0}\eta_{lm}F_{lM}\chi_{iM}F_{mM}\delta u_{i,L}dV \tag{5.92}$$

$$\left(\mathcal{K}^{e,h}_{\phi u}\right)_7 = (\nu-\sigma)\int_{\mathcal{B}^e_0}\{\boldsymbol{\alpha}^e\}^T\cdot[\boldsymbol{N}^{\chi,e}]^T\cdot[\boldsymbol{J}_{17}]\cdot[\boldsymbol{GRAD}\left(\boldsymbol{N}^{u,e}\right)]\cdot\{\delta\boldsymbol{d}^e\}\,dV \tag{5.93}$$

$$[\boldsymbol{\mathcal{J}}^e_{17}] = (\nu-\sigma)\int_{\mathcal{B}^e_0}[\boldsymbol{N}^{\chi,e}]^T\cdot[\boldsymbol{J}_{17}]\cdot[\boldsymbol{GRAD}\left(\boldsymbol{N}^{u,e}\right)]\,dV \tag{5.94}$$

$$\left(\mathcal{K}^{h}_{\phi u}\right)_7 = \mathop{\mathbf{A}}_{e=1}^{n_{\text{el}}}\{\boldsymbol{\alpha}^e\}^T\cdot[\boldsymbol{\mathcal{J}}^e_{17}]\cdot\{\delta\boldsymbol{d}^e\} \tag{5.95}$$

The ninth term is:

$$(\nu-\sigma)\int_{\mathcal{B}_0}\eta_{lm}F_{lM}F_{iL}\left(\chi_{iM}\right)\ F_{mM}dV = (\nu-\sigma)\int_{\mathcal{B}_0}\eta_{lm}F_{lM}F_{iL}F_{mM}\delta\Phi_{iM}dV \tag{5.96}$$

$$\left(\mathcal{K}^{e,h}_{\phi\phi}\right)_2 = (\nu-\sigma)\int_{\mathcal{B}^e_0}\{\boldsymbol{\alpha}^e\}^T\cdot[\boldsymbol{N}^{\chi,e}]^T\cdot[\boldsymbol{J}_{22}]\cdot[\boldsymbol{N}^{\chi,e}]\cdot\{\delta\boldsymbol{\phi}^e\}\,dV \tag{5.97}$$

$$[\boldsymbol{\mathcal{J}}^e_{22}] = (\nu-\sigma)\int_{\mathcal{B}^e_0}[\boldsymbol{N}^{\chi,e}]^T\cdot[\boldsymbol{J}_{22}]\cdot[\boldsymbol{N}^{\chi,e}]\,dV \tag{5.98}$$

$$\left(\mathcal{K}^{h}_{\phi\phi}\right)_2 = \mathop{\mathbf{A}}_{e=1}^{n_{\text{el}}}\{\boldsymbol{\alpha}^e\}^T\cdot[\boldsymbol{\mathcal{J}}^e_{22}]\cdot\{\delta\boldsymbol{\phi}^e\} \tag{5.99}$$

The tenth term is:

$$(\kappa-\sigma)\int_{\mathcal{B}_0}\eta_{lm}F_{lM}\delta\left(F_{iM}\right)\chi_{iL}F_{mM}dV = (\kappa-\sigma)\int_{\mathcal{B}_0}\eta_{lm}F_{lM}\chi_{iL}F_{mM}\delta u_{i,M}dV \tag{5.100}$$

$$\left(\mathcal{K}^{e,h}_{\phi u}\right)_8 = (\kappa-\sigma)\int_{\mathcal{B}^e_0}\{\boldsymbol{\alpha}^e\}^T\cdot[\boldsymbol{N}^{\chi,e}]^T\cdot[\boldsymbol{J}_{18}]\cdot[\boldsymbol{GRAD}\left(\boldsymbol{N}^{u,e}\right)]\cdot\{\delta\boldsymbol{d}^e\}\,dV \tag{5.101}$$

$$[\boldsymbol{\mathcal{J}}^e_{18}] = (\kappa-\sigma)\int_{\mathcal{B}^e_0}[\boldsymbol{N}^{\chi,e}]^T\cdot[\boldsymbol{J}_{18}]\cdot[\boldsymbol{GRAD}\left(\boldsymbol{N}^{u,e}\right)]\,dV \tag{5.102}$$

$$\left(\mathcal{K}^{h}_{\phi u}\right)_8 = \mathop{\mathbf{A}}_{e=1}^{n_{\text{el}}}\{\boldsymbol{\alpha}^e\}^T\cdot[\boldsymbol{\mathcal{J}}^e_{18}]\cdot\{\delta\boldsymbol{d}^e\} \tag{5.103}$$

The eleventh term is:

$$(\kappa-\sigma)\int_{\mathcal{B}_0}\eta_{lm}F_{lM}F_{iM}\left(\chi_{iL}\right)\ F_{mM}dV=(\kappa-\sigma)\int_{\mathcal{B}_0}\eta_{lm}F_{lM}F_{iM}F_{mM}\delta\Phi_{iL}dV \tag{5.104}$$

$$\left(\mathcal{K}^{e,h}_{\phi\phi}\right)_3=(\kappa-\sigma)\int_{\mathcal{B}^e_0}\{\boldsymbol{\alpha}^e\}^T\cdot[\boldsymbol{N}^{\chi,e}]^T\cdot[\boldsymbol{J}_{23}]\cdot[\boldsymbol{N}^{\chi,e}]\cdot\{\delta\boldsymbol{\phi}^e\}\,dV \tag{5.105}$$

$$[\boldsymbol{\mathcal{J}}^e_{23}]=(\kappa-\sigma)\int_{\mathcal{B}^e_0}[\boldsymbol{N}^{\chi,e}]^T\cdot[\boldsymbol{J}_{23}]\cdot[\boldsymbol{N}^{\chi,e}]\,dV \tag{5.106}$$

$$\left(\mathcal{K}^{h}_{\phi\phi}\right)_3=\mathop{\mathbf{A}}_{e=1}^{n_{\text{el}}}\{\boldsymbol{\alpha}^e\}^T\cdot[\boldsymbol{\mathcal{J}}^e_{23}]\cdot\{\delta\boldsymbol{\phi}^e\} \tag{5.107}$$

The twelfth term is:

$$\int_{\mathcal{B}_0}\eta_{lm}F_{lL}\left(\Sigma_{LM}-S_{LM}\right)\delta\left(F_{mM}\right)dV=\int_{\mathcal{B}_0}\eta_{lm}F_{lL}\left(\Sigma_{LM}-S_{LM}\right)\delta u_{m,M}dV \tag{5.108}$$

$$\left(\mathcal{K}^{e,h}_{\phi u}\right)_9=\int_{\mathcal{B}^e_0}\{\boldsymbol{\alpha}^e\}^T\cdot[\boldsymbol{N}^{\chi,e}]^T\cdot[\boldsymbol{J}_{19}]\cdot[\boldsymbol{GRAD}\left(\boldsymbol{N}^{u,e}\right)]\cdot\{\delta\boldsymbol{d}^e\}\,dV \tag{5.109}$$

$$[\boldsymbol{\mathcal{J}}^e_{19}]=\int_{\mathcal{B}^e_0}[\boldsymbol{N}^{\chi,e}]^T\cdot[\boldsymbol{J}_{19}]\cdot[\boldsymbol{GRAD}\left(\boldsymbol{N}^{u,e}\right)]\,dV \tag{5.110}$$

$$\left(\mathcal{K}^{h}_{\phi u}\right)_9=\mathop{\mathbf{A}}_{e=1}^{n_{\text{el}}}\{\boldsymbol{\alpha}^e\}^T\cdot[\boldsymbol{\mathcal{J}}^e_{19}]\cdot\{\delta\boldsymbol{d}^e\} \tag{5.111}$$

The thirteenth term is:

$$\begin{aligned}&\int_{\mathcal{B}_0}\eta_{lm,k}F_{kK}\delta\left(F_{lL}\right)M_{KLM}\chi_{mM}dV=\int_{\mathcal{B}_0}\eta_{lm,A}F^{-1}_{Ak}F_{kK}\delta\left(F_{lL}\right)M_{KLM}\chi_{mM}dV\\&=\int_{\mathcal{B}_0}\eta_{lm,K}\delta\left(F_{lL}\right)M_{KLM}\chi_{mM}dV=\int_{\mathcal{B}_0}\eta_{lm,K}M_{KLM}\chi_{mM}\delta u_{l,L}dV\end{aligned} \tag{5.112}$$

$$\left(\mathcal{KM}^{e}_{\phi u}\right)_1=\int_{\mathcal{B}^e_0}\{\boldsymbol{\alpha}^e\}^T\cdot[\boldsymbol{GRAD}\left(\boldsymbol{N}^{\chi,e}\right)]^T\cdot[\boldsymbol{M}_1]\cdot[\boldsymbol{GRAD}\left(\boldsymbol{N}^{u,e}\right)]\cdot\{\delta\boldsymbol{d}^e\}\,dV \tag{5.113}$$

$$[\boldsymbol{\mathfrak{M}}^e_1]=\int_{\mathcal{B}^e_0}[\boldsymbol{GRAD}\left(\boldsymbol{N}^{\chi,e}\right)]^T\cdot[\boldsymbol{M}_1]\cdot[\boldsymbol{GRAD}\left(\boldsymbol{N}^{u,e}\right)]\,dV \tag{5.114}$$

$$\left(\mathcal{KM}^{h}_{\phi u}\right)_1=\mathop{\mathbf{A}}_{e=1}^{n_{\text{el}}}\{\boldsymbol{\alpha}^e\}^T\cdot[\boldsymbol{\mathfrak{M}}^e_1]\cdot\{\delta\boldsymbol{d}^e\} \tag{5.115}$$

The examples given in the next chapters uses only one parameter τ_7 in the definition of higher order couple stress tensor. Hence, we present the linearization of only one term related to

τ_7. Then, the fourteenth term is:

$$\int_{\mathcal{B}_0} \eta_{lm,K} F_{lL} \delta\left(M_{KLM}\right) \chi_{mM} dV = \int_{\mathcal{B}_0} \eta_{lm,K} F_{lL} \delta\left(M_{KLM}\right) \chi_{mM} dV$$
$$= \tau_7 \int_{\mathcal{B}_0} \eta_{lm,K} F_{lL} \delta\left(F_{iK}\right) \chi_{iL,M} \chi_{mM} dV = \tau_7 \int_{\mathcal{B}_0} \eta_{lm,K} F_{lL} \chi_{iL,M} \chi_{mM} \delta u_{i,K} dV \tag{5.116}$$

$$\left(\mathcal{KM}^e_{\phi u}\right)_2 = \tau_7 \int_{\mathcal{B}^e_0} \{\boldsymbol{\alpha}^e\}^T \cdot \left[\boldsymbol{GRAD}\left(\boldsymbol{N}^{\chi,e}\right)\right]^T \cdot [\boldsymbol{M}_2] \cdot \left[\boldsymbol{GRAD}\left(\boldsymbol{N}^{u,e}\right)\right] \cdot \{\delta \boldsymbol{d}^e\} \, dV \tag{5.117}$$

$$[\mathfrak{M}^e_2] = \tau_7 \int_{\mathcal{B}^e_0} \left[\boldsymbol{GRAD}\left(\boldsymbol{N}^{\chi,e}\right)\right]^T \cdot [\boldsymbol{M}_2] \cdot \left[\boldsymbol{GRAD}\left(\boldsymbol{N}^{u,e}\right)\right] dV \tag{5.118}$$

$$\left(\mathcal{KM}^h_{\phi u}\right)_2 = \mathop{\mathbf{A}}_{e=1}^{n_{\text{el}}} \{\boldsymbol{\alpha}^e\}^T \cdot [\mathfrak{M}^e_2] \cdot \{\delta \boldsymbol{d}^e\} \tag{5.119}$$

The fifteenth term is:

$$\tau_7 \int_{\mathcal{B}_0} \eta_{lm,K} F_{lL} F_{iK} \delta\left(\chi_{iL,M}\right) \chi_{mM} dV = \tau_7 \int_{\mathcal{B}_0} \eta_{lm,K} F_{lL} F_{iK} \chi_{mM} \delta \Phi_{iL,M} dV \tag{5.120}$$

$$\left(\mathcal{KM}^e_{\phi\phi}\right)_1 = \tau_7 \int_{\mathcal{B}^e_0} \{\boldsymbol{\alpha}^e\}^T \cdot \left[\boldsymbol{GRAD}\left(\boldsymbol{N}^{\chi,e}\right)\right]^T \cdot [\boldsymbol{M}_3] \cdot \left[\boldsymbol{GRAD}\left(\boldsymbol{N}^{\chi,e}\right)\right] \cdot \{\delta \boldsymbol{\phi}^e\} \, dV \tag{5.121}$$

$$[\mathfrak{M}^e_3] = \tau_7 \int_{\mathcal{B}^e_0} \left[\boldsymbol{GRAD}\left(\boldsymbol{N}^{\chi,e}\right)\right]^T \cdot [\boldsymbol{M}_3] \cdot \left[\boldsymbol{GRAD}\left(\boldsymbol{N}^{\chi,e}\right)\right] dV \tag{5.122}$$

$$\left(\mathcal{KM}^h_{\phi\phi}\right)_1 = \mathop{\mathbf{A}}_{e=1}^{n_{\text{el}}} \{\boldsymbol{\alpha}^e\}^T \cdot [\mathfrak{M}^e_3] \cdot \{\delta \boldsymbol{\phi}^e\} \tag{5.123}$$

The sixteenth term is:

$$\int_{\mathcal{B}_0} \eta_{lm,K} F_{lL} M_{KLM} \delta\left(\chi_{mM}\right) dV = \int_{\mathcal{B}_0} \eta_{lm,K} F_{lL} M_{KLM} \delta \Phi_{mM} dV \tag{5.124}$$

$$\left(\mathcal{KM}^e_{\phi\phi}\right)_2 = \int_{\mathcal{B}^e_0} \{\boldsymbol{\alpha}^e\}^T \cdot \left[\boldsymbol{GRAD}\left(\boldsymbol{N}^{\chi,e}\right)\right]^T \cdot [\boldsymbol{M}_4] \cdot [\boldsymbol{N}^{\chi,e}] \cdot \{\delta \boldsymbol{\phi}^e\} \, dV \tag{5.125}$$

$$[\mathfrak{M}^e_4] = \int_{\mathcal{B}^e_0} \left[\boldsymbol{GRAD}\left(\boldsymbol{N}^{\chi,e}\right)\right]^T \cdot [\boldsymbol{M}_4] \cdot [\boldsymbol{N}^{\chi,e}] \, dV \tag{5.126}$$

$$\left(\mathcal{KM}^h_{\phi\phi}\right)_2 = \mathop{\mathbf{A}}_{e=1}^{n_{\text{el}}} \{\boldsymbol{\alpha}^e\}^T \cdot [\mathfrak{M}^e_4] \cdot \{\delta \boldsymbol{\phi}^e\} \tag{5.127}$$

These matrices determined above are constructing the global consistent tangent, in a same way presented in the section 4.8, to be used in the Newton-Raphson algorithm. To avoid repeating it, we omit those details here. The next chapter demonstrates the convenience of use of reference configuration in the implementation, together with examples.

Chapter 6

Finite Element Implementation and Numerical Examples of Finite Strain Micromorphic Elasticity

Previous Chapters 4 and 5 presented the finite element formulation together with the linearizations of the balance equations at current configuration and reference configuration respectively. In numerical examples, firstly, we provide a three dimensional finite strain micromorphic materially linear isotropic elastic model formulated in two ways for finite element implementation (Isbuga and Regueiro (2011), Regueiro and Isbuga (2011)): (i) direct finite strain elasticity , and (ii) rate form with semi-implicit time integration. The model is based upon the finite strain isotropic micromorphic elasticity model proposed by Eringen and Suhubi (1964); Suhubi and Eringen (1964). For (i), the direct formulation, the constitutive equations are calculated in the reference configuration, and the resulting stresses are mapped to the current configuration as shown in Chapter 5. For (ii), the rate formulation, the constitutive equations are integrated in time in the current configuration using the Truesdell objective stress rates as presented in Chapter 4. The comparison of two implementation shows the computational effectiveness of direct implementation and the following numerical examples present the applications of the formulation.

Three dimensional numerical examples are analyzed to compare the two formulations (i) and (ii) for standard finite strain isotropic elasticity, and the formulation (i) is used to demonstrate the elastic length scale effects that come through the higher order couple stress in the micromorphic theory (Regueiro and Isbuga (2011), Isbuga and Regueiro (2011)). The

following examples also provide the boundary condition effects as well as insights about three dimensional micromorphic continuum.

6.0.4 Element Used in Finite Element Implementation

We use a mixed 27 node hexahedral element for finite element implementation (Fig.6.1): 27 nodes for $\boldsymbol{u}^h$ and 8 vertex nodes for $\boldsymbol{\Phi}^h$ (Q27P8), where h is the discretization parameter. For the rate form (ii) of the model, (4.4) and (4.23) are written in Galerkin form (Hughes, 1987), and the time-integrated stress equations (3.134), (3.136), and (4.37) are used. The mixed formulation is employed in recognition that $\boldsymbol{\Phi}^h$ is a micro-displacement tensor (no gradient is calculated on a micro-displacement $\boldsymbol{u}'^h$, but $\boldsymbol{\Phi}^h$ is analogous to $\partial \boldsymbol{u}^h/\partial \boldsymbol{X}$ when comparing $\boldsymbol{F}^h$ and $\boldsymbol{\chi}^h$), where the gradient of a quadratic interpolation is linear, such that $\boldsymbol{\nabla u}^h$ and $\boldsymbol{\Phi}^h$ would be of approximate same order interpolation. Such mixed methods are shown to be convergent (Hughes, 1987) for the small strain case, but no formal proof of convergence is presented here; i.e., we do not show in a proof that $\boldsymbol{u} = \lim_{h\to 0} \boldsymbol{u}^h$ and $\boldsymbol{\Phi} = \lim_{h\to 0} \boldsymbol{\Phi}^h$. One of the numerical examples (Section 6.2.4) will provide a mesh refinement study to demonstrate the convergence of the mixed FE solution. The global nodal displacement vector is $\boldsymbol{d}$ and the nodal micro-displacement tensor in vector form is $\boldsymbol{\phi}$. Displacement vector u_k^h is interpolated at each node shown by solid dots, and the micro-displacement tensor Φ_{kK}^h is interpolated only at the vertices shown by open circles in Fig.6.1, such that

$$u_k^{h^e}(\boldsymbol{\xi}) = \sum_{a=1}^{n_{en}^u} N_a^u(\boldsymbol{\xi}) d_{k(a)}^e \ , \ \Phi_{kK}^{h^e}(\boldsymbol{\xi}) = \sum_{b=1}^{n_{en}^\phi} N_b^\Phi(\boldsymbol{\xi}) \phi_{kK(b)}^e \tag{6.1}$$

where $\boldsymbol{\xi} = [\xi \ \eta \ \zeta]$ are the natural coordinates, $N_a^u(\boldsymbol{\xi})$ the tri-quadratic interpolation functions, $N_b^\Phi(\boldsymbol{\xi})$ the tri-linear interpolation functions, $d_{k(a)}^e$ the displacement vector at node a of element e, and $\phi_{kK(b)}^e$ the micro-displacement tensor at node b in element e.

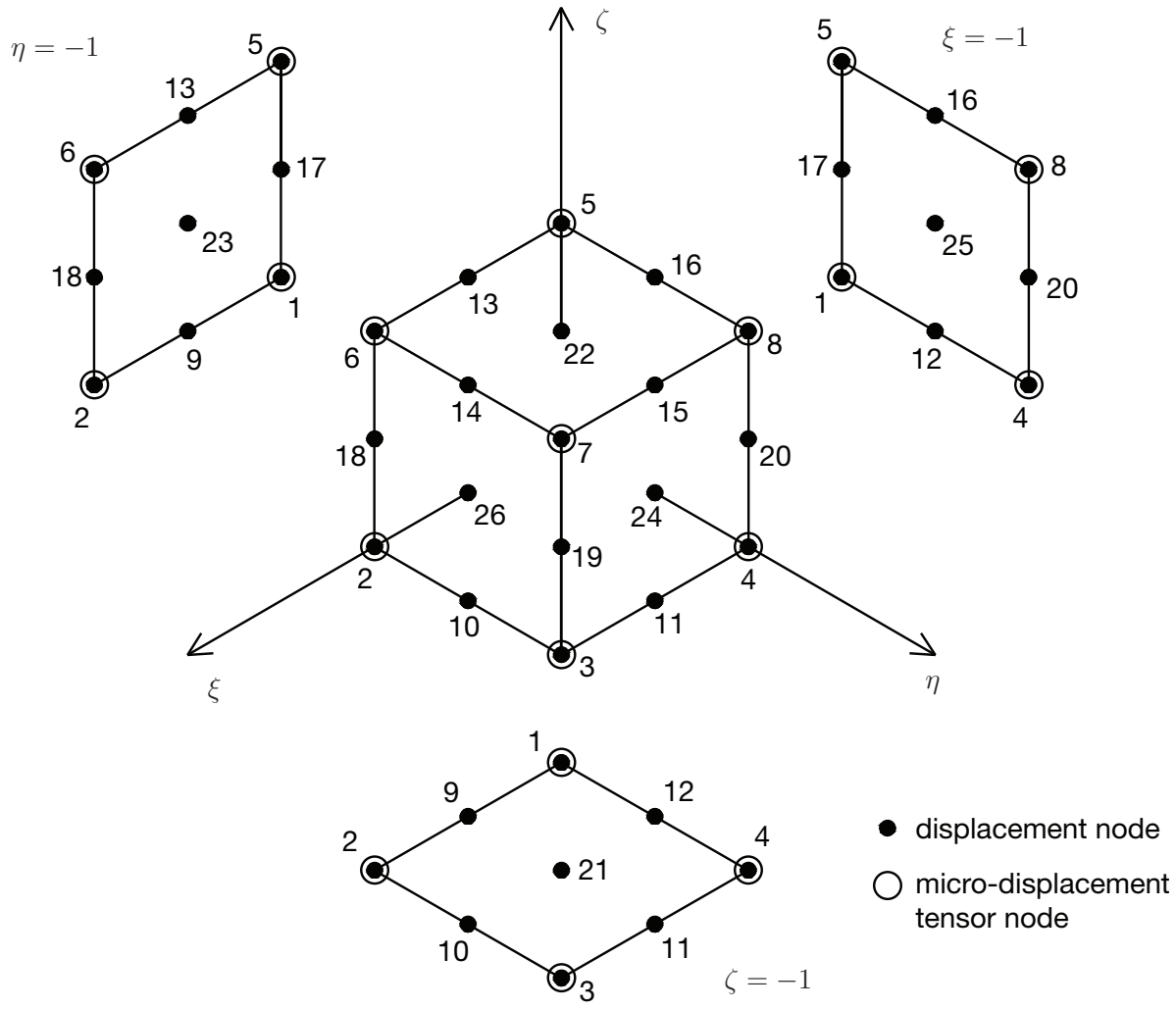

Figure 6.1: Mixed 27 node hexahedral element: quadratic in displacement and linear in micro-displacement tensor interpolations. Node numbering and geometry shown in the natural coordinate space (Hughes, 1987). The number of element nodes for displacement and micro-displacement tensor, respectively, are $n^u_{en} = 27$ and $n^\phi_{en} = 8$.

6.1 One-dimensional (1D) micromorphic uniaxial strain in compression formulation and FE implementation for 'verification' of 3D micromorphic FE model

As a form of verification for our three-dimensional finite strain coupled micromorphic finite element implementation in an opensource C++ code Tahoe, we formulate and imple-

ment a simpler one-dimensional uniaxial strain compression problem. It entails an assumed displacement only in the X_3 direction, and likewise only a component of $\boldsymbol{\Phi}$ in the X_3 direction. The resulting kinematics are as follows:

$$\boldsymbol{u} = \begin{bmatrix} 0 \\ 0 \\ u \end{bmatrix}, \quad \boldsymbol{\Phi} = \begin{bmatrix} 0 & 0 & 0 \\ 0 & 0 & 0 \\ 0 & 0 & \Phi \end{bmatrix} \tag{6.2}$$

where $u_3 = u(X_3)$ and $\Phi_{33} = \Phi(X_3)$. The resulting deformation measures are as follows:

$$\boldsymbol{F} = \begin{bmatrix} 1 & 0 & 0 \\ 0 & 1 & 0 \\ 0 & 0 & 1 + \frac{\partial u}{\partial X_3} \end{bmatrix}, \quad \boldsymbol{\chi} = \begin{bmatrix} 1 & 0 & 0 \\ 0 & 1 & 0 \\ 0 & 0 & 1 + \Phi \end{bmatrix} \tag{6.3}$$

$$\boldsymbol{E} = (\boldsymbol{C} - \boldsymbol{1})/2 = \begin{bmatrix} 0 & 0 & 0 \\ 0 & 0 & 0 \\ 0 & 0 & \frac{1}{2}\frac{\partial u}{\partial X_3}\left(2 + \frac{\partial u}{\partial X_3}\right) \end{bmatrix} \tag{6.4}$$

$$\boldsymbol{\mathcal{E}} = \begin{bmatrix} 0 & 0 & 0 \\ 0 & 0 & 0 \\ 0 & 0 & \Phi + \frac{\partial u}{\partial X_3} + \Phi\frac{\partial u}{\partial X_3} \end{bmatrix} \tag{6.5}$$

$$\Gamma_{333} = \frac{\partial \Phi}{\partial X_3}\left(1 + \frac{\partial u}{\partial X_3}\right) \tag{6.6}$$

When substituting these deformation measures in (6.4)-(6.6) into the constitutive equations (2.113)-(2.115), and in turn the linearized variational equations in (4.4) and (4.23), a one-dimensional coupled finite element formulation results. We use a mixed element formulation similar to the 3D hexahedral element in Fig.6.1, where axial displacement $u^h(X_3)$ is interpolated quadratically and axial micro-displacement tensor component $\Phi^h(X_3)$ is interpolated linearly. This is the same as the column compression problem in Section 6.2.4, where the two models (3D and 1D) are compared in Section 6.2.3.

6.2 Numerical examples

6.2.1 Choice of elastic parameters

In the Cauchy continuum, the constitutive equations involve two Lamé parameters for linear isotropic elasticity, which we call here λ^* and μ^*, to distinguish from the micromorphic elastic parameters λ and μ. The isotropic micromorphic elasticity approach introduces seven elastic moduli $(\lambda, \mu, \eta, \tau, \kappa, \nu, \sigma)$ in the unsymmetric Cauchy stress tensor $\boldsymbol{\sigma}$ and the symmetric microstress tensor $\boldsymbol{s}$, and eleven elastic constants $(\tau_1, \ldots, \tau_{11})$ in the higher order couple stress tensor $\boldsymbol{m}$, for a total of eighteen micromorphic linear isotropic elastic parameters. For the form of our constitutive equations in (2.113)-(2.115), (Smith, 1968) proposed restrictions among the elastic parameters in the form of inequalities to achieve the positive definiteness of a quadratic strain energy function in Section 2.5. Only the results are provided here. The numerical values may be chosen by a set of relations between Lamé parameters, λ^* and μ^*, and the micromorphic elastic parameters given below. The set of relations in (6.7) and (6.8) satisfy the positive definiteness of strain energy for numerical values of Lamé parameters $\lambda^* = 6400$ MPa and $\mu^* = 6400$ MPa for Nuozhadu granite (Zhou et al., 2010), and will be used in the numerical examples.

$$
\begin{aligned}
\tau_1 &\approx 0.15\lambda^*\ell_1^2 & \tau_7 &\approx 1.15\mu^*\ell_7^2 \\
\tau_2 = \tau_3 &\approx 0.25\lambda^*\ell_2^2 & \tau_8 = \tau_9 &\approx 0.85\mu^*\ell_8^2 \\
\tau_4 &\approx 0.275\lambda^*\ell_4^2 & \tau_{10} &\approx 0.70\mu^*\ell_{10}^2 \\
\tau_5 &\approx 0.135\lambda^*\ell_5^2 & \tau_{11} &\approx 0.85\mu^*\ell_{11}^2 \\
\tau_6 &\approx 0.345\lambda^*\ell_6^2
\end{aligned}
\tag{6.7}
$$

and

$$\begin{aligned} \eta &\approx 2\lambda^* & \kappa &\approx 1.4\mu^* \\ \tau &\approx 0.33\lambda^* & \nu &\approx 1.15\mu^* \\ \lambda &\approx 0.67\lambda^* & \sigma &\approx 0.70\mu^* \\ \mu &\approx 0.7\mu^* \end{aligned} \tag{6.8}$$

where ℓ_i $(i = 1, \ldots, 11)$ are elastic length scale parameters. Numerical values for the elastic parameters were calculated by relations given in (6.7) and (6.8) and are reported in Tables 6.1 and 6.2. In this paper, we do not attempt to relate the micromorphic elastic parameters to microstructural elastic parameters used in the analysis of a representative volume element (RVE) of the material, as in (Neff and Forest, 2007) for a metallic foam. Instead, we choose micromorphic elastic parameters that satisfy positive definiteness of the strain energy, as determined by (Smith, 1968) for the linearized form of our constitutive equations in (2.113)-(2.115).

Table 6.1: Isotropic micromorphic elastic parameters. Stress in MPa and length in micrometers (μm).

λ	μ	η	ν	κ	τ	σ
4267	4480	12800	7360	8960	2133	1920

Table 6.2: Isotropic micromorphic elastic parameters for $\boldsymbol{m}$. Stress $\tilde{\tau}_i$ in MPa and length ℓ_i in μm, where $\tau_i = \tilde{\tau}_i \ell_i^2$.

$\tilde{\tau}_1$	$\tilde{\tau}_2$	$\tilde{\tau}_3$	$\tilde{\tau}_4$	$\tilde{\tau}_5$	$\tilde{\tau}_6$	$\tilde{\tau}_7$	$\tilde{\tau}_8$	$\tilde{\tau}_9$	$\tilde{\tau}_{10}$	$\tilde{\tau}_{11}$
1600	1600	1600	1760	864	2208	7360	5440	5440	4480	5440
ℓ_1	ℓ_2	ℓ_3	ℓ_4	ℓ_5	ℓ_6	ℓ_7	ℓ_8	ℓ_9	ℓ_{10}	ℓ_{11}
0	0	0	0	0	0	0.1,1,10	0	0	0	0

In Table 6.2, we assume that the micromorphic elastic parameters $\tilde{\tau}_i$ may have different length scales than each other. It maybe also assumed that they all have the same length scales as in the future examples.

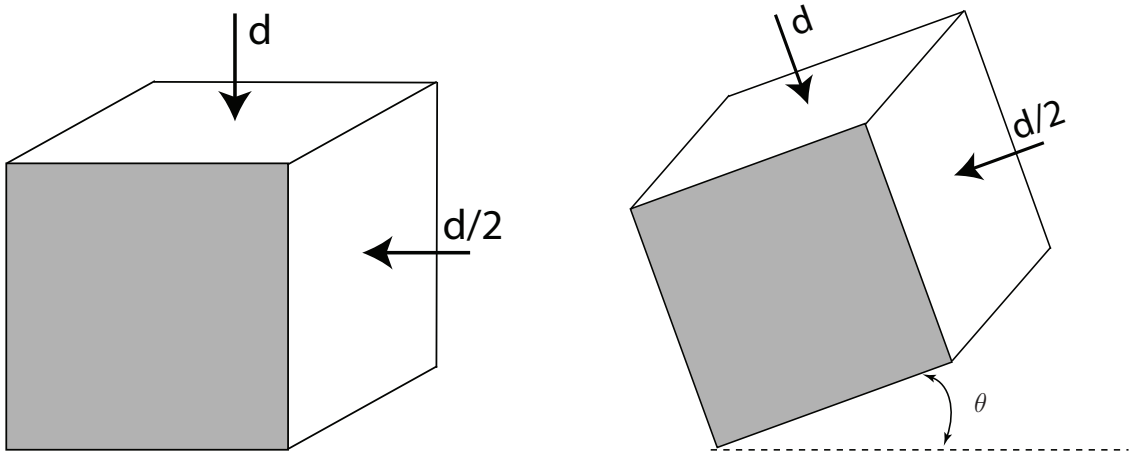

(a) (b)

Figure 6.2: (a) Plane strain compression with prescribed boundary displacements for non-rotating case. Front and back faces have zero normal displacements to generate a plane strain condition using a hexahedral element. (b) Plane strain compression with prescribed boundary displacements for rotating case through angle $\theta = 0 - 90^{\circ}$.

6.2.2 Small strain compression with large rotation

The first example provides a comparison of the (i) direct and (ii) incremental rate formulations of standard (not micromorphic) finite strain materially linear isotropic elasticity for a small strain compression, large rotation problem. The purpose of this example is to compare how the two formulations and FE implementations perform for a large rotation example, for future finite strain elasto-plastic micromorphic constitutive model implementation. We already know that the materially linear elasticity assumption is valid only for small elastic strains, where we expect large plastic strains to develop for the problems of interest to us (e.g., coupling to particulate mechanics models in a multiscale framework). A single $1 \times 1 \times 1$m cube tri-quadratic hexahedral element is used in the simulation, with a plane strain condition imposed three-dimensionally (out-of-plane), and large rotation prescribed to the boundary displacements, as shown in Fig.6.2. The Lamé parameters used in the analysis are $\lambda^* = 29$MPa and $\mu^* = 7$MPa (for a geomaterial), and the applied displacement is $d = 0.002$m.

Because of the semi-implicit time integration in (3.134), (3.136), and (4.37), it is ob-

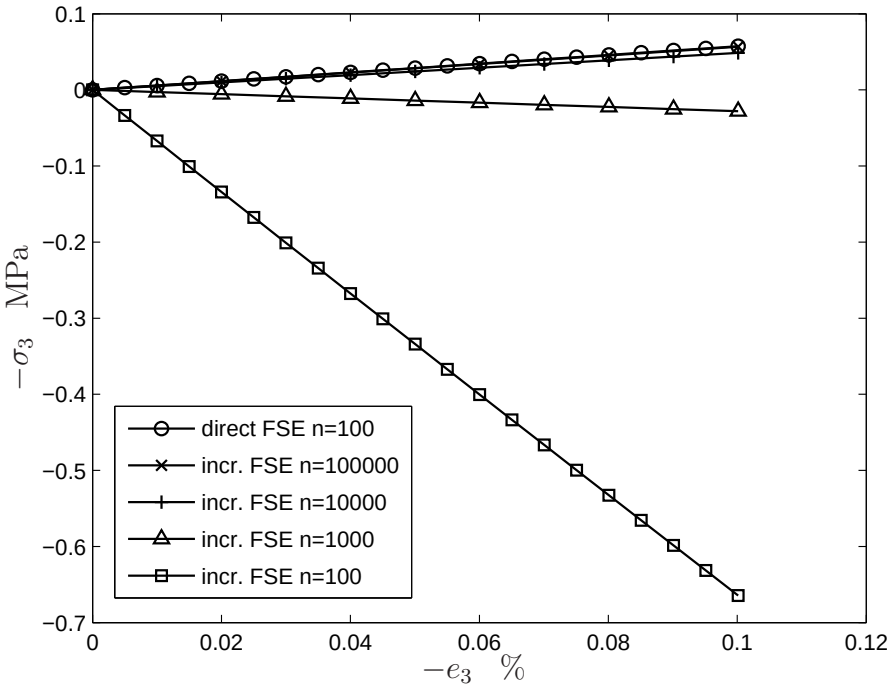

Figure 6.3: For large rotation example in Fig.6.2(b), the plots provide a comparison of the third principal Cauchy stress σ_3 versus the third principal Almansi strain e_3 obtained by (i) direct finite strain elasticity (FSE), and (ii) semi-implicit incremental FSE formulation, with different number of time steps, n. It shows that as the time steps are refined, the incremental formulation (ii) result approaches the direct formulation (i) result.

served in Fig.6.3 that during the large rotation example, we need many more time steps (i.e., smaller time increments) to achieve a proper level of accuracy for the incremental rate formulation of the model than compared to the direct formulation. In Fig.6.4, the minor principal stress-strain curve shows a good comparison between direct and incremental rate formulations of the standard elasticity model for same number of time steps for no rotation, and also a comparison with the rotation example to show that the principal stress values are the same. The advantage to using the incremental rate formulation (ii) for micromorphic elasto-plasticity (Regueiro, 2009) is when it is implemented within an explicit solution method, whether quasi-static or dynamic. For these solution methods, small time steps are used to ensure stability, and thus a semi-implicit time integration of a rate formulation of

micromorphic elasto-plasticity would be more computationally efficient than the direct formulation. For implicit solution methods (Regueiro and Ebrahimi, 2010), however, the direct formulation is better suited because time steps can be larger.

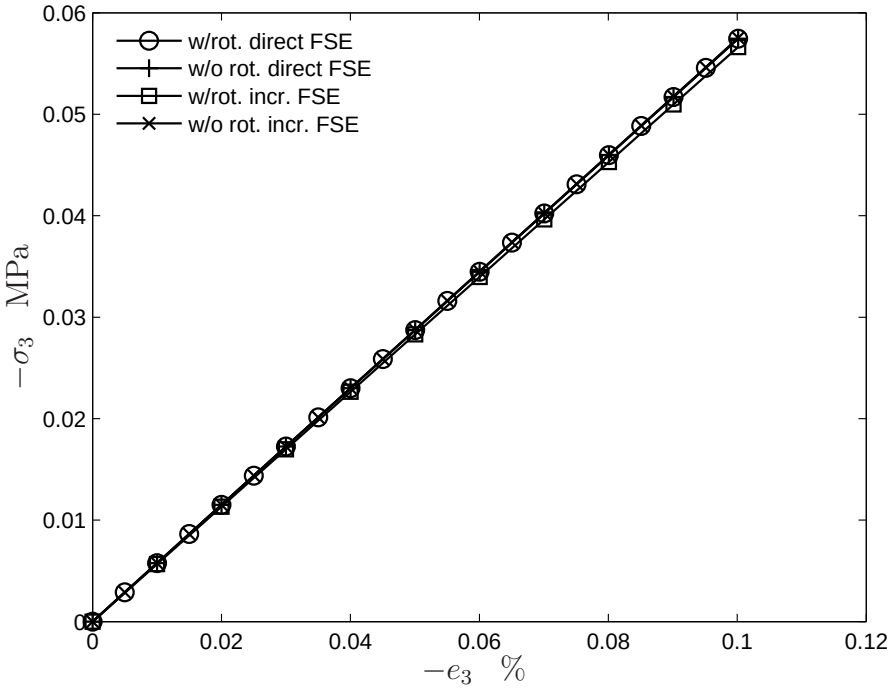

Figure 6.4: Comparison of the third principal Cauchy stress σ_3 vs. Almansi strain plots for small strain e_3 with large rotation, and small strain without rotation cases obtained by both (i) direct FSE, and (ii) semi-implicit incremental FSE formulations.

6.2.3 1D 'verification' example

We compare our 1D finite element model presented in Section 6.1 to the 3D model results in Section 6.2.4. We assume same elastic parameters, and an eight element mesh in the X_3 direction, with $u_3 = -1\mu m$ at $X_3 = 100\mu m$. We consider three cases: (1) Φ^h_{33} free along X_3; (2) $\Phi^h_{33} = 0$ at $X_3 = 0$, with $\ell_7 = 0$; (3) $\Phi^h_{33} = 0$ at $X_3 = 0$, with $\ell_7 = 10\mu m$. The results are reported in Figs.6.5-6.7. We see nearly exact agreement between our one-dimensional micromorphic FE results and the 3D results. Thus, our 3D micromorphic FE

results are verified against a separate 1D micromorphic FE formulation and implementation.

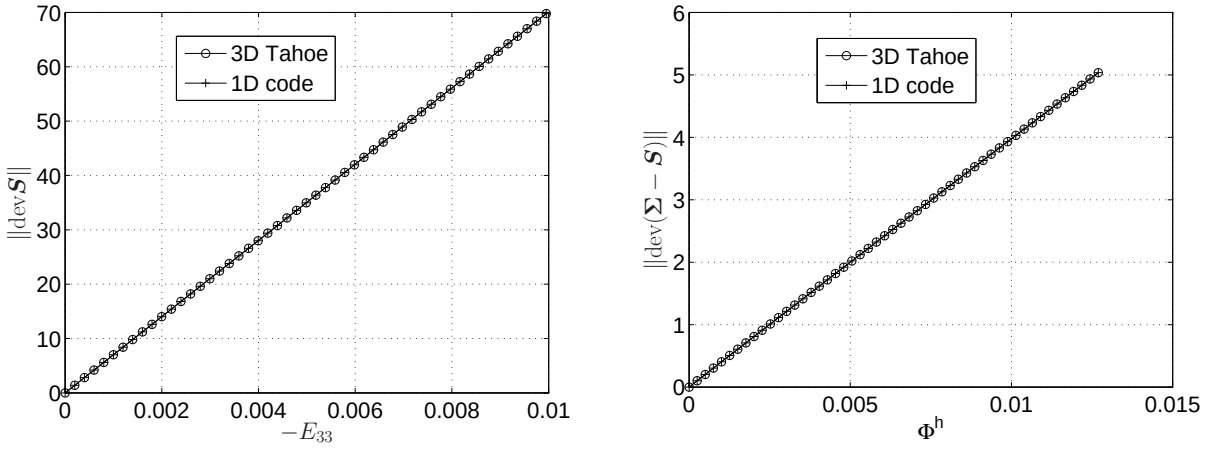

(a) (b)

Figure 6.5: (1) For Φ^h_{33} free along X_3: (a) Comparison of $\|\mathrm{dev}\boldsymbol{S}\|$ for 3D and 1D column compression. (b) Comparison of $\|\mathrm{dev}(\boldsymbol{\Sigma}-\boldsymbol{S})\|$ for 3D and 1D column compression.

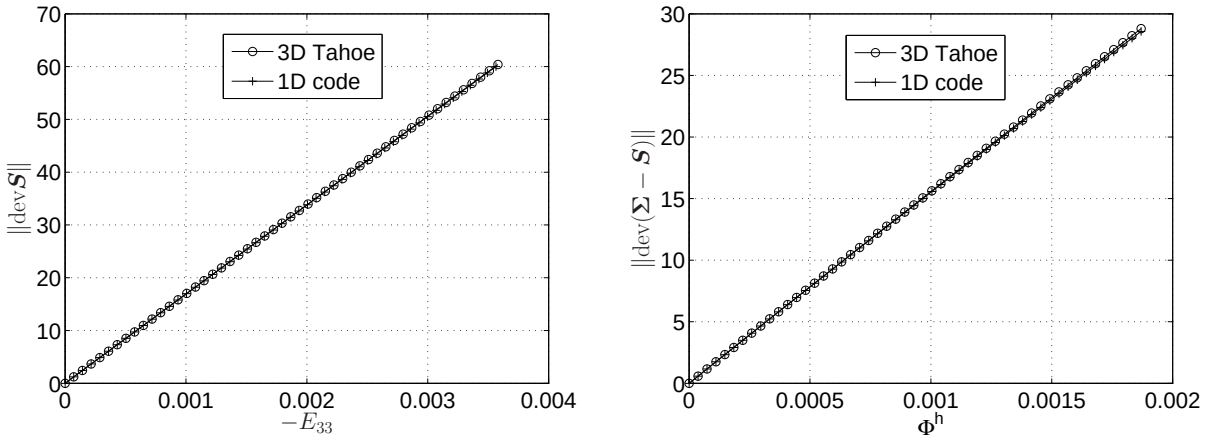

(a) (b)

Figure 6.6: (2) For $\Phi^h_{33}=0$ at $X_3=0$ and $\ell_7=0$: (a) Comparison of $\|\mathrm{dev}\boldsymbol{S}\|$ for 3D and 1D column compression. (b) Comparison of $\|\mathrm{dev}(\boldsymbol{\Sigma}-\boldsymbol{S})\|$ for 3D and 1D column compression.

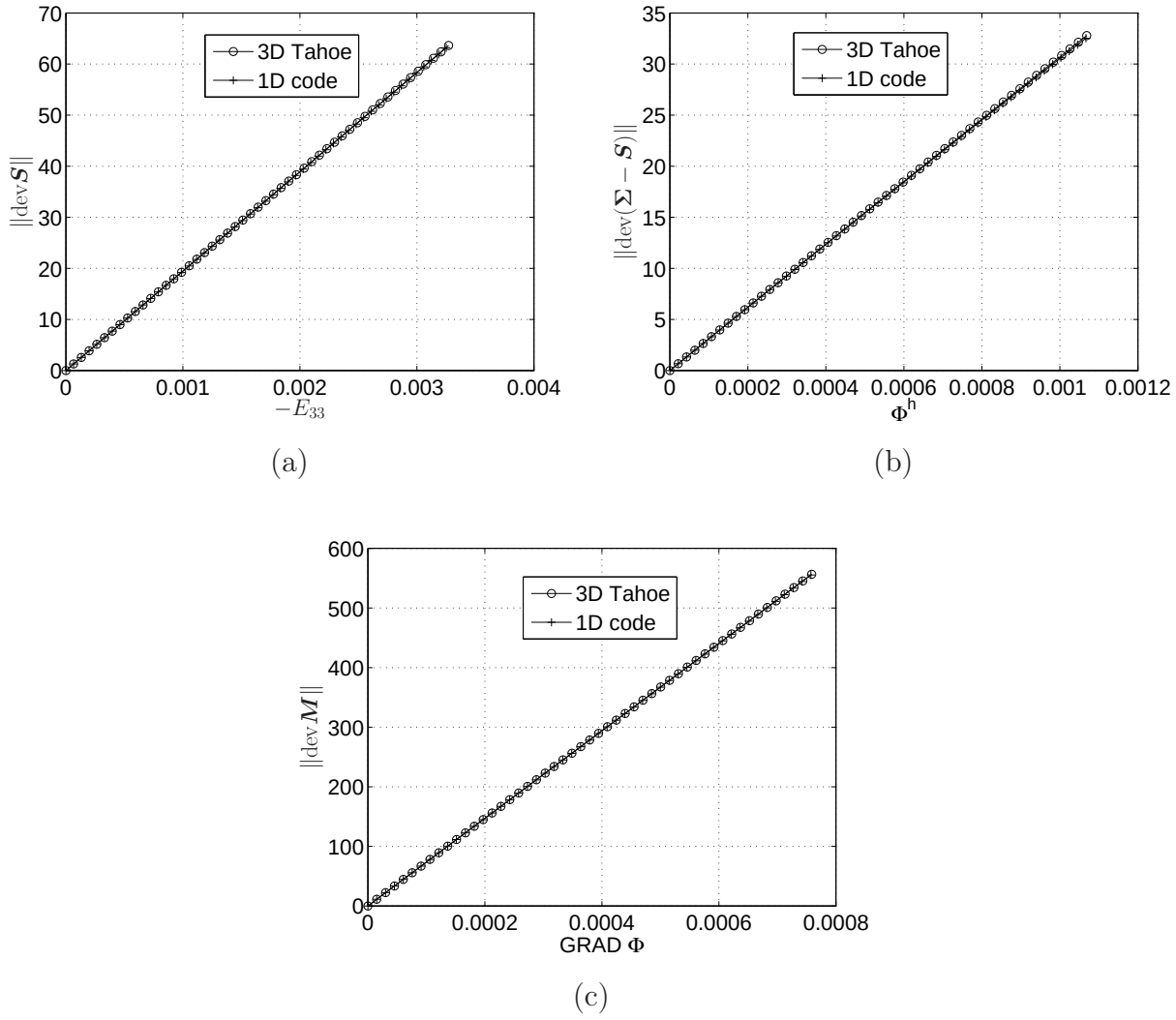

Figure 6.7: (3) For $\Phi^h_{33} = 0$ at $X_3 = 0$ and $\ell_7 = 10\mu m$: (a) Comparison of $\|\mathrm{dev}\boldsymbol{S}\|$ for 3D and 1D column compression. (b) Comparison of $\|\mathrm{dev}(\boldsymbol{\Sigma} - \boldsymbol{S})\|$ for 3D and 1D column compression. (c) Comparison of $\|\mathrm{dev}\boldsymbol{M}\|$ for 3D and 1D column compression.

6.2.4 Finite strain column compression with length scale effects

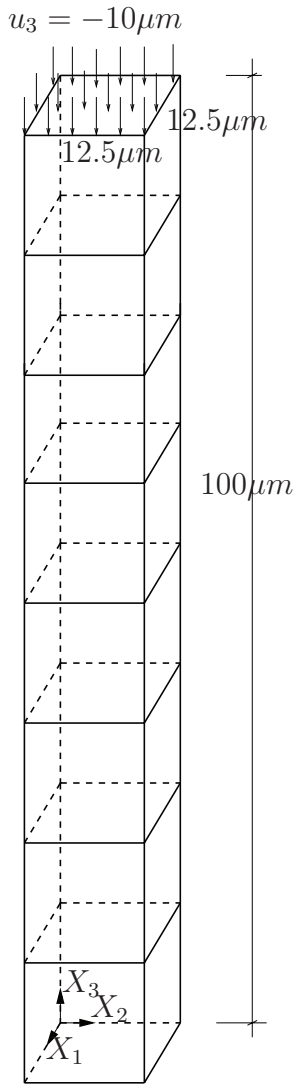

Figure 6.8: A 100 μm long column with a 156.25 $(\mu m)^2$ cross sectional area compressed with a displacement loading $u_3 = -10\mu m$ assuming different length scales ℓ_7.

Figure 6.8 shows a column compression example, with coarsest eight Q27P8 element mesh, which will demonstrate the length scale effect in the higher order stress term, and also be used for a mesh refinement study. This example is like a one-dimensional version of the cubical microindentation test in Section 6.2.6. The displacement boundary condition $u_3 = -10\mu$m is applied to the top surface at $X_3 = 100\mu m$. The displacement boundary conditions were chosen to provide a uniaxial strain compression problem: $u_1 = 0$ on $\pm X_1$ faces, $u_2 = 0$ on $\pm X_2$ faces, and $u_3 = 0$ on $-X_3$ face. All the micro-displacement tensor components Φ_{iI} are set $= 0$ except the micro-displacement tensor component Φ_{33} in the X_3 direction, where $\Phi_{33} = 0$ at $X_3 = 0$.

Figure 6.9, for a 32 element column mesh, shows the variation over quasi-static loading time of the deviatoric stress norms $||\text{dev}\boldsymbol{\sigma}||$, $||\text{dev}\,(\boldsymbol{s} - \boldsymbol{\sigma})\,||$, and $||\text{dev}\boldsymbol{m}||$ and traces $\text{tr}\boldsymbol{\sigma}$ and $\text{tr}\,(\boldsymbol{s} - \boldsymbol{\sigma})$, and norm of trace $||\text{tr}\boldsymbol{m}||$ for the unsymmetric Cauchy stress tensor $\boldsymbol{\sigma}$, the relative stress tensor $(\boldsymbol{s} - \boldsymbol{\sigma})$, and the higher order couple stress tensor $\boldsymbol{m}$, respectively, at $X_3 = 2.773$ μm where we have a gradient in Φ^h_{33} values which generates higher order stress tensor components due to the definition $\boldsymbol{M} = \tau_7\boldsymbol{\Gamma}$. Figure 6.9 also provides a comparison of these invariants for the three choices of length scale ℓ_7 in Table 6.2. Figures 6.10, 6.11, and 6.12 provide comparisons of the stress invariants with

different number of elements along the column length in X_3 at different heights from the bottom surface in Fig.6.8. Definitions of these stress invariant measures are

$$\begin{aligned} ||\mathrm{dev}\boldsymbol{\sigma}|| &= \sqrt{(\mathrm{dev}\sigma_{ij})(\mathrm{dev}\sigma_{ij})} \\ ||\mathrm{dev}\left(\boldsymbol{s}-\boldsymbol{\sigma}\right)|| &= \sqrt{[\mathrm{dev}(s_{ij}-\sigma_{ij})][\mathrm{dev}(s_{ij}-\sigma_{ij})]} \\ ||\mathrm{dev}\boldsymbol{m}|| &= \sqrt{(\mathrm{dev}m_{ijk})(\mathrm{dev}m_{ijk})} \\ \mathrm{tr}\boldsymbol{\sigma} &= \sigma_{kk} \\ \mathrm{tr}\left(\boldsymbol{s}-\boldsymbol{\sigma}\right) &= (s_{kk}-\sigma_{kk}) \\ ||\mathrm{tr}\boldsymbol{m}|| &= \sqrt{m_{aak}m_{bbk}} \end{aligned} \tag{6.9}$$

where

$$\begin{aligned} \mathrm{dev}\sigma_{ij} &= \sigma_{ij} - \left(\frac{1}{3}\sigma_{kk}\right)\delta_{ij} \\ \mathrm{dev}\left(s_{ij}-\sigma_{ij}\right) &= \left(s_{ij}-\sigma_{ij}\right) - \left(\frac{1}{3}\left(s_{kk}-\sigma_{kk}\right)\right)\delta_{ij} \\ \mathrm{dev}m_{ijk} &= m_{ijk} - \frac{1}{3}\delta_{ij}m_{aak} \end{aligned} \tag{6.10}$$

Note that based on its definition, $\mathrm{dev}m_{ijk}$ is traceless:

$$\mathrm{trace}(\mathrm{dev}m_{ijk}) = \mathrm{dev}m_{iik} = m_{iik} - \frac{1}{3}(3)m_{aak} = 0 \tag{6.11}$$

Recall the definition of the higher order stress m_{ijk} (Eringen, 1999), equation (2.1.5):

$$m_{ijk}n_i da \overset{\mathrm{def}}{=} \int_{da} \sigma'_{ij}\xi_k n'_i da' \tag{6.12}$$

where n_i is the unit normal vector to macro-element differential area da in the current configuration $\mathcal{B}$, σ'_{ij} is the micro-element symmetric Cauchy stress, ξ_k is the relative position vector of the micro-element centroid with respect to the macro-element centroid, n'_i is the unit normal vector to micro-element differential area da' in the current configuration $\mathcal{B}$. Based on the definition of m_{ijk} through (6.12), since we plan to implement a pressure-sensitive micromorphic elasto-plasticity model (Regueiro, 2009), we need a "higher order

mean-couple-stress" and "deviatoric stress" definition. Equation (6.10), based on (6.12), satisfies this definition, where we see the micro-element mean Cauchy stress is $p' = \sigma'_{aa}/3$, such that the higher order mean-couple-stress is $p_k = m_{aak}/3$.

In Fig.6.9, for all the invariants, the effect of increasing length scale ℓ_7 is what we expect for all plots except Fig.6.9(a): as the length scale increases, the stress response is higher, which is consistent with a larger value of $\tau_7 = \tilde{\tau}_7 \ell_7^2$. This is a compression problem with shear, where only $\Phi^h_{33} \neq 0$, but we will see for the cubical microindentation test next that when three-dimensional stress effects are enabled, the trends are not as simple to interpret.

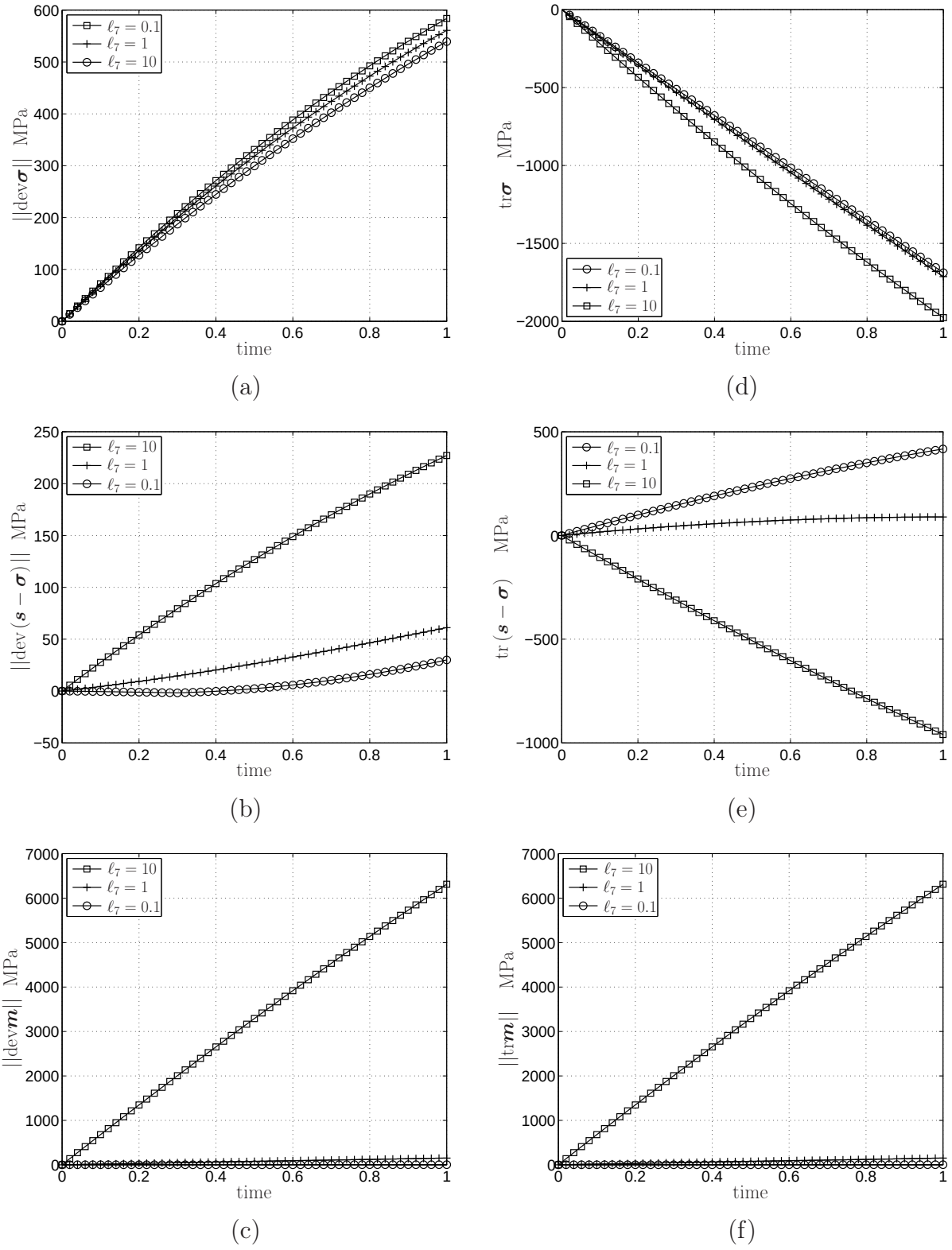

Figure 6.9: For 32 element column compression example and different length scale values of ℓ_7, a comparison of deviatoric stress invariants (a) $||\mathrm{dev}\boldsymbol{\sigma}||$, (b) $||\mathrm{dev}(\boldsymbol{s}-\boldsymbol{\sigma})||$, and (c) $||\mathrm{dev}\boldsymbol{m}||$, and also the first stress invariants (d) $\mathrm{tr}\boldsymbol{\sigma}$, (e) $\mathrm{tr}(\boldsymbol{s}-\boldsymbol{\sigma})$, and (f) $||\mathrm{tr}\boldsymbol{m}||$ at $X_3 = 2.773\mu m$.

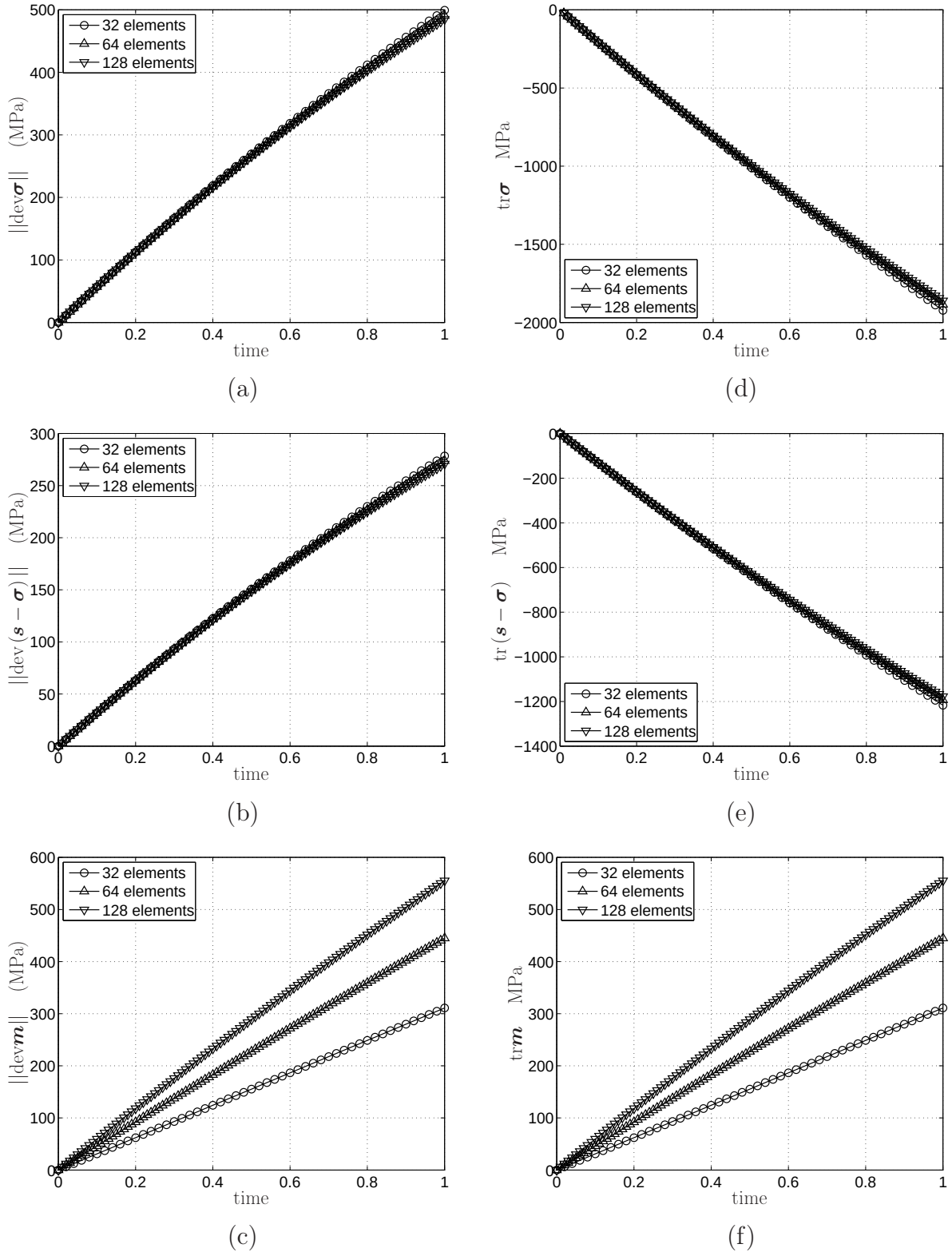

Figure 6.10: Comparison of stress invariants at $X_3 = 0$ with different number of elements in the X_3 direction for $\ell_7 = 1\mu m$.

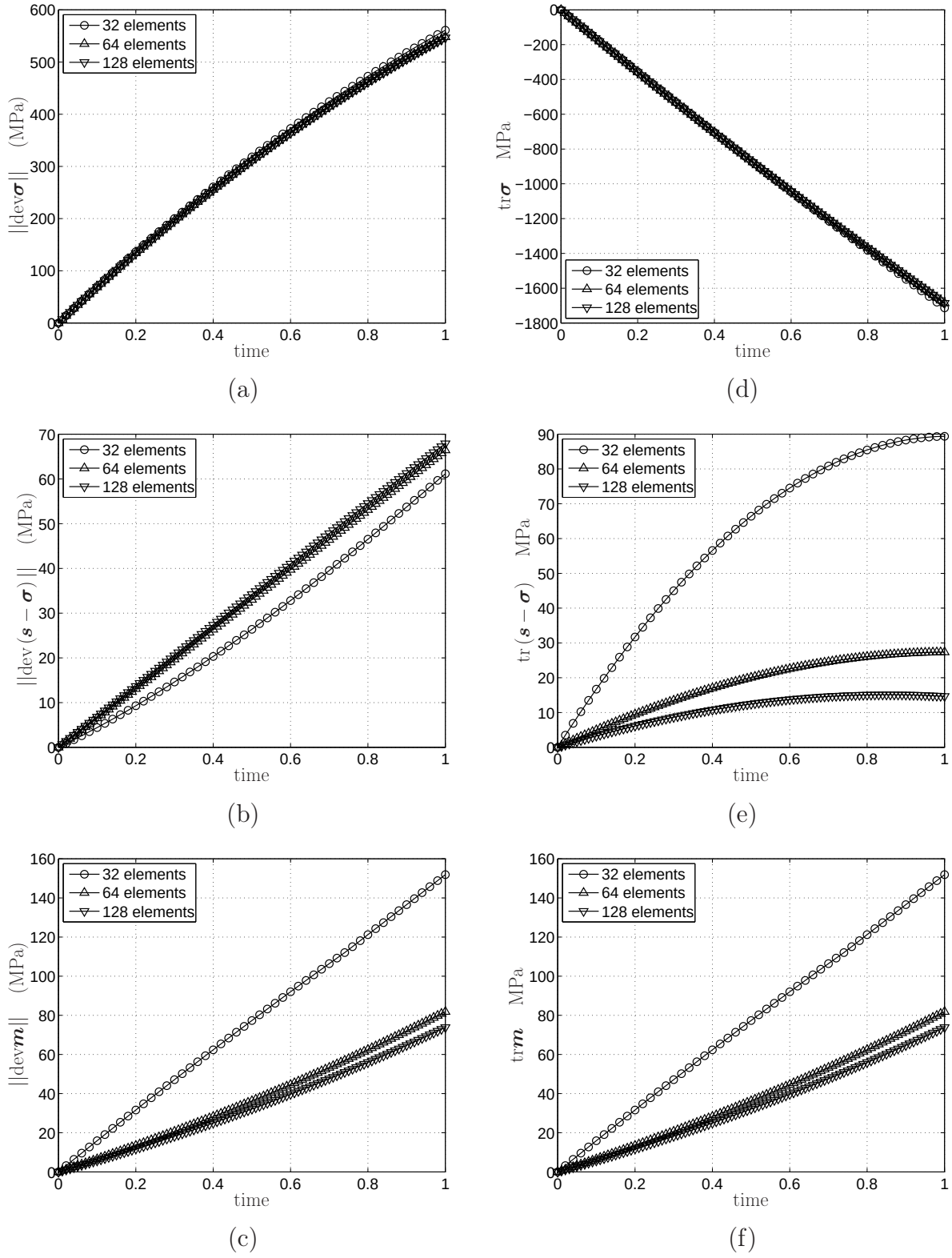

Figure 6.11: Comparison of stress invariants at $X_3 = 3.125$ μm with different number of elements in the X_3 direction for $\ell_7 = 1\mu m$.

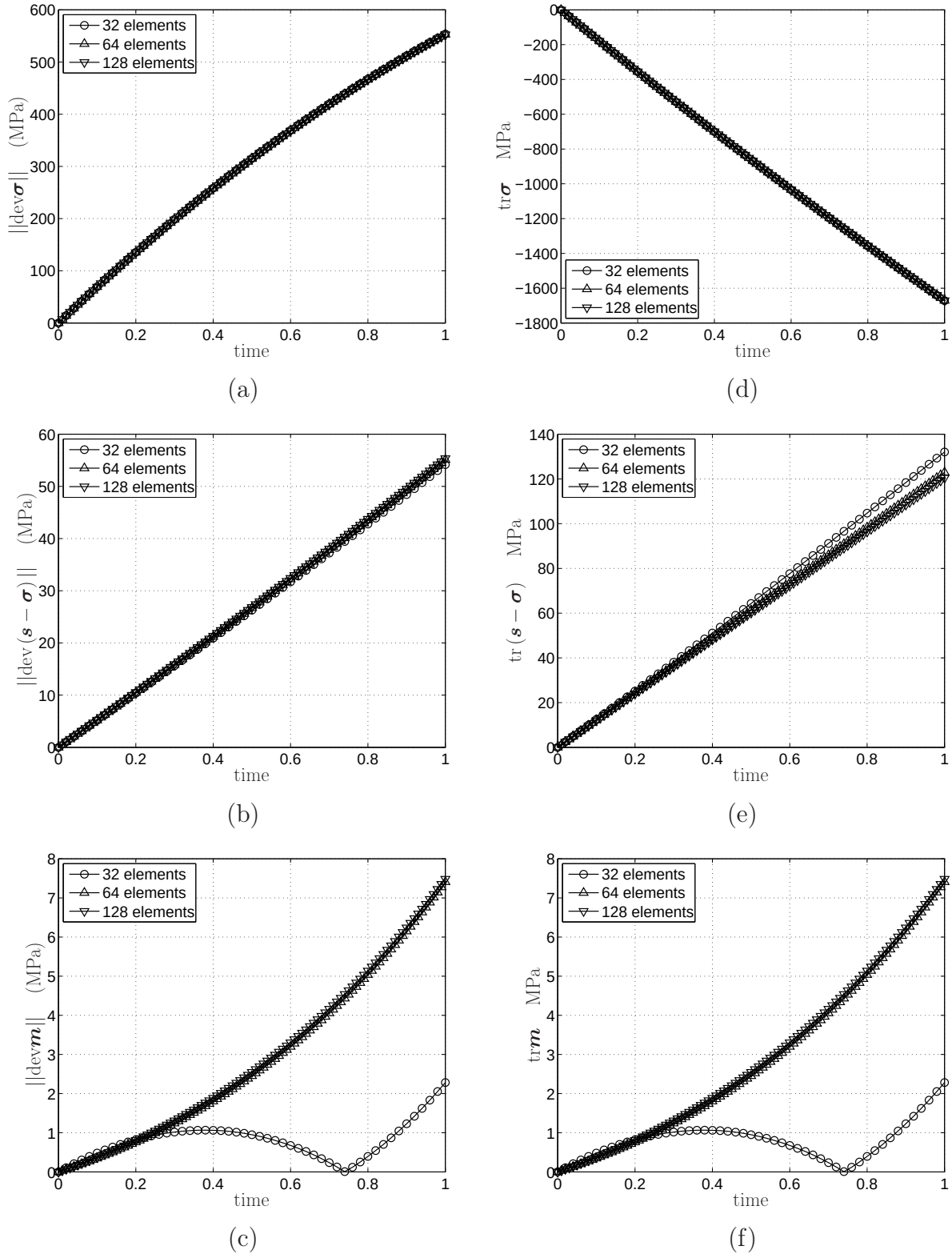

Figure 6.12: Comparison of stress invariants at $X_3 = 6.25$ μm with different number of elements in the X_3 direction for $\ell_7 = 1\mu m$.

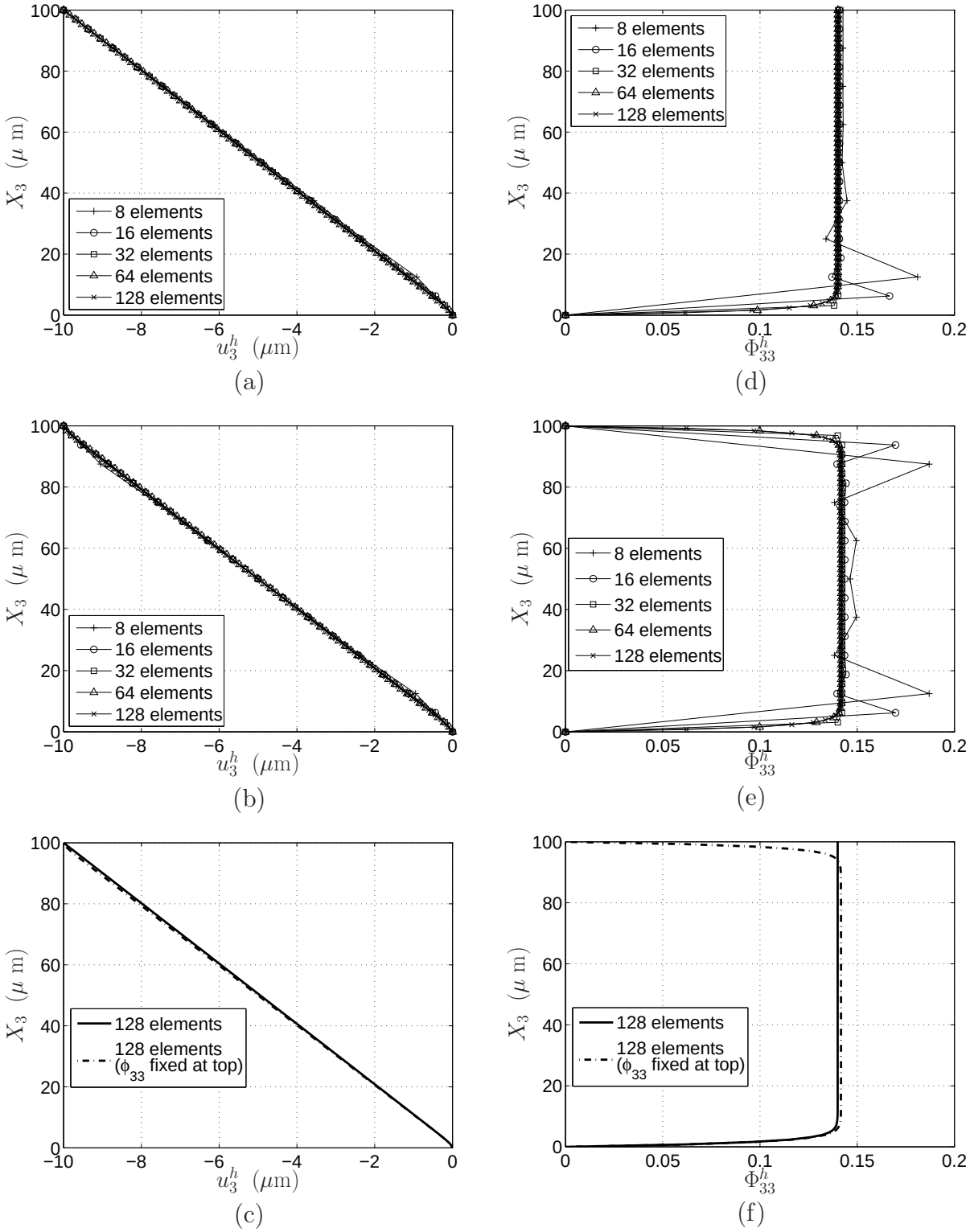

Figure 6.13: Comparison of u_3^h and Φ_{33}^h profiles versus X_3, for different number of elements in the X_3 direction for $\ell_7 = 1\mu m$.

As evident in Figs.6.10-6.12, as the column mesh in Fig.6.8 is refined in the X_3 direction, the results converge to a unique solution. In Fig.6.10(c) and (f), the convergence is not so obvious because these higher order stress $\boldsymbol{m}$ invariants are plotted at the boundary node at $X_3 = 0$ where the gradient $\boldsymbol{\nabla\Phi}^h$ is highest. In Fig.6.13, the convergence trend is more clear. Figure 6.13 shows comparisons of u_3^h and Φ_{33}^h profiles with different number of elements together with one additional boundary condition for Φ_{33}^h which is fixed at $X_3 = 100\mu m$. It is clear that, for 8 elements and 16 elements meshes, there are oscillations at the proximity of the boundary where we have high gradients in Φ_{33}^h. Although this behavior seems to be related to a coarse mesh, this influence of the boundary is seen when $\ell_7 = 1\mu m$. Figure 6.14 (a) shows that the oscillations disappear with a higher length scale $\ell_7 = 10\mu m$.

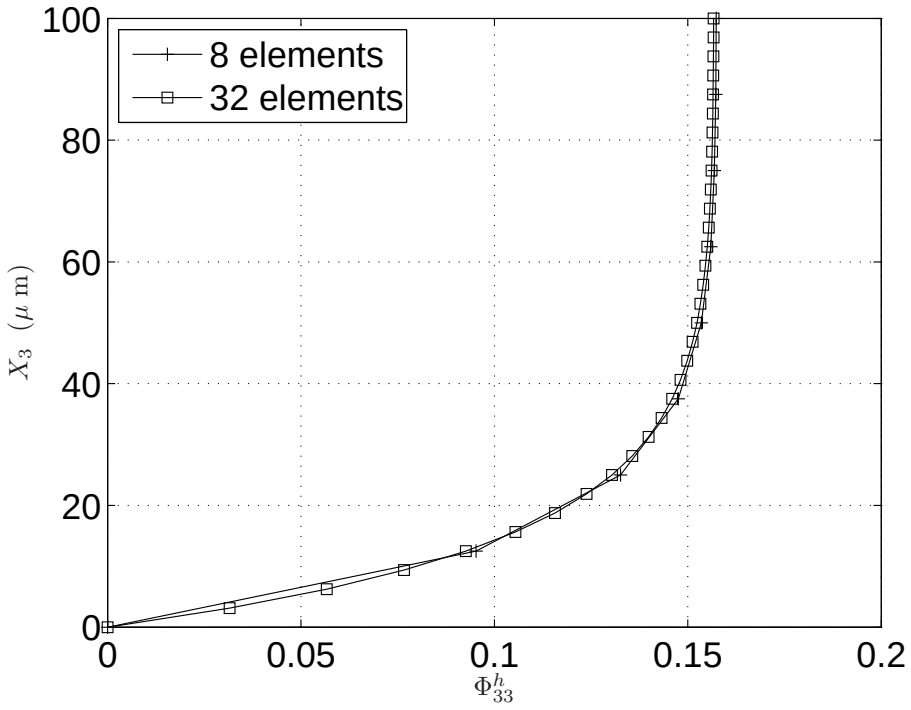

Figure 6.14: Comparison of Φ_{33}^h profile: different number of elements with $\ell_7 = 10\mu m$.

6.2.5 Comparison of full and quarter microindentation to evaluate boundary conditions on $\boldsymbol{\Phi}^h$

Before conducting the microindentation simulations in Section 6.2.6, we investigate the boundary condition on $\boldsymbol{\Phi}^h$. For a coarse mesh indentation considering the full $4\,(\mu\text{m})^2$ indentation area in Fig.6.15(a) and one quarter area $1\,(\mu\text{m})^2$ of the indentation area in Fig.6.15(b), we compare the results in Table 6.3 for the node at the center of the punch area indicated in Fig.6.15. We see that displacement $\boldsymbol{u}^h$ boundary conditions between full and quarter indent areas match (i.e., zero in X_1 and X_2 directions at the center node), whereas the BCs for micro-displacement tensor $\boldsymbol{\Phi}^h$ do not match (i.e., $\Phi^h_{11} = \Phi^h_{22} = 0$ for quarter indent area, and $\Phi^h_{11} = \Phi^h_{22} = 0.72956$ for full indent area). Thus the microindentation simulations in Section 6.2.6 are what we will call **corner indentation** simulations rather than assuming quarter symmetry, which does not hold for the BCs we choose in Fig.6.16 for $\boldsymbol{\Phi}^h$.

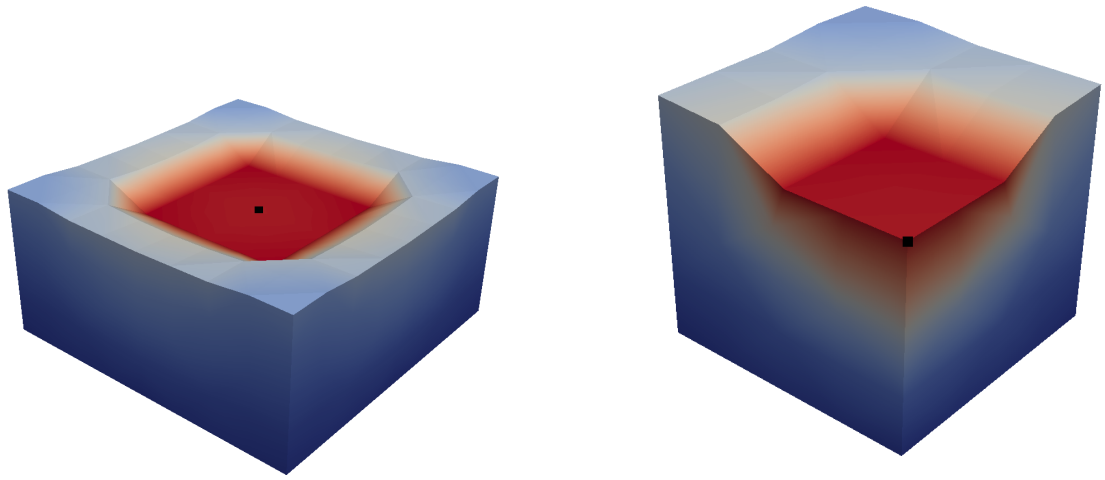

(a) (b)

Figure 6.15: (a) Whole domain is considered with a $4\,(\mu\text{m})^2$ square indent area with a magnitude of $u_3 = -0.5$ μm at the middle of the top surface of the cube domain with dimensions of $4\times4\times2$ μm, (b) quarter model of the whole domain is considered with a $1\,(\mu\text{m})^2$ square indent area with the same magnitude on the corner of the top surface of the cube domain with dimensions of $2\times2\times2$ μm. Results are reported in Table 6.3 at the nodes marked by black squares, respectively, at the center of the indent area of the whole domain and at the corner of the indent area of the quarter domain.

Table 6.3: Comparison of values at nodes indicated by black squares in Fig.6.15 for full and quarter indent areas. Quarter symmetry holds for $\boldsymbol{u}^h$ but not for Φ^h.

	quarter indent area	full indent area
Φ^h_{11}	0	0.72956
Φ^h_{22}	0	0.72956
Φ^h_{33}	0.37	0.35649
u^h_1	0	0
u^h_2	0	0
u^h_3	$-0.5\mu m$	$-0.5\mu m$

6.2.6 Finite strain cubical corner microindentation with length scale effects

This example is a three dimensional corner square microindentation problem to demonstrate the three dimensionality of the finite element implementation as well as the elastic length scale effects through the higher order stress tensor $\boldsymbol{m}$ when three-dimensional stress effects are enabled. It is a 100μm cube with 25μm square area loaded with downward prescribed displacement $u_3 = -10\mu$m (see Fig.6.16). Note that all simulations were run to finite strains ($\approx 10\%$) where the assumption that elastic strains are small in equations (2.113) and (2.114) (but rotations can still be large) would be invalid. But this implementation will eventually be used as a precursor to a finite strain elasto-plastic micromorphic model implementation, where plastic strains can be large for such materials like soil, rock, concrete, metals, etc., where elastic strains are typically small. We assumed that only three micro-displacement tensor components Φ^h_{11}, Φ^h_{22}, and Φ^h_{33} are free, and all the shear terms $\Phi^h_{iI} = 0\,(i \neq I)$. The boundary conditions on micro-displacement tensor are chosen as: $\Phi^h_{11} = 0$ at $X_1 = 0\,\text{and}\,100\mu m$, $\Phi^h_{22} = 0$ at $X_2 = 0\,\text{and}\,100\mu m$, and $\Phi^h_{33} = 0$ at $X_3 = 0$. Micromorphic elastic parameters given in Tables 6.1 and 6.2 were used in the analysis. An 8*8*8=512 Q27P8 element mesh is used.

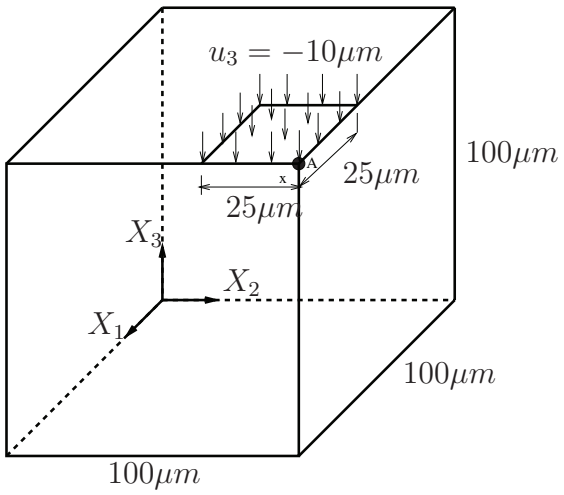

Figure 6.16: Cubical microindentation example geometry and loading configuration.

Figure 6.17 shows the variation over quasi-static loading time and comparison for various length scale values ℓ_7 of the deviatoric stress invariant measures $||\text{dev}\boldsymbol{\sigma}||$, $||\text{dev}\,(\boldsymbol{s} - \boldsymbol{\sigma})\,||$, and $||\text{dev}\boldsymbol{m}||$, and first stress invariant measures $\text{tr}\boldsymbol{\sigma}$, $\text{tr}\,(\boldsymbol{s} - \boldsymbol{\sigma})$, and $||\text{tr}\boldsymbol{m}||$ at the Gauss point near node A underneath the indent area.

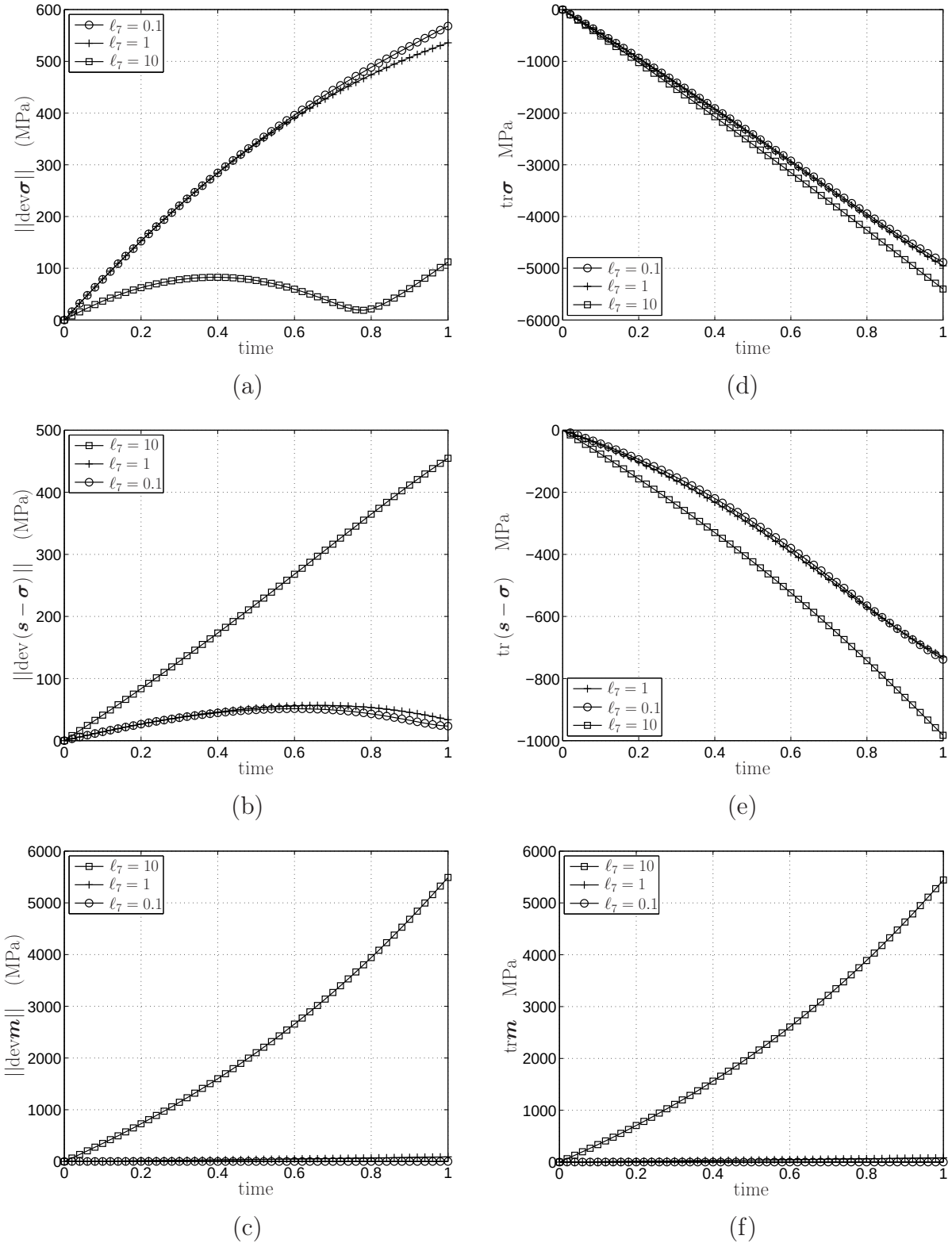

Figure 6.17: For corner punch problem and different length scale values of ℓ_7, a comparison of the deviatoric stress invariants (a) $||\mathrm{dev}\boldsymbol{\sigma}||$, (b) $||\mathrm{dev}(\boldsymbol{s}-\boldsymbol{\sigma})||$, and (c) $||\mathrm{dev}\boldsymbol{m}||$, also the first stress invariants (d) $\mathrm{tr}\boldsymbol{\sigma}$, (e) $\mathrm{tr}(\boldsymbol{s}-\boldsymbol{\sigma})$, and (f) $||\mathrm{tr}\boldsymbol{m}||$ at Gauss point near node A under the indent area.

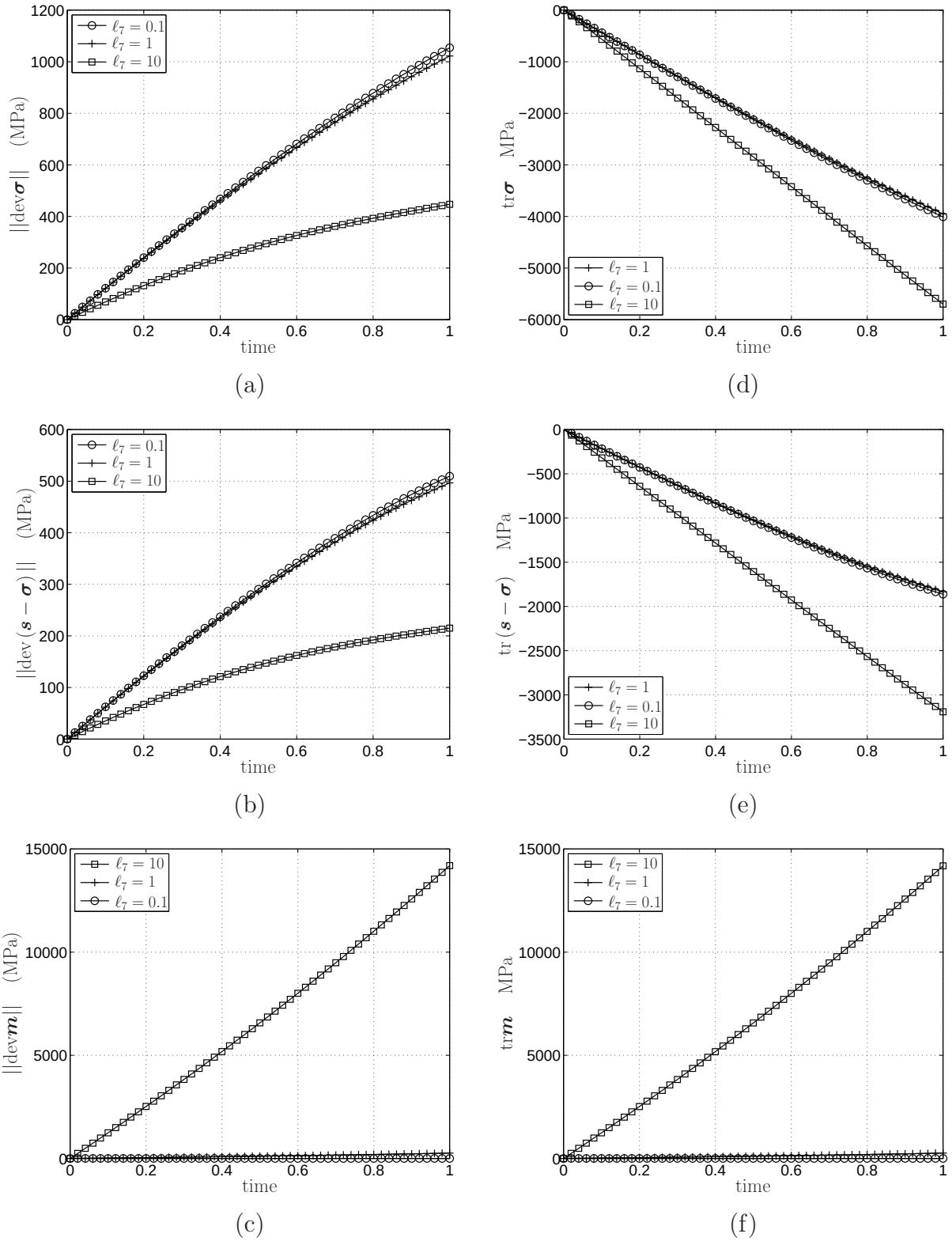

Figure 6.18: For the corner punch problem with $\Phi^h_{33} = 0$ under the punch area, and different length scale values of ℓ_7, a comparison of the deviatoric stress invariants (a) $||\mathrm{dev}\boldsymbol{\sigma}||$, (b) $||\mathrm{dev}(\boldsymbol{s}-\boldsymbol{\sigma})||$, and (c) $||\mathrm{dev}\boldsymbol{m}||$, also the first stress invariants (d) $\mathrm{tr}\boldsymbol{\sigma}$, (e) $\mathrm{tr}(\boldsymbol{s}-\boldsymbol{\sigma})$, and (f) $||\mathrm{tr}\boldsymbol{m}||$ at Gauss point near node A under the indent area.

Figure 6.17, which is plotted for the Gauss point nearest node A under the corner of the square indent area, shows that the highest values for the deviatoric stress invariant $||\text{dev}\boldsymbol{\sigma}||$ is for the smallest length scale value $\ell_7 = 0.1\mu$m, whereas the next highest is $\ell_7 = 1\mu$m, and the lowest values for $\ell_7 = 10\mu$m. Because the variation over loading time is not as smooth as for the column compression result in Fig.6.9(a) (there is an apparent oscillation), the fact that the $\ell_7 = 0.1\mu$m result is more higher than with $\ell_7 = 1\mu$m and $\ell_7 = 10\mu$m can be attributed to the three-dimensionality of the simulation, development of shear at the indent area, and possibly the resolution of the mesh. Conversely, in Fig.6.17(d), the first stress invariant $\text{tr}\boldsymbol{\sigma}$ shows a consistently higher stress values in compression result with increasing length scale ℓ_7. In Figs.6.17(b) and (e), for the relative stress $\boldsymbol{s} - \boldsymbol{\sigma}$, the invariants show trends with varying length scale ℓ_7 that are consistent: higher stress values with increasing length scale ℓ_7. Again, this can be attributed to the three-dimensionality of the problem, an effect that is oftentimes missed in many strain-gradient elasticity models formulated only for 1D and 2D problems. This effect comes in naturally through the 3D micromorphic FE model. The question then becomes how to fit these elastic parameters (and in the future, plastic parameters) to experimental data to have physically meaningful results. We envision using multiscale techniques, whereby an underlying grain-scale model (like the discrete element method (Cundall and Strack, 1979)) is used to upscale to the micromorphic continuum model through an overlapping region (Regueiro and Yan, 2011). In Figs.6.17(c) and (f), for the higher order couple stress $\boldsymbol{m}$, the invariant trends follow a higher stress values with increasing length scale, a result that is likely due to the decoupling of $\boldsymbol{m}$ from $\boldsymbol{\sigma}$ and $\boldsymbol{s} - \boldsymbol{\sigma}$ through the constitutive equations (2.113)-(2.115); note that the stresses are still coupled through the balance of linear momentum and balance of first moment of momentum. The stress state and deformation is three dimensional, so unlike the previous simpler example of column compression, the combination of deformation and micromorphic elastic parameters can lead to unexpected trends in stress.

In Fig.6.18, the trends for increasing length scale ℓ_7 are similar as in Fig.6.17, except

in Fig.6.18(b), which shows an opposite trend: smallest ℓ_7 leads to the highest values of $||\text{dev}\,(\boldsymbol{s}-\boldsymbol{\sigma})\,||$ result. Because the results in Figs.6.18 and 6.17 are plotted at a Gauss point beneath the punch area, the boundary condition $\Phi^h_{33}=0$ under the punch area influences the results reported in Fig.6.18 at this Gauss point more significantly than at a Gauss point further from the punch area.

These results signify the importance of the selection of elastic micromorphic length scale parameters ℓ_i in addition to micro-displacement tensor $\boldsymbol{\Phi}^h$ boundary conditions.

The stress invariant measures $||\text{dev}\boldsymbol{\sigma}||$, $||\text{dev}\,(\boldsymbol{s}-\boldsymbol{\sigma})\,||$, $||\text{dev}\boldsymbol{m}||$, $\text{tr}\boldsymbol{\sigma}$, $\text{tr}\,(\boldsymbol{s}-\boldsymbol{\sigma})$, and $||\text{tr}\boldsymbol{m}||$ used in this work will provide a basis for a future implementation of the three dimensional micromorphic finite strain elasto-plastic pressure sensitive model in which three yield functions are defined for macro-scale, micro-scale, and micro-scale gradient plasticity concept (Regueiro, 2009, 2010).

6.2.7 Boundary condition effect on uniaxial cube compression

This example is a one element 2m cube uniaxial stress in compression analysis, allowing one free micro-displacement tensor degree of freedom Φ^h_{33} with various combinations of micromorphic isotropic elastic material parameters. As mentioned in Section 6.2.1, the numerical values may be chosen by a set of relations between Lamé parameters λ^* and μ^* and the other micromorphic elastic parameters. The following set of relations satisfy the positive definiteness of strain energy for specific values of $\lambda^*=39$ MPa and $\mu^*=12$ MPa for a geomaterial as:

$$\begin{array}{rlrlllll}
\tau_1 & \approx 0.111\lambda^* L_c^2 & \tau_7 & \approx 0.670\mu^* L_c^2 & \lambda & \approx 0.7435\lambda^* & \mu & \approx 0.583\mu^* \\
\tau_2=\tau_3 & \approx 0.185\lambda^* L_c^2 & \tau_8=\tau_9 & \approx 0.495\mu^* L_c^2 & \tau & \approx 0.256\lambda^* & \nu & \approx 0.667\mu^* \\
\tau_4 & \approx 0.204\lambda^* L_c^2 & \tau_{10} & \approx 0.408\mu^* L_c^2 & \eta & \approx 1.53\lambda^* & \sigma & \approx 0.4167\mu^* \\
\tau_5 & \approx 0.1\lambda^* L_c^2 & \tau_{11} & \approx 0.495\mu^* L_c^2 & & & \kappa & \approx 0.833\mu^* \\
\tau_6 & \approx 0.256\lambda^* L_c^2 & & & & & &
\end{array} \tag{6.13}$$

As mentioned before, we assume in this example and the next following two examples that only one length scale L_c (not ℓ_7) exists that is associated with the elastic parameter τ_7.

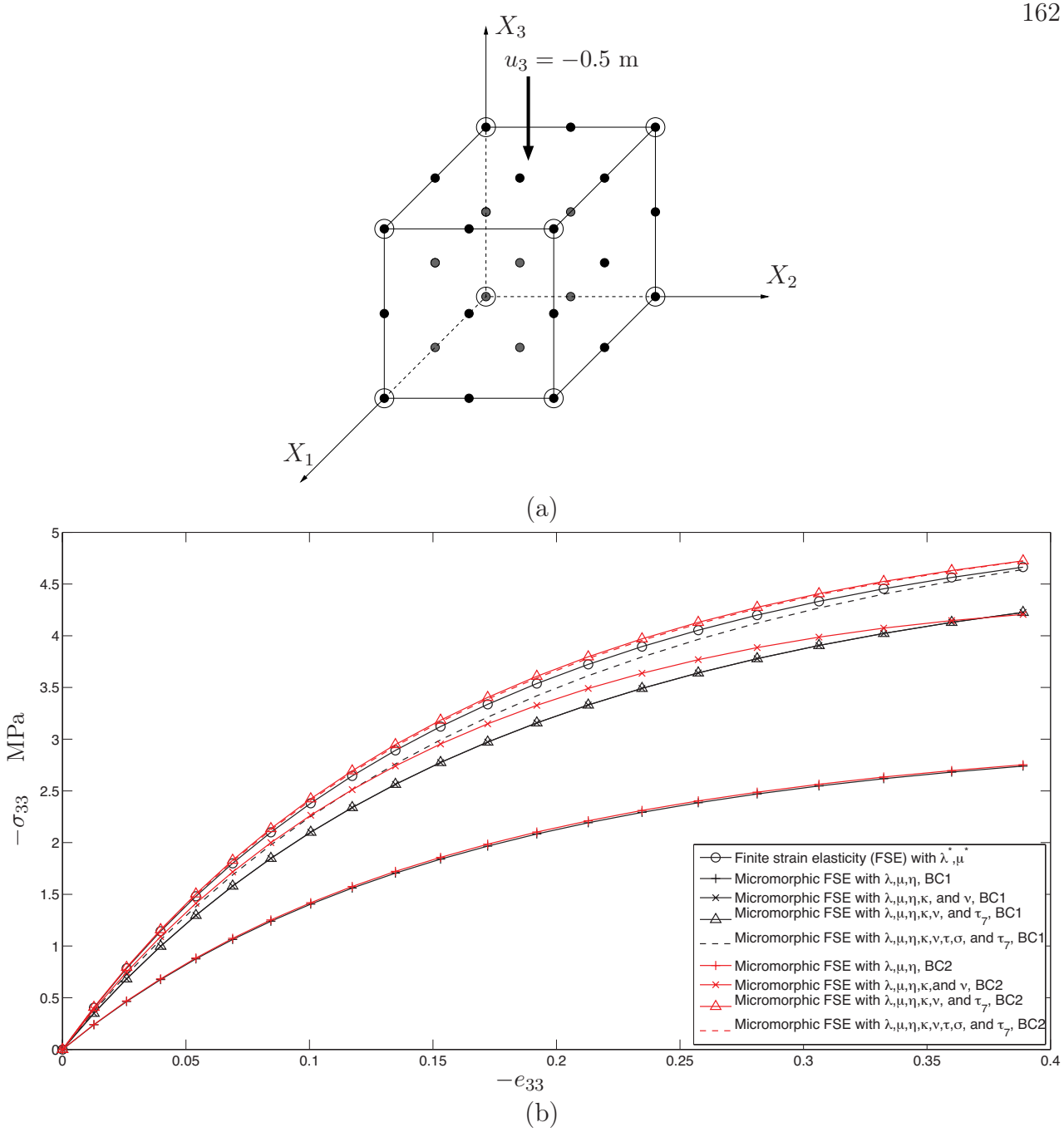

Figure 6.19: (a) 2x2x2 m cube compression example with a one element mesh. (b) Comparison of Cauchy stress tensor component σ_{33} obtained by standard finite strain elasticity (FSE) and finite strain micromorphic elasticity with various combinations of micromorphic elastic material parameters as well as different BCs.

Numerical values for the micromorphic elastic material parameters are then calculated as

$$\lambda = 29.10^3 \text{ kPa} \quad \mu = 7.10^3 \text{ kPa} \quad \eta = 60.10^3 \text{ kPa}$$
$$\nu = 8.10^3 \text{ kPa} \quad \kappa = 10.10^3 \text{ kPa} \quad \tau = 10.10^3 \text{ kPa} \quad \sigma = 5.10^3 \text{ kPa} \tag{6.14}$$

Note that to simplify the computations from the set of relations which satisfy the positive definiteness of strain energy expressed in (6.13), we take

$$\tau_1 = \tau_2 = \tau_3 = \tau_4 = \tau_5 = \tau_6 = \tau_8 = \tau_9 = \tau_{10} = \tau_{11} = 0 \ , \ \tau_7 = 8.10^3 \text{ kPa.m}^2 \tag{6.15}$$

where the characteristic length is assumed to be $L_c = 1$ m.

Figure 6.19(a) shows the compression example 1 element mesh. The displacement boundary condition $u_3 = -0.5$ m is applied to the top surface in the negative X_3 direction. The displacement boundary conditions were chosen to constrain the rigid body motions as: $u_1 = 0$ on $-X_1$ face, $u_2 = 0$ on $-X_2$ face, and $u_3 = 0$ on $-X_3$ face. We considered two different sets of boundary conditions for $\mathbf{\Phi}^h$: (1) all the micro-displacement tensor components Φ^h_{iI} are set $= 0$ except the component Φ^h_{33} in the X_3 direction as boundary condition type 1 (BC1); (2) Φ^h_{33} is free on the top surface of the cube ($X_3 = 2$m), and $\Phi^h_{33} = 0$ at $X_3 = 0$ for boundary condition type 2 (BC2). The different BCs will show the effect of the gradient of Φ^h_{33} in the X_3 direction. Another example in Fig.6.20 illustrates a boundary layer effect.

Figure 6.19(b) is the comparison of Cauchy stress tensor component σ_{33} obtained by standard finite strain elasticity (FSE) with the same stress component in micromorphic finite strain elasticity calculated by equations (2.87) and (2.113). Figure 6.19(b) shows that the micromorphic approach may result in lower stress for BC1 as compared to BC2. In Fig.6.19(b), for BC1, all the Φ^h_{33} are the same which, in turn, gives zero gradient of micro-displacement tensor $\mathbf{\nabla \Phi} = \mathbf{0}$ between the top and the bottom surfaces of the cube. For BC2, there is a gradient of Φ^h_{33} between the top and bottom surfaces of the cube element that generates a non-zero higher order stress tensor $\boldsymbol{m}$ which results in different relative

stress $\boldsymbol{s} - \boldsymbol{\sigma}$, and different Cauchy stress $\boldsymbol{\sigma}$ in the first moment of momentum balance due to the coupling between the two balance equations. Figure 6.19(b) shows an increase in σ_{33} by including additional parameters $\eta, \kappa, \nu, \tau,$ and σ where for BC1, no contribution from the parameter τ_7 is expected due to zero gradient of $\boldsymbol{\Phi}$.

6.2.8 Boundary condition effect on finite strain column compression

In this example, we consider a similar geometry and boundary conditions with that of the previous column example but with different dimensions and parameters. The effect of boundary conditions on the micro-displacement tensor $\mathbf{\Phi}$ may be presented more clearly in this example in which a 10m column with a 1×1 m^2 cross section is loaded on the $+X_3$ surface (top surface) with a prescribed displacement, $u_3 = -1$m. Similar boundary conditions to the one element cube example (BC1 and BC2) are employed, except displacements in X_1 and X_2 directions are zero. Figure 6.20(a) shows the boundary effect on micro-displacement tensor where we have slightly lower values of Φ^h_{33} near the bottom surface that is causing a gradient in micro-displacement tensor which results in different values of the higher order stress tensor $\boldsymbol{m}$ at different heights of the column as shown in Figs.6.20 (c) and (d). We see higher values for invariants of the higher order stress tensor at locations where we have a higher gradient of Φ^h_{33} near $X_3 = 0$ (see Fig.6.20(b)) which is expected because of the definition of the higher order stress tensor in the reference configuration, for this specific example, $\boldsymbol{M} = \tau_7\mathbf{\Gamma}$ where $\mathbf{\Gamma} = \boldsymbol{F}^T\boldsymbol{\nabla\chi}$. We do not see a similar behavior for BC1 in which $\boldsymbol{\nabla\Phi} = \mathbf{0}$, that makes the higher order stress tensor zero; therefore, for BC1, stress invariants given in Figs.6.20 (c), (d), (e), and (f) are the same at different heights along the column (i.e., the stress is uniform along the height of the column for BC1).

6.2.9 Boundary condition effect on square corner punch problem

The third example is a three dimensional square corner punch problem to demonstrate the three dimensionality of the finite element implementation.This example also considers a similar geometry and the same boundary conditions with that of the previous corner punch example; however, it uses different parameters as well as dimensions. It is a 10m cube with different $l_i\times l_i$m^2 square areas loaded with downward prescribed displacement $u_3 = -1$m (see Fig.6.21). We assumed that only three micro-displacement tensor components Φ^h_{11}, Φ^h_{22}, and

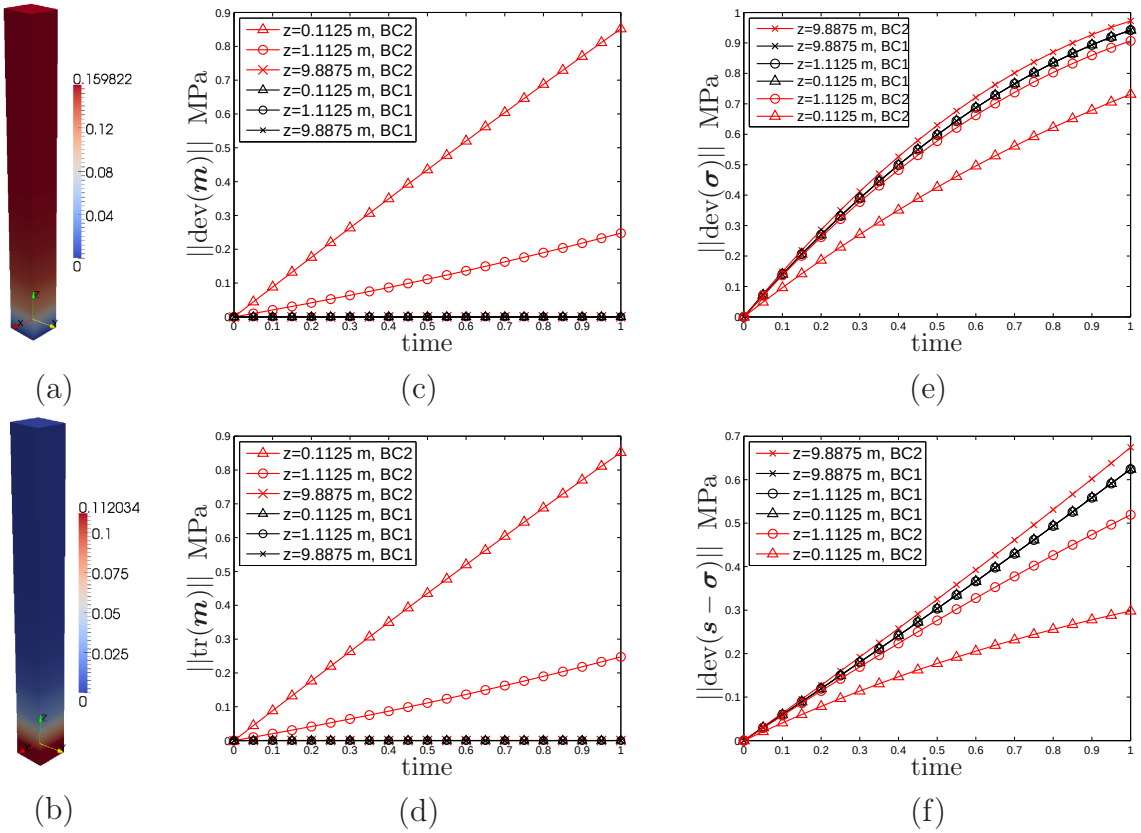

Figure 6.20: (a) Variation of norm of micro-displacement tensor, $||\boldsymbol{\Phi}||$, through the column height that shows the boundary effect on $\boldsymbol{\Phi}$, (b) norm of gradient of micro-displacement tensor, $||\boldsymbol{\nabla\Phi}||$, that generates non-zero $\boldsymbol{m}$, (c) norm of deviatoric higher order stress $||\mathrm{dev}\,(\boldsymbol{m})\,||$, which is largest where the highest gradient is observed, (d) norm of trace of $\boldsymbol{m}$, $||\mathrm{tr}\,(\boldsymbol{m})\,||$, (e) norm of deviatoric Cauchy stress, $||\mathrm{dev}\,(\boldsymbol{\sigma})\,||$, (f) norm of deviatoric relative stress, $||\mathrm{dev}\,(\boldsymbol{s}-\boldsymbol{\sigma})\,||$.

Φ^h_{33} are free, and all the other shear components $\Phi^h_{iI} = 0\,(i \neq I)$. The boundary conditions on micro-displacement tensor are chosen as: $\Phi^h_{11} = 0$ on $\pm X_1$ faces, $\Phi^h_{22} = 0$ on $\pm X_2$ faces, and $\Phi^h_{33} = 0$ on $-X_3$ face according to Fig.6.21. Elastic parameters given in (6.14) and (6.15) were used in the analysis.

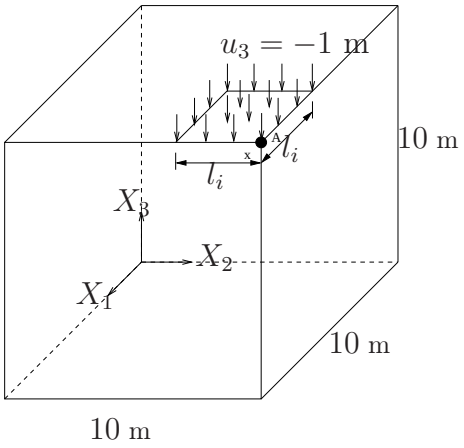

Punch area label (s_i)	**Punch area** $(l_i \times l_i$ in $m^2)$
s_1	3×3
s_2	2.5×2.5
s_3	2×2
s_4	1.5×1.5
s_5	1×1

Iteration number	**Relative error**
1^{st}	7.293805×10^{-02}
2^{nd}	5.935305×10^{-04}
3^{rd}	9.067026×10^{-07}
4^{th}	3.401397×10^{-09}
5^{th}	1.186506×10^{-11}

Figure 6.21: (left) 10x10x10 m cube with various square punch areas, s_i (top right), showing Gauss point as `X` near nodal point A where stresses are plotted in Fig.6.22. Convergence profile obtained by Newton-Raphson algorithm at the first time step for the largest punch area (bottom right). The time step is $\Delta t = 0.025$ and total time = 1. There are $10 * 10 * 10 = 1000$ mixed Q27P8 hexahedral elements in the mesh.

Figure 6.22 shows the variation over loading of the norms of deviatoric stress $||\text{dev}\boldsymbol{\sigma}||$, $||\text{dev}\,(\boldsymbol{s} - \boldsymbol{\sigma})\,||$, and $||\text{dev}\boldsymbol{m}||$ and traces $\text{tr}\boldsymbol{\sigma}$, $\text{tr}\,(\boldsymbol{s} - \boldsymbol{\sigma})$, and $||\text{tr}\boldsymbol{m}||$ for the unsymmetric Cauchy stress tensor $\boldsymbol{\sigma}$, the relative stress tensor $(\boldsymbol{s} - \boldsymbol{\sigma})$, and the higher order couple stress tensor $\boldsymbol{m}$, respectively, at the Gauss point near the node A underneath the punch area. Figures 6.22(a) and (b) show the deviatoric stress norms for various combinations of elastic parameters $\lambda, \mu, \eta, \kappa, \nu, \tau, \sigma, \tau_7$. Upon including terms with τ and σ, $||\text{dev}\boldsymbol{\sigma}||$ and $||\text{dev}\,(\boldsymbol{s} - \boldsymbol{\sigma})\,||$ decrease until the end of loading, when they increase. The stress state and deformation is three dimensional, so unlike the previous simple examples of uniaxial compression, the combination of deformation and micromorphic elastic parameters can lead to unexpected trends in stress. Upon introducing τ_7 to include the effect of higher order stress tensor $\boldsymbol{m}$, the relative deviatoric stress norm $||\text{dev}\,(\boldsymbol{s} - \boldsymbol{\sigma})\,||$ tends to decrease, whereas $||\text{dev}\boldsymbol{\sigma}||$

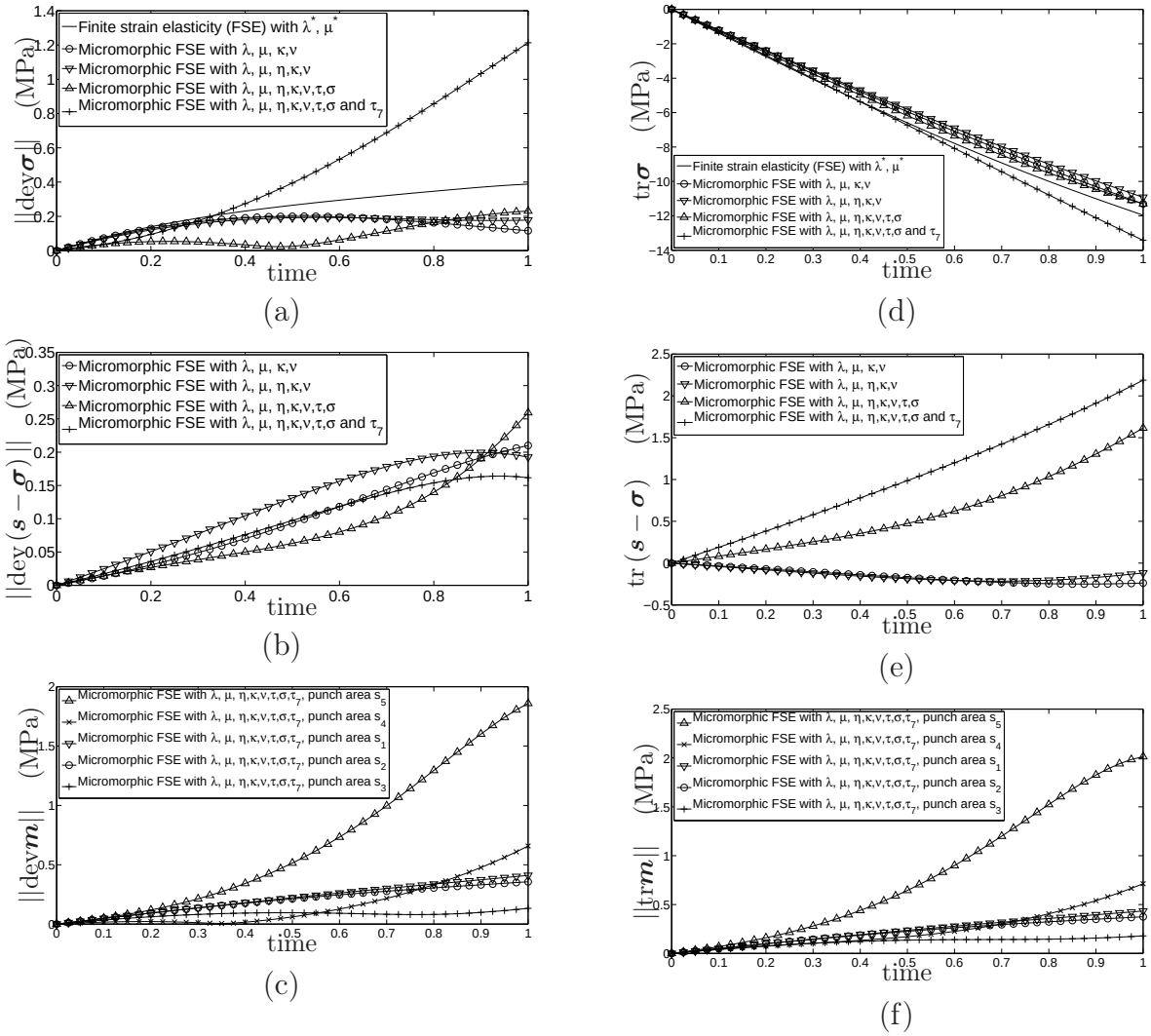

Figure 6.22: Deviatoric stress norms (a) $||\text{dev}\boldsymbol{\sigma}||$, (b) $||\text{dev}\,(\boldsymbol{s}-\boldsymbol{\sigma})\,||$, and (c) $||\text{dev}\boldsymbol{m}||$, and traces (d) $\text{tr}\boldsymbol{\sigma}$, (e) $\text{tr}\,(\boldsymbol{s}-\boldsymbol{\sigma})$, and norm of trace of $\boldsymbol{m}$ (f) $||\text{tr}\boldsymbol{m}||$ at the Gauss point closest to the node A under the punch area. Plots (c) and (f) show the results under five different punch areas.

increases. For $||\text{dev}\,(\boldsymbol{s}-\boldsymbol{\sigma})\,||$, this behavior is also observed in the column compression example: $||\text{dev}\,(\boldsymbol{s}-\boldsymbol{\sigma})\,||$ is smaller where higher gradient of Φ^h_{33} is seen that causes higher values of higher order stress tensor. Figures 6.22 (c) and (f) agree with results shown in Figs6.20 (c) and (d) regarding the effect of the gradient of micro-displacement tensor $\boldsymbol{\nabla\Phi}$ which leads to an increase in magnitude of higher order stress tensor $\boldsymbol{m}$ that in turn induces a change in relative and Cauchy stress tensors, $\boldsymbol{s}-\boldsymbol{\sigma}$ and $\boldsymbol{\sigma}$, respectively. Figures 6.22(d-f) show the first invariants of $\boldsymbol{\sigma}$, $(\boldsymbol{s}-\boldsymbol{\sigma})$, and $\boldsymbol{m}$. Figure 6.22(d) shows decreased first invari-

ant (increasing compressive stress, which is negative) for tr$\boldsymbol{\sigma}$, while tr$(\boldsymbol{s}-\boldsymbol{\sigma})$ in Fig.6.22(e) goes into tension when τ and σ are introduced. Because of the definition $||\text{tr}\boldsymbol{m}||$, it is always positive, a measure that must be changed to reflect the sign of tr$\boldsymbol{m}$ (tension or compression) when used in a pressure-sensitive plasticity model (Regueiro, 2009). Recall that only τ_7 is nonzero in (6.15), so that the higher order stress is $m_{klm} = \tau_7 F_{kK} F_{lL} \Gamma_{LMK} \chi_{mM}/J$, $\Gamma_{LMK} = F_{iL}\chi_{iM,K}$. The stress measures $||\text{dev}\boldsymbol{\sigma}||$, $||\text{dev}(\boldsymbol{s}-\boldsymbol{\sigma})||$, $||\text{dev}\boldsymbol{m}||$, tr$\boldsymbol{\sigma}$, tr$(\boldsymbol{s}-\boldsymbol{\sigma})$, and $||\text{tr}\boldsymbol{m}||$ used in this work will provide a basis for a future implementation of the three dimensional micromorphic finite strain elasto-plastic pressure sensitive model in which three yield functions are defined for macro-scale, micro-scale, and micro-scale gradient plasticity concept (Regueiro, 2009, 2010). Figures 6.22(a) and (d) also include the comparison of $||\text{dev}\boldsymbol{\sigma}||$ and tr$\boldsymbol{\sigma}$ for the standard finite strain symmetric Cauchy stress tensor with those of micromorphic finite strain unsymmetric Cauchy stress tensor with the various combinations of micromorphic isotropic elastic parameters. The micromorphic results, depending on the deformation history, show either higher values or lower values of stresses than standard elasticity. These results signify the importance of the selection of micromorphic elastic parameters in addition to micro-displacement tensor $\boldsymbol{\Phi}^h$ boundary conditions. The table in Fig.6.21 illustrates the global convergence profile at time the first time step for the large deformation punch problem, with parameters $\lambda, \mu, \eta, \kappa, \nu, \tau, \sigma$ and τ_7.

6.3 Conclusions from micromorphic finite strain elasticity FE implementation

We have implemented a three dimensional finite element model for finite deformation micromorphic materially linear isotropic elasticity into an open source finite element code Tahoe via two formulations: (i) direct finite elasticity, and (ii) rate form with semi-implicit time integration (ignoring the micromorphic contribution). This chapter compared the two implementations for standard elasticity (no micromorphic terms) for a small strain compression, large rotation example. The incremental rate form required many more time steps to

be accurate enough to handle the large rotation, whereas the direct implementation converged quickly and was accurate with relatively few time steps. The advantage to using the incremental rate formulation in the future will become apparent when implementing a micromorphic elasto-plasticity model (Regueiro, 2009) within an explicit time solution method, whether quasi-static or dynamic. For these solution methods, small time steps are used to ensure stability, and thus a semi-implicit time integration of a rate formulation of micromorphic elasto-plasticity would be more computationally efficient than a direct formulation. For implicit solution methods (Regueiro and Ebrahimi, 2010), however, the direct formulation is warranted and will give accurate results for larger time steps.

In the numerical examples, the effect of one of the elastic length scale parameters ℓ_7 is not so transparent. For some cases, increasing ℓ_7 leads to higher values of stresses, whereas in other cases increasing ℓ_7 can lead to lower values of stresses. Further study on using multiscale techniques to up-scale underlying grain-scale simulation results to the micromorphic continuum finite element implementation will likely help to interpret how the elastic micromorphic parameters are calibrated. Currently, these elastic parameters are chosen to satisfy positive definiteness of elastic strain energy following Smith1968.

With regard to nanomechanics, we envision relating the micromorphic elastic parameters of our 3D FE model to an underlying microstructural representative volume element (RVE) of a material (composed of grains and/or platelets) subjected to nanoindentation, such as nacre (Barthelat et al., 2006) or porous nanocomposite cementitious materials (Bobko and Ulm, 2008; Bobko et al., 2009).

This chapter also presented preliminary results of the model applied to three 3 dimensional examples. These results motivate further study of the meaning of certain micromorphic isotropic elastic parameters and boundary conditions on micro-displacement tensor $\mathbf{\Phi}$, as well as their influence on the simulations. In the numerical examples, micromorphic elastic parameters have been chosen to satisfy the positive definiteness of strain energy that obey the inequalities proposed by Smith (1968). Numerical values have been chosen in a similiar

way followed by Neff and Forest (2007) and Zervos et al. (2009). The boundary conditions on $\boldsymbol{\Phi}$ may not be explicitly anticipated from the physical problem as discussed by Eringen (1968a). In addition, we noticed from several analyses that $\boldsymbol{\Phi}$ boundary conditions together with the associated micromorphic elastic parameters play an important role in convergence of the nonlinear Newton-Raphson solution algorithm. Even for the comparatively simple example of uniaxial compression, specification of the boundary conditions on $\boldsymbol{\Phi}$ and the choice of micromorphic elastic parameters may affect the numerical results. A square corner punch problem demonstrated the full three dimensionality of the finite element implementation and some interesting trends in stress response at a Gauss point beneath the punch with various combinations of micromorphic elastic parameters, and the length scale effect for various punch areas.

Chapter 7

Extension of Finite Element Formulation and Implementation to Drucker-Prager Plasticity

This section shows the extension of finite strain micromorphic isotropic elasticity to Drucker-Prager plasticity formulated in the intermediate configuration $\bar{\mathcal{B}}$ (Fig. 1.6), assuming a multiplicative decomposition of deformation gradient $\boldsymbol{F}$ and micro-deformation tensor $\boldsymbol{\chi}$.

Kinematics, governing equations, and mapping of the balance of momenta equations, and thermodynamic equations into intermediate configuration, and outline of the theory to extend to plasticity were presented in Chapter 4. This section presents detailed formulation, developed and implemented, for Drucker-Prager plasticity with some numerical examples. Different than anticipated formulation given in Chapter 4, we also introduce another approach for yield function and plastic potential function formulations which involve combination of the stress tensors together with cohesion, friction angle, dilation angle, micro-scale cohesion, micro-scale friction angle, and micro-scale dilation angle. This will be called "combined plasticity" formulation to distinguish from the three-scale plasticity formulation in Chapter 4. We first present the three-scale plasticity formulation and implementation which was previously mentioned in Chapter 4. Then, we show combined plasticity formulation and implementation.

The three different scale yield functions presented in Chapter 4 express that plasticity may govern at these scales separately and/or at the same time. The first case may include the

plasticity in macro-scale which is already different than classical plasticity due to additional terms appearing in classical stress tensor. Here, we call it "macro-plasticity" which aims to express the micro-continuum effects considered, but plasticity governs at macro-scale which in turns mean only macro-scale plasticity function yielded. Similarly, if only the micro-scale plasticity function yields, it will be called "micro-plasticity". It may be the case that these two scales may yield at the same time which will require to solve for two different plastic multipliers solved in a coupled way that will be called "coupled plasticity".

7.0.1 Solving for macro-plastic multiplier locally for three scale approach

To solve for macro-scale plastic multiplier $\Delta\bar{\gamma}$, we solve the yield function at current time step t_{n+1}

$$\bar{F}_{n+1}\left(\Delta\bar{\gamma}_{n+1}\right) = 0, \Delta\bar{\gamma}^{\chi}_{n+1} = 0 \tag{7.1}$$

$$\bar{F}^{k} + \left(\frac{\partial \bar{F}}{\partial \Delta\bar{\gamma}}\right)^{k} \delta\left(\Delta\bar{\gamma}\right)^{k} = 0,\ \delta\left(\Delta\bar{\gamma}\right) = -\frac{\bar{F}^{k}}{\left(\frac{\partial \bar{F}}{\partial \Delta\bar{\gamma}}\right)^{k}} \tag{7.2}$$

$$\Delta\bar{\gamma}^{k+1} = \Delta\bar{\gamma}^{k} + \delta\left(\Delta\bar{\gamma}\right)^{k} \tag{7.3}$$

which from the discrete Kuhn-Tucker conditions, $\bar{F}_{n+1}\Delta\bar{\gamma}_{n+1} = 0 \Rightarrow \bar{F}_{n+1} = 0, \Delta\bar{\gamma}_{n+1} > 0$ for plasticity loading, where $(\bullet)^{k}$ denotes the previous iteration values and $(\bullet)^{k+1}$ denotes updated value. The subscript $(\bullet)_{n+1}$ is dropped for these terms assumed to be at the current time step t_{n+1}. To determine the local consistent tangent $\partial\bar{F}/\partial\Delta\bar{\gamma}$ where yield and plastic potential functions were defined in Section 3.4, we start to derive the derivative of each term with respect to $\Delta\bar{\gamma}$ as:

$$\frac{\partial \bar{\boldsymbol{S}}}{\partial \Delta\bar{\gamma}} = (\lambda+\tau)\,\mathrm{tr}\left(\frac{\partial \bar{\boldsymbol{E}}^e}{\partial \Delta\bar{\gamma}}\right)\mathbf{1} + 2\,(\mu+\sigma)\left(\frac{\partial \bar{\boldsymbol{E}}^e}{\partial \Delta\bar{\gamma}}\right) + \eta \mathrm{tr}\left(\frac{\partial \bar{\boldsymbol{\mathcal{E}}}^e}{\partial \Delta\bar{\gamma}}\right)\mathbf{1}$$
$$+ \kappa\left(\frac{\partial \bar{\boldsymbol{\mathcal{E}}}^e}{\partial \Delta\bar{\gamma}}\right) + \nu\left(\frac{\partial \bar{\boldsymbol{\mathcal{E}}}^e}{\partial \Delta\bar{\gamma}}\right)^T \tag{7.4}$$

$$\left(\frac{\partial \bar{\boldsymbol{E}}^e}{\partial \Delta\bar{\gamma}}\right) = \frac{1}{2}\left(\left(\frac{\partial \boldsymbol{F}^e}{\partial \Delta\bar{\gamma}}\right)^T \boldsymbol{F}^e + \boldsymbol{F}^{eT}\frac{\partial \boldsymbol{F}^e}{\partial \Delta\bar{\gamma}}\right) \tag{7.5}$$

$$\left(\frac{\partial \bar{\boldsymbol{\mathcal{E}}}^e}{\partial \Delta\bar{\gamma}}\right) = \left(\frac{\partial \boldsymbol{F}^e}{\partial \Delta\bar{\gamma}}\right)^T \boldsymbol{\chi}^e + \boldsymbol{F}^{eT}\left(\frac{\partial \boldsymbol{\chi}^e}{\partial \Delta\bar{\gamma}}\right) \tag{7.6}$$

$$\left(\frac{\partial \boldsymbol{F}^e}{\partial \Delta\bar{\gamma}}\right) = -\boldsymbol{F}^e\left(\frac{\partial \boldsymbol{F}^p}{\partial \Delta\bar{\gamma}}\right)\boldsymbol{F}^{p-1} \tag{7.7}$$

where

$$\left(\frac{\partial \boldsymbol{F}^p}{\partial \Delta\bar{\gamma}}\right) = \bar{\boldsymbol{C}}_n^{e-1}\left(\frac{\partial \bar{G}}{\partial \bar{\boldsymbol{S}}}\right)_n^T \boldsymbol{F}_n^p \tag{7.8}$$

and $\boldsymbol{F}^p$ is defined in Section 7.0.7. Here, we have only macro-scale plasticity; hence, $\partial\boldsymbol{\chi}^p/\partial\Delta\bar{\gamma} = \mathbf{0}$ and $\partial\boldsymbol{\chi}^e/\partial\Delta\bar{\gamma} = \mathbf{0}$. When we have micro-scale plasticity in combined plasticity approach, this condition will change. Furthermore, we have the derivatives

$$\frac{\partial ||\mathrm{dev}\bar{\boldsymbol{S}}||}{\partial \Delta\bar{\gamma}} = \frac{\partial \mathrm{dev}\bar{\boldsymbol{S}}}{\partial \Delta\bar{\gamma}} : \frac{\mathrm{dev}\boldsymbol{S}}{||\mathrm{dev}\bar{\boldsymbol{S}}||} \tag{7.9}$$

$$\frac{\partial \mathrm{dev}\bar{\boldsymbol{S}}}{\partial \Delta\bar{\gamma}} = \frac{\partial \bar{\boldsymbol{S}}}{\partial \Delta\bar{\gamma}} - \frac{\partial \bar{p}}{\partial \Delta\bar{\gamma}}\mathbf{1} \tag{7.10}$$

$$\frac{\partial \bar{p}}{\partial \Delta\bar{\gamma}} = \frac{1}{3}\left(\mathbf{1} : \frac{\partial \bar{\boldsymbol{S}}}{\partial \Delta\bar{\gamma}}\right) \tag{7.11}$$

$$\left(\frac{\partial \bar{G}}{\partial \bar{\boldsymbol{S}}}\right)_n = \left(\frac{\mathrm{dev}\bar{\boldsymbol{S}}}{||\mathrm{dev}\bar{\boldsymbol{S}}||}\right)_n + \frac{1}{3}B^\psi\mathbf{1} \tag{7.12}$$

$$\left(\frac{\partial \bar{c}}{\partial \Delta\bar{\gamma}}\right) = H^c h_n^c \tag{7.13}$$

where

$$h_n^c = -\left(\frac{\partial \bar{G}}{\partial \bar{c}}\right)_n = A^\psi \tag{7.14}$$

Then, the local consistent tangent can be found as:

$$\frac{\partial \bar{F}}{\partial \Delta\bar{\gamma}} = \frac{\partial ||\mathrm{dev}\bar{\boldsymbol{S}}||}{\partial \Delta\bar{\gamma}} - \left(A^\phi\frac{\partial \bar{c}}{\partial \Delta\bar{\gamma}} - B^\phi\frac{\partial \bar{p}}{\partial \Delta\bar{\gamma}}\right) \tag{7.15}$$

where all the terms in equation 7.15 were determined above.

7.0.2 Solving for micro-plastic multiplier locally for three scale approach

Similar to the previous section, we form the local consistent tangent $\partial \bar{F}^{\chi}/\partial \Delta\bar{\gamma}^{\chi}$ for micro-scale plasticity as

$$\bar{F}^{\chi}_{n+1}\left(\Delta\bar{\gamma}^{\chi}_{n+1}\right) = 0, \Delta\bar{\gamma}_{n+1} = 0 \tag{7.16}$$

$$\frac{\partial\left(\bar{\boldsymbol{\Sigma}} - \bar{\boldsymbol{S}}\right)}{\partial\Delta\bar{\gamma}^{\chi}} = (\eta - \tau)\,\mathrm{tr}\left(\frac{\partial\bar{\boldsymbol{\mathcal{E}}}^{e}}{\partial\Delta\bar{\gamma}^{\chi}}\right)\mathbf{1} + (\nu - \sigma)\left(\frac{\partial\bar{\boldsymbol{\mathcal{E}}}^{e}}{\partial\Delta\bar{\gamma}^{\chi}}\right) + (\kappa - \sigma)\left(\frac{\partial\bar{\boldsymbol{\mathcal{E}}}^{e}}{\partial\Delta\bar{\gamma}^{\chi}}\right) \tag{7.17}$$

If we have only micro-scale plasticity, we have $\partial\boldsymbol{F}^{e}/\partial\Delta\bar{\gamma} = \mathbf{0}$, and for separate scale plasticity $\partial\boldsymbol{F}^{e}/\partial\Delta\bar{\gamma}^{\chi} = \mathbf{0}$. Then,

$$\frac{\partial\bar{\boldsymbol{\mathcal{E}}}^{e}}{\partial\Delta\bar{\gamma}^{\chi}} = \boldsymbol{F}^{eT}\left(\frac{\partial\boldsymbol{\chi}^{e}}{\partial\Delta\bar{\gamma}^{\chi}}\right) \tag{7.18}$$

where

$$\frac{\partial\boldsymbol{\chi}^{e}}{\partial\Delta\bar{\gamma}^{\chi}} = -\boldsymbol{\chi}^{e}\left(\frac{\partial\boldsymbol{\chi}^{p}}{\partial\Delta\bar{\gamma}^{\chi}}\right)\boldsymbol{\chi}^{p-1} \tag{7.19}$$

and

$$\frac{\partial\boldsymbol{\chi}^{p}}{\partial\Delta\bar{\gamma}^{\chi}} = -\boldsymbol{F}^{eT}\boldsymbol{\chi}^{e}\bar{\boldsymbol{\Psi}}^{e-1}_{n}\left(\frac{\partial\bar{G}^{\chi}}{\partial\left(\bar{\boldsymbol{\Sigma}} - \bar{\boldsymbol{S}}\right)}\right)^{T}_{n}\bar{\boldsymbol{\Psi}}^{e-T}_{n}\bar{\boldsymbol{C}}^{\chi,e}_{n}\boldsymbol{\chi}^{p}_{n}\boldsymbol{\chi}^{p-1} \tag{7.20}$$

$$\frac{\partial||\mathrm{dev}\left(\bar{\boldsymbol{\Sigma}} - \bar{\boldsymbol{S}}\right)||}{\partial\Delta\bar{\gamma}^{\chi}} = \frac{\partial\mathrm{dev}\left(\bar{\boldsymbol{\Sigma}} - \bar{\boldsymbol{S}}\right)}{\partial\Delta\bar{\gamma}^{\chi}} : \frac{\mathrm{dev}\left(\bar{\boldsymbol{\Sigma}} - \bar{\boldsymbol{S}}\right)}{||\mathrm{dev}\left(\bar{\boldsymbol{\Sigma}} - \bar{\boldsymbol{S}}\right)||} \tag{7.21}$$

$$\frac{\partial\mathrm{dev}\left(\bar{\boldsymbol{\Sigma}} - \bar{\boldsymbol{S}}\right)}{\partial\Delta\bar{\gamma}^{\chi}} = \frac{\partial\left(\bar{\boldsymbol{\Sigma}} - \bar{\boldsymbol{S}}\right)}{\partial\Delta\bar{\gamma}^{\chi}} - \frac{\partial\bar{p}^{\chi}}{\partial\Delta\bar{\gamma}^{\chi}}\mathbf{1} \tag{7.22}$$

$$\frac{\partial\bar{p}^{\chi}}{\partial\Delta\bar{\gamma}^{\chi}} = \frac{1}{3}\left(\mathbf{1} : \frac{\partial\left(\bar{\boldsymbol{\Sigma}} - \bar{\boldsymbol{S}}\right)}{\partial\Delta\bar{\gamma}^{\chi}}\right) \tag{7.23}$$

$$\left(\frac{\partial\bar{G}^{\chi}}{\partial\left(\bar{\boldsymbol{\Sigma}} - \bar{\boldsymbol{S}}\right)}\right)_{n} = \frac{\mathrm{dev}\left(\bar{\boldsymbol{\Sigma}} - \bar{\boldsymbol{S}}\right)}{||\mathrm{dev}\left(\bar{\boldsymbol{\Sigma}} - \bar{\boldsymbol{S}}\right)||} + \frac{1}{3}B^{\psi,\chi}\mathbf{1} \tag{7.24}$$

$$\frac{\partial\bar{c}^{\chi}}{\partial\Delta\bar{\gamma}^{\chi}} = H^{c,\chi}h^{c,\chi}_{n} \tag{7.25}$$

where

$$h^{c,\chi}_{n} = -\left(\frac{\partial\bar{G}}{\partial\bar{c}}\right)_{n} = A^{\psi,\chi} \tag{7.26}$$

Then, the local consistent tangent for the micro scale can be found as:

$$\frac{\partial \bar{F}^{\chi}}{\partial \Delta \bar{\gamma}^{\chi}} = \frac{\partial ||\text{dev}\left(\bar{\boldsymbol{\Sigma}} - \bar{\boldsymbol{S}}\right)||}{\partial \Delta \bar{\gamma}^{\chi}} - \left(A^{\phi,\chi} \frac{\partial \bar{c}^{\chi}}{\partial \Delta \bar{\gamma}^{\chi}} - B^{\phi,\chi} \frac{\partial \bar{p}^{\chi}}{\partial \Delta \bar{\gamma}^{\chi}} \right) \tag{7.27}$$

7.0.3 Solving for plastic multipliers locally for coupled plasticity for three scale approach

The last two sections presented the formulation to solve for plastic multipliers when macro-scale and micro-scale plasticity exist separately. This section considers to solve for plastic multipliers in case of these two scales are coupled which means that plastic multipliers will be obtained in a coupled way as follows,

$$\bar{F}_{n+1}\left(\Delta \bar{\gamma}_{n+1}, \Delta \bar{\gamma}^{\chi}_{n+1}\right) = 0, \Delta \bar{\gamma}_{n+1} > 0 \tag{7.28}$$

$$\bar{F}^{\chi}_{n+1}\left(\Delta \bar{\gamma}_{n+1}, \Delta \bar{\gamma}^{\chi}_{n+1}\right) = 0, \Delta \bar{\gamma}^{\chi}_{n+1} > 0 \tag{7.29}$$

$$\bar{F}^{k} + \left(\frac{\partial \bar{F}}{\partial \Delta \bar{\gamma}}\right)^{k} \delta\left(\Delta \bar{\gamma}\right)^{k} + \left(\frac{\partial \bar{F}}{\partial \Delta \bar{\gamma}^{\chi}}\right)^{k} \delta\left(\Delta \bar{\gamma}^{\chi}\right)^{k} = 0 \tag{7.30}$$

$$\bar{F}^{\chi k} + \left(\frac{\partial \bar{F}^{\chi}}{\partial \Delta \bar{\gamma}}\right)^{k} \delta\left(\Delta \bar{\gamma}\right)^{k} + \left(\frac{\partial \bar{F}^{\chi}}{\partial \Delta \bar{\gamma}^{\chi}}\right)^{k} \delta\left(\Delta \bar{\gamma}^{\chi}\right)^{k} = 0 \tag{7.31}$$

To solve for $\delta\left(\Delta \bar{\gamma}\right)$ and $\delta\left(\Delta \bar{\gamma}^{\chi}\right)$, we create the local consistent tangent as:

$$\begin{bmatrix} \frac{\partial \bar{F}}{\partial \Delta \bar{\gamma}} & \frac{\partial \bar{F}}{\partial \Delta \bar{\gamma}^{\chi}} \\ \frac{\partial \bar{F}^{\chi}}{\partial \Delta \bar{\gamma}} & \frac{\partial \bar{F}^{\chi}}{\partial \Delta \bar{\gamma}^{\chi}} \end{bmatrix}^{k} \begin{Bmatrix} \delta\left(\Delta \bar{\gamma}\right) \\ \delta\left(\Delta \bar{\gamma}^{\chi}\right) \end{Bmatrix}^{k} = \begin{Bmatrix} -\bar{F} \\ -\bar{F}^{\chi} \end{Bmatrix}^{k} \tag{7.32}$$

Definitions of $\frac{\partial \bar{F}}{\partial \Delta \bar{\gamma}}$ and $\frac{\partial \bar{F}^{\chi}}{\partial \Delta \bar{\gamma}^{\chi}}$ were already given in equations 7.15 and 7.27, where the off diagonal terms can be found as:

$$\frac{\partial \bar{\boldsymbol{S}}}{\partial \Delta \bar{\gamma}^{\chi}} = \eta \text{tr}\left(\frac{\partial \bar{\boldsymbol{\mathcal{E}}}^{e}}{\partial \Delta \bar{\gamma}^{\chi}}\right)\mathbf{1} + \kappa\left(\frac{\partial \bar{\boldsymbol{\mathcal{E}}}^{e}}{\partial \Delta \bar{\gamma}^{\chi}}\right) + \nu\left(\frac{\partial \bar{\boldsymbol{\mathcal{E}}}^{e}}{\partial \Delta \bar{\gamma}^{\chi}}\right)^{T} \tag{7.33}$$

where

$$\frac{\partial||\mathrm{dev}\bar{\boldsymbol{S}}||}{\partial\Delta\bar{\gamma}^{\chi}} = \frac{\partial \mathrm{dev}\bar{\boldsymbol{S}}}{\partial\Delta\bar{\gamma}^{\chi}} : \frac{\mathrm{dev}\boldsymbol{S}}{||\mathrm{dev}\bar{\boldsymbol{S}}||} \tag{7.34}$$

$$\frac{\partial \mathrm{dev}\bar{\boldsymbol{S}}}{\partial\Delta\bar{\gamma}^{\chi}} = \frac{\partial\bar{\boldsymbol{S}}}{\partial\Delta\bar{\gamma}^{\chi}} - \frac{\partial\bar{p}}{\partial\Delta\bar{\gamma}^{\chi}}\mathbf{1} \tag{7.35}$$

$$\frac{\partial\bar{p}}{\partial\Delta\bar{\gamma}^{\chi}} = \frac{1}{3}\left(\mathbf{1} : \frac{\partial\bar{\boldsymbol{S}}}{\partial\Delta\bar{\gamma}^{\chi}}\right) \tag{7.36}$$

$$\left(\frac{\partial\bar{c}}{\partial\Delta\bar{\gamma}^{\chi}}\right) = 0 \tag{7.37}$$

then, we get

$$\frac{\partial\bar{F}}{\partial\Delta\bar{\gamma}^{\chi}} = \frac{\partial||\mathrm{dev}\bar{\boldsymbol{S}}||}{\partial\Delta\bar{\gamma}^{\chi}} + B^{\phi}\frac{\partial\bar{p}}{\partial\Delta\bar{\gamma}^{\chi}} \tag{7.38}$$

also

$$\begin{aligned}\frac{\partial\left(\bar{\boldsymbol{\Sigma}} - \bar{\boldsymbol{S}}\right)}{\partial\Delta\bar{\gamma}} &= \tau \mathrm{tr}\left(\frac{\partial\bar{\boldsymbol{E}}^{e}}{\partial\Delta\bar{\gamma}}\right)\mathbf{1} + 2\sigma\left(\frac{\partial\bar{\boldsymbol{E}}^{e}}{\partial\Delta\bar{\gamma}}\right) + (\eta - \tau)\,\mathrm{tr}\left(\frac{\partial\bar{\boldsymbol{\mathcal{E}}}^{e}}{\partial\Delta\bar{\gamma}}\right)\mathbf{1} \\ &+ (\nu - \sigma)\left(\frac{\partial\bar{\boldsymbol{\mathcal{E}}}^{e}}{\partial\Delta\bar{\gamma}}\right) + (\kappa - \sigma)\left(\frac{\partial\bar{\boldsymbol{\mathcal{E}}}^{e}}{\partial\Delta\bar{\gamma}}\right)^{T}\end{aligned} \tag{7.39}$$

and

$$\frac{\partial||\mathrm{dev}\left(\bar{\boldsymbol{\Sigma}} - \bar{\boldsymbol{S}}\right)||}{\partial\Delta\bar{\gamma}} = \frac{\partial \mathrm{dev}\left(\bar{\boldsymbol{\Sigma}} - \bar{\boldsymbol{S}}\right)}{\partial\Delta\bar{\gamma}} : \frac{\mathrm{dev}\left(\bar{\boldsymbol{\Sigma}} - \bar{\boldsymbol{S}}\right)}{||\mathrm{dev}\bar{\boldsymbol{S}}||} \tag{7.40}$$

$$\frac{\partial \mathrm{dev}\left(\bar{\boldsymbol{\Sigma}} - \bar{\boldsymbol{S}}\right)}{\partial\Delta\bar{\gamma}} = \frac{\partial\left(\bar{\boldsymbol{\Sigma}} - \bar{\boldsymbol{S}}\right)}{\partial\Delta\bar{\gamma}} - \frac{\partial\bar{p}^{\chi}}{\partial\Delta\bar{\gamma}}\mathbf{1} \tag{7.41}$$

$$\frac{\partial\bar{p}^{\chi}}{\partial\Delta\bar{\gamma}} = \frac{1}{3}\left(\mathbf{1} : \frac{\partial\left(\bar{\boldsymbol{\Sigma}} - \bar{\boldsymbol{S}}\right)}{\partial\Delta\bar{\gamma}}\right) \tag{7.42}$$

$$\left(\frac{\partial\bar{c}^{\chi}}{\partial\Delta\bar{\gamma}}\right) = 0 \tag{7.43}$$

which gives

$$\frac{\partial\bar{F}^{\chi}}{\partial\Delta\bar{\gamma}} = \frac{\partial||\mathrm{dev}\left(\bar{\boldsymbol{\Sigma}} - \bar{\boldsymbol{S}}\right)||}{\partial\Delta\bar{\gamma}} + B^{\phi,\chi}\frac{\partial\bar{p}^{\chi}}{\partial\Delta\bar{\gamma}} \tag{7.44}$$

7.0.4 Solving for plastic multipliers globally for separate plasticity

In this section, we present the formulation to construct the global consistent tangent. We show how to obtain the global $\delta\left(\Delta\bar{\gamma}\right)$ and $\delta\left(\Delta\bar{\gamma}^{\chi}\right)$ in terms of $\delta\boldsymbol{u}$ and $\delta\boldsymbol{\Phi}$ by applying a

variational approach in the context of a linearization of the weak form of the coupled balance of linear momentum and balance of first moment of momentum.

For macro-scale plasticity:

$$\delta\bar{F}\left(\bar{\boldsymbol{S}},\bar{c}\right)=\frac{\partial\bar{F}}{\partial\bar{\boldsymbol{S}}}:\delta\bar{\boldsymbol{S}}+\frac{\partial\bar{F}}{\partial\bar{c}}\delta\bar{c}=0 \tag{7.45}$$

where

$$\delta\bar{\boldsymbol{S}}=\left(\lambda+\tau\right)\mathrm{tr}\left(\delta\bar{\boldsymbol{E}}^{e}\right)\mathbf{1}+2\left(\mu+\sigma\right)\delta\bar{\boldsymbol{E}}^{e}+\eta\mathrm{tr}\left(\delta\bar{\boldsymbol{\mathcal{E}}}^{e}\right)\mathbf{1}+\kappa\delta\bar{\boldsymbol{\mathcal{E}}}^{\boldsymbol{e}}+\nu\delta\bar{\boldsymbol{\mathcal{E}}}^{eT} \tag{7.46}$$

where

$$\delta\bar{\boldsymbol{E}}^{e}=\frac{1}{2}\left[\boldsymbol{B}^{T}-\boldsymbol{A}^{T}\delta\left(\Delta\bar{\gamma}\right)+\boldsymbol{B}-\boldsymbol{A}\delta\left(\Delta\bar{\gamma}\right)\right] \tag{7.47}$$

$$\delta\bar{\boldsymbol{\mathcal{E}}}^{e}=\boldsymbol{M}^{T}-\boldsymbol{N}\delta\left(\Delta\bar{\gamma}\right)+\boldsymbol{P}-\boldsymbol{D}\delta\left(\Delta\bar{\gamma}^{\chi}\right) \tag{7.48}$$

$$\boldsymbol{A}=\boldsymbol{F}^{eT}\boldsymbol{F}^{e}\bar{\boldsymbol{C}}_{n}^{e-1}\left(\frac{\partial\bar{G}}{\partial\bar{\boldsymbol{S}}}\right)_{n}^{T}\boldsymbol{F}_{n}^{p}\boldsymbol{F}^{p-1} \tag{7.49}$$

$$\boldsymbol{B}=\boldsymbol{F}^{eT}\boldsymbol{GRAD}\left(\delta\boldsymbol{u}\right)\boldsymbol{F}^{p-1} \tag{7.50}$$

$$\boldsymbol{M}=\boldsymbol{\chi}^{eT}\boldsymbol{GRAD}\left(\delta\boldsymbol{u}\right)\boldsymbol{F}^{p-1} \tag{7.51}$$

$$\boldsymbol{N}=\boldsymbol{\chi}^{eT}\boldsymbol{F}^{e}\bar{\boldsymbol{C}}_{n}^{e-1}\left(\frac{\partial\bar{G}}{\partial\bar{\boldsymbol{S}}}\right)_{n}^{T}\boldsymbol{F}_{n}^{p}\boldsymbol{F}^{p-1} \tag{7.52}$$

$$\boldsymbol{P}=\boldsymbol{F}^{eT}\delta\boldsymbol{\Phi}\boldsymbol{\chi}^{p-1} \tag{7.53}$$

$$\boldsymbol{D}=\boldsymbol{F}^{eT}\boldsymbol{\chi}^{e}\bar{\boldsymbol{\Psi}}_{n}^{e-1}\left(\frac{\partial\bar{G}^{\chi}}{\partial\left(\bar{\boldsymbol{\Sigma}}-\bar{\boldsymbol{S}}\right)}\right)_{n}^{T}\bar{\boldsymbol{\Psi}}_{n}^{e-T}\bar{\boldsymbol{C}}_{n}^{\chi,e}\boldsymbol{\chi}_{n}^{p}\boldsymbol{\chi}^{p-1} \tag{7.54}$$

If we insert equations 7.47 and 7.48 into 7.46, we get

$$\begin{aligned}\delta\bar{\boldsymbol{S}}&=\left(\lambda+\tau\right)\mathrm{tr}\left(\boldsymbol{B}\right)\mathbf{1}-\left(\lambda+\tau\right)\mathrm{tr}\left(\boldsymbol{A}^{T}\right)\mathbf{1}\delta\left(\Delta\bar{\gamma}\right)\\&+\left(\mu+\sigma\right)\left(\boldsymbol{B}^{T}+\boldsymbol{B}\right)-\left(\mu+\sigma\right)\left(\boldsymbol{A}^{T}+\boldsymbol{A}\right)\delta\left(\Delta\bar{\gamma}\right)\\&+\eta\mathrm{tr}\left(\boldsymbol{M}^{T}\right)\mathbf{1}-\eta\mathrm{tr}\left(\boldsymbol{N}^{T}\right)\mathbf{1}\delta\left(\Delta\bar{\gamma}\right)\\&+\eta\mathrm{tr}\left(\boldsymbol{P}\right)\mathbf{1}-\eta\mathrm{tr}\left(\boldsymbol{D}\right)\mathbf{1}\delta\left(\Delta\bar{\gamma}^{\chi}\right)\\&+\kappa\boldsymbol{M}^{T}-\kappa\boldsymbol{N}^{T}\delta\left(\Delta\bar{\gamma}\right)+\kappa\boldsymbol{P}-\kappa\boldsymbol{D}\delta\left(\Delta\bar{\gamma}^{\chi}\right)\\&+\nu\boldsymbol{M}-\nu\boldsymbol{N}\delta\left(\Delta\bar{\gamma}\right)+\nu\boldsymbol{P}^{T}-\nu\boldsymbol{D}^{T}\delta\left(\Delta\bar{\gamma}^{\chi}\right)\end{aligned} \tag{7.55}$$

and

$$\delta\bar{c} = H^c h_n^c \delta\left(\Delta\bar{\gamma}\right) \tag{7.56}$$

$$\frac{\partial\bar{F}}{\partial\bar{c}} = -A^{\phi} \tag{7.57}$$

where $h_n^c = -A^{\psi}$. If equations 7.56,7.57, and 7.55 are inserted in equation 7.45 and collect the terms $\delta\left(\Delta\bar{\gamma}\right)$ and $\delta\left(\Delta\bar{\gamma}^{\chi}\right)$ on one side, we get:

$$\mathcal{C}_1\delta\left(\Delta\bar{\gamma}\right) + \mathcal{C}_2\delta\left(\Delta\bar{\gamma}^{\chi}\right) = \mathcal{F}_1\left(\delta\boldsymbol{u}, \delta\boldsymbol{\Phi}\right) \tag{7.58}$$

where

$$\begin{aligned}\mathcal{F}_1\left(\delta\boldsymbol{u}, \delta\boldsymbol{\Phi}\right) &= \left(\lambda+\tau\right)\left(\frac{\partial\bar{F}}{\partial\bar{\boldsymbol{S}}} : \mathbf{1}\right)\mathrm{tr}\left(\boldsymbol{B}^T\right) + \left(\mu+\sigma\right)\frac{\partial\bar{F}}{\partial\bar{\boldsymbol{S}}} : \left(\boldsymbol{B}^T + \boldsymbol{B}^T\right) + \eta\left(\frac{\partial\bar{F}}{\partial\bar{\boldsymbol{S}}} : \mathbf{1}\right)\mathrm{tr}\left(\boldsymbol{M}^T\right) \\ &+ \eta\left(\frac{\partial\bar{F}}{\partial\bar{\boldsymbol{S}}} : \mathbf{1}\right)\mathrm{tr}\left(\boldsymbol{P}\right) + \kappa\frac{\partial\bar{F}}{\partial\bar{\boldsymbol{S}}} : \boldsymbol{M}^T + \kappa\frac{\partial\bar{F}}{\partial\bar{\boldsymbol{S}}} : \boldsymbol{P} + \nu\frac{\partial\bar{F}}{\partial\bar{\boldsymbol{S}}} : \boldsymbol{M} + \nu\frac{\partial\bar{F}}{\partial\bar{\boldsymbol{S}}} : \boldsymbol{P}^T\end{aligned} \tag{7.59}$$

$$\begin{aligned}\mathcal{C}_1 = \Bigg[&\left(\lambda+\tau\right)\left(\frac{\partial\bar{F}}{\partial\bar{\boldsymbol{S}}}\right)\mathrm{tr}\left(\boldsymbol{A}^T\right) + \left(\mu+\sigma\right)\frac{\partial\bar{F}}{\partial\bar{\boldsymbol{S}}} : \left(\boldsymbol{A}^T + \boldsymbol{A}\right) + \eta\left(\frac{\partial\bar{F}}{\partial\bar{\boldsymbol{S}}} : \mathbf{1}\right)\mathrm{tr}\left(\boldsymbol{N}^T\right) \\ &+\kappa\frac{\partial\bar{F}}{\partial\bar{\boldsymbol{S}}} : \boldsymbol{N}^T + \nu\frac{\partial\bar{F}}{\partial\bar{\boldsymbol{S}}} : \boldsymbol{N} - \frac{\partial\bar{F}}{\partial\bar{c}}H^c h_n^c\Bigg]\end{aligned} \tag{7.60}$$

$$\mathcal{C}_2 = \left[\eta\left(\frac{\partial\bar{F}}{\partial\bar{\boldsymbol{S}}} : \mathbf{1}\right)\mathrm{tr}\left(\boldsymbol{D}\right) + \kappa\frac{\partial\bar{F}}{\partial\bar{\boldsymbol{S}}} : \boldsymbol{D} + \nu\frac{\partial\bar{F}}{\partial\bar{\boldsymbol{S}}} : \boldsymbol{D}^T\right] \tag{7.61}$$

For micro-scale plasticity:

$$\bar{F}^{\chi}\left(\left(\bar{\boldsymbol{\Sigma}} - \bar{\boldsymbol{S}}\right), \bar{c}^{\chi}\right) = \frac{\partial\bar{F}^{\chi}}{\partial\left(\bar{\boldsymbol{\Sigma}} - \bar{\boldsymbol{S}}\right)} : \delta\left(\bar{\boldsymbol{\Sigma}} - \bar{\boldsymbol{S}}\right) + \frac{\partial\bar{F}^{\chi}}{\partial\bar{c}^{\chi}}\delta\bar{c}^{\chi} = 0 \tag{7.62}$$

where

$$\begin{aligned}\delta\left(\bar{\boldsymbol{\Sigma}} - \bar{\boldsymbol{S}}\right) &= \tau\mathrm{tr}\left(\boldsymbol{B}^T\right)\mathbf{1} - \tau\mathrm{tr}\left(\boldsymbol{A}^T\right)\mathbf{1}\delta\left(\Delta\bar{\gamma}\right) + \sigma\left(\boldsymbol{B}^T + \boldsymbol{B}\right) - \sigma\left(\boldsymbol{A}^T + \boldsymbol{A}^T\right)\delta\left(\Delta\bar{\gamma}\right) \\ &+ \left(\eta-\tau\right)\mathrm{tr}\left(\boldsymbol{M}^T\right)\mathbf{1} - \left(\eta-\tau\right)\mathrm{tr}\left(\boldsymbol{N}\right)\mathbf{1}\delta\left(\Delta\bar{\gamma}\right) + \left(\eta-\tau\right)\mathrm{tr}\left(\boldsymbol{P}\right)\mathbf{1} - \left(\eta-\tau\right)\mathrm{tr}\left(\boldsymbol{D}\right)\mathbf{1}\delta\left(\Delta\bar{\gamma}^{\chi}\right) \\ &+ \left(\nu-\sigma\right)\boldsymbol{M}^T - \left(\nu-\sigma\right)\boldsymbol{N}^T\delta\left(\Delta\bar{\gamma}\right) + \left(\nu-\sigma\right)\boldsymbol{P} - \left(\nu-\sigma\right)\boldsymbol{D}\delta\left(\Delta\bar{\gamma}^{\chi}\right) \\ &+ \left(\kappa-\sigma\right)\boldsymbol{M} - \left(\kappa-\sigma\right)\boldsymbol{N}\delta\left(\Delta\bar{\gamma}\right) + \left(\kappa-\sigma\right)\boldsymbol{P}^T - \left(\kappa-\sigma\right)\boldsymbol{D}^T\delta\left(\Delta\bar{\gamma}^{\chi}\right)\end{aligned} \tag{7.63}$$

and

$$\delta\bar{c}^{\chi} = H^{c,\chi} h_n^{c,\chi} \delta\left(\Delta\bar{\gamma}^{\chi}\right) \tag{7.64}$$

$$\frac{\partial\bar{F}^{\chi}}{\partial\bar{c}^{\chi}} = -A^{\phi,\chi} \tag{7.65}$$

where $h_n^{c,\chi} = -A^{\psi,\chi}$. Again, if we insert 7.64, 7.65, and 7.63 into equation 7.62 and collect the terms multiplied by $\delta\left(\Delta\bar{\gamma}\right)$ and $\delta\left(\Delta\bar{\gamma}^{\chi}\right)$ on one side, we get:

$$\mathcal{C}_3\delta\left(\Delta\bar{\gamma}\right) + \mathcal{C}_4\delta\left(\Delta\bar{\gamma}^{\chi}\right) = \mathcal{F}_2\left(\delta\boldsymbol{u}, \delta\boldsymbol{\Phi}\right) \tag{7.66}$$

where

$$\begin{aligned}
\mathcal{F}_2\left(\delta\boldsymbol{u}, \delta\boldsymbol{\Phi}\right) &= \tau\left(\frac{\partial\bar{F}^{\chi}}{\partial\left(\bar{\boldsymbol{\Sigma}} - \bar{\boldsymbol{S}}\right)} : \mathbf{1}\right)\mathrm{tr}\left(\boldsymbol{B}\right) + \sigma\frac{\partial\bar{F}^{\chi}}{\partial\left(\bar{\boldsymbol{\Sigma}} - \bar{\boldsymbol{S}}\right)} : \left(\boldsymbol{B}^T + \boldsymbol{B}\right) \\
&+ \left(\eta - \tau\right)\left(\frac{\partial\bar{F}^{\chi}}{\partial\left(\bar{\boldsymbol{\Sigma}} - \bar{\boldsymbol{S}}\right)} : \mathbf{1}\right)\mathrm{tr}\left(\boldsymbol{M}^T\right) + \left(\eta - \tau\right)\left(\frac{\partial\bar{F}^{\chi}}{\partial\left(\bar{\boldsymbol{\Sigma}} - \bar{\boldsymbol{S}}\right)} : \mathbf{1}\right)\mathrm{tr}\left(\boldsymbol{P}\right) \\
&+ \left(\nu - \sigma\right)\frac{\partial\bar{F}^{\chi}}{\partial\left(\bar{\boldsymbol{\Sigma}} - \bar{\boldsymbol{S}}\right)} : \boldsymbol{M}^T + \left(\nu - \sigma\right)\frac{\partial\bar{F}^{\chi}}{\partial\left(\bar{\boldsymbol{\Sigma}} - \bar{\boldsymbol{S}}\right)} : \boldsymbol{P} \\
&+ \left(\kappa - \sigma\right)\frac{\partial\bar{F}^{\chi}}{\partial\left(\bar{\boldsymbol{\Sigma}} - \bar{\boldsymbol{S}}\right)} : \boldsymbol{M} + \left(\kappa - \sigma\right)\frac{\partial\bar{F}^{\chi}}{\partial\left(\bar{\boldsymbol{\Sigma}} - \bar{\boldsymbol{S}}\right)} : \boldsymbol{P}^T
\end{aligned} \tag{7.67}$$

$$\begin{aligned}
\mathcal{C}_3 = \Bigg[&\tau\left(\frac{\partial\bar{F}^{\chi}}{\partial\left(\bar{\boldsymbol{\Sigma}} - \bar{\boldsymbol{S}}\right)} : \mathbf{1}\right)\mathrm{tr}\left(\boldsymbol{A}^T\right) + \sigma\frac{\partial\bar{F}^{\chi}}{\partial\left(\bar{\boldsymbol{\Sigma}} - \bar{\boldsymbol{S}}\right)} : \left(\boldsymbol{A}^T + \boldsymbol{A}\right) \\
&+ \left(\eta - \tau\right)\left(\frac{\partial\bar{F}^{\chi}}{\partial\left(\bar{\boldsymbol{\Sigma}} - \bar{\boldsymbol{S}}\right)} : \mathbf{1}\right)\mathrm{tr}\left(\boldsymbol{N}^T\right) + \left(\nu - \sigma\right)\frac{\partial\bar{F}^{\chi}}{\partial\left(\bar{\boldsymbol{\Sigma}} - \bar{\boldsymbol{S}}\right)} : \boldsymbol{N}^T \\
&+ \left(\kappa - \sigma\right)\frac{\partial\bar{F}^{\chi}}{\partial\left(\bar{\boldsymbol{\Sigma}} - \bar{\boldsymbol{S}}\right)} : \boldsymbol{N}\Bigg]
\end{aligned} \tag{7.68}$$

$$\begin{aligned}
\mathcal{C}_4 = \Bigg[&\left(\eta - \tau\right)\left(\frac{\partial\bar{F}^{\chi}}{\partial\left(\bar{\boldsymbol{\Sigma}} - \bar{\boldsymbol{S}}\right)} : \mathbf{1}\right)\mathrm{tr}\left(\boldsymbol{D}\right) + \left(\nu - \sigma\right)\frac{\partial\bar{F}^{\chi}}{\partial\left(\bar{\boldsymbol{\Sigma}} - \bar{\boldsymbol{S}}\right)} : \boldsymbol{D} \\
&+ \left(\kappa - \sigma\right)\frac{\partial\bar{F}^{\chi}}{\partial\left(\bar{\boldsymbol{\Sigma}} - \bar{\boldsymbol{S}}\right)} : \boldsymbol{D}^T - \frac{\partial\bar{F}^{\chi}}{\partial\bar{c}^{\chi}}H^{c,\chi}h_n^{c,\chi}\Bigg]
\end{aligned} \tag{7.69}$$

Here, we consider three different cases. When we have only macro-scale plasticity, micro-scale plasticity, and coupled plasticity. When we have only macro-scale plasticity $\delta\left(\Delta\bar{\gamma}^{\chi}\right) = 0$, then from 7.58 we find:

$$\begin{aligned}
\mathcal{C}_1\delta\left(\Delta\bar{\gamma}\right) + \mathcal{C}_2\delta\left(\Delta\bar{\gamma}^{\chi}\right) &= \mathcal{F}_1\left(\delta\boldsymbol{u}, \delta\boldsymbol{\Phi}\right) \\
\delta\left(\Delta\bar{\gamma}\right) &= \frac{1}{\mathcal{C}_1}\mathcal{F}_1\left(\delta\boldsymbol{u}, \delta\boldsymbol{\Phi}\right)
\end{aligned} \tag{7.70}$$

Similarly, when we have only micro-scale plasticity $\delta\left(\Delta\bar{\gamma}\right)=0$.

$$\begin{aligned}\mathcal{C}_3\delta\left(\Delta\bar{\gamma}\right)+\mathcal{C}_4\delta\left(\Delta\bar{\gamma}^{\chi}\right)&=\mathcal{F}_2\left(\delta\boldsymbol{u},\delta\boldsymbol{\Phi}\right)\\ \delta\left(\Delta\bar{\gamma}^{\chi}\right)&=\frac{1}{\mathcal{C}_4}\mathcal{F}_2\left(\delta\boldsymbol{u},\delta\boldsymbol{\Phi}\right)\end{aligned}\tag{7.71}$$

When we have coupled plasticity, we get:

$$\begin{bmatrix}\mathcal{C}_1 & \mathcal{C}_2\\ \mathcal{C}_3 & \mathcal{C}_4\end{bmatrix}\begin{Bmatrix}\delta\left(\Delta\bar{\gamma}\right)\\ \delta\left(\Delta\bar{\gamma}^{\chi}\right)\end{Bmatrix}=\begin{Bmatrix}\mathcal{F}_1\left(\delta\boldsymbol{u},\delta\boldsymbol{\Phi}\right)\\ \mathcal{F}_2\left(\delta\boldsymbol{u},\delta\boldsymbol{\Phi}\right)\end{Bmatrix}\tag{7.72}$$

Then,

$$\delta\left(\Delta\bar{\gamma}\right)=\mathcal{A}_1\mathcal{F}_1\left(\delta\boldsymbol{u},\delta\boldsymbol{\Phi}\right)+\mathcal{A}_2\mathcal{F}_2\left(\delta\boldsymbol{u},\delta\boldsymbol{\Phi}\right)\tag{7.73}$$

$$\delta\left(\Delta\bar{\gamma}^{\chi}\right)=\mathcal{A}_3\mathcal{F}_1\left(\delta\boldsymbol{u},\delta\boldsymbol{\Phi}\right)+\mathcal{A}_4\mathcal{F}_2\left(\delta\boldsymbol{u},\delta\boldsymbol{\Phi}\right)\tag{7.74}$$

where

$$\begin{aligned}\mathcal{A}_1&=\frac{\mathcal{C}_4}{\mathcal{C}_1\mathcal{C}_4-\mathcal{C}_2\mathcal{C}_3},\qquad \mathcal{A}_2=-\frac{\mathcal{C}_2}{\mathcal{C}_1\mathcal{C}_4-\mathcal{C}_2\mathcal{C}_3},\\ \mathcal{A}_3&=-\frac{\mathcal{C}_3}{\mathcal{C}_1\mathcal{C}_4-\mathcal{C}_2\mathcal{C}_3},\qquad \mathcal{A}_4=\frac{\mathcal{C}_1}{\mathcal{C}_1\mathcal{C}_4-\mathcal{C}_2\mathcal{C}_3},\end{aligned}\tag{7.75}$$

Even though we proposed a yield function for the micro-scale gradient plasticity in previous chapters, we will assume that micro-scale gradient will stay elastic in this work, for now. The formulation for its contribution to plasticity as well as global consistent tangent will be given in the next sections.

7.0.5 Solving for plastic multiplier locally for combined plasticity

In combined plasticity, we have one yield function including the terms shown in separate scale plasticity. Having one plastic multiplier for $\boldsymbol{F}^p$ and $\boldsymbol{\chi}^p$ actually dictates that they plastify at the same time; they evolve plastically the same and there is only one intermediate

configuration at which these two variables evolve. The combined yield function can be expressed as:

$$\bar{F}(\bar{\boldsymbol{S}},\bar{c},\left(\bar{\boldsymbol{\Sigma}}-\bar{\boldsymbol{S}}\right),\bar{c}^{\chi}) \overset{\text{def}}{=} \left[\text{dev}\bar{\boldsymbol{S}}:\text{dev}\bar{\boldsymbol{S}}+\text{dev}(\bar{\boldsymbol{\Sigma}}-\bar{\boldsymbol{S}}):\text{dev}(\bar{\boldsymbol{\Sigma}}-\bar{\boldsymbol{S}})\right]^{\frac{1}{2}} - \left(A^{\phi}\bar{c}-B^{\phi}\bar{p}+A^{\chi,\phi}\bar{c}^{\chi}-B^{\chi,\phi}\bar{p}^{\chi}\right)\leq 0 \tag{7.76}$$

and combined plastic potential function

$$\bar{G}(\bar{\boldsymbol{S}},\bar{c},\left(\bar{\boldsymbol{\Sigma}}-\bar{\boldsymbol{S}}\right),\bar{c}^{\chi}) \overset{\text{def}}{=} \left[\text{dev}\bar{\boldsymbol{S}}:\text{dev}\bar{\boldsymbol{S}}+\text{dev}(\bar{\boldsymbol{\Sigma}}-\bar{\boldsymbol{S}}):\text{dev}(\bar{\boldsymbol{\Sigma}}-\bar{\boldsymbol{S}})\right]^{\frac{1}{2}} - \left(A^{\psi}\bar{c}-B^{\psi}\bar{p}+A^{\chi,\psi}\bar{c}^{\chi}-B^{\chi,\psi}\bar{p}^{\chi}\right) \tag{7.77}$$

To obtain local consistent tangent $\partial\bar{F}/\partial\left(\Delta\bar{\gamma}\right)$, we first determine the relations given below. Different than the definitions given in previous sections, we define some derivatives as: Let's call

$$||\boldsymbol{N}|| = \left[\text{dev}\bar{\boldsymbol{S}}:\text{dev}\bar{\boldsymbol{S}}+\text{dev}(\bar{\boldsymbol{\Sigma}}-\bar{\boldsymbol{S}}):\text{dev}(\bar{\boldsymbol{\Sigma}}-\bar{\boldsymbol{S}})\right]^{\frac{1}{2}} \tag{7.78}$$

Then,

$$\frac{\partial||\boldsymbol{N}||}{\partial\Delta\bar{\gamma}} = \frac{1}{||\boldsymbol{N}||}\left(\text{dev}\bar{\boldsymbol{S}}:\frac{\partial\text{dev}\bar{\boldsymbol{S}}}{\partial\Delta\bar{\gamma}}+\text{dev}(\bar{\boldsymbol{\Sigma}}-\bar{\boldsymbol{S}}):\frac{\partial\text{dev}(\bar{\boldsymbol{\Sigma}}-\bar{\boldsymbol{S}})}{\partial\Delta\bar{\gamma}}\right) \tag{7.79}$$

$$\left(\frac{\partial\bar{\boldsymbol{\mathcal{E}}}^{e}}{\partial\Delta\bar{\gamma}}\right) = \left(\frac{\partial\boldsymbol{F}^{e}}{\partial\Delta\bar{\gamma}}\right)^{T}\boldsymbol{\chi}^{e}+\boldsymbol{F}^{eT}\left(\frac{\partial\boldsymbol{\chi}^{e}}{\partial\Delta\bar{\gamma}}\right) \tag{7.80}$$

$$\left(\frac{\partial\boldsymbol{\chi}^{e}}{\partial\Delta\bar{\gamma}}\right) = -\boldsymbol{\chi}^{e}\left(\frac{\partial\boldsymbol{\chi}^{p}}{\partial\Delta\bar{\gamma}}\right)\boldsymbol{\chi}^{p-1} \tag{7.81}$$

$$\frac{\partial\boldsymbol{\chi}^{p}}{\partial\Delta\bar{\gamma}} = -\boldsymbol{F}^{eT}\boldsymbol{\chi}^{e}\bar{\boldsymbol{\Psi}}_{n}^{e-1}\left(\frac{\partial\bar{G}}{\partial\left(\bar{\boldsymbol{\Sigma}}-\bar{\boldsymbol{S}}\right)}\right)_{n}^{T}\bar{\boldsymbol{\Psi}}_{n}^{e-T}\bar{\boldsymbol{C}}_{n}^{\chi,e}\boldsymbol{\chi}_{n}^{p}\boldsymbol{\chi}^{p-1} \tag{7.82}$$

where $\partial\text{dev}\bar{\boldsymbol{S}}/\partial\Delta\bar{\gamma}$ was defined before in equation (7.10) and $\partial\text{dev}(\bar{\boldsymbol{\Sigma}}-\bar{\boldsymbol{S}})/\partial\Delta\bar{\gamma}$ can be

expressed as:

$$\frac{\partial\left(\bar{\boldsymbol{\Sigma}}-\bar{\boldsymbol{S}}\right)}{\partial\Delta\bar{\gamma}}=\tau\mathrm{tr}\left(\frac{\partial\bar{\boldsymbol{E}}^{e}}{\partial\Delta\bar{\gamma}}\right)\mathbf{1}+2\sigma\left(\frac{\partial\bar{\boldsymbol{E}}^{e}}{\partial\Delta\bar{\gamma}}\right)+(\eta-\tau)\,\mathrm{tr}\left(\frac{\partial\bar{\boldsymbol{\mathcal{E}}}^{e}}{\partial\Delta\bar{\gamma}}\right)\mathbf{1}+(\nu-\sigma)\left(\frac{\partial\bar{\boldsymbol{\mathcal{E}}}^{e}}{\partial\Delta\bar{\gamma}}\right)$$
$$+(\kappa-\sigma)\left(\frac{\partial\bar{\boldsymbol{\mathcal{E}}}^{e}}{\partial\Delta\bar{\gamma}}\right) \tag{7.83}$$

$$\frac{\partial\mathrm{dev}(\bar{\boldsymbol{\Sigma}}-\bar{\boldsymbol{S}})}{\partial\Delta\bar{\gamma}}=\frac{\partial\left(\bar{\boldsymbol{\Sigma}}-\bar{\boldsymbol{S}}\right)}{\partial\Delta\bar{\gamma}}-\frac{\partial\bar{p}^{\chi}}{\partial\Delta\bar{\gamma}}\mathbf{1} \tag{7.84}$$

$$\frac{\partial\bar{p}^{\chi}}{\partial\Delta\bar{\gamma}}=\frac{1}{3}\frac{\partial\mathrm{tr}(\bar{\boldsymbol{\Sigma}}-\bar{\boldsymbol{S}})}{\partial\Delta\bar{\gamma}} \tag{7.85}$$

$$\frac{\partial\bar{c}^{\chi}}{\partial\Delta\bar{\gamma}}=H^{c,\chi}A^{\psi,\chi} \tag{7.86}$$

The other derivatives $\partial\bar{p}/\partial\Delta\bar{\gamma}$ and $\partial\bar{c}/\partial\Delta\bar{\gamma}$ were defined previously in equations (7.11) and (7.13).

7.0.6 Solving for plastic multiplier globally for combined plasticity

We presented the plasticity contribution into the global consistent tangent in separate plasticity assumption. Now, we follow a similar approach to determine $\delta\left(\Delta\bar{\gamma}\right)$ in combined plasticity formulation. We start with

$$\delta\bar{F}=\frac{\partial\bar{F}}{\partial\bar{\boldsymbol{S}}}:\delta\bar{\boldsymbol{S}}+\frac{\partial\bar{F}}{\partial\bar{c}}\delta\bar{c}+\frac{\partial\bar{F}^{\chi}}{\partial\left(\bar{\boldsymbol{\Sigma}}-\bar{\boldsymbol{S}}\right)}:\delta\left(\bar{\boldsymbol{\Sigma}}-\bar{\boldsymbol{S}}\right)+\frac{\partial\bar{F}^{\chi}}{\partial\bar{c}^{\chi}}\delta\bar{c}^{\chi}=0 \tag{7.87}$$

with updated definitions for

$$\frac{\partial\bar{F}}{\partial\bar{\boldsymbol{S}}}=\frac{\mathrm{dev}\bar{\boldsymbol{S}}}{||\boldsymbol{N}||}+\frac{1}{3}B^{\phi}\mathbf{1} \tag{7.88}$$

$$\frac{\partial\bar{G}}{\partial\bar{\boldsymbol{S}}}=\frac{\mathrm{dev}\bar{\boldsymbol{S}}}{||\boldsymbol{N}||}+\frac{1}{3}B^{\psi}\mathbf{1} \tag{7.89}$$

$$\frac{\partial\bar{F}}{\partial\left(\bar{\boldsymbol{\Sigma}}-\bar{\boldsymbol{S}}\right)}=\frac{\mathrm{dev}\left(\bar{\boldsymbol{\Sigma}}-\bar{\boldsymbol{S}}\right)}{||\boldsymbol{N}||}+\frac{1}{3}B^{\phi,\chi}\mathbf{1} \tag{7.90}$$

$$\frac{\partial\bar{G}}{\partial\left(\bar{\boldsymbol{\Sigma}}-\bar{\boldsymbol{S}}\right)}=\frac{\mathrm{dev}\left(\bar{\boldsymbol{\Sigma}}-\bar{\boldsymbol{S}}\right)}{||\boldsymbol{N}||}+\frac{1}{3}B^{\psi,\chi}\mathbf{1} \tag{7.91}$$

If we carry out the calculations similar to the separate plasticity, we can see that we can use the same expressions defined for separate scale plasticity approach. In this case $\bar{F}=\bar{F}^{\chi}$,

$\delta\left(\Delta\bar{\gamma}\right) = \delta\left(\Delta\bar{\gamma}\right)^{\chi}$, and $\mathcal{C}_1$, $\mathcal{C}_2$, $\mathcal{C}_3$, and $\mathcal{C}_4$ are already defined in equations (7.60), (7.61), (7.68), and (7.69).

$$\delta\left(\Delta\bar{\gamma}\right) = \delta\left(\Delta\bar{\gamma}\right)^{\chi} = \frac{\mathcal{F}_1 + \mathcal{F}_2}{\mathcal{C}_1 + \mathcal{C}_2 + \mathcal{C}_3 + \mathcal{C}_4} \tag{7.92}$$

7.0.7 Forming global consistent tangent for different plasticity assumptions

In this part, we like to present the contribution to global consistent tangent for different scale plasticity and combined plasticity assumptions due to linearization of the balance of momenta equations. Based on the previous chapters, we have the linearization of the balance equations already presented, in addition to that, we just show the effect of the $\delta\left(\Delta\bar{\gamma}\right)$ and $\delta\left(\Delta\bar{\gamma}^{\chi}\right)$ for separate scale plasticity and just $\delta\left(\Delta\bar{\gamma}\right) = \delta\left(\Delta\bar{\gamma}^{\chi}\right)$ for the combined plasticity. We follow the semi-implicit numerical integration algorithm outlined in (Regueiro, 2010) as:

Given: $\boldsymbol{F}_{n+1}$, $\boldsymbol{\chi}_{n+1}$, $\bar{\boldsymbol{C}}^{e}_{n}$, $\bar{\boldsymbol{\Psi}}^{e}_{n}$, $\boldsymbol{F}^{p}_{n}$, $\boldsymbol{\chi}^{e}_{n}$, $\bar{Z}_n$, $\bar{Z}^{\chi}_{n}$, $\bar{c}_n$, $\bar{c}^{\chi}_{n}$, $\left(\partial\bar{G}/\partial\bar{\boldsymbol{S}}\right)_n$, $\left(\partial\bar{G}^{\chi}/\partial\left(\bar{\boldsymbol{\Sigma}} - \bar{\boldsymbol{S}}\right)\right)_n$

(1) Calculate trial values and yield functions

$$\begin{aligned}
\boldsymbol{F}^{etr} &= \boldsymbol{F}_{n+1}\boldsymbol{F}^{p-1}_{n} \\
\bar{\boldsymbol{C}}^{etr} &= \boldsymbol{F}^{etrT}\boldsymbol{F}^{etr} \\
\bar{\boldsymbol{E}}^{etr} &= \left(\bar{\boldsymbol{C}}^{etr} - \mathbf{1}\right) \\
\boldsymbol{\chi}^{etr} &= \boldsymbol{\chi}_{n+1}\boldsymbol{\chi}^{p-1}_{n} \\
\boldsymbol{\Psi}^{etr} &= \boldsymbol{F}^{etrT}\boldsymbol{\chi}^{etr} \\
\boldsymbol{E}^{etr} &= \boldsymbol{\Psi}^{etr} - \mathbf{1} \\
\text{Calculate} \quad & \bar{\boldsymbol{S}}^{tr}, \left(\bar{\boldsymbol{\Sigma}}^{tr} - \bar{\boldsymbol{S}}^{tr}\right)
\end{aligned}$$

For separate plasticity:

$$\begin{aligned}
\bar{F}^{tr} &= \bar{F}\left(\bar{\boldsymbol{S}}^{tr}, \bar{\boldsymbol{E}}^{etr}, \bar{\boldsymbol{\mathcal{E}}}^{etr}, \bar{c}_n\right) \\
\bar{F}^{\chi,tr} &= \bar{F}^{\chi}\left(\left(\bar{\boldsymbol{\Sigma}}^{tr} - \bar{\boldsymbol{S}}^{tr}\right), \bar{\boldsymbol{E}}^{etr}, \bar{\boldsymbol{\mathcal{E}}}^{etr}, \bar{c}^{\chi}_{n}\right)
\end{aligned}$$

For combined plasticity:

$$\bar{F}^{tr} = \bar{F}\left(\bar{\boldsymbol{S}}^{tr}, \left(\bar{\boldsymbol{\Sigma}}^{tr} - \bar{\boldsymbol{S}}^{tr}\right), \bar{\boldsymbol{E}}^{etr}, \bar{\boldsymbol{\mathcal{E}}}^{etr}, \bar{c}_n, \bar{c}_n^{\chi}\right)$$

(2) Integrate plastic part of deformation gradient $\boldsymbol{F}_{n+1}^{p}$ and micro deformation tensor $\boldsymbol{\chi}_{n+1}^{p}$:

$$\bar{\boldsymbol{C}}_n^e \dot{\boldsymbol{F}}_{n+1}^{p} \boldsymbol{F}_n^{p-1} = \dot{\bar{\gamma}}_{n+1} \left(\frac{\partial \bar{G}}{\partial \bar{\boldsymbol{S}}^{tr}}\right)_n^T \tag{7.93}$$

$$\boldsymbol{F}_{n+1}^{p} = \left[\boldsymbol{F}_n^{p} + \Delta\bar{\gamma}\bar{\boldsymbol{C}}_n^{e-1}\left(\frac{\partial \bar{G}}{\partial \bar{\boldsymbol{S}}^{tr}}\right)_n^T \boldsymbol{F}_n^{p}\right] \tag{7.94}$$

$$\bar{\boldsymbol{\Psi}}_n^e \dot{\boldsymbol{\chi}}_{n+1}^{p} \boldsymbol{\chi}_n^{p-1} \bar{\boldsymbol{C}}_n^{\chi,e} \bar{\boldsymbol{\Psi}}_n^{eT} = \dot{\bar{\gamma}}_{n+1}^{\chi} \left(\frac{\partial \bar{G}^{\chi}}{\partial\left(\bar{\boldsymbol{\Sigma}} - \bar{\boldsymbol{S}}\right)}\right)_n^T \tag{7.95}$$

$$\boldsymbol{\chi}_{n+1}^{p} = \left[\boldsymbol{\chi}_n^{p} + \Delta\bar{\gamma}^{\chi}\bar{\boldsymbol{\Psi}}_n^{e-1}\left(\frac{\partial \bar{G}^{\chi}}{\partial\left(\bar{\boldsymbol{\Sigma}} - \bar{\boldsymbol{S}}\right)}\right)_n^T \bar{\boldsymbol{\Psi}}_n^{e-T} \bar{\boldsymbol{C}}_n^{\chi,e} \boldsymbol{\chi}_n^{p}\right] \tag{7.96}$$

(3) Update elastic deformation:

$$\boldsymbol{F}_{n+1}^{e} = \boldsymbol{F}_{n+1}\boldsymbol{F}_{n+1}^{p-1}, \quad \bar{\boldsymbol{C}}_{n+1}^{e} = \boldsymbol{F}_{n+1}^{eT}\boldsymbol{F}_{n+1}^{e}, \quad \bar{\boldsymbol{E}}_{n+1}^{e} = \left(\bar{\boldsymbol{C}}_{n+1}^{e} - \bar{\mathbf{1}}\right)/2 \tag{7.97}$$

$$\boldsymbol{\chi}_{n+1}^{e} = \boldsymbol{\chi}_{n+1}\boldsymbol{\chi}_{n+1}^{p-1}, \quad \bar{\boldsymbol{\Psi}}_{n+1}^{e} = \boldsymbol{F}_{n+1}^{eT}\boldsymbol{\chi}_{n+1}^{e}, \quad \bar{\boldsymbol{\mathcal{E}}}_{n+1}^{e} = \bar{\boldsymbol{\Psi}}_{n+1}^{e} - \bar{\mathbf{1}} \tag{7.98}$$

(4) Update stresses:

$$\bar{\boldsymbol{S}}_{n+1} = \bar{\boldsymbol{S}}\left(\bar{\boldsymbol{E}}_{n+1}^{e}, \bar{\boldsymbol{\mathcal{E}}}_{n+1}^{e}\right), \quad \left(\bar{\boldsymbol{\Sigma}} - \bar{\boldsymbol{S}}\right)_{n+1} = \left(\bar{\boldsymbol{\Sigma}} - \bar{\boldsymbol{S}}\right)\left(\bar{\boldsymbol{E}}_{n+1}^{e}, \bar{\boldsymbol{\mathcal{E}}}_{n+1}^{e}\right) \tag{7.99}$$

(5) Integrate strain-like ISVs, then update stress-like ISVs $\bar{c}$ and $\bar{c}^{\chi}$:

For separate plasticity:

$$\bar{c}_{n+1} = \bar{c}_n + \left(\Delta\bar{\gamma}\right) H^{c} h_n^{c} \tag{7.100}$$

$$\bar{c}_{n+1}^{\chi} = \bar{c}_n^{\chi} + \left(\Delta\bar{\gamma}\right)^{\chi} H^{c,\chi} h_n^{c,\chi} \tag{7.101}$$

For combined plasticity:

$$\bar{c}_{n+1} = \bar{c}_n + (\Delta\bar{\gamma})\, H^c h_n^c \tag{7.102}$$

$$\bar{c}^{\chi}_{n+1} = \bar{c}^{\chi}_n + (\Delta\bar{\gamma})\, H^{c,\chi} h_n^{c,\chi} \tag{7.103}$$

As expressed previously, in intermediate configuration assumption, we have $\boldsymbol{F} = \boldsymbol{F}^e\boldsymbol{F}^p$ and $\boldsymbol{\chi} = \boldsymbol{\chi}^e\boldsymbol{\chi}^p$.

For separate plasticity assumption, if we linearize these expressions, we get:

$$\boldsymbol{F}^e = \boldsymbol{F}\boldsymbol{F}^{p-1} \tag{7.104}$$

$$\delta\boldsymbol{F}^e = \delta\boldsymbol{F}\boldsymbol{F}^{p-1} + \boldsymbol{F}\delta\left(\boldsymbol{F}^{p-1}\right) \tag{7.105}$$

$$= \delta\boldsymbol{F}\boldsymbol{F}^{p-1} - \boldsymbol{F}\boldsymbol{F}^{p-1}\delta\left(\boldsymbol{F}^p\right)\boldsymbol{F}^{p-1} \tag{7.106}$$

where

$$\delta\boldsymbol{F}^p = \bar{\boldsymbol{C}}_n^{e-1}\left(\frac{\partial\bar{G}}{\partial\bar{\boldsymbol{S}}}\right)_n^T \boldsymbol{F}_n^p\delta\left(\Delta\bar{\gamma}\right) \tag{7.107}$$

then,

$$\delta\boldsymbol{F}^e = \frac{\partial\delta\boldsymbol{u}}{\partial\boldsymbol{X}}\boldsymbol{F}^{p-1} - \boldsymbol{F}^e\bar{\boldsymbol{C}}_n^{e-1}\left(\frac{\partial\bar{G}}{\partial\bar{\boldsymbol{S}}}\right)_n^T \boldsymbol{F}_n^p\boldsymbol{F}^{p-1}\delta\left(\Delta\bar{\gamma}\right) \tag{7.108}$$

Similarly,

$$\boldsymbol{\chi}^e = \boldsymbol{\chi}\boldsymbol{\chi}^{p-1} \tag{7.109}$$

$$\delta\boldsymbol{\chi}^e = \delta\boldsymbol{\chi}\boldsymbol{\chi}^{p-1} + \boldsymbol{\chi}\delta\left(\boldsymbol{\chi}^{p-1}\right) \tag{7.110}$$

$$= \delta\boldsymbol{\chi}\boldsymbol{\chi}^{p-1} - \boldsymbol{\chi}\boldsymbol{\chi}^{p-1}\delta\left(\boldsymbol{\chi}^p\right)\boldsymbol{\chi}^{p-1} \tag{7.111}$$

where

$$\delta\boldsymbol{\chi}^p = \bar{\boldsymbol{\Psi}}_n^{e-1}\left(\frac{\partial\bar{G}^{\chi}}{\partial\left(\bar{\boldsymbol{\Sigma}} - \bar{\boldsymbol{S}}\right)}\right)_n^T \bar{\boldsymbol{\Psi}}_n^{e-T}\bar{\boldsymbol{C}}_n^{\chi,e}\boldsymbol{\chi}_n^p\delta\left(\Delta\bar{\gamma}^{\chi}\right) \tag{7.112}$$

then,

$$\delta\boldsymbol{\chi}^e = \delta\boldsymbol{\Phi}\ \boldsymbol{\chi}^{p-1} - \boldsymbol{\chi}^e\bar{\boldsymbol{\Psi}}_n^{e-1}\left(\frac{\partial\bar{G}^{\chi}}{\partial\left(\bar{\boldsymbol{\Sigma}} - \bar{\boldsymbol{S}}\right)}\right)_n^T \bar{\boldsymbol{\Psi}}_n^{e-T}\bar{\boldsymbol{C}}_n^{\chi,e}\boldsymbol{\chi}_n^p\boldsymbol{\chi}^{p-1}\delta\left(\Delta\bar{\gamma}^{\chi}\right) \tag{7.113}$$

7.0.8 Contribution to global consistent tangent from plasticity

In addition to the terms which were previously determined in the global consistent tangent, we just give the additional terms which will contribute to the global consistent tangent when plasticity is introduced. Hence, the additional terms will be from the terms including $\delta\left(\Delta\bar{\gamma}\right)$ and/or $\delta\left(\Delta\bar{\gamma}^{\chi}\right)$. Starting with the balance of linear momentum, if we write the constitutive equation in intermediate configuration and apply linearization process with respect to reference configuration, and also if we ignore the boundary term, the body force vector, and the acceleration vector, we get:

$$\begin{aligned}
&\int_{\mathcal{B}_0} J^p \boldsymbol{\nabla w} : \left(\boldsymbol{F}^e \bar{\boldsymbol{S}} \boldsymbol{F}^{eT}\right) dV + \delta\left(\int_{\mathcal{B}_0} J^p \boldsymbol{\nabla w} : \left(\boldsymbol{F}^e \bar{\boldsymbol{S}} \boldsymbol{F}^{eT}\right) dV\right) \\
&= \int_{\mathcal{B}_0} J^p \boldsymbol{\nabla w} : \left(\boldsymbol{F}^e \bar{\boldsymbol{S}} \boldsymbol{F}^{eT}\right) dV \\
&+ \int_{\mathcal{B}_0} J^p \left(\delta\left(\boldsymbol{\nabla w}\right) : \left(\boldsymbol{F}^e \bar{\boldsymbol{S}} \boldsymbol{F}^{eT}\right) + \delta\left(J^p\right) \boldsymbol{\nabla w} : \left(\boldsymbol{F}^e \bar{\boldsymbol{S}} \boldsymbol{F}^{eT}\right) + J^p \boldsymbol{\nabla w} : \left(\delta\left(\boldsymbol{F}^e\right) \bar{\boldsymbol{S}} \boldsymbol{F}^{eT}\right)\right. \\
&\left. + J^p \boldsymbol{\nabla w} : \left(\boldsymbol{F}^e \delta\left(\bar{\boldsymbol{S}}\right) \boldsymbol{F}^{eT}\right) + J^p \boldsymbol{\nabla w} : \left(\boldsymbol{F}^e \bar{\boldsymbol{S}} \delta\left(\boldsymbol{F}^{eT}\right)\right)\right) dV = 0
\end{aligned} \tag{7.114}$$

where

$$\delta\left(\boldsymbol{\nabla w}\right) = \left(\boldsymbol{\nabla}_0 \boldsymbol{w}\right) \delta \boldsymbol{F}^{-1} = -\left(\boldsymbol{\nabla}_0 \boldsymbol{w}\right) \boldsymbol{F}^{-1} \delta \boldsymbol{F} \boldsymbol{F}^{-1} \tag{7.115}$$

$$\delta\left(\det \boldsymbol{F}^p\right) = \det \boldsymbol{F}^p \mathrm{tr}\left(\boldsymbol{F}^{p-1} \delta \boldsymbol{F}^p\right) = J^p \mathrm{tr}\left(\boldsymbol{F}^{p-1} \delta \boldsymbol{F}^p\right) \tag{7.116}$$

where $\boldsymbol{\nabla}_0\left(\bullet\right) = \boldsymbol{GRAD}\left(\bullet\right) = \left[\left(\bullet\right)_{,K}\right]$ and we used the Piola transform as:

$$\boldsymbol{\sigma} = \frac{1}{J^e} \boldsymbol{F}^e \bar{\boldsymbol{S}} \boldsymbol{F}^{eT},\ dv = J^e d\bar{V} \tag{7.117}$$

Then, we employ equations 7.107, 7.108, and 7.113 also insert them into equation 7.114 as:

$$\begin{aligned}
&\int_{\mathcal{B}_0} \left[(\boldsymbol{\nabla}_0 \boldsymbol{w})\, \boldsymbol{F}^{-1}\right] : J^p \boldsymbol{F}^e \bar{\boldsymbol{S}} \boldsymbol{F}^{eT} dV + \int_{\mathcal{B}_0} \left(- \left[(\boldsymbol{\nabla}_0 \boldsymbol{w})\, \boldsymbol{F}^{-1} \left(\frac{\partial \delta \boldsymbol{u}}{\partial \boldsymbol{X}}\right) \boldsymbol{F}^{-1}\right] : \left(J^p \boldsymbol{F}^e \bar{\boldsymbol{S}} \boldsymbol{F}^{eT}\right) \right. \\
&+ \left[(\boldsymbol{\nabla}_0 \boldsymbol{w})\, \boldsymbol{F}^{-1}\right] : \left(J^p \mathrm{tr} \left(\boldsymbol{F}^{p-1} \bar{\boldsymbol{C}}_n^{e-1} \left(\frac{\partial \bar{G}}{\partial \bar{\boldsymbol{S}}}\right)_n^T \boldsymbol{F}_n^p \right) \boldsymbol{F}^e \bar{\boldsymbol{S}} \boldsymbol{F}^{eT} \delta\left(\Delta \bar{\gamma}\right) \right) \\
&+ \left[(\boldsymbol{\nabla}_0 \boldsymbol{w})\, \boldsymbol{F}^{-1}\right] : \left(J^p \left(\frac{\partial \delta \boldsymbol{u}}{\partial \boldsymbol{X}} \boldsymbol{F}^{p-1} - \boldsymbol{F}^e \bar{\boldsymbol{C}}_n^{e-1} \left(\frac{\partial \bar{G}}{\partial \bar{\boldsymbol{S}}}\right)_n^T \boldsymbol{F}_n^p \boldsymbol{F}^{p-1} \right) \bar{\boldsymbol{S}} \boldsymbol{F}^{eT} \delta\left(\Delta \bar{\gamma}\right) \right) \\
&+ \left[(\boldsymbol{\nabla}_0 \boldsymbol{w})\, \boldsymbol{F}^{-1}\right] : \left(J^p \boldsymbol{F}^e \delta\left(\bar{\boldsymbol{S}}\right) \boldsymbol{F}^{eT}\right) \\
&+ \left. \left[(\boldsymbol{\nabla}_0 \boldsymbol{w})\, \boldsymbol{F}^{-1}\right] : \left(J^p \boldsymbol{F}^e \bar{\boldsymbol{S}} \left(\frac{\partial \delta \boldsymbol{u}}{\partial \boldsymbol{X}} \boldsymbol{F}^{p-1} - \boldsymbol{F}^e \bar{\boldsymbol{C}}_n^{e-1} \left(\frac{\partial \bar{G}}{\partial \bar{\boldsymbol{S}}}\right)_n^T \boldsymbol{F}_n^p \boldsymbol{F}^{p-1} \right)^T \delta\left(\Delta \bar{\gamma}\right) \right) \right) dV = 0
\end{aligned} \tag{7.118}$$

where $\delta \bar{\boldsymbol{S}}$ was defined in equation 7.55. Similarly, for the balance of first moment of momentum if we ignore the boundary term, the body couple, and the micro-spin inertia tensors, we have:

$$\begin{aligned}
&\int_{\mathcal{B}_0} \boldsymbol{\eta} : \left(\boldsymbol{F}^e \bar{\boldsymbol{\Sigma}} \boldsymbol{F}^{eT} - \boldsymbol{F}^e \bar{\boldsymbol{S}} \boldsymbol{F}^{eT}\right) J^p dV + \int_{\mathcal{B}_0} (\boldsymbol{\nabla} \boldsymbol{\eta}) \vdots \left(\boldsymbol{F}^e \left(\boldsymbol{F}^e \odot \bar{\boldsymbol{M}} \boldsymbol{\chi}^{eT}\right) J^p\right) dV \\
&+ \delta \left(\int_{\mathcal{B}_0} \boldsymbol{\eta} : \left[\boldsymbol{F}^e \bar{\boldsymbol{\Sigma}} \boldsymbol{F}^{eT} - \boldsymbol{F}^e \bar{\boldsymbol{S}} \boldsymbol{F}^{eT}\right] J^p dV + \int_{\mathcal{B}_0} (\boldsymbol{\nabla} \boldsymbol{\eta}) \vdots \left(\boldsymbol{F}^e \left(\boldsymbol{F}^e \odot \bar{\boldsymbol{M}} \boldsymbol{\chi}^{eT}\right) J^p\right) dV \right) = 0
\end{aligned} \tag{7.119}$$

carrying over the calculations gives:

$$\begin{aligned}
&\int_{\mathcal{B}_0} \boldsymbol{\eta} : \left(\boldsymbol{F}^e \bar{\boldsymbol{\Sigma}} \boldsymbol{F}^{eT} - \boldsymbol{F}^e \bar{\boldsymbol{S}} \boldsymbol{F}^{eT}\right) J^p dV + \int_{\mathcal{B}_0} (\boldsymbol{\nabla} \boldsymbol{\eta}) \vdots \left(\boldsymbol{F}^e \left(\boldsymbol{F}^e \odot \bar{\boldsymbol{M}} \boldsymbol{\chi}^{eT}\right) J^p\right) dV \\
&\int_{\mathcal{B}_0} \left(\boldsymbol{\eta} : \left(\delta \boldsymbol{F}^e \left(\bar{\boldsymbol{\Sigma}} - \bar{\boldsymbol{S}}\right) \boldsymbol{F}^{eT} J^p\right) + \boldsymbol{\eta} : \left(\boldsymbol{F}^e \delta \left(\bar{\boldsymbol{\Sigma}} - \bar{\boldsymbol{S}}\right) \boldsymbol{F}^{eT} J^p\right) + \boldsymbol{\eta} : \left(\boldsymbol{F}^e \left(\bar{\boldsymbol{\Sigma}} - \bar{\boldsymbol{S}}\right) \delta \boldsymbol{F}^{eT} J^p\right) \right. \\
&+ \boldsymbol{\eta} : \left(\boldsymbol{F}^e \left(\bar{\boldsymbol{\Sigma}} - \bar{\boldsymbol{S}}\right) \boldsymbol{F}^{eT}\right) \delta\left(J^p\right)\Big) dV + \int_{\mathcal{B}_0} \left(\delta (\boldsymbol{\nabla} \boldsymbol{\eta}) \vdots \left(\boldsymbol{F}^e \left(\boldsymbol{F}^e \odot \bar{\boldsymbol{M}} \boldsymbol{\chi}^{eT}\right)\right) J^p \right. \\
&+ (\boldsymbol{\nabla} \boldsymbol{\eta}) \vdots \left(\delta \boldsymbol{F}^e \left(\boldsymbol{F}^e \odot \bar{\boldsymbol{M}} \boldsymbol{\chi}^{eT}\right)\right) J^p + (\boldsymbol{\nabla} \boldsymbol{\eta}) \vdots \left(\boldsymbol{F}^e \left(\delta \boldsymbol{F}^e \odot \bar{\boldsymbol{M}} \boldsymbol{\chi}^{eT}\right)\right) J^p \\
&+ (\boldsymbol{\nabla} \boldsymbol{\eta}) \vdots \left(\boldsymbol{F}^e \left(\boldsymbol{F}^e \odot \delta \bar{\boldsymbol{M}} \boldsymbol{\chi}^{eT}\right)\right) J^p + (\boldsymbol{\nabla} \boldsymbol{\eta}) \vdots \left(\boldsymbol{F}^e \left(\boldsymbol{F}^e \odot \bar{\boldsymbol{M}} \delta \boldsymbol{\chi}^{eT}\right)\right) J^p \\
&+ \left. (\boldsymbol{\nabla} \boldsymbol{\eta}) \vdots \left(\boldsymbol{F}^e \left(\boldsymbol{F}^e \odot \bar{\boldsymbol{M}} \boldsymbol{\chi}^{eT}\right)\right) \delta J^p \right) dV = 0
\end{aligned} \tag{7.120}$$

Again, if we apply equations 7.108, 7.113, and 7.107 in equation 7.120, we get:

$$
\begin{aligned}
&\int_{\mathcal{B}_0} \boldsymbol{\eta} : \left(\boldsymbol{F}^e \bar{\boldsymbol{\Sigma}} \boldsymbol{F}^{eT} - \boldsymbol{F}^e \bar{\boldsymbol{S}} \boldsymbol{F}^{eT}\right) J^p dV + \int_{\mathcal{B}_0} (\boldsymbol{\nabla}\boldsymbol{\eta}) \vdots \left(\boldsymbol{F}^e \left(\boldsymbol{F}^e \odot \bar{\boldsymbol{M}}\boldsymbol{\chi}^{eT}\right)\right) J^p dV \\
&+ \int_{\mathcal{B}_0} \left(\boldsymbol{\eta} : \left(\left(\frac{\partial \delta \boldsymbol{u}}{\partial \boldsymbol{X}} \boldsymbol{F}^{p-1} - \boldsymbol{F}^e \bar{\boldsymbol{C}}_n^{e-1} \left(\frac{\partial \bar{G}}{\partial \bar{\boldsymbol{S}}} \right)_n^T \boldsymbol{F}_n^p \boldsymbol{F}^{p-1} \right) \left(\bar{\boldsymbol{\Sigma}} - \bar{\boldsymbol{S}}\right) \boldsymbol{F}^{eT} \right) J^p \delta\left(\Delta\bar{\gamma}\right) \right. \\
&+ \boldsymbol{\eta} : \left(\boldsymbol{F}^e \delta\left(\bar{\boldsymbol{\Sigma}} - \bar{\boldsymbol{S}}\right) \boldsymbol{F}^{eT}\right) J^p \\
&+ \boldsymbol{\eta} : \left(\boldsymbol{F}^e \left(\bar{\boldsymbol{\Sigma}} - \bar{\boldsymbol{S}}\right) \left(\frac{\partial \delta \boldsymbol{u}}{\partial \boldsymbol{X}} \boldsymbol{F}^{p-1} - \boldsymbol{F}^e \bar{\boldsymbol{C}}_n^{e-1} \left(\frac{\partial \bar{G}}{\partial \bar{\boldsymbol{S}}} \right)_n^T \boldsymbol{F}_n^p \boldsymbol{F}^{p-1} \right)^T \right) J^p \delta\left(\Delta\bar{\gamma}\right) \\
&+ \boldsymbol{\eta} : \left(\boldsymbol{F}^e \left(\bar{\boldsymbol{\Sigma}} - \bar{\boldsymbol{S}}\right) \boldsymbol{F}^{eT} J^p \mathrm{tr}\left(\boldsymbol{F}^{p-1} \bar{\boldsymbol{C}}_n^{e-1} \left(\frac{\partial \bar{G}}{\partial \bar{\boldsymbol{S}}} \right)_n^T \boldsymbol{F}_n^p \right) \right) \delta\left(\Delta\bar{\gamma}\right) \Big) dV \\
&+ \int_{\mathcal{B}_0} \left(- \left((\boldsymbol{\nabla}_0 \boldsymbol{\eta}) \boldsymbol{F}^{-1} \frac{\partial \delta \boldsymbol{u}}{\partial \boldsymbol{X}} \boldsymbol{F}^{-1} \right) \vdots \left(\boldsymbol{F}^e \left(\boldsymbol{F}^e \odot \bar{\boldsymbol{M}}\boldsymbol{\chi}^{eT}\right)\right) J^p \right. \\
&+ \left((\boldsymbol{\nabla}_0 \boldsymbol{\eta}) \boldsymbol{F}^{-1}\right) \vdots \left(\left(\frac{\partial \delta \boldsymbol{u}}{\partial \boldsymbol{X}} \boldsymbol{F}^{p-1} - \boldsymbol{F}^e \bar{\boldsymbol{C}}_n^{e-1} \left(\frac{\partial \bar{G}}{\partial \bar{\boldsymbol{S}}} \right)_n^T \boldsymbol{F}_n^p \boldsymbol{F}^{p-1} \right) \left(\boldsymbol{F}^e \odot \bar{\boldsymbol{M}}\boldsymbol{\chi}^{eT}\right) \right) J^p \delta\left(\Delta\bar{\gamma}\right) \\
&+ \left((\boldsymbol{\nabla}_0 \boldsymbol{\eta}) \boldsymbol{F}^{-1}\right) \vdots \left(\boldsymbol{F}^e \left(\left(\frac{\partial \delta \boldsymbol{u}}{\partial \boldsymbol{X}} \boldsymbol{F}^{p-1} - \boldsymbol{F}^e \bar{\boldsymbol{C}}_n^{e-1} \left(\frac{\partial \bar{G}}{\partial \bar{\boldsymbol{S}}} \right)_n^T \boldsymbol{F}_n^p \boldsymbol{F}^{p-1} \right) \odot \bar{\boldsymbol{M}}\boldsymbol{\chi}^{eT} \right) \right) J^p \delta\left(\Delta\bar{\gamma}\right) \\
&+ \left((\boldsymbol{\nabla}_0 \boldsymbol{\eta}) \boldsymbol{F}^{-1}\right) \vdots \left(\boldsymbol{F}^e \left(\boldsymbol{F}^e \odot \delta\bar{\boldsymbol{M}}\boldsymbol{\chi}^{eT}\right)\right) J^p \\
&+ \left((\boldsymbol{\nabla}_0 \boldsymbol{\eta}) \boldsymbol{F}^{-1}\right) \vdots \left(\boldsymbol{F}^e \left(\boldsymbol{F}^e \odot \bar{\boldsymbol{M}} \left(\delta\boldsymbol{\Phi}\, \boldsymbol{\chi}^{p-1} - \boldsymbol{\chi}^e \bar{\boldsymbol{\Psi}}_n^{e-1} \left(\frac{\partial \bar{G}^\chi}{\partial \left(\bar{\boldsymbol{\Sigma}} - \bar{\boldsymbol{S}}\right)} \right)_n^T \right. \right. \right. \\
&\left. \left. \left. \bar{\boldsymbol{\Psi}}_n^{e-T} \bar{\boldsymbol{C}}_n^{\chi,e} \boldsymbol{\chi}_n^p \boldsymbol{\chi}^{p-1} \right)^T \right) \right) J^p \delta\left(\Delta\bar{\gamma}^\chi\right) \\
&\left. + \left((\boldsymbol{\nabla}_0 \boldsymbol{\eta}) \boldsymbol{F}^{-1}\right) \vdots \left(\boldsymbol{F}^e \left(\boldsymbol{F}^e \odot \bar{\boldsymbol{M}}\boldsymbol{\chi}^{eT}\right)\right) J^p \mathrm{tr}\left(\boldsymbol{F}^{p-1} \bar{\boldsymbol{C}}_n^{e-1} \left(\frac{\partial \bar{G}}{\partial \bar{\boldsymbol{S}}} \right)_n^T \boldsymbol{F}_n^p \right) \delta\left(\Delta\bar{\gamma}\right) \right) dV = 0
\end{aligned}
\tag{7.121}
$$

where $\delta\left(\bar{\boldsymbol{\Sigma}} - \bar{\boldsymbol{S}}\right)$ was defined in equation 7.63. Definition of $\delta\bar{\boldsymbol{M}}$ requires to determine $\delta\left(\bar{\boldsymbol{\nabla}}\boldsymbol{\chi}^e\right)$ which can be found as:

$$
\chi^e_{i\bar{A},\bar{L}} = \chi_{iK,L} F^{p-1}_{L\bar{L}} \chi^{p-1}_{K\bar{A}} - \chi^e_{i\bar{R}} \chi^p_{\bar{R}B,L} F^{p-1}_{L\bar{L}} \chi^{p-1}_{B\bar{A}} \tag{7.122}
$$

The constitutive assumption which considers the gradient of the micro-deformation tensor $\boldsymbol{\nabla}_0\boldsymbol{\chi}^p$ as a separate variable results in very complicated linearization process; therefore, we

will assume that $\boldsymbol{\nabla}_0\boldsymbol{\chi}^p = \mathbf{0}$ and derive the relations based on this assumption. Then, the equation above reduces to:

$$\begin{aligned}
\bar{\boldsymbol{\nabla}}\boldsymbol{\chi}^e &= \boldsymbol{\nabla}_0\boldsymbol{\chi}\boldsymbol{F}^{p-1}\boldsymbol{\chi}^{p-1} \\
\delta\left(\bar{\boldsymbol{\nabla}}\boldsymbol{\chi}^e\right) &= \boldsymbol{\nabla}_0\delta\boldsymbol{\Phi}\boldsymbol{F}^{p-1}\,\boldsymbol{\chi}^{p-1} - \left(\boldsymbol{\nabla}_0\boldsymbol{\chi}\right)\boldsymbol{F}^{p-1}\bar{\boldsymbol{C}}_n^{e-1}\left(\frac{\partial\bar{G}}{\partial\bar{\boldsymbol{S}}}\right)_n^T\boldsymbol{F}_n^p\boldsymbol{F}^{p-1}\boldsymbol{\chi}^{p-1}\delta\left(\Delta\bar{\gamma}\right) \\
&\quad - \left(\boldsymbol{\nabla}_0\boldsymbol{\chi}\right)\boldsymbol{F}^{p-1}\boldsymbol{\chi}^{p-1}\bar{\boldsymbol{\Psi}}_n^{e-1}\left(\frac{\partial\bar{G}^\chi}{\partial\left(\bar{\boldsymbol{\Sigma}}-\bar{\boldsymbol{S}}\right)}\right)_n^T\bar{\boldsymbol{\Psi}}_n^{e-T}\bar{\boldsymbol{C}}_n^{\chi,e}\boldsymbol{\chi}_n^p\boldsymbol{\chi}^{p-1}\delta\left(\Delta\bar{\gamma}^\chi\right)
\end{aligned} \tag{7.123}$$

This gives us the simplified definition of $\delta\bar{\boldsymbol{M}}$ as:

$$\delta\bar{\boldsymbol{M}} = \tau_7\delta\boldsymbol{F}^{eT}\bar{\boldsymbol{\nabla}}\boldsymbol{\chi}^e + \tau_7\boldsymbol{F}^{eT}\delta\left(\bar{\boldsymbol{\nabla}}\boldsymbol{\chi}^e\right) \tag{7.124}$$

where $\delta\boldsymbol{F}^e$ and $\delta\left(\bar{\boldsymbol{\nabla}}\boldsymbol{\chi}^e\right)$ were defined in equations 7.108 and 7.123 respectively.

As mentioned above, additional contribution to the global consistent tangent will come from the terms which include $\delta\left(\Delta\bar{\gamma}\right)$ and/or $\delta\left(\Delta\bar{\gamma}^\chi\right)$. The definitions $\delta\left(\Delta\bar{\gamma}\right)$ and $\delta\left(\Delta\bar{\gamma}^\chi\right)$ depend on which plasticity approach we use. If we use separate scale plasticity, these definitions will be obtained as described in Section 7.0.4, and if we use combined plasticity we obtain those definitions as described in Section 7.0.6.

7.1 Numerical Examples

In this section, we present some examples to demonstrate the micromorphic Drucker-Prager plasticity and Drucker-Prager-like plasticity. We chose different yield functions as well as plastic potential functions accordingly to account for the behavior of geomaterials. As mentioned in detail above, we assumed three different yield criteria: (1) Standard Drucker-Prager (DP) yield function which involves no micromorphic terms ($\boldsymbol{\Phi}^h = \mathbf{0}$ in governing equations, and balance of first moment of momentum is not solved); (2) Macro-scale DP yield function (MDP) which has the same form of DP yield criterion but involves the second Piola-Kirchhoff stress tensor $\bar{\boldsymbol{S}}$ including additional micromorphic elastic terms; (3) Combined DP like yield function (CDP) that involves the combination of the second Piola-Kirchhoff stress

tensor $\bar{\boldsymbol{S}}$ and the relative stress tensor $\left(\bar{\boldsymbol{\Sigma}} - \bar{\boldsymbol{S}}\right)$ measures, along with micromorphic elastic terms.

7.2 Finite Strain Column Compression with Different Yield Criteria

We start with a one dimensional column example: uniaxial strain in compression. The column geometry considered in this section was previously described in detail in Section 6.2.4 shown in Fig 6.8. We use a similar geometry with the boundary conditions and present a comparison of the results obtained by using different yield functions on this one dimensional example and also investigate the effect of elastic length scale on this geometry as well as the influence of micromorphic boundary conditions on the simulations. The elastic parameters used in this column example are chosen as

$$\begin{aligned} &\lambda = 29.10^3 \text{ kPa} \quad \mu = 7.10^3 \text{ kPa} \quad \eta = 40.10^3 \text{ kPa} \\ &\nu = 8.10^3 \text{ kPa} \quad \kappa = 10.10^3 \text{ kPa} \quad \tau = 10.10^3 \text{ kPa} \quad \sigma = 5.10^3 \text{ kPa} \end{aligned} \tag{7.125}$$

Discussion of the results regarding this example is given in Section 7.2.4.

7.2.1 Case 1

In the first case, the column has a height of 10 m and a cross section of $1.25 \times 1.25\ m^2$. A displacement boundary condition $u_3 = -1\ m$ is applied to the top surface at $X_3 = 10m$. The displacement boundary conditions were chosen to provide a uniaxial strain compression problem: $u_1 = 0$ on $\pm X_1$ faces, $u_2 = 0$ on $\pm X_2$ faces, and $u_3 = 0$ on $-X_3$ face. All the micro-displacement tensor components Φ^h_{iI} are set $= 0$ except the micro-displacement tensor component Φ^h_{33} in the X_3 direction. In figures 7.2, 7.5, and 7.8 , we show the stress paths which were obtained by the different yield function assumptions. We demonstrate the initial yield surface with F_0 and final yield surface with F. We plot using the stress measures S_c,

S_m, and S_s versus pressure terms $\bar{p}_c$, $\bar{p}_m$, and $\bar{p}$ respectively. These terms are defined as:

$$S_c = \left(\text{dev}\bar{\boldsymbol{S}} : \text{dev}\bar{\boldsymbol{S}} + \text{dev}(\bar{\boldsymbol{\Sigma}} - \bar{\boldsymbol{S}}) : \text{dev}(\bar{\boldsymbol{\Sigma}} - \bar{\boldsymbol{S}})\right)^{\frac{1}{2}} \tag{7.126}$$

$$S_m = S_s = \|\text{dev}\bar{\boldsymbol{S}}\| \tag{7.127}$$

$$\bar{p}_c = B^{\phi}\bar{p} + B^{\phi,\chi}\bar{p}^{\chi} \tag{7.128}$$

$$\bar{p}^{\chi} = \frac{\text{tr}(\bar{\boldsymbol{\Sigma}} - \bar{\boldsymbol{S}})}{3} \tag{7.129}$$

$$\bar{p}_m = \bar{p} = \frac{\text{tr}\bar{\boldsymbol{S}}}{3} \tag{7.130}$$

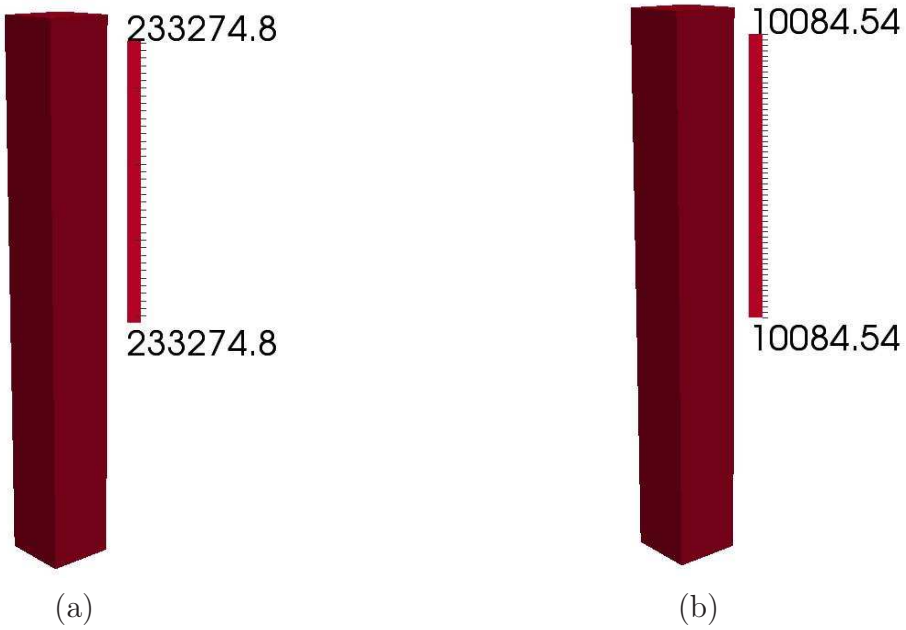

Figure 7.1: Case 1: Contour plots of (a) $||\text{dev}\boldsymbol{\sigma}||$ (Pa) and (b) cohesion c (Pa) distribution along the column height. Gauss point values extrapolated to nodes were obtained by using CDP yield criterion.

and other yield and plastic potential function parameters were chosen in Table 7.1.

Table 7.1: Parameters used in yield and plastic potential functions for column example.

ϕ (rad.)	ψ (rad.)	H^c (Pa)	c (Pa)	ϕ^{χ} (rad.)	ψ^{χ} (rad.)	$H^{c,\chi}$ (Pa)	c^{χ} (Pa)	τ_7 (Pa. m^2)
0.15	0.1	1×10^3	1×10^4	0.0	0.0	10	1×10^2	1×10^7

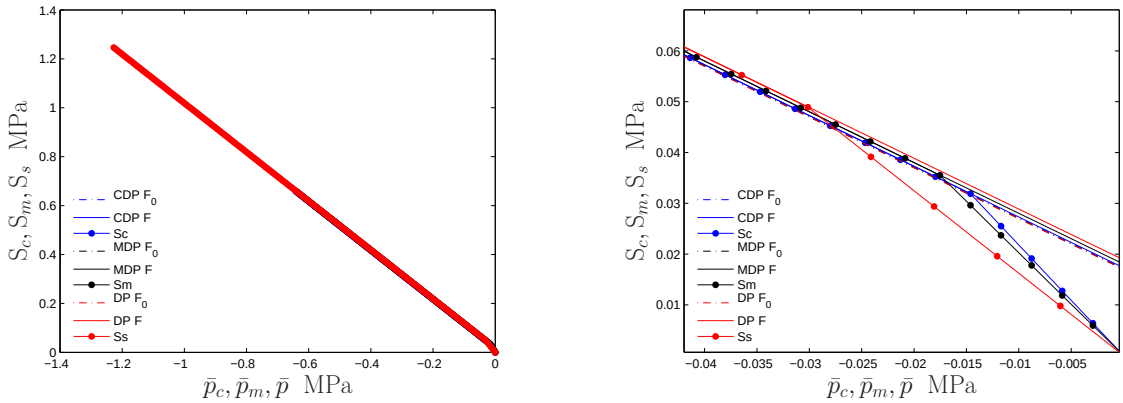

Figure 7.2: Case 1: Comparison of (a) stress paths obtained by using different yield criteria, (b) the initial parts of the stress paths that shows the different behaviors with different yield function assumptions.

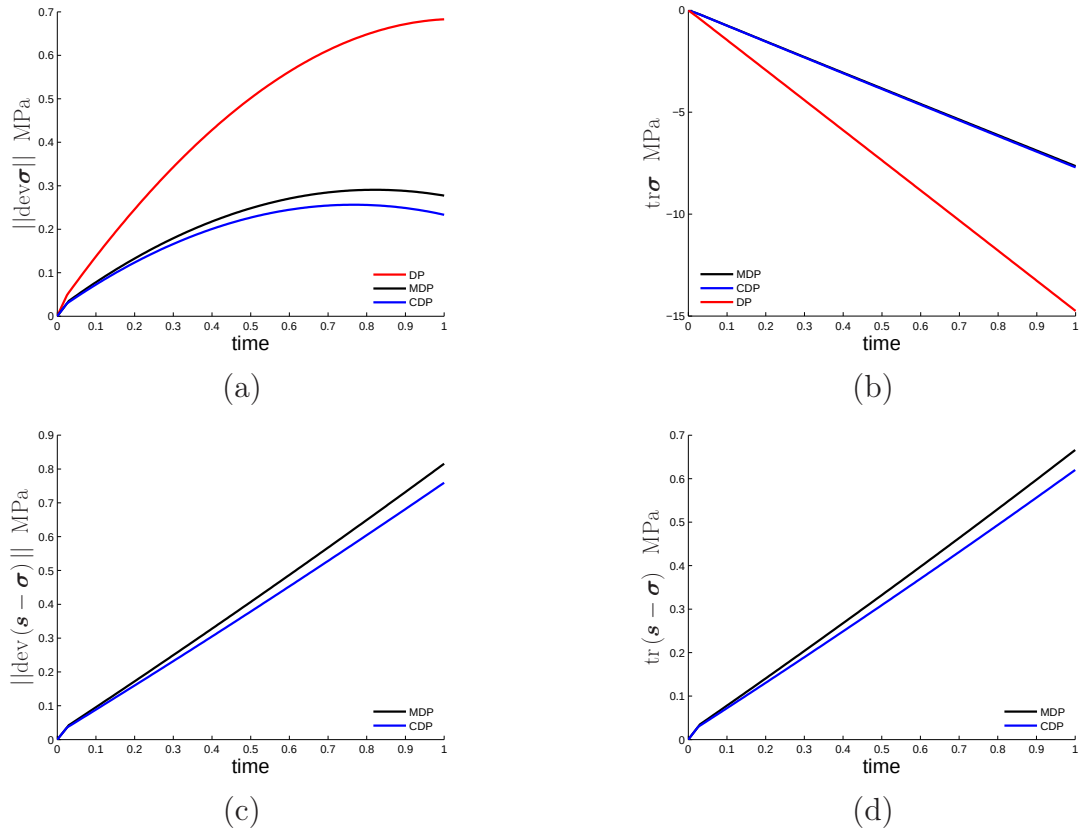

Figure 7.3: Case 1: Comparison of (a) the norm of the deviatoric part of unsymmetric Cauchy stress tensor $||\text{dev}\boldsymbol{\sigma}||$ in current configuration, (b) the first invariant of the unsymmetric Cauchy stress tensor $\text{tr}\boldsymbol{\sigma}$, (c) the deviatoric part of relative stress tensor measure $||\text{dev}(\boldsymbol{s}-\boldsymbol{\sigma})||$ in current configuration, (d) the first invariant of the relative stress tensor $\text{tr}(\boldsymbol{s}-\boldsymbol{\sigma})$.

7.2.2 Case 2

In the second case, we consider the case where $\Phi^h_{33} = 0$ at $X_3 = 0$ that creates a gradient in micro-displacement tensor Φ^h_{33} values as shown in Figure 7.4 (a); however, $\tau_7 = 0$ so that the higher order couple stress tensor will disappear due to one term approach that is explained already in Chapter 6.

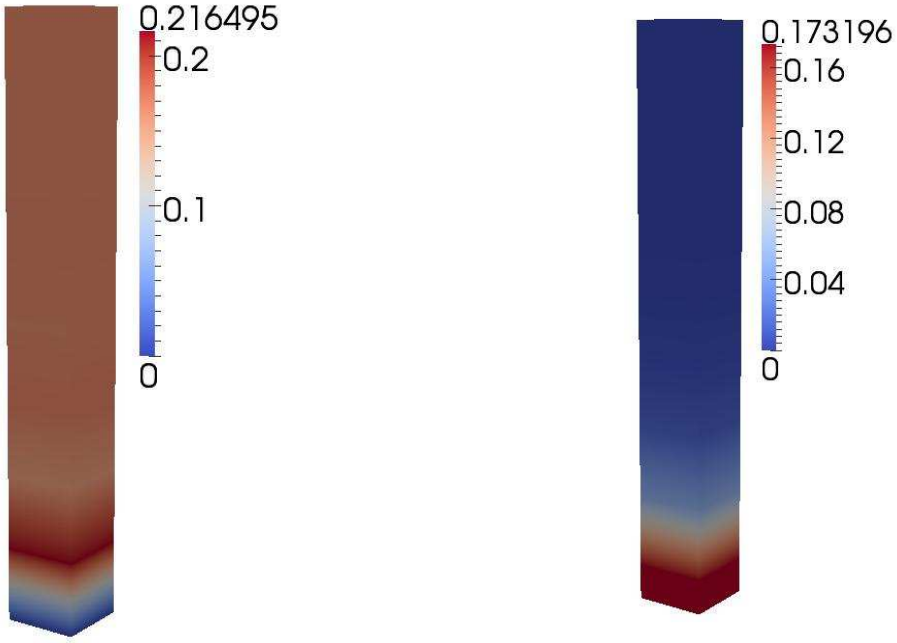

(a) (b)

Figure 7.4: Case 2: Contour plot of (a) $||\boldsymbol{\Phi}^h||$ and (b) $||\boldsymbol{\nabla}\boldsymbol{\Phi}^h||$ values at nodes obtained by using CDP yield criterion.

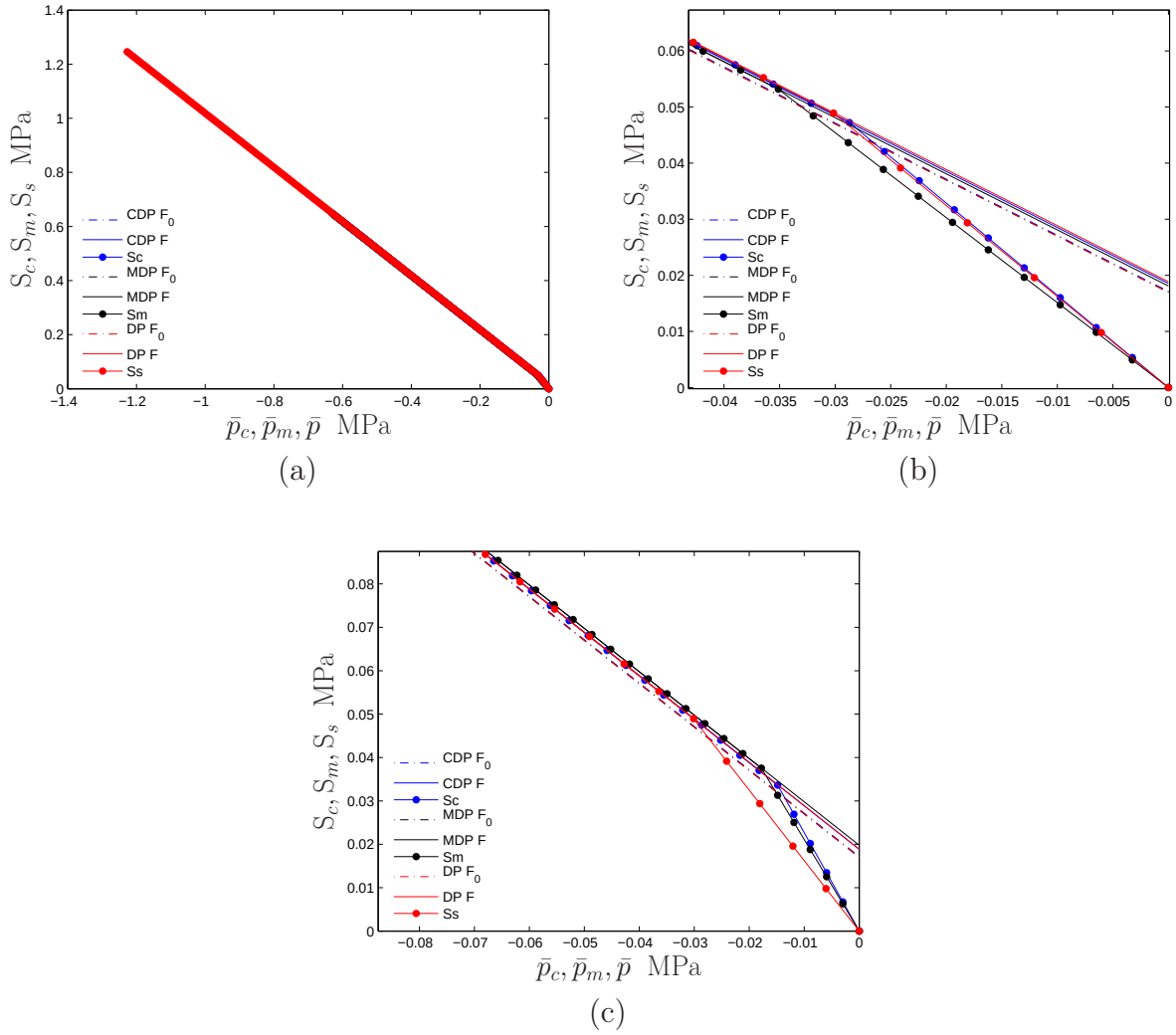

Figure 7.5: Case 2: Comparison of (a) stress paths obtained by using different yield criteria, (b) the initial parts of the stress paths that shows the different behaviors with different yield function assumptions at $X_3 = 0.14$m, (c) the initial parts of the stress at $X_3 = 1.10$m.

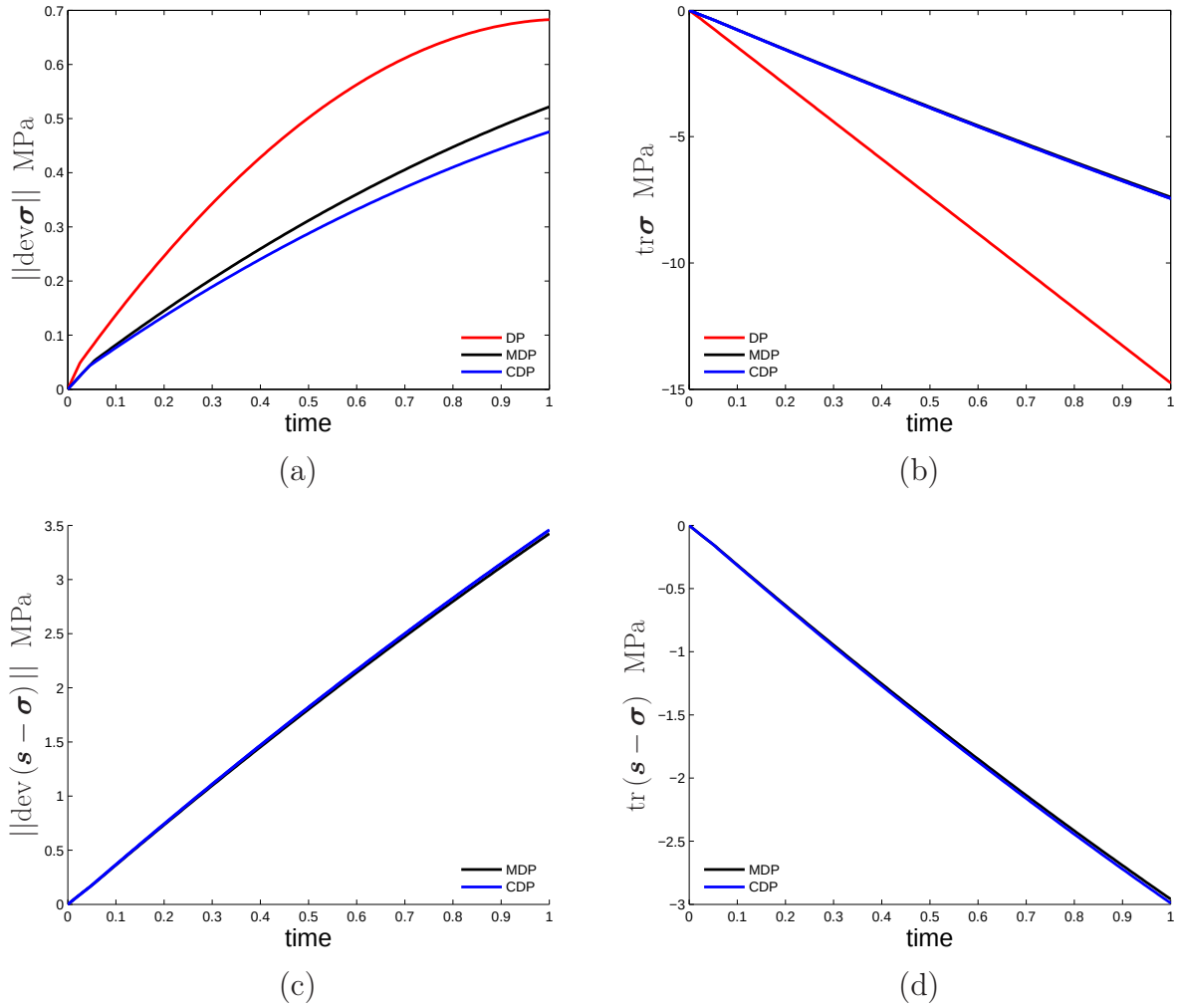

Figure 7.6: Case 2: Comparison of (a) the deviatoric part of unsymmetric Cauchy stress tensor measure $||\text{dev}\boldsymbol{\sigma}||$ in current configuration, (b) the first invariant of the unsymmetric Cauchy stress tensor $\text{tr}\boldsymbol{\sigma}$, (c) the deviatoric part of relative stress tensor norm $||\text{dev}\,(\boldsymbol{s}-\boldsymbol{\sigma})\,||$ in current configuration, (d) the first invariant of the relative stress tensor $\text{tr}\,(\boldsymbol{s}-\boldsymbol{\sigma})$ at $X_3 = 0.14$m.

7.2.3 Case 3

In the last case, we consider the same boundary condition used above but we also include the elastic length scale parameter $\ell_c = 1\text{m}$ which is introduced by τ_7. Note that, as in previous examples, we used one parameter approach for the higher order stress tensor as $\boldsymbol{M} = \tau_7 \boldsymbol{\Gamma}$. We employed the Preconditioned Conjugate Gradient method explained in A.2.2.

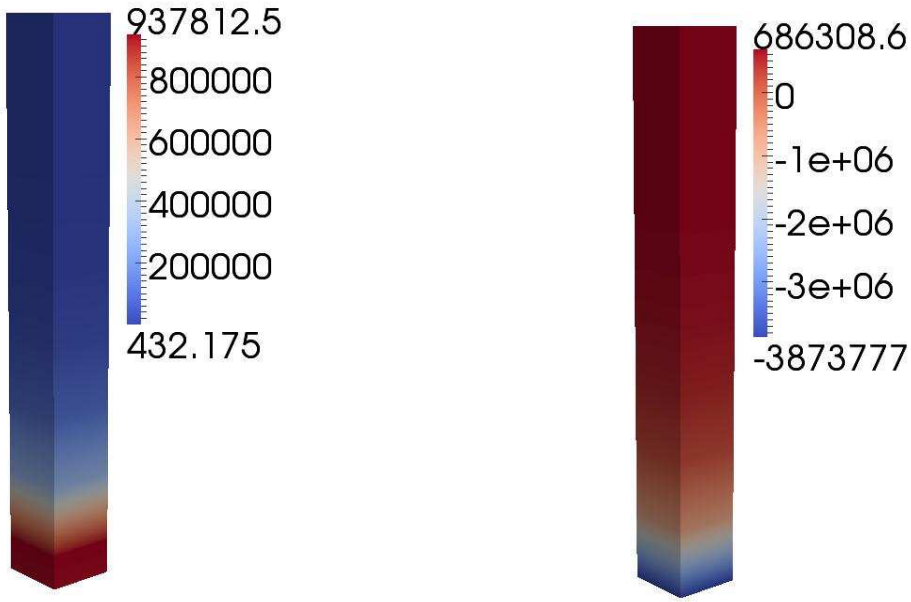

(a) (b)

Figure 7.7: Case 3: Contour plot of (a) $||\text{tr}\boldsymbol{m}||$ in Pa and (b) $\text{tr}\,(\boldsymbol{s} - \boldsymbol{\sigma})$ in Pa values at nodes obtained by using CDP yield criterion.

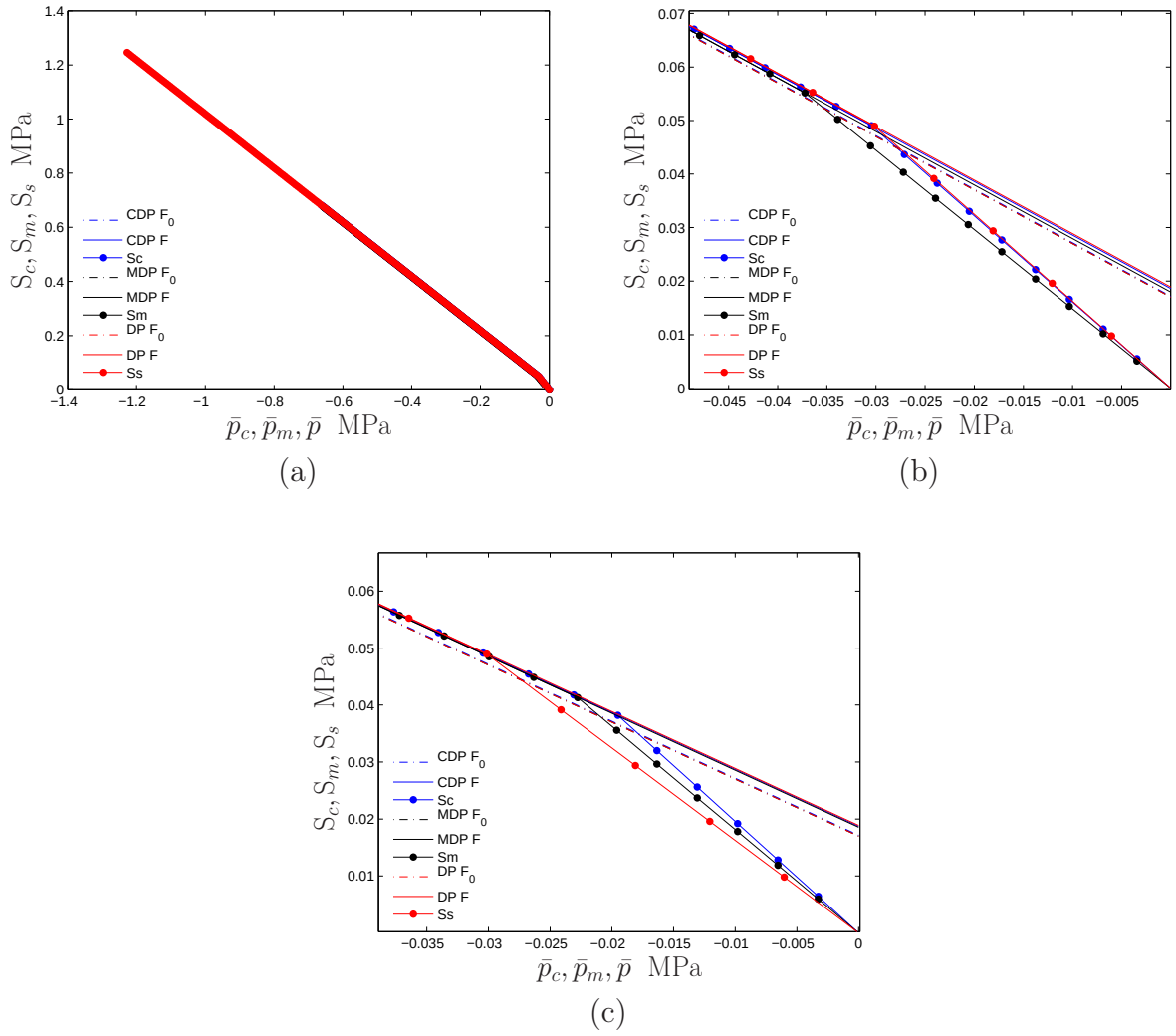

Figure 7.8: Case 3: Comparison of (a) stress paths obtained by using different yield criteria, (b) the initial parts of the stress paths that shows the different behaviors with different yield function assumptions at $X_3 = 0.14$m, (c) the initial parts of the stress at $X_3 = 1.10$m.

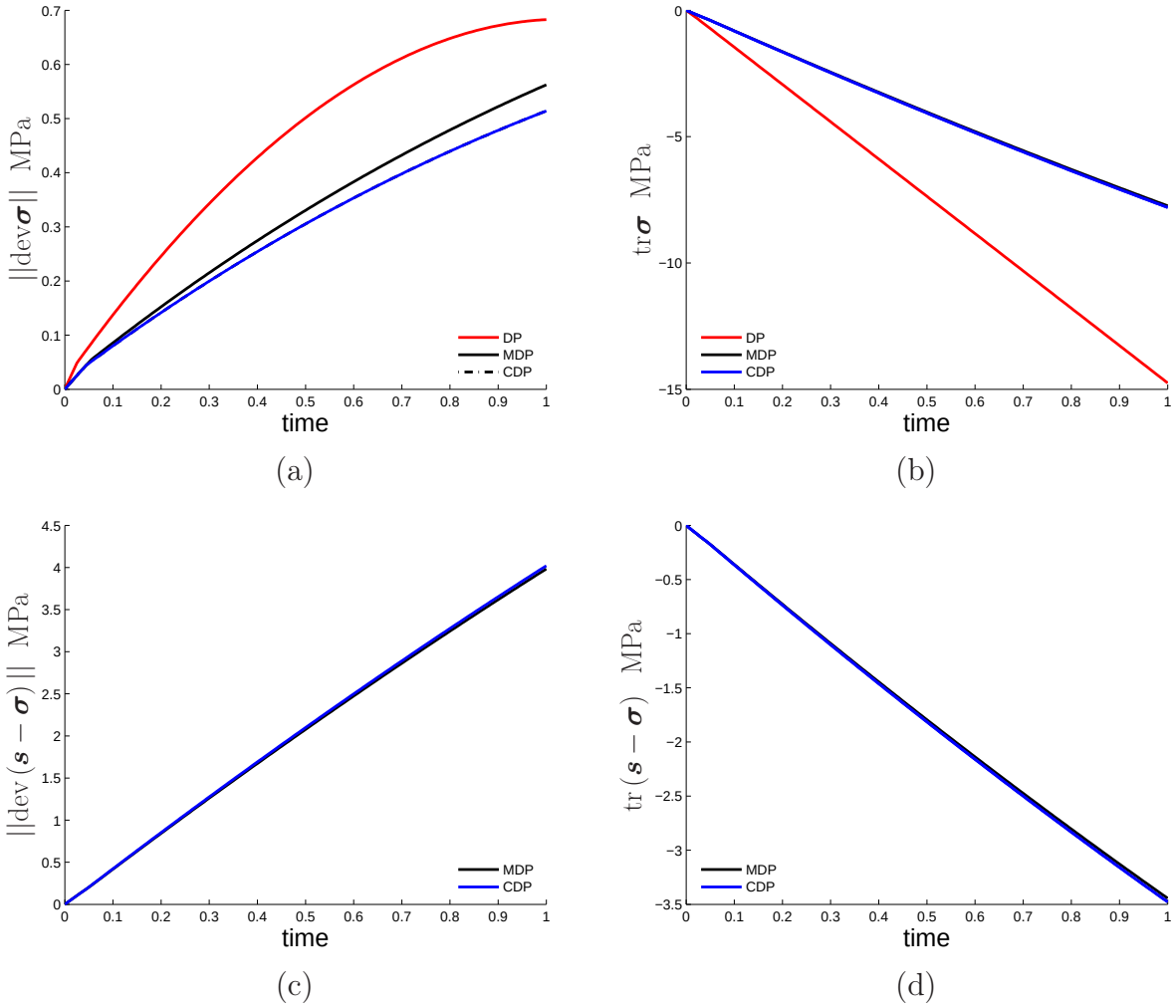

Figure 7.9: Case 3: Comparison of (a) the deviatoric part of unsymmetric Cauchy stress tensor norm $||\text{dev}\boldsymbol{\sigma}||$ in current configuration, (b) the first invariant of the unsymmetric Cauchy stress tensor $\text{tr}\boldsymbol{\sigma}$, (c) the deviatoric part of relative stress tensor measure $||\text{dev}\,(\boldsymbol{s}-\boldsymbol{\sigma})\,||$ in current configuration, (d) the first invariant of the relative stress tensor $\text{tr}\,(\boldsymbol{s}-\boldsymbol{\sigma})$ at $X_3 = 0.14$m.

7.2.4 Discussion of the results

Figure 7.1 shows that when additional micromorphic degree of freedom Φ^h_{33} is involved and there is no boundary effect, we have the homogeneous distribution of the norm of unsymmetric Cauchy stress tensor $||\text{dev}\boldsymbol{\sigma}||$ and cohesion c as expected in the standard DP model.

Figure 7.4 shows the boundary effect for Case 2. Since we do not have τ_7 for this case, the gradient in Φ^h_{33} values will not generate any value for the higher order couple stress tensor $\boldsymbol{m}$. One may think that for the region in which Φ^h_{33} is close to zero, the model should reduce to standard DP model. However, micromorphic models should present different results due to the additional micromorphic elastic moduli appearing in the constitutive equations. Note that even if there is no Φ^h_{33} involved, the micro-deformation tensor $\boldsymbol{\chi}^e = \mathbf{1}$. Since $\boldsymbol{\mathcal{E}}^e = \boldsymbol{F}^{eT}\boldsymbol{\chi}^e$ and $\boldsymbol{F}^e \neq \mathbf{0}$, then $\boldsymbol{\mathcal{E}}^e \neq \mathbf{0}$. This shows that due to coupling in strain tensors even if we set all the additional degrees of freedom to zero but involve the additional micromorphic elastic moduli, we will have different results from the standard plasticity approach as long as we have non zero $\boldsymbol{F}^e$.

Figures 7.2(a), 7.5(a), and 7.8(a) show the total stress paths comparison of all the models. A closer look at the initial parts of these paths in sections (b) and (c) of the same figures will give more insights. Figures 7.5(b) and 7.8(b) show that in the vicinity of the bottom surface boundary $X_3 = 0.14$m, the difference between CDP model and DP model vanish. However, this is valid for the stress path plots which does not necessarily indicate that models present the same behavior. Note that we plot the stress paths with S_c, S_m, and S_s vs. their associated pressure values, respectively, $\bar{p}_c$, $\bar{p}_m$, and $\bar{p}$ where the definitions were given in equations (7.128) and (7.130). If we look at the unsymmetric deviatoric Cauchy stress tensor norm $||\text{dev}\boldsymbol{\sigma}||$ as well as the relative stress tensor norm $||\text{dev}\,(\boldsymbol{s} - \boldsymbol{\sigma})\,||$, respectively, in Figures 7.10 and 7.11 in the same region, we see a noticeable difference in the behaviors.

Stress path comparison in Figures 7.2(b), 7.5(c), and 7.8(c) show that at $X_3 = 1.10$ m

as we go further from the boundary where $\Phi^h_{33} = 0$, micromorphic contribution in MDP and CDP models causes different stress path compared to DP model. The difference between MDP and CDP models is because of the evolution of $\boldsymbol{\chi}^p$ which is assumed to evolve with same plastic multiplier $\Delta\bar{\gamma}$ with $\boldsymbol{F}^p$ in CDP model. Note that MDP model does not include the evolution of $\boldsymbol{\chi}^p$ but only $\boldsymbol{F}^p$. Figure 7.7 shows the opposite trend of the contour plots of the stress measures $||\mathrm{tr}\,(\boldsymbol{m})\,||$ and $\mathrm{tr}\,(\boldsymbol{s}-\boldsymbol{\sigma})$ throughout the column length such that $\mathrm{tr}\,(\boldsymbol{s}-\boldsymbol{\sigma})$ value is higher where $||\mathrm{tr}\,(\boldsymbol{m})\,||$ is lower for Case 3. Note that these two stress tensors $(\boldsymbol{s}-\boldsymbol{\sigma})$ and $\boldsymbol{\nabla m}$ appear in the balance of first moment of momentum that they should balance each other.

Comparison of the three cases

Figures 7.10 and 7.11 show the difference in stresses, and Figure 7.12 shows different stress paths that are obtained by CDP criterion for the three different cases mentioned above: (1) no boundary effect (homogeneous distribution of Φ^h_{33} value throughout the column height), (2) boundary effect (gradient in micro displacement $\boldsymbol{\nabla}\Phi^h_{33}$ but without the higher order couple stress tensor), and (3) boundary effect together with the length scale effect which is introduced by the higher order couple stress tensor. Although the deviatoric stress norms $||\mathrm{dev}\boldsymbol{\sigma}||$ and $||\mathrm{dev}\,(\boldsymbol{s}-\boldsymbol{\sigma})\,||$ in Figures 7.3, 7.6, and 7.9 obtained by same models show similar behaviours to each other for all the cases, closer comparisons provided in Figures 7.10 and 7.11 (obtained by CDP model) show that they differ in values. For the Figures 7.10 and 7.11, we may say that introducing τ_7 causes higher values of the deviatoric stress norms $||\mathrm{dev}\boldsymbol{\sigma}||$ and $||\mathrm{dev}\,(\boldsymbol{s}-\boldsymbol{\sigma})\,||$ obtained by CDP model in the vicinity of the boundary, and different stress paths as shown in Figure 7.12. In Section 6.2.8, we saw a trend for the stress norms, that is, higher the gradient of $\boldsymbol{\Phi}^h$, lower the values of these stress norms. Here, neither the deviatoric relative stress tensor norm $||\mathrm{dev}\,(\boldsymbol{s}-\boldsymbol{\sigma})\,||$, nor unsymmetric deviatoric Cauchy stress norm $||\mathrm{dev}\boldsymbol{\sigma}||$ present similar trend in the vicinity of the bottom boundary. In the absence of τ_7, the unsymmetric Cauchy stress tensor has lower values of $||\mathrm{dev}\boldsymbol{\sigma}||$, likewise

for the relative stress tensor measure $||\text{dev}\,(\boldsymbol{s}-\boldsymbol{\sigma})\,||$. However, this effect is reversed when τ_7 is introduced.

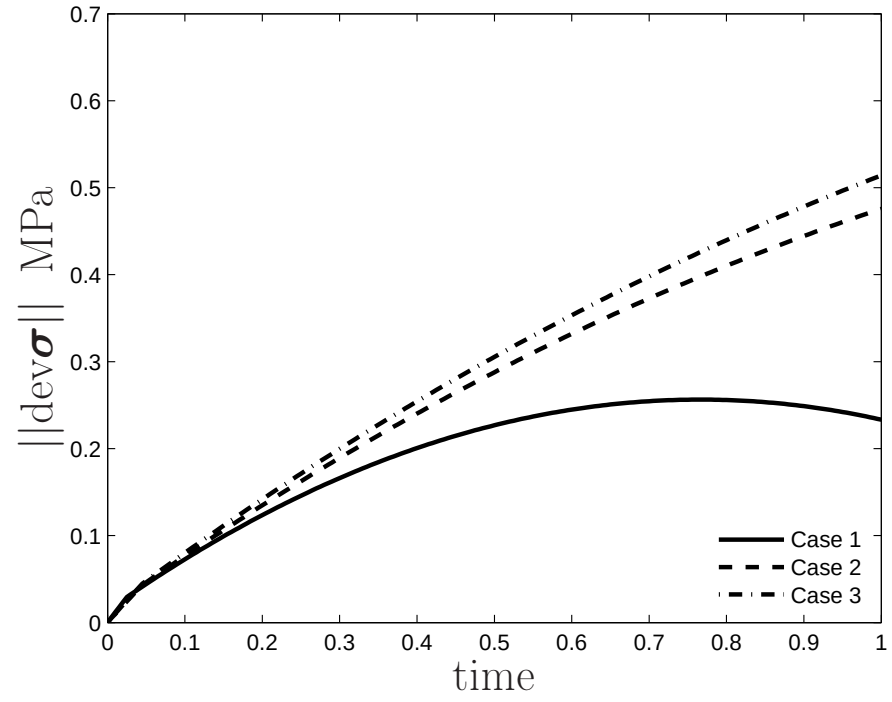

(a)

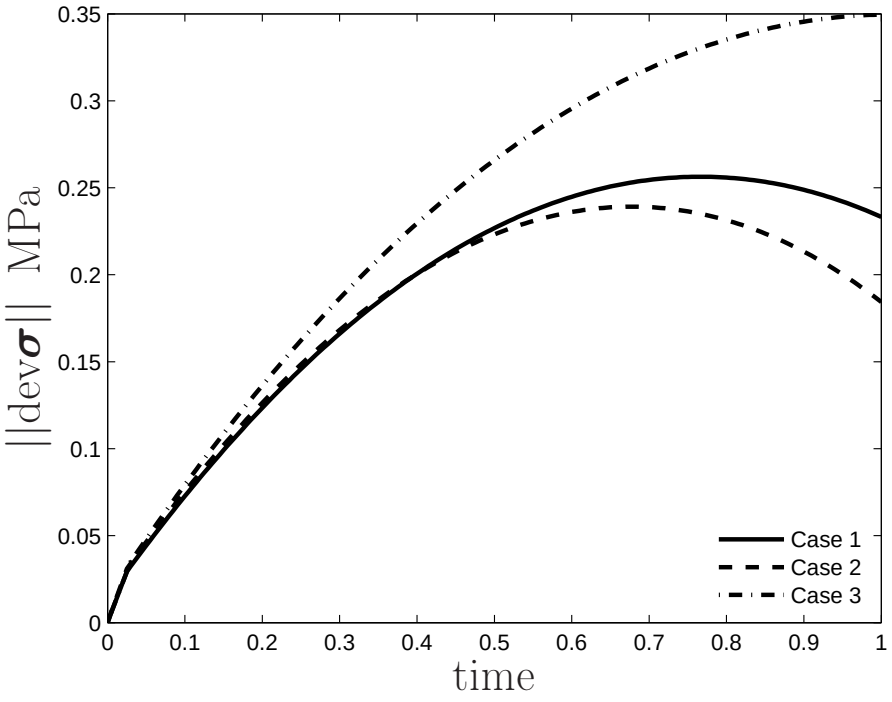

(b)

Figure 7.10: Comparison of the deviatoric stress norms $||\text{dev}\boldsymbol{\sigma}||$ obtained by CDP model at (a) $X_3 = 0.14$m, (b) $X_3 = 1.10$m for all the cases in column example.

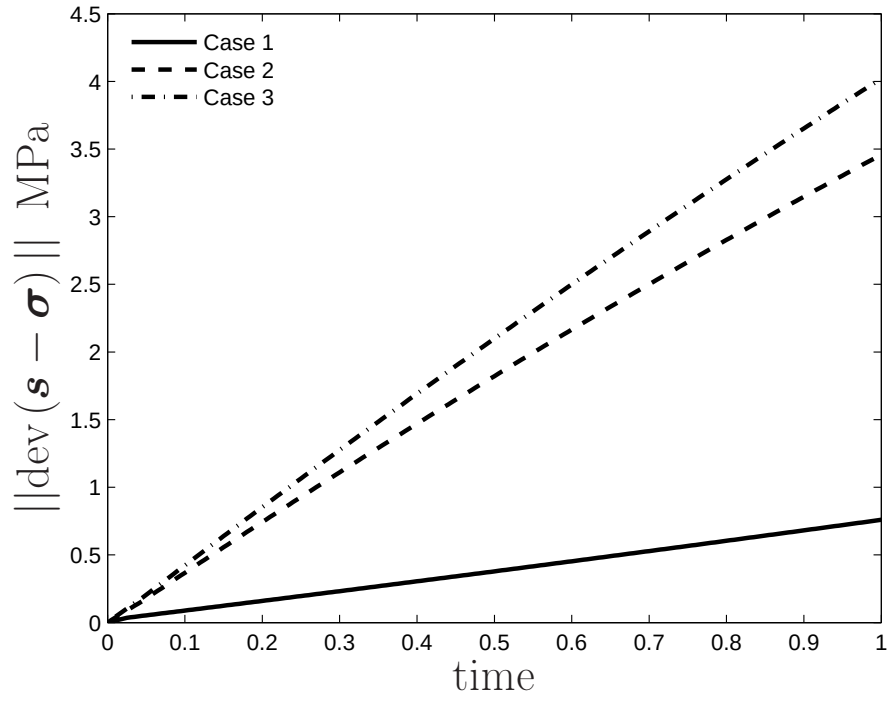

(a)

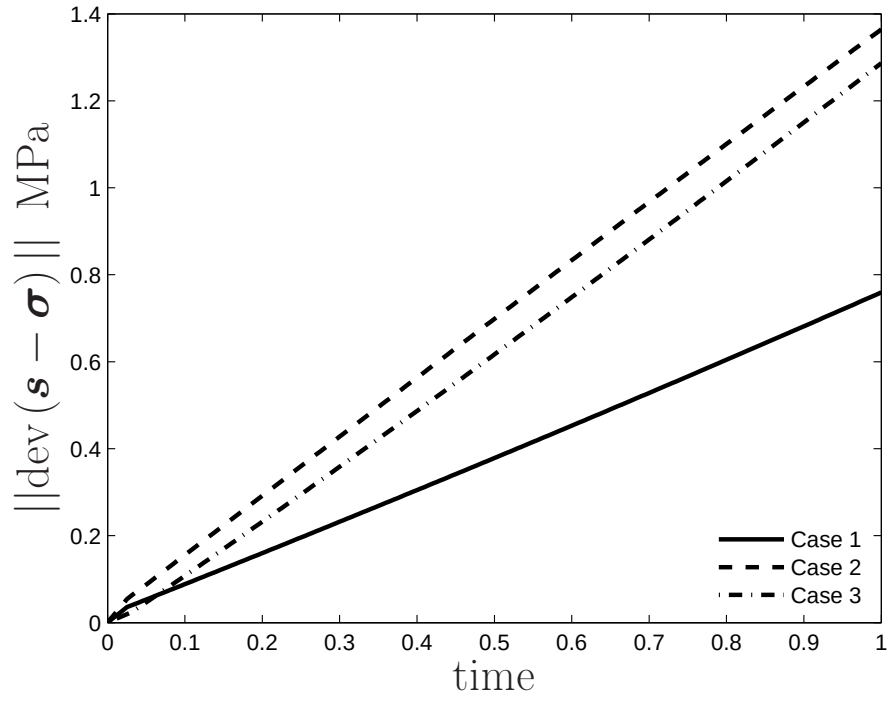

(b)

Figure 7.11: Comparison of the deviatoric relative stress norms $||\mathrm{dev}\,(\boldsymbol{s}-\boldsymbol{\sigma})||$ obtained by CDP model at (a) $X_3 = 0.14$m, (b) $X_3 = 1.10$m for all the cases in column example.

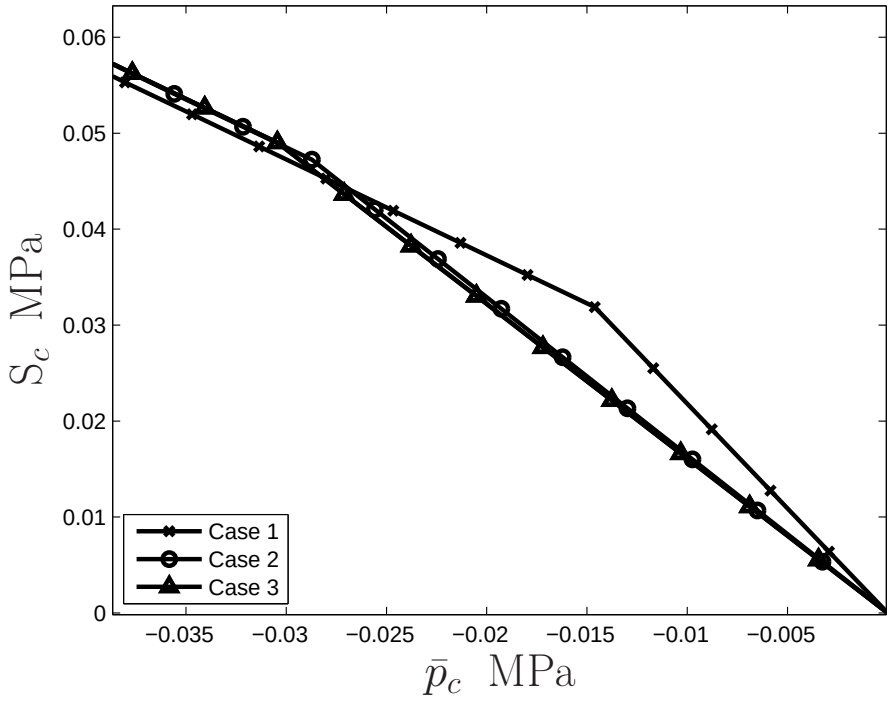

(a)

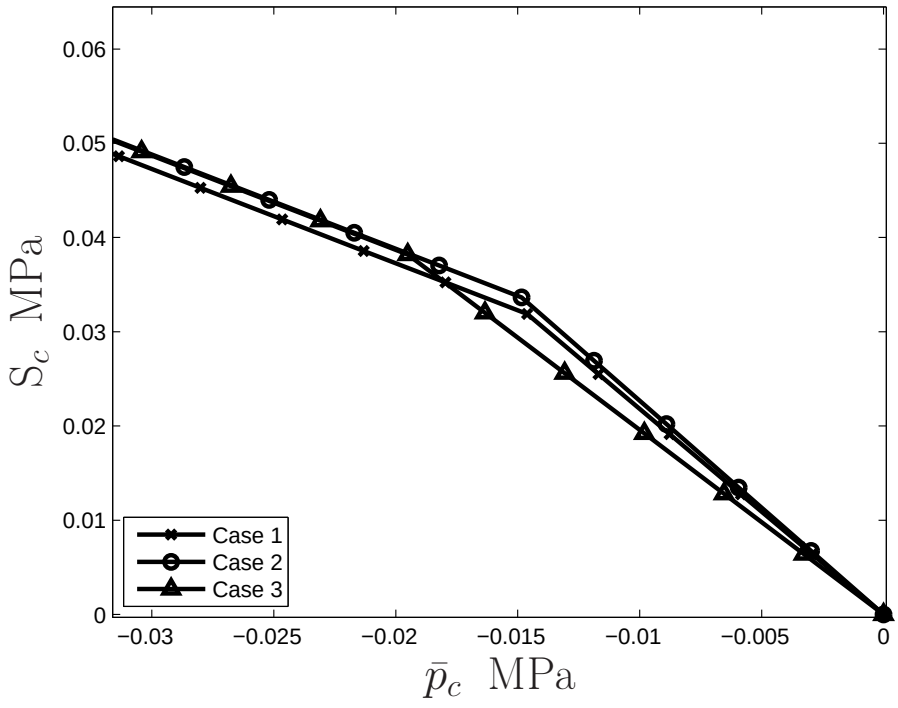

(b)

Figure 7.12: Comparison of the stress paths at (a) $X_3 = 0.14$m, and (b) $X_3 = 1.10$m for all the cases in column example.

7.3 Plane Strain Example

In this section, we consider a 3D geometry under plain strain condition with different number of additional degrees of freedom through $\mathbf{\Phi}^h$. The height of the sample is chosen as 0.08 m and the width is 0.04m (the geometry is given in Figure 7.13). Confining pressures of $\sigma_c = 0.1$ MPa and $\sigma_c = 0.2$ MPa are applied on the side surfaces for the different examples, and displacement boundary condition is applied on the top surface. The parameters chosen in this analysis are given in Tables 7.2 and 7.3. We consider four different cases: (i) only two additional degrees of freedom are chosen which are in plane dilation/stretch degrees of freedom Φ^h_{22}, Φ^h_{33}; (ii) three additional degrees of freedom which are one out of plane degree of freedom Φ^h_{11}, and two in plane degrees of freedom Φ^h_{22}, Φ^h_{33}; (iii) we turn on the in plane degrees of freedom in Z- Y plane as well to see the effect of those degrees of freedom, and the total degrees of freedom are four that are: $\Phi^h_{22}, \Phi^h_{33}, \Phi^h_{23}, \Phi^h_{32}$; (iv) we consider the most general case and have nine additional degrees of freedom, whole micro-displacement tensor $\mathbf{\Phi}^h$ involved to investigate the contribution of all degrees of freedom introduced by micromorphic theory. For this example, we initially applied 10% of initial height which is 0.08m as a displacement boundary condition $u = 0.008$m, but some analysis and standard plasticity could not complete the entire analysis because of Newton-Raphson algorithm convergence problems. Since we use semi implicit time integration method, using smaller time steps may solve the problem. However, we constrain our attention to the effect of micromorphic theory and postpone the convergence problems which are due to computational power limitations to a future time.

In Figure 7.14, we show the stages of the applied loads. The first stage, the region between the points “a” and “b”, shows the application of the confining pressure. The confining pressure is chosen to be small enough not to cause yielding at this initial stage to better observe the differences in the stress paths. The lateral confining pressure is applied incrementally till point “b” where it reaches its maximum, and kept constant till the end

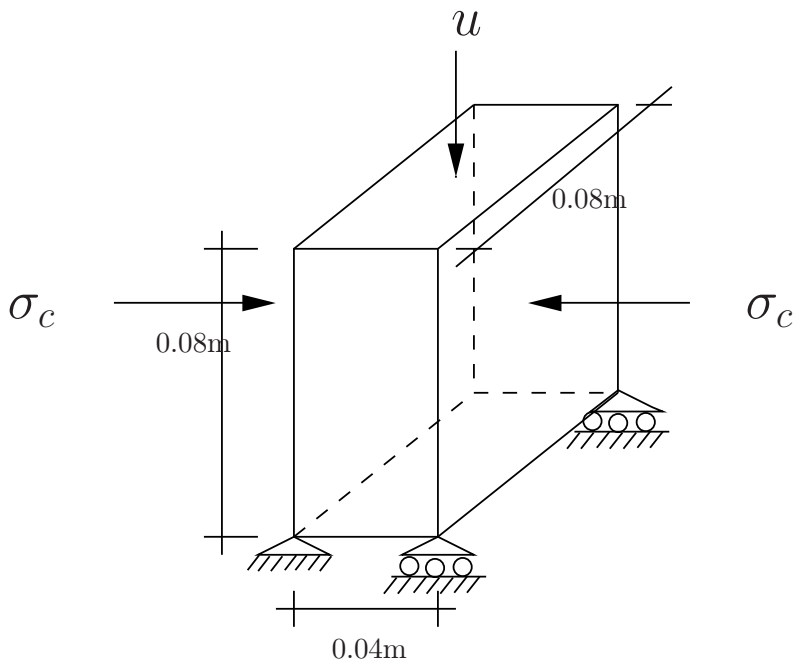

Figure 7.13: plane strain example.

of the analyses. The second stage, the region between two points marked by “b” and “c”, demonstrates the beginning of the application of displacement boundary condition on the top surface. It initially causes a decreases in deviatoric stress norms; however, due to plane strain conditions together with increasing applied displacement on top surface, the stress norms increase and touch the yield surface at the point “d”. The last state shows that stress paths touch the yield surface and stay on the yield surface as expected. Similar patterns can be seen in the plots 7.16, 7.17, and 7.18 which include the stress norms as well.

From Figures 7.14, 7.15, and 7.16 , we see that micromorphic plasticity results present different behavior compared to standard plasticity as expected; however, we may say that there is no noticeable difference between cases with different numbers of degrees of freedom. We can easily say that the shear degrees of freedom are found to have no significant effect on the simulations; therefore, for the future examples these degrees of freedom can be neglected to gain more computational power in plane strain examples. In Figure 7.15, we see that the effect of micromorphic degrees of freedom is that micromorphic continuum tends to provide

a less stiff behavior at a Gauss point in an element at the top surface. Note that we have the coupled strain tensor $\bar{\boldsymbol{\mathcal{E}}}^e$ which is defined as $\bar{\boldsymbol{\mathcal{E}}}^e = \boldsymbol{F}^{eT}\boldsymbol{\chi}^e - \mathbf{1}$ that means the effect of the micro-structure is coupled with the macro-structure, and it does not represent the micro-structural response purely. This coupled micro strain tensor effect is amplified when multiplied by higher values of micromorphic elastic moduli η, κ, and ν. Here, we again express the importance of the choice of micromorphic elastic material moduli that will be the most significant point to model the material response. Since we have not considered a real physical material, this behavior can be more meaningful when a homogenization procedure is applied to determine the micromorphic elastic parameters in a completely overlapped coupled region with an underlying microstructural model like the discrete element for granular materials.

To investigate further the additional degrees of freedom with the plane strain conditions, we increase the confining pressure to $\sigma_c = 0.2$ MPa (and elastic parameters are given for this case in Table 7.4) so that we may activate the out of plane degree of freedom Φ^h_{11} more under a higher pressure. We choose only the cases which include only the micro dilation/ stretch degrees of freedom. For the case (i) we consider only Φ^h_{22}, Φ^h_{33} and for case (ii) we have only $\Phi^h_{11}, \Phi^h_{22}, \Phi^h_{33}$.

Figures 7.17, and 7.18 show that increasing confining pressure changes the response, and now a clear difference between these two cases is seen compared to the previous example which was under less confining pressure. From these figures, we may conclude that the out of plane degree of freedom Φ^h_{11} actually does have an effect on the results, and it caused a different stress path as in Figure 7.17 as well as mostly lower values of $||\text{dev}\bar{\boldsymbol{S}}||$ at initial part of Figure 7.18.

Table 7.2: Micromorphic elastic parameters used in plane strain problem with confining pressure $\sigma_c = 0.1$ MPa .

λ (MPa)	μ (MPa)	η (MPa)	ν (MPa)	κ (MPa)	τ (MPa)	σ (MPa)	τ_7 (Pa. m^2)
19	5	40	8	10	10	2	1×10^2

Table 7.3: Parameters used in plane strain example.

ϕ (rad.)	ψ (rad.)	H^c (Pa)	c (Pa)	ϕ^χ (rad.)	ψ^χ (rad.)	$H^{c,\chi}$ (Pa)	c^χ (Pa)
0.15	0.1	0.0	1×10^4	0.0	0.0	0.0	10

Table 7.4: Micromorphic elastic parameters used in plane strain problem with confining pressure $\sigma_c = 0.2$ MPa.

λ (MPa)	μ (MPa)	η (MPa)	ν (MPa)	κ (MPa)	τ (MPa)	σ (MPa)	τ_7 (Pa. m^2)
29	7	40	8	10	10	5	1×10^2

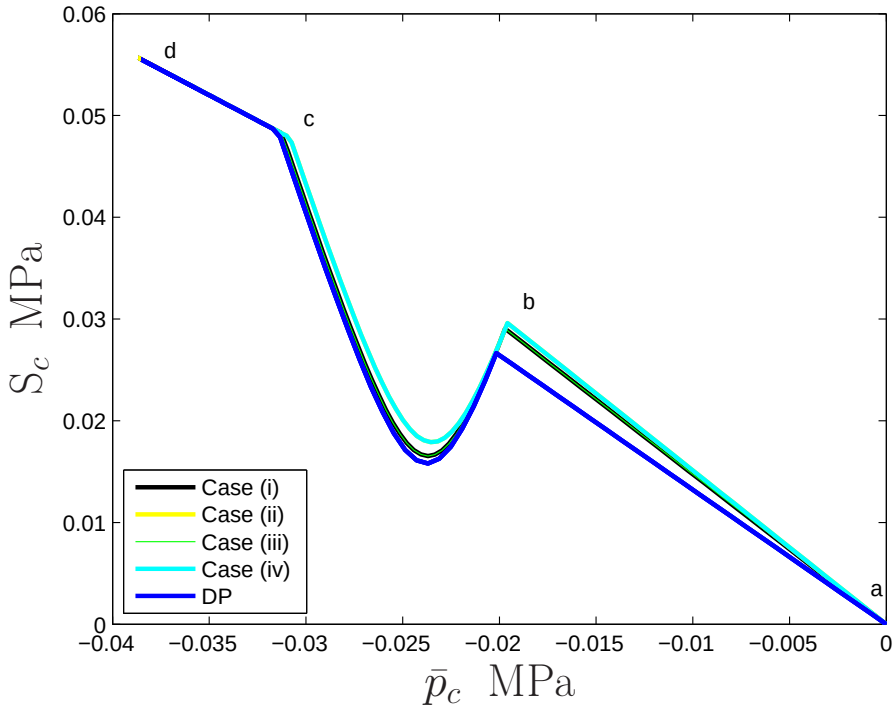

Figure 7.14: Comparison of stress paths of the different cases for plane strain example for confining pressure $\sigma_c = 0.1$ MPa.

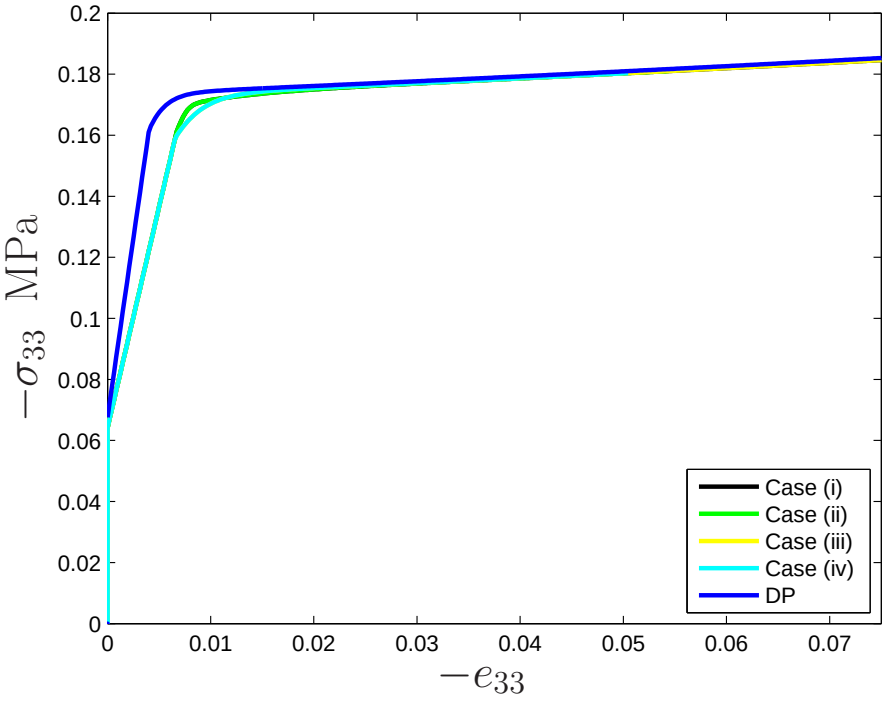

Figure 7.15: Comparison of stress strain plots for different cases with standard Drucker-Prager (DP) plasticity result for plane strain example for confining pressure $\sigma_c = 0.1$ MPa .

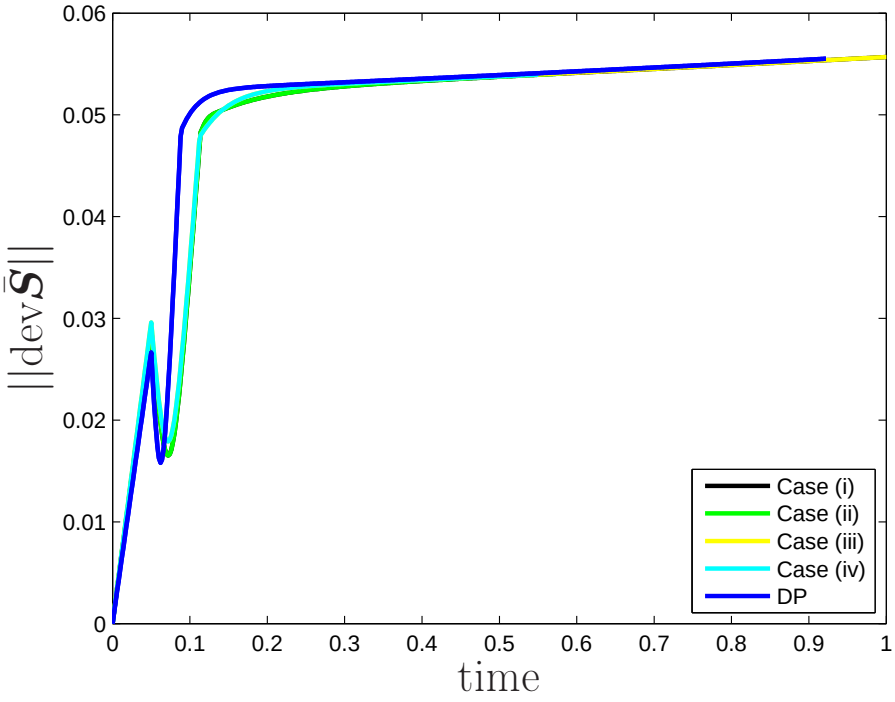

Figure 7.16: Comparison of deviatoric stress norms $||\mathrm{dev}\bar{\boldsymbol{S}}||$ for different cases for plane strain example for confining pressure $\sigma_c = 0.1$ MPa.

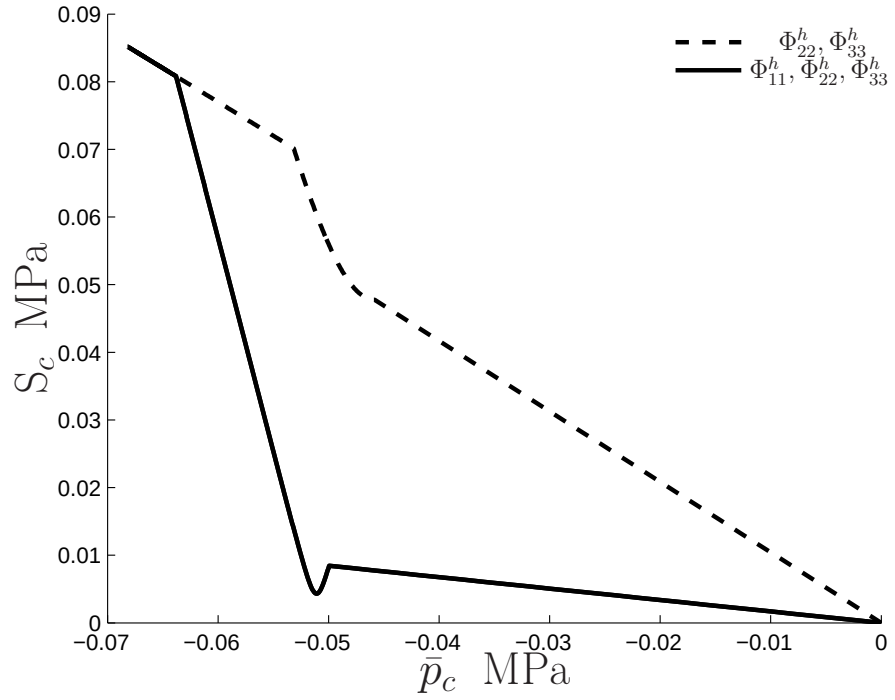

Figure 7.17: Comparison of stress paths of the two different cases for plane strain example for confining pressure $\sigma_c = 0.2$ MPa.

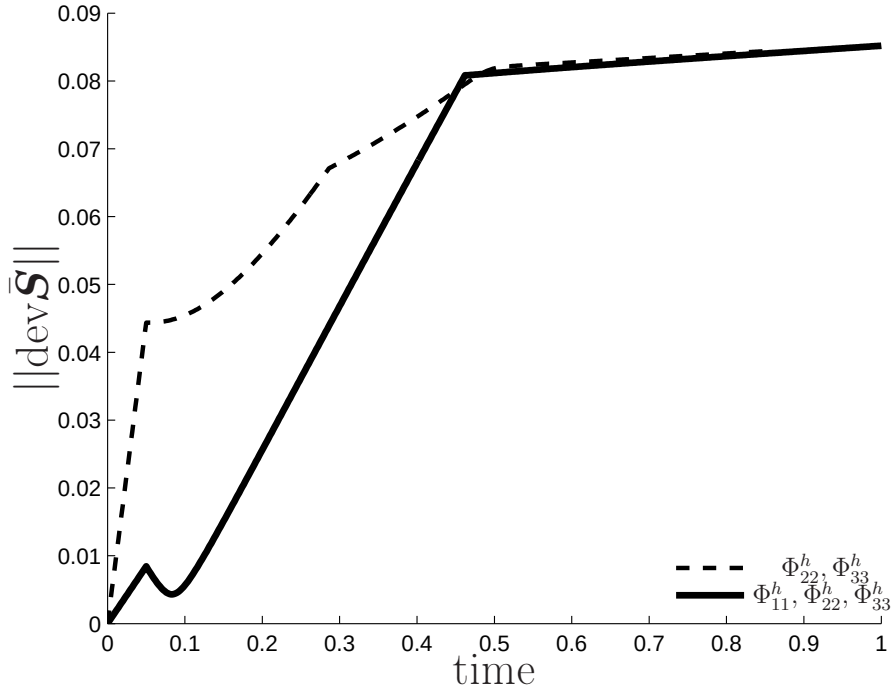

Figure 7.18: Comparison of deviatoric stress norms of $||\mathrm{dev}\bar{\boldsymbol{S}}||$ for two different cases for plane strain example for confining pressure $\sigma_c = 0.2$ MPa.

In this study, we developed and implemented a model for nonlinear finite element analysis for finite strain micromorphic elastoplastic geomaterials to be used in a multiscale approach explained in the beginning of this work. These numerical examples conclude this study. More exciting problems such as strain softening, localizations, etc. as well as overlap coupling micro-structural model can be investigated by using micromorphic theory. The results, challenges, findings, targets in conjunction with the suggestions for a future study are summarized in the next Chapter.

Chapter 8

Conclusions and Future work

We investigated the various aspects of the micromorphic continuum within the context of finite strain isotropic elasticity and elastoplasticity. Results indicate that the micromorphic contribution causes different behaviors depending on number of additional degrees of freedom $\boldsymbol{\Phi}^h$, length scale, and boundary conditions on micro-displacement tensor. Three dimensional stress state with the combination of deformation and additional micromorphic elastic parameters, together with the different plasticity criteria, and plasticity parameters lead to different trends. Influences of micro-displacement tensor $\boldsymbol{\Phi}^h$ boundary conditions and length scale on results were found to be very significant factors on convergence and results of the simulations as well. It is possible to have convergence issues if proper $\boldsymbol{\Phi}^h$ boundary conditions together with micromorphic elastic moduli are not chosen. We proved that symmetry conditions are not applicable on $\boldsymbol{\Phi}^h$ in this approach that requires considering whole domain that means additional computational work.

Based on the findings and results obtained by the analyses, extending micromorphic FE implementation to current configuration, and including inertia terms will possibly eliminate the convergence issues with regard to plasticity since we will plan to use an explicit formulation and implementation. The constitutive assumption which has been made to consider the plastic part of the gradient of micro-deformation tensor $\boldsymbol{\nabla\chi}^p$ as a separate internal variable rather than taking the derivative of the plastic part of the micro-deformation tensor $\boldsymbol{\chi}^p$ is found to be one point to be improved and to be changed to make it dependent to

the plastic part of the micro-deformation tensor $\boldsymbol{\chi}^p$ due to the convergence difficulties. It is because when the gradient of the plastic part of the micro-deformation tensor $\boldsymbol{\nabla}\boldsymbol{\chi}^p$ is treated as a separate internal variable, and assuming micro-scale gradient plasticity did not occur (micro-scale gradient stayed elastic $\boldsymbol{\nabla}\boldsymbol{\chi}^p = \mathbf{0}$), but when we have plasticity in micro-scale which indicates $\boldsymbol{\chi} = \boldsymbol{\chi}^e\boldsymbol{\chi}^p$,then, for this case $\boldsymbol{\chi}^p$ will exist, and the gradient of the plastic part of the micro-deformation tensor $\boldsymbol{\nabla}\boldsymbol{\chi}^p$ may not be zero as it was assumed. Therefore, assuming $\boldsymbol{\nabla}\boldsymbol{\chi}^p = \mathbf{0}$ will cause non compatible values of the gradient of the elastic part of the micro-deformation $\boldsymbol{\nabla}\boldsymbol{\chi}^e$, hence, $\boldsymbol{\nabla}\boldsymbol{\chi}^e = \boldsymbol{\nabla}\left(\boldsymbol{\chi}\boldsymbol{\chi}^{p-1}\right)$ that affects the global consistent tangent. One way to add this property is to introduce the gradient of the plastic part of micro-deformation tensor $\boldsymbol{\nabla}\boldsymbol{\chi}^p$ as additional degrees of freedom at the nodes of elements such as micro-displacement tensor $\boldsymbol{\Phi}^h$. This approach will bring more computational cost compared to the current approach; however, it will possibly increase the effectiveness of the implementation and help to further analyze the length scale related problems such as strain localization problems. The additional convergence problems resulting from the use of semi-implicit time integration algorithm and introducing additional $\boldsymbol{\Phi}^h$ degrees of freedom will need to be further investigated. To resolve the problem caused by semi implicit time integration, it may be possible to use very small time steps. The additional computational power can be addressed by parallel processing which can be a useful tool to overcome the necessity of more computational power. Although we had some convergence issues with the rigid punch example given in Chapter 6 when we turned on all additional degrees of freedom $\boldsymbol{\Phi}^h$, a mesh refinement study shown in the same chapter showed that the element used in finite element analysis is convergent. The reason that caused non-convergent results with respect to Newton-Raphson solver (not spatial discretization) may be caused by the additional shear degrees of freedom in the shear dominated region. To better involve the micromorphic additional degrees of freedom, one can use a finer mesh in the shear dominated region. Note that, we were able to involve all the additional degrees of freedom in the example considered in Section 7.3. Coupling of lower length scale region modeled by DEM (or FEM for

bound particulate materials) with the micromophic continuum region modeled by FEM as a multi-scale approach will be the ultimate aim of the future work of this study to address the artificial influence of boundaries of the lower length scale on the simulations.

In coupling of these two scales, the influence of the boundary conditions on micro-displacement tensor $\mathbf{\Phi}^h$ may be important. In this work, we only considered one type of essential boundary condition on the micro-displacement tensor which is $\Phi^h_{33} = 0$. However, the motion of the underlying particles in the region where FE mesh is extended in the DE region may be supplied by DEM, and it will be introduced by the micro-displacement tensor $\mathbf{\Phi}^h$ that may require to apply prescribed values dictated by DEM to the micro-displacement tensor $\mathbf{\Phi}^h$. To capture the inherent behavior of micro-structure, it may be the best to turn on all the micro-displacement degrees of freedom in a three dimensional problem so that overall response of the micro-field such as microdilation/stretch, microrotations, and microshear can be represented by the micromorphic theory. The spatial variation of the values of $\mathbf{\Phi}^h$ will always create a gradient in the field in which the length scale effect will be taken into account by the higher order couple stress tensor $\boldsymbol{m}$ that will be an interesting problem to investigate in this multiscale approach between DEM and FEM. Currently, the couple traction boundary condition is not implemented, and that will also have an influence on the boundary conditions. Further investigation of essential boundary conditions through $\mathbf{\Phi}^h$, and natural boundary conditions through the couple traction are required, with coupling between DEM and FEM helping to interpret the physical meaning of these boundary conditions.

Bibliography

Anandarajah, A. (1994). Discrete-element method for simulating behavior of cohesive soil. ASCE J. Geotech. Eng. Div., 120(9):1593–1613.

Barthelat, F., Li, C.-M., Comi, C., and Espinosa, H. (2006). Mechanical properties of nacre constituents and their impact on mechanical performance. J. Mater. Res., 21(8):1977 – 86.

Bashir, Y. and Goddard, J. (1991). A novel simulation method for the quasi-static mechanics of granular assemblages. J. Rheol., 35:849–885.

Bilby, B., Bullough, R., and Smith, E. (1955). Continuous distributions of dislocations: a new application of the methods of non-Riemannian geometry. Proc. R. Soc. Lond. A, Math. Phys. Eng. Sci., 231:263–273.

Bobko, C., Gathier, B., Borges, L., and Ulm, F.-J. (2009). The nanogranular origin of friction and cohesion in shale - a strength homogenization approach to interpretation of nanoindentation results. in revision, Journal of the Mechanics and Physics of Solids.

Bobko, C. and Ulm, F.-J. (2008). The nano-mechanical morphology of shale. Mech. Mater., 40(4-5):318 – 37.

Bonet, J. and Wood, R. D. (1997). Nonlinear Continuum Mechanics For Finite Element Analysis. Cambridge University Press.

Chambon, R., Caillerie, D., and Matsuchima, T. (2001a). Plastic continuum with microstructure, local second gradient theories for geomaterials: localization studies. International Journal of Solids and Structures, 38(46-47):8503 – 8527.

Chambon, R., Caillerie, D., and Tamagnini, C. (2001b). A finite deformation second gradient theory of plasticity. Comptes Rendus de l'Académie des Sciences - Series IIB - Mechanics, 329(11):797 – 802.

Chambon, R., Caillerie, D., and Tamagnini, C. (2004). A strain space gradient plasticity theory for finite strain. Computer Methods in Applied Mechanics and Engineering, 193(27-29):2797 – 2826.

Chang, C. S., Kabir, M. G., and Chung, Y. (1992). Micromechanics modeling for stress-strain behavior of granular soils. ii: Evaluation. Journal of Geotechnical Engineering, 118(12):1975–1992.

Christoffersen, J., Mehrabadi, M., and Nemat-Nasser, S. (1981). A micromechanical description of granular material behavior. J. App. Mech., 48:339–344.

Coleman, B. D. and Noll, W. (1963). The thermodynamics of elastic materials with heat conduction and viscosity. Arch. Ration. Mech. Anal., 13:167–178.

Cosserat, E. and Cosserat, F. (1909). Theorie des corps deformables. Hermann, Paris.

Cundall, P. and Strack, O. (1979). A discrete numerical model for granular assemblies. Geotechnique, 29:47–65.

E. Kröner, ed. (1968). Mechanics of Generalized Continua. Springer-Verlag.

E.H. Lee and D.T. Liu (1967). Finite-strain elastic-plastic theory with application to plane-wave analysis. J. App. Phys., 38:19–27.

Eringen, A. (1968a). Theory of micropolar elasticity. In Liebowitz, H., editor, Fracture, An Advanced Treatise, volume 2, pages 622–729. Academic Press.

Eringen, A. (1968b). Theory of Micropolar Elasticity, volume 2 of Fracture, An Advanced Treatise, chap. 7, pages 622–729. Academic Press, New York, 1^{st} edition.

Eringen, A. (1999). Microcontinuum Field Theories I: Foundations and Solids. Springer-Verlag.

Eringen, A. C. and Suhubi, E. S. (1964). Nonlinear theory of simple micro-elastic solids–1. International Journal of Engineering Science, 2(2):189 – 203.

Fish, J. (2006). Bridging the scales in nano engineering and science. J. Nanoparticle Res., 8(5):577 – 94.

Forest, S. and Sievert, R. (2003). Elastoviscoplastic constitutive frameworks for generalized continua. Acta Mechanica, 160(1-2):71 – 111.

Forest, S. and Sievert, R. (2006). Nonlinear microstrain theories. International Journal of Solids and Structures, 43(24):7224 – 7245.

Gardiner, B. S. and Tordesillas, A. (2004). Micromechanics of shear bands. International Journal of Solids and Structures, 41(21):5885 – 5901. Granular Mechanics.

Germain, P. (1973). The method of virtual power in continuum mechanics. part 2: Microstructure. SIAM Journal on Applied Mathematics, 25(3):556–575.

Grammenoudis, P., Tsakmakis, C., and Hofer, D. (2009). Micromorphic continuum. part ii: Finite deformation plasticity coupled with damage. International Journal of Non-Linear Mechanics, 44(9):957 – 974.

Grammenoudis, P., Tsakmakis, C., and Hofer, D. (2010). Micromorphic continuum. part iii: Small deformation plasticity coupled with damage. International Journal of Non-Linear Mechanics, 45(2):140 – 148.

Green, A. E. and Naghdi, P. M. (1995). A unified procedure for construction of theories of deformable media. ii. generalized continua. Proceedings of the Royal Society of London. Series A: Mathematical and Physical Sciences, 448(1934):357–377.

Hughes, T. J. R. (1987). The Finite Element Method. Prentice-Hall: New Jersey.

Isbuga, V. and Regueiro, R. A. (2011). Three-dimensional finite element analysis of finite deformation micromorphic linear isotropic elasticity. International Journal of Engineering Science, 49(12):1326 – 1336.

Jefferson, G., Haritos, G. K., and McMeeking, R. M. (2002). The elastic response of a cohesive aggregate–a discrete element model with coupled particle interaction. Journal of the Mechanics and Physics of Solids, 50(12):2539 – 2575.

Kafadar, C. and Eringen, A. C. (1971). Micropolar media: I the classical theory. Int. J. Eng. Sci., 9:271–305.

Klein, P. and Zimmerman, J. (2006). Coupled atomistic-continuum simulations using arbitrary overlapping domains. Journal of Computational Physics, 213(1):86 – 116.

Kolymbas, D., editor (2000). Constitutive Modelling of Granular Materials. Springer-Verlag.

Kondo, K. (1952). On the geometrical and physical foundations of the theory of yielding. In Proceedings of the 2nd Japan National Congress for Appl. Mech., pages 41–47.

Kraft, R., Molinari, J., Ramesh, K., and Warner, D. (2008). Computational micromechanics of dynamic compressive loading of a brittle polycrystalline material using a distribution of grain boundary properties. J. Mech. Phys. Solids, 56:2618–41.

Kröner, E. (1960). Allgemeine kontinuumstheorie der versetzungen and eigenspannungen. Arch. Ration. Mech. Anal., 4:273–334.

Lee, E. (1969). Elastic-plastic deformation at finite strains. J. App. Mech., 36:1–6.

Lee, J. D. and Chen, Y. (2003). Constitutive relations of micromorphic thermoplasticity. International Journal of Engineering Science, 41(3-5):387 – 399.

Liu, W. K., Karpov, E. G., and Park, H. S. (2006). Nano Mechanics and Materials: Theory, Multiscale Methods, and Applications. John Wiley&Sons Ltd., 1 edition.

Lubliner, J. (1990). Plasticity Theory. Macmillan Pub., NY.

Luding, S. (2004). Micro-macro transition for anisotropic, frictional granular packings. International Journal of Solids and Structures, 41(21):5821 – 5836. Granular Mechanics.

Luding, S., Latzel, M., Volk, W., Diebels, S., and Herrmann, H. (2001). From discrete element simulations to a continuum model. Comp. Meth. App. Mech. Engr., 191(1-2):21 – 28.

Masson, S. and Martinez, J. (2001). Micromechanical analysis of the shear behavior of a granular material. J. Eng. Mech., 127(10):1007 – 1016.

Matsushima, T., Chambon, R., and Caillerie, D. (2000). Second gradient models as a particular case of microstructured models: a large strain finite elements analysis. Comptes Rendus de l'Académie des Sciences - Series IIB - Mechanics-Physics-Astronomy, 328(2):179 – 186.

Mindlin, R. (1964). Micro-structure in linear elasticity. Archs ration. Mech. Analysis, 16:51–78.

Mindlin, R. and Eshel, N. (1968). On first strain-gradient theories in linear elasticity. International Journal of Solids and Structures, 4(1):109 – 124.

Moran, B., Ortiz, M., and Shih, C. (1990). Formulation of implicit finite-element methods for multiplicative finite deformation plasticity. Int. J. Numer. Methods Eng., 29(3):483–514.

Neff, P. and Forest, S. (2007). A geometrically exact micromorphic model for elastic metallic foams accounting for affine microstructure. modelling, existence of minimizers, identification of moduli and computational results. Journal of Elasticity, 87(2):239–276.

Nemat-Nasser, S. (2004). Plasticity: a treatise on the finite deformation of heterogeneous inelastic materials. Cambridge University Press.

Peters, J. (2005). Some fundamental aspects of the continuumization problem in granular media. J. Eng. Math., 52(1-3):231 – 50.

Ramaswamy, S. and Aravas, N. (1998). Finite element implementation of gradient plasticity models. Part I: Gradient-dependent yield functions. Comp. Meth. App. Mech. Engr., 163:11–32.

Regueiro, R. (2009). Finite strain micromorphic pressure-sensitive plasticity. J. Eng. Mech., 135:178–191.

Regueiro, R. (2010). On finite strain micromorphic elastoplasticity. Int. J. Solids Struct., 47:786–800.

Regueiro, R. and Ebrahimi, D. (2010). Implicit dynamic three-dimensional finite element analysis of an inelastic biphasic mixture at finite strain. Part 1: application to a simple geomaterial. Comp. Meth. App. Mech. Engr., 199:2024–2049.

Regueiro, R. and Yan, B. (2011). Concurrent multiscale computational modeling for dense dry granular materials interfacing deformable solid bodies, pages 251–273. Bifurcations, Instabilities and Degradations in Geomaterials; Springer Series in Geomechanics and Geoengineering. Springer-Verlag, Berlin.

Regueiro, R. A. and Isbuga, V. (2011). Length scale effects in finite strain micromorphic linear isotropic elasticity: finite element analysis of three-dimensional cubical microindentation. Proceedings of the Institution of Mechanical Engineers, Part N: Journal of Nanoengineering and Nanosystems.

Rothenburg, L. and Selvadurai, A. (1981). Micromechanical definition of the Cauchy stress tensor for particulate media. In Selvadurai, A., editor, Mechanics of Structured Media, pages 469–486. Elsevier Scientific.

Sansour, C. (1998). Unified concept of elastic-viscoplastic cosserat and micromorphic continua. Journal De Physique. IV, 8(8):341 – 348.

Sansour, C., Skatulla, S., and Zbib, H. (2010). A formulation for the micromorphic continuum at finite inelastic strains. International Journal of Solids and Structures, 47(11-12):1546 – 1554.

Scott, R. and Craig, M. (1980). Computer modeling of clay structure and mechanics. ASCE J. Geotech. Eng. Div., 106(1):17–33.

Shewchuk, J. R. (1994). An introduction to the conjugate gradient method without the agonizing pain. `http://www.cs.berkeley.edu/~jrs/jrspapers.html#cg`.

Simo, J. C. (1998). Numerical Analysis and Simulation of Plasticity. In Ciarlet, P. and Lions, J., editors, Handbook of Numerical Analysis. Elsevier Science.

Smith, A. C. (1968). Inequalities between the constants of a linear micro-elastic solid. International Journal of Engineering Science, 6(2):65 – 74.

Suhubi, E. and Eringen, A. (1964). Nonlinear theory of simple micro-elastic solids–ii. Int. J. Engr. Sci., 2(2):389–404.

Tamagnini, C., Chambon, R., and Caillerie, D. (2001). A second gradient elastoplastic cohesive-frictional model for geomaterials. Comptes Rendus de l'AcadÃ©mie des Sciences - Series IIB - Mechanics, 329(10):735 – 739.

Truesdell, C. and Toupin, R. (1960). The classical field theories. Handbuch der Physik, Springer, Berlin.

Vernerey, F., Liu, W., and Moran, B. (2007). Multi-scale micromorphic theory for hierarchical materials. J. Mech. Phys. Solids, 55(12):2603 – 2651.

Voyiadjis, G. Z. and Al-Rub, R. K. A. (2005). Gradient plasticity theory with a variable length scale parameter. International Journal of Solids and Structures, 42(14):3998 – 4029.

Wagner, G. J. and Liu, W. K. (2003). Coupling of atomistic and continuum simulations using a bridging scale decomposition. Journal of Computational Physics, 190(1):249 – 274.

Wren, J.R. and Borja, R.I. (1997). Micromechanics of granular media. Part II: Overall tangential moduli and localization model for periodic assemblies of circular disks. Comp. Meth. App. Mech. Engr., 141(3–4):221–246.

Yan, B., Regueiro, R., and Sture, S. (2010). Three dimensional discrete element modeling of granular materials and its coupling with finite element facets. Eng. Comput., 27(4):519–550.

Zervos, A., Papanastasiou, A. P., and Vardoulakis, A. I. (2001). A finite element displacement formulation for gradient elastoplasticity. International Journal for Numerical Methods in Engineering, 50(6):1369–1388.

Zervos, A., Papanicolopulos, S.-A., and Vardoulakis, I. (2009). Two finite-element discretizations for gradient elasticity. Journal of Engineering Mechanics, 135(3):203–213.

Zhang, Z., Liu, Z., Liu, X., Gao, Y., and Zhuang, Z. (2011a). Wedge indentation of a thin film on a substrate based on micromorphic plasticity. Acta Mechanica, 221:133–145. 10.1007/s00707-011-0483-1.

Zhang, Z., Zhuang, Z., Gao, Y., Liu, Z., and Nie, J. (2011b). Cyclic plastic behavior analysis based on the micromorphic mixed hardening plasticity model. Computational Materials Science, 50(3):1136 – 1144.

Zhou, J., Xu, W., and Yang, X. (2010). A microcrack damage model for brittle rocks under uniaxial compression. Mechanics Research Communications, 37(4):399 – 405.

Appendix A

Variations of Representative Terms Appearing in the Balance Equations

Variation of some terms which are used in linearization of balance equations are given below.

(1) Variation of J :

$$\delta(J) = J div\,(\delta \boldsymbol{u}) \tag{A.1}$$

(2) Variation of $\boldsymbol{F}$: In matrix form :

$$\delta\,(\boldsymbol{F}) = \boldsymbol{grad}(\delta \boldsymbol{u})\boldsymbol{F} \tag{A.2}$$

In indicial form :

$$\begin{aligned} x_i &= X_i + u_i \\ \frac{\partial x_i}{\partial X_I} &= \frac{\partial X_i}{\partial X_I} + \frac{\partial u_i}{\partial X_I} \\ F_{iI} &= \delta_{iI} + u_{i,I} \\ \delta\,(F_{iI}) &= \delta\left(\frac{\partial u_i}{\partial X_I}\right) = \frac{\partial \delta u_i}{\partial X_I} \\ \delta\,(F_{iI}) &= \delta\,(u_{i,j})\,F_{jI} \end{aligned}$$

(3) Variation of $\boldsymbol{F}^{-1}$:

$$\delta(\boldsymbol{F}^{-1}) = -\boldsymbol{F}^{-1}\delta(\boldsymbol{F})\boldsymbol{F}^{-1} = -\boldsymbol{F}^{-1}\boldsymbol{grad}(\delta \boldsymbol{u}) \tag{A.3}$$

(4) Variation of $\boldsymbol{\nabla w}$:

$$\begin{aligned}
\boldsymbol{\nabla w} &= \frac{\partial \boldsymbol{w}}{\partial \boldsymbol{x}} = \frac{\partial \boldsymbol{w}}{\partial \boldsymbol{X}}\frac{\partial \boldsymbol{X}}{\partial \boldsymbol{x}} = \frac{\partial \boldsymbol{w}}{\partial \boldsymbol{X}}\boldsymbol{F}^{-1} \\
\Rightarrow \delta\boldsymbol{\nabla w} &= \delta\left(\frac{\partial \boldsymbol{w}}{\partial \boldsymbol{X}}\boldsymbol{F}^{-1}\right) \\
&= \delta\left(\frac{\partial \boldsymbol{w}}{\partial \boldsymbol{X}}\right)\boldsymbol{F}^{-1} + \frac{\partial \boldsymbol{w}}{\partial \boldsymbol{X}}\delta\left(\boldsymbol{F}^{-1}\right) \\
\delta\boldsymbol{\nabla w} &= \delta\left(\frac{\partial \boldsymbol{w}}{\partial \boldsymbol{X}}\right)\boldsymbol{F}^{-1} - \frac{\partial \boldsymbol{w}}{\partial \boldsymbol{X}}\boldsymbol{F}^{-1}\boldsymbol{grad}(\delta\boldsymbol{u})
\end{aligned} \tag{A.4}$$

(5) Variation of $\Delta t\boldsymbol{\ell}_{n+1}$:

$$\begin{aligned}
\boldsymbol{\ell}_{n+1} &= \dot{\boldsymbol{F}}_{n+1}\boldsymbol{F}_{n+1}^{-1} \\
\Delta t\boldsymbol{\ell}_{n+1} &= \Delta t\dot{\boldsymbol{F}}_{n+1}\boldsymbol{F}_{n+1}^{-1} \\
\Delta t\boldsymbol{\ell}_{n+1} &= \left(\boldsymbol{F}_{n+1} - \boldsymbol{F}_n\right)\boldsymbol{F}_{n+1}^{-1} \\
\delta(\Delta t\boldsymbol{\ell}_{n+1}) &= \boldsymbol{F}_n\boldsymbol{F}^{-1}\boldsymbol{grad}(\delta\boldsymbol{u})
\end{aligned} \tag{A.5}$$

(6) Variation of $\Delta t\boldsymbol{d}_{n+1}$:

$$\begin{aligned}
\delta(\Delta t\boldsymbol{d}_{n+1}) &= \frac{1}{2}\delta\left(\Delta t\boldsymbol{\ell}_{n+1}^{e} + \Delta t\boldsymbol{\ell}_{n+1}^{eT}\right) \\
\delta(\Delta t\boldsymbol{d}_{n+1}) &= \frac{1}{2}\left(\boldsymbol{F}_n\boldsymbol{F}^{-1}\boldsymbol{grad}(\delta\boldsymbol{u}) + \left(\boldsymbol{F}_n\boldsymbol{F}^{-1}\boldsymbol{grad}(\delta\boldsymbol{u})\right)^{T}\right)
\end{aligned} \tag{A.6}$$

(7) Variation of $tr\left(\Delta t\boldsymbol{d}_{n+1}\right)$:

$$\begin{aligned}
tr\left(\delta\left(\Delta t\boldsymbol{d}_{n+1}\right)\right) &= tr\left(\delta\left(\Delta t\boldsymbol{\ell}_{n+1}\right)\right) \\
tr\left(\delta\left(\Delta t\boldsymbol{d}_{n+1}\right)\right) &= tr\left(\boldsymbol{F}_n\boldsymbol{F}^{-1}\boldsymbol{grad}(\delta\boldsymbol{u})\right)
\end{aligned} \tag{A.7}$$

(8) Variation of the micro deformation tensor $\boldsymbol{\chi}$ for micro motion:

$$\begin{aligned}
\boldsymbol{\chi} &= \mathbf{1} + \boldsymbol{\Phi} \\
\Rightarrow \delta\left(\boldsymbol{\chi}\right) &= \delta\left(\mathbf{1}\right) + \delta\left(\boldsymbol{\Phi}\right) \\
\delta\left(\boldsymbol{\chi}\right) &= \delta\left(\boldsymbol{\Phi}\right)
\end{aligned} \tag{A.8}$$

(9) Variation of the inverse of the micro deformation tensor $\boldsymbol{\chi}$ for micro motion:

$$\delta\left(\boldsymbol{\chi}^{-1}\right)=\boldsymbol{\chi}^{-1}\left(\delta\boldsymbol{\chi}\right)\boldsymbol{\chi}^{-1} \tag{A.9}$$

$$\delta\left(\boldsymbol{\chi}^{-1}\right)=\boldsymbol{\chi}^{-1}\left(\delta\boldsymbol{\Phi}\right)\boldsymbol{\chi}^{-1} \tag{A.10}$$

(10) Variation of $\boldsymbol{\nabla\chi}$:

$$\begin{aligned}
\boldsymbol{\nabla}\boldsymbol{\chi}_{n+1}&=\frac{\partial\boldsymbol{\chi}}{\partial\boldsymbol{x}}=\frac{\partial\boldsymbol{\chi}}{\partial\boldsymbol{X}}\frac{\partial\boldsymbol{X}}{\partial\boldsymbol{x}}=\frac{\partial\boldsymbol{\chi}}{\partial\boldsymbol{X}}\boldsymbol{F}^{-1}\\
\delta\left(\boldsymbol{\nabla\chi}\right)&=\frac{\partial\delta\left(\boldsymbol{\chi}\right)}{\partial\boldsymbol{X}}\boldsymbol{F}^{-1}+\frac{\partial\boldsymbol{\chi}}{\partial\boldsymbol{X}}\delta\left(\boldsymbol{F}^{-1}\right)\\
\delta\left(\boldsymbol{\nabla\chi}\right)&=\boldsymbol{GRAD}\left(\delta\boldsymbol{\Phi}\right)\boldsymbol{F}^{-1}-\boldsymbol{GRAD}\left(\boldsymbol{\chi}\right)\boldsymbol{F}^{-1}\boldsymbol{grad}(\delta\boldsymbol{u})
\end{aligned} \tag{A.11}$$

(11) Variation of $\Delta t\boldsymbol{\nu}^{e}_{n+1}$:

$$\begin{aligned}
\Delta t\boldsymbol{\varepsilon}^{e}_{n+1}&=\Delta t\boldsymbol{\nu}^{e}_{n+1}+\left(\Delta t\boldsymbol{\ell}^{e}_{n+1}\right)^{T}\\
\Delta t\boldsymbol{\nu}^{e}_{n+1}&=\Delta t\boldsymbol{\nu}_{n+1}-\Delta t\boldsymbol{\nu}^{p}_{n+1}\\
\Delta t\boldsymbol{\nu}^{p}_{n+1}&=0\qquad\text{for elastic case}\\
\Delta t\boldsymbol{\nu}_{n+1}&=\left(\Delta\boldsymbol{\chi}_{n+1}\right)\boldsymbol{\chi}^{-1}_{n+1}=\left(\boldsymbol{\chi}_{n+1}-\boldsymbol{\chi}_{n}\right)\boldsymbol{\chi}^{-1}_{n+1}\\
\delta\left(\Delta t\boldsymbol{\nu}_{n+1}\right)&=\delta\left(\boldsymbol{\chi}_{n+1}-\boldsymbol{\chi}_{n}\right)\boldsymbol{\chi}^{-1}_{n+1}+\left(\boldsymbol{\chi}_{n+1}-\boldsymbol{\chi}_{n}\right)\delta\left(\boldsymbol{\chi}^{-1}_{n+1}\right)\\
\delta\left(\Delta t\boldsymbol{\nu}_{n+1}\right)&=\delta\left(\boldsymbol{\chi}_{n+1}\right)\boldsymbol{\chi}^{-1}_{n+1}+\left(\boldsymbol{\chi}_{n+1}-\boldsymbol{\chi}_{n}\right)\delta\left(\boldsymbol{\chi}^{-1}_{n+1}\right)\\
\delta\left(\Delta t\boldsymbol{\nu}_{n+1}\right)&=\delta\left(\boldsymbol{\Phi}_{n+1}\right)\boldsymbol{\chi}^{-1}_{n+1}-\left(\boldsymbol{\chi}_{n+1}-\boldsymbol{\chi}_{n}\right)\boldsymbol{\chi}^{-1}_{n+1}\delta\left(\boldsymbol{\Phi}_{n+1}\right)\boldsymbol{\chi}^{-1}_{n+1}\\
\delta\left(\Delta t\boldsymbol{\nu}_{n+1}\right)&=\delta\left(\boldsymbol{\Phi}_{n+1}\right)\boldsymbol{\chi}^{-1}_{n+1}-\left(\boldsymbol{\chi}_{n+1}-\boldsymbol{\chi}_{n}\right)\boldsymbol{\chi}^{-1}_{n+1}\delta\left(\boldsymbol{\Phi}_{n+1}\right)\boldsymbol{\chi}^{-1}_{n+1}\\
\delta\left(\Delta t\boldsymbol{\nu}_{n+1}\right)&=\delta\left(\boldsymbol{\Phi}_{n+1}\right)\boldsymbol{\chi}^{-1}_{n+1}-\overbrace{\boldsymbol{\chi}_{n+1}\boldsymbol{\chi}^{-1}_{n+1}}^{\mathbf{1}}\delta\left(\boldsymbol{\Phi}_{n+1}\right)\boldsymbol{\chi}^{-1}_{n+1}+\boldsymbol{\chi}_{n}\boldsymbol{\chi}^{-1}_{n+1}\delta\left(\boldsymbol{\Phi}_{n+1}\right)\boldsymbol{\chi}^{-1}_{n+1}\\
\delta\left(\Delta t\boldsymbol{\nu}_{n+1}\right)&=\boldsymbol{\chi}_{n}\boldsymbol{\chi}^{-1}_{n+1}\delta\left(\boldsymbol{\Phi}_{n+1}\right)\boldsymbol{\chi}^{-1}_{n+1}
\end{aligned} \tag{A.12}$$

(12) Variation of $\Delta t\boldsymbol{\varepsilon}^{e}_{n+1}$:

$$\Delta t\boldsymbol{\varepsilon}^{e}_{n+1}=\Delta t\boldsymbol{\nu}^{e}_{n+1}+\Delta t\boldsymbol{\ell}^{eT}_{n+1}$$

$$\delta\left(\Delta t\boldsymbol{\varepsilon}^{e}_{n+1}\right)=\boldsymbol{\chi}_{n}\boldsymbol{\chi}^{-1}_{n+1}\delta\left(\boldsymbol{\Phi}_{n+1}\right)\boldsymbol{\chi}^{-1}_{n+1}+\left(\boldsymbol{F}_{n}\boldsymbol{F}^{-1}_{n+1}\boldsymbol{grad}(\delta\boldsymbol{u}_{n+1})\right)^{T} \tag{A.13}$$

$$\delta\left(\Delta t\boldsymbol{\varepsilon}^{e}_{n+1}\right)=\boldsymbol{\chi}_{n}\boldsymbol{\chi}^{-1}\delta\left(\boldsymbol{\Phi}\right)\boldsymbol{\chi}^{-1}+\left(\boldsymbol{F}_{n}\boldsymbol{F}^{-1}\boldsymbol{grad}(\delta\boldsymbol{u})\right)^{T} \tag{A.14}$$

(13) The indicial notation of some of these expressions can be given as:

$$\Delta t\ell^e_{lk} = \delta_{lk} - (F_n)_{lK} F^{-1}_{Kk}$$

$$(\Delta t d_{lk}) = \frac{1}{2}(\Delta t\ell_{lk} + \Delta t\ell_{kl})$$

$$\Delta t d^e_{lk} = \frac{1}{2}\left(\delta_{lk} - (F_n)_{lK} F^{-1}_{Kk} + \delta_{kl} - (F_n)_{kK} F^{-1}_{Kl}\right)$$

$$\Delta t\nu^e_{lk} = \Delta t\nu_{lk} - \Delta t\nu^p_{lk}$$

$$\Delta t\nu_{lk} = (\Delta\chi_{lL})\,\chi^{-1}_{Lk} = (\chi_{lL} - (\chi_n)_{lL})\,\chi^{-1}_{Lk}$$

$$\Delta t\varepsilon^e_{lk} = \Delta t\nu^e_{lk} + \Delta t\ell^e_{kl}$$

$$\Delta t\varepsilon^e_{lk} = (\chi_{lL} - (\chi_n)_{lL})\,\chi^{-1}_{Lk} + \delta_{lk} - (F_n)_{lK} F^{-1}_{Kk}$$

A.1 Algorithm to form element stiffness matrix for each term

Linearization procedure of individual terms and determining the element stiffness matrix contribution to form global consistent tangent matrix can be very time consuming and maybe impossible to implement for the most of the terms presented in this work. This small algorithm given below, as an example, for the specific term shows how to form the element stiffness matrix for that term. Let's consider the term given in equations 5.28-5.30

$$2(\mu+\sigma)\int_{\mathcal{B}_0} w_{k,L} F^{-1}_{Ll} F_{lL}\delta(F_{iL})\,F_{iK}F_{kK}dV = 2(\mu+\sigma)\int_{\mathcal{B}_0} w_{k,L} F^{-1}_{Ll} F_{lL}F_{iK}F_{kK}\delta u_{i,L}dV \tag{A.15}$$

$$\left(\mathcal{K}^{e,h}_{uu}\right)_5 = 2(\mu+\sigma)\int_{\mathcal{B}^e_0} \{\boldsymbol{c}^e\}^T\cdot[\boldsymbol{GRAD}(\boldsymbol{N}^{u,e})]^T\cdot[\boldsymbol{I}_{15}]\cdot[\boldsymbol{GRAD}(\boldsymbol{N}^{u,e})]\cdot\{\delta\boldsymbol{d}^e\}\,dV \tag{A.16}$$

$$[\mathfrak{J}^e_{15}] = 2(\mu+\sigma)\int_{\mathcal{B}^e_0} [\boldsymbol{GRAD}(\boldsymbol{N}^{u,e})]^T\cdot[\boldsymbol{I}_{15}]\cdot[\boldsymbol{GRAD}(\boldsymbol{N}^{u,e})]\,dV \tag{A.17}$$

To calculate the matrix $\left(\mathcal{K}^{e,h}_{uu}\right)_5$ at a Gauss point for each element, we use this portion of the code

```
fTemp_matrix_nudof_x_nudof.MultATBC(fShapeDisplGrad,I1_5,fShapeDisplGad);
scale = scale_const*(fMaterial_Params[kMu]+fMaterial_Params[kSigma_const]);
fTemp_matrix_nudof_x_nudof *= scale;
fKu_5 += fTemp_matrix_nudof_x_nudof;
```

and $[\boldsymbol{I}_{15}]$ is obtained by the algorithm used in the given function below.

```
void FSMicromorphic3DT::Form_I1_5()
{
    int row;
    int col=0;
    I1_5=0.0;

    for(int K=0;K<3;K++)
    {
        for(int i=0;i<3;i++)
        {
            row=K*3;
            for(int l=0;l<3;l++)
            {
                for(int L=0;L<3;L++)
                {
                    I1_5(row,col)+=fDeformation_Gradient(l,L)
                                   *fDeformation_Gradient(i,L);
                }
                row++;
            }
            col++;
        }
    }
```

A.2 Finite element matrices

A.2.1 Notations in Chapter 4

It is a very time consuming to show all the matrices in open form with their components. Here we present some of them, other matrices can be obtained in a similar way. Note that

some of these matrices may have a different order in components in Chapter 5.

$$\{\boldsymbol{GRAD}(\boldsymbol{w})\}^T = \left\{ \begin{array}{ccccccccc} w_{1,1} & w_{1,2} & w_{1,3} & w_{2,1} & w_{2,2} & w_{2,3} & w_{3,1} & w_{3,2} & w_{3,3} \end{array} \right\} \tag{A.18}$$

$$\{\boldsymbol{GRAD}(\delta\boldsymbol{u})\}^T = \left\{ \begin{array}{ccccccccc} \delta u_{1,1} & \delta u_{2,1} & \delta u_{3,1} & \delta u_{1,2} & \delta u_{2,2} & \delta u_{3,2} & \delta u_{3,1} & \delta u_{3,2} & \delta u_{3,3} \end{array} \right\} \tag{A.19}$$

$$[\boldsymbol{N}^{u,e}]^T = \begin{bmatrix} N_1^u(\boldsymbol{\xi}) & 0 & 0 \\ 0 & N_1^u(\boldsymbol{\xi}) & 0 \\ 0 & 0 & N_1^u(\boldsymbol{\xi}) \\ N_2^u(\boldsymbol{\xi}) & 0 & 0 \\ 0 & N_2^u(\boldsymbol{\xi}) & 0 \\ 0 & 0 & N_2^u(\boldsymbol{\xi}) \\ \vdots & \vdots & \vdots \\ N_{n_{en}^u}^u(\boldsymbol{\xi}) & 0 & 0 \\ 0 & N_{n_{en}^u}^u(\boldsymbol{\xi}) & 0 \\ 0 & 0 & N_{n_{en}^u}^u(\boldsymbol{\xi}) \end{bmatrix}_{n_{dof}^{u,e} \times n_{sd}} \tag{A.20}$$

$$[\boldsymbol{GRAD}\,(\boldsymbol{N}^{u,e})]^T =$$

$$\begin{bmatrix} N_{1,1}^u(\boldsymbol{\xi}) & 0 & 0 & N_{1,2}^u(\boldsymbol{\xi}) & 0 & 0 & N_{1,3}^u(\boldsymbol{\xi}) & 0 & 0 \\ 0 & N_{1,1}^u(\boldsymbol{\xi}) & 0 & 0 & N_{1,2}^u(\boldsymbol{\xi}) & 0 & 0 & N_{1,3}^u(\boldsymbol{\xi}) & 0 \\ 0 & 0 & N_{1,1}^u(\boldsymbol{\xi}) & 0 & 0 & N_{1,2}^u(\boldsymbol{\xi}) & 0 & 0 & N_{1,3}^u(\boldsymbol{\xi}) \\ \vdots & \vdots & \vdots & \vdots & \vdots & \vdots & \vdots & \vdots & \vdots \\ N_{n_{en}^u,1}^u(\boldsymbol{\xi}) & 0 & 0 & N_{n_{en}^u,2}^u(\boldsymbol{\xi}) & 0 & 0 & N_{n_{en}^u,3}^u(\boldsymbol{\xi}) & 0 & 0 \\ 0 & N_{n_{en}^u,1}^u(\boldsymbol{\xi}) & 0 & 0 & N_{n_{en}^u,2}^u(\boldsymbol{\xi}) & 0 & 0 & N_{n_{en}^u,3}^u(\boldsymbol{\xi}) & 0 \\ 0 & 0 & N_{n_{en}^u,1}^u(\boldsymbol{\xi}) & 0 & 0 & N_{n_{en}^u,2}^u(\boldsymbol{\xi}) & 0 & 0 & N_{n_{en}^u,3}^u(\boldsymbol{\xi}) \end{bmatrix}_r \tag{A.21}$$

$$[\boldsymbol{GRAD}\,(\boldsymbol{N}^{\chi,e})] =$$

$$\left[\begin{array}{cccccccccc}
N^{\chi}_{1,1}(\boldsymbol{\xi}) & 0 & \dots & N^{\chi}_{2,1}(\boldsymbol{\xi}) & 0 & \dots & N^{\chi}_{n^{\chi}_{en},1}(\boldsymbol{\xi}) & 0\dots & \dots \\
N^{\chi}_{1,2}(\boldsymbol{\xi}) & 0 & \dots & N^{\chi}_{2,2}(\boldsymbol{\xi}) & 0 & \dots & N^{\chi}_{n^{\chi}_{en},2}(\boldsymbol{\xi}) & 0\dots & \dots \\
N^{\chi}_{1,3}(\boldsymbol{\xi}) & 0 & \dots & N^{\chi}_{2,3}(\boldsymbol{\xi}) & 0 & \dots & N^{\chi}_{n^{\chi}_{en},3}(\boldsymbol{\xi}) & 0\dots & \dots \\
\vdots & \ddots & \vdots & \vdots & \ddots & \vdots & \vdots & \ddots & \vdots \\
0 & 0 & \dots & N^{\chi}_{1,1}(\boldsymbol{\xi}) & 0 & \dots & \dots & 0\dots & N^{\chi}_{n^{\chi}_{en},1}(\boldsymbol{\xi}) \\
0 & 0 & \dots & N^{\chi}_{1,2}(\boldsymbol{\xi}) & 0 & \dots & \dots & 0\dots & N^{\chi}_{n^{\chi}_{en},1}(\boldsymbol{\xi}) \\
0 & 0 & \dots & N^{\chi}_{1,3}(\boldsymbol{\xi}) & 0 & \dots & \dots & 0\dots & N^{\chi}_{n^{\chi}_{en},1}(\boldsymbol{\xi})
\end{array}\right]_{(n_{sd}*n_{sd}*n_{sd})\times n^{\chi,e}_{dof}} \tag{A.22}$$

$$[\boldsymbol{N}^{\chi,e}] = \left[\begin{array}{cccccccccc}
N^{\chi}_{1}(\boldsymbol{\xi}) & 0 & \dots & N^{\chi}_{2}(\boldsymbol{\xi}) & 0 & \dots & N^{\chi}_{8}(\boldsymbol{\xi}) & 0\dots & 0 \\
0 & \ddots & \vdots & \vdots & \ddots & \vdots & \vdots & \ddots & \vdots \\
0 & 0 & \dots & N^{\chi}_{1}(\boldsymbol{\xi}) & 0 & \dots & \dots & 0\dots & N^{\chi}_{8}(\boldsymbol{\xi})
\end{array}\right]_{(n_{sd}*n_{sd})\times n^{\chi,e}_{dof}} \tag{A.23}$$

A.2.2 Preconditioned Conjugate Gradients

Shewchuk (1994) gives a very brief summary of preconditioned conjugate gradient method which is used in Section 7.2.3.

$$
\begin{aligned}
&i \Leftarrow 0\\
&r \Leftarrow b - Ax\\
&d \Leftarrow M^{-1}r\\
&\delta_{new} \Leftarrow r^T d\\
&\delta_0 \Leftarrow \delta_{new}\\
&\text{While } \; i < i_{max} \text{ and } \; \delta_{new} > \epsilon^2 \delta_0\\
&\quad q \Leftarrow Ad\\
&\quad \alpha \Leftarrow \frac{\delta_{new}}{d^T q}\\
&\quad x \Leftarrow x + \alpha d\\
&\quad \text{If } i \text{ is divisible by } 50\\
&\quad\quad r \Leftarrow b - Ax\\
&\quad \text{else}\\
&\quad\quad r \Leftarrow r - \alpha q\\
&\quad s \Leftarrow M^{-1}r\\
&\quad \delta_{old} \Leftarrow \delta_{new}\\
&\quad \delta_{new} \Leftarrow r^T s\\
&\quad \beta \Leftarrow \frac{\delta_{new}}{\delta_{old}}\\
&\quad d \Leftarrow s + \beta d\\
&\quad i \Leftarrow i + 1
\end{aligned}
\tag{A.24}
$$

where A, b are inputs, M is preconditioner, and x is a starting value. Shewchuk (1994) states that the perfect preconditioner is $M = A$.